Field Trial of Residual LNAPL Recovery Using CO_2-Supersaturated Water Injection in the Borden Aquifer

by

Leif Carl Nelson

A thesis
presented to the University of Waterloo
in fulfillment of the
thesis requirement for the degree of

Master of Science
in
Earth Sciences

Waterloo, Ontario, Canada, 2007

I hereby declare that I am the sole author of this thesis. This is a true copy of this thesis, including any required final revisions, as accepted by my examiners.

I understand that my thesis may be made electronically available to the public.

Abstract

The ability of supersaturated water injection (SWI) to recover non-aqueous phase liquids (NAPLs) was studied at the field scale as part of an ongoing program to evaluate the applicability of this technology to groundwater remediation. SWI uses *Gas inFusion*™ technology to efficiently dissolve gases into liquids at elevated pressures.

SWI has been shown to both volatilize and mobilize residual NAPL ganglia in laboratory experiments (Li, 2004). During SWI pressurized water containing high concentrations of CO_2 is injected into the subsurface below the zone of contamination. Once the injected water is in the aquifer the pressure drops substantially and the concentration of CO_2 is no longer in equilibrium with the water and as a result CO_2 bubbles nucleate. These bubbles then migrate upwards through the contaminated zone towards the water table. As they move they come into contact with residual NAPL ganglia and they either volatilize this NAPL, resulting in a bubble comprised of CO_2 and gaseous NAPL, or mobilize this NAPL, resulting in a film of NAPL surrounding the bubble. In either case the bubbles continue to rise until they reach the water table at which point they are removed from the subsurface by a dual phase extraction system.

In this work, a known amount of NAPL was emplaced below the water table at residual concentrations to represent a residual source of weathered gasoline. The NAPL contained 80 liters of pentane, 80 liters hexane and 40 liters of Soltrol 130. The source was created in a hydraulically isolated cell in an unconfined sand aquifer at CFB Borden, Ontario. After the source was emplaced SWI was used to remove as much of the contaminant mass as possible in 22.25 days of operation over three months. To quantify the mass of each of the contaminants removed from the cell, vapour and water samples were taken frequently, the concentration of volatile organic compounds was continuously monitored and recorded as was the rate at which water and vapour were extracted from the cell. Based on this data the mass removed over time could be calculated.

Based on this data it was calculated that 44% of the volatile compounds (pentane and hexane) were removed but that a negligible amount of the non-volatile Soltrol was removed. At this point several soil cores were taken and they revealed that there were still high concentrations of NAPL in the center of the cell. Modeling of the flow paths of the injected water showed that water capable of releasing CO_2 bubbles did not likely reach the center of the cell. As a result another phase of remediation was launched that targeted that area. During this phase another 20% was removed, making the total 64% of the initial mass of volatile compounds. Additional soil coring following phase two showed that NAPL concentrations had decreased significantly, with the highest concentrations being predominantly hexane and located near the water table. Hexane is less volatile than pentane so this may indicate that mobilization is occurring and that some of the Soltrol in the cell may have been mobilized to the water table but there was insufficient volume to create a free phase that could have been drawn into a well. However, there is no direct evidence of Soltrol mobilization so it is recommended that soil sampling be conducted to evaluate the vertical distribution of Soltrol in the cell.

The goal of this project was to determine if SWI was capable of removing residual NAPL at a field site. It was successful in removing volatile NAPL but not non-volatile NAPL. 64% of the volatile compounds were removed but contaminant mass was still being removed when the system was shut down so with continued operation more mass would have been removed. There is no way of knowing how much more would have been removed had the project continued. These results indicate that continued development of the technology is warranted.

Acknowledgements

I would like to begin by thanking my advisor, Dr. Jim Barker, for his support, guidance and reassuring advice throughout this project. My other two committee members, Dr. Neil Thomson and Dr. Mario Ioannidis, were also very supportive of the project and invaluable sources of guidance and information.

Tom Li from inVentures technologies Inc. provided a tremendous amount of support for the project including technical knowledge of the GI generators and their operation, field monitoring during the final stage and thesis chapter edits. In addition I would like to thanks inVentures for their financial support, Wade Campbell of Inventures in Fredericton for technical support and John Archibald for supporting the project and providing help and guidance along the way.

This project would not have been possible without the tremendous amount of logistical and technical support I received from fellow students and staff at Waterloo. First and foremost I would like to thank Claudia Naas for helping to coordinate things at Borden and helping me wade through university paperwork (or doing it for me). Marianne van der Griendt and Shirley Chatten did a wonderful job analyzing the various types of samples I brought in from the field and getting me high quality results. Bob Ingelton and Paul Johnson provided invaluable assistance and guidance on well drilling and soil sampling. Scott Piggott did several days of geophysical field work and provided me with a detailed report. Dr. John Chatzis provided lots of guidance and helped me to look at the project from different perspectives. My fellow students did so much to help out with field work, sample couriering, discussing results and proving encouragement and support. So, Cindy Doughty, Alex Oiffer, Michelle Fraser, Juliana de Freitas, Jiri Beranek, Ken Clogg-Wright, Barb Fletcher, Jo Passmore, Christian Gardios, Marian Mocanu, Albanie Tremblay, Colby Steelman, Jacqueline Kreller, Dinah Augustine and whoever I am forgetting, thank you. And also thanks to Nick La Posta for spending a rainy Saturday helping me drill wells.

Minh Le and C3 Environmental provided financial and infrastructure support at Borden. Mike Campbell and SCG Industries provided the dual phase extraction system used in phase I and Don Kierstad did a great job helping us set it up and get it running. I would also like to acknowledge the American Petroleum Institute (API), the Natural Science and Engineering Research Council (NSERC) of Canada, and the Canadian Foundation for Innovation (CFI) for their financial support.

Last but definitely not least, I would like to thank Heather Sutton and my family, Jon and Marie Nelson and Anna Nelson whose unwavering encouragement, support and understanding made this possible.

Table of Contents

List of Tables

List of Figures

1. Introduction and Background

1.1. Groundwater Contamination

Groundwater contamination is a significant concern in Canada, the United States and much of the rest of the world. Groundwater is a source of drinking water for millions of people and it supplies flow to creeks, rivers, lakes and wetlands. As a result attempts to keep it free from contamination or to remove any contamination that occurs are very important. In the United States millions of dollars are spent each year to design, construct and operate groundwater remediation systems and it is estimated that it will cost over $750 billion dollars over the next thirty years to remediate the more than 300 000 sites in the United States with groundwater contamination (Kent & Bianchi Mosquera, 2001).

There are many sources of groundwater contamination and one of the most common is the release of gasoline or other petroleum products into the subsurface through spills, leaking storage tanks or improper disposal. Most petroleum products have low solubility in water so they form a separate liquid phase in the subsurface and are termed non aqueous phase liquids (NAPLs). NAPLs that are less dense than water, such as most petroleum products are termed light non aqueous phase liquids (LNAPLs) while those denser than water, such as chlorinated solvents, are termed DNAPLs. LNAPLs tend to pool above the water table and slowly dissolve into the groundwater as it flows by. However when the water table fluctuates, so will the position of the pooled NAPL and this results in some trapping of NAPL ganglia below the water table. These NAPL ganglia trapped below the water table are termed a residual source and can remain after the pool of NAPL has been removed.

Due to their low solubility, NAPL source zones (comprised of either or both pools of NAPL and residual NAPL) can continue to dissolve into groundwater for decades and act as continuing sources of groundwater contamination. Source zones can be difficult and expensive to clean up, a total cost of $500 000 to $1 000 000 is typical in the United States (Kent & Bianchi Mosquera, 2001). As a result much research has been done to develop technologies capable of remediating source zones (Khan et al, 2004; Soga et al, 2004).

1.2. Air Sparging

Air sparging is a method of groundwater remediation applicable to both sources zones and plumes of volatile organic contaminants, such as gasoline. Air is injected below the water table (typically a few meters below) and removes contaminants by a combination of volatilization and aerobic biodegradation (Figure 1.1). As the injected air moves up through the saturated zone, volatile contaminants partition from the sorbed, aqueous and NAPL phases into the vapour phase and flow up into the unsaturated zone. The injected

air contains oxygen that partitions from the vapour phase into the water, stimulating biodegradation (Johnson et al, 1993).

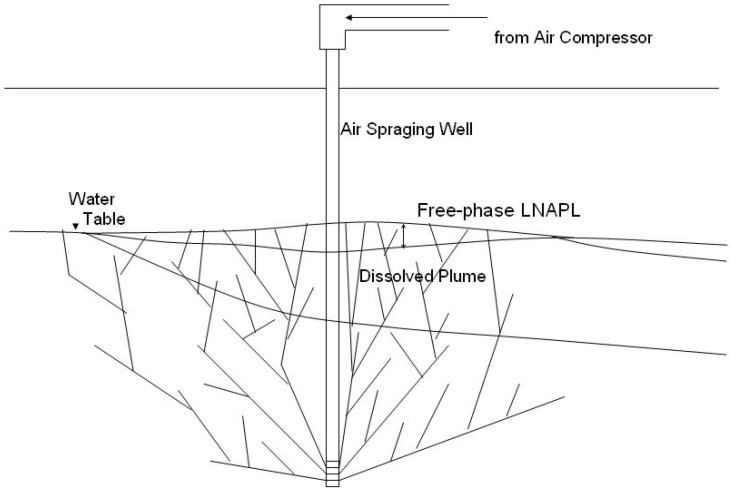

Figure 1.1 Conceptual model of the application of air sparging at a site contaminated with free phase and dissolved LNAPL.

In order to control and collect the contaminant vapours, air sparging is commonly used in tandem with soil vapour extraction (SVE). Air sparging and air sparging/SVE systems are relatively inexpensive and easy to build (Johnson et al, 1993).

1.2.1. Air Distribution

Considerable research has been conducted into how injected sparge air flows in saturated porous media, whether it is dominated by flow as bubbles or flow as fingers/channels. This work has important implications for the zone of influence of air sparging systems and their efficiency at removing contaminants (Ji et al, 1993). If sparged air moves in discrete channels then there is great potential for large areas of the subsurface to be bypassed. If that is the case, remediation will be limited by aqueous phase diffusion and therefore considerably less effective than if the air contacted the NAPL directly (Ahlfeld et al, 1994).

Ji et al (1993) conducted laboratory experiments using glass beads in a large tank and found that the type of flow observed primarily depended upon grain size. In gravel-sized beads (grain diameters greater than four mm) air flowed as discrete bubbles while in sand-, silt- and clay-sized beads (diameters less than 0.75 mm) air flowed in channels. So under most natural subsurface conditions, channel flow will dominate, based on their results. They also found that in homogeneous media with uniform grain sizes the air flow patterns were symmetrical about the vertical axis through the injection point. However, when mixtures of grain sizes were used the air flow patterns were no longer symmetrical due to slight spatial variations in the bead mixture and the resulting pore scale heterogeneities. Since natural subsurface environments are essentially never perfectly homogeneous, air flow patterns at real sites will not be symmetrical. In addition, they

found that the presence of large scale heterogeneities will have a significant impact on air flow patterns. Layers of lower permeability will block air flow, causing the area directly above them to be inaccessible to direct air flow. As a result contaminants in these areas will not be efficiently remediated. The presence of lower permeability layers is common in natural subsurface environments so this will likely impact the effectiveness of air sparging at most sites.

Ahfeld et al (1994) observe that when given air flow dominated by channeling, the important factors are location of the channels (especially with respect to free- or residual-phase contaminants) and their density (number of channels per unit area of cross section). The location of channels will be determined by pore scale heterogeneities, as the air pressure increases and overcomes the capillary pressure. Since the smallest capillary pressure occurs in pores with the largest radius of curvature, channels will preferentially form where there are the largest pore sizes. Since larger pores generally correlate to higher permeabilities, air flow will become channeled along pathways of relatively high permeability and the overall pattern of air flow will be governed by heterogeneities in permeability. This means that higher air pressures are required to enter smaller pores. Poorly sorted sand will result in a larger zone of influence than a well sorted sand due to the lower permeability and increased tortuosity resulting from the smaller pore sizes in the poorly sorted sand (Reddy & Adams, 2001). At a given air injection flow rate the channel density (air saturation) will be less in the poorly sorted sand. In a gravel, where flow is as discrete bubbles, the zone of influence is even smaller.

One potential way to increase the volume of aquifer impacted and air saturation by air sparging is to use horizontal wells. In laboratory tests Plummer et al (1997) showed that for a given injection rate, a horizontal well causes a more laterally extensive channeling network and displaces more water (increases air saturation).

Clayton (1998) argues that there are two types of channeling possible during air sparging, pore-scale fingering and macroscopic channeling. Pore-scale fingering is described as many small fingers resulting in good coverage of the subsurface and high air saturation, while macroscopic channeling is the channeling described by other researchers where channels are large and widely spaced. Clayton contends that pore scale fingering is much more common than macroscopic channeling. Evidence of high air saturation in homogeneous fine sands is used to support the presence of pore scale air fingering as opposed to macroscopic channeling. As a result, fine sands are expected to provide optimal conditions for air sparging. However, Brooks et al (1999) provide additional experimental and theoretical evidence that macroscopic channel flow dominates in sand, silts and clays while bubble dominated flow only occurs in gravels.

Reddy and Adams (2001) examined the effects of soil heterogeneity on sparged air flow patterns in the laboratory. They found that when the permeability ratio between two adjoining layers was greater than 10:1, with the less permeable layer underlain by the more permeable layer, that air would bypass the less permeable layer. The large impact of relatively small changes in permeability was observed by Tomlinson et al (2003) at a field site through the use of geophysical tools to monitor in situ air saturation during air

sparging. Extensive air pockets were observed to form beneath less permeable layers; however, air was able to migrate through these layers. It is not known whether this migration was due to the air pressure building up high enough to enter the low permeability layer or if the air flow "short circuited" the layer by flowing through a well casing or stratigrapic window or if it flowed around the edge of the layer.

To date multiphase flow models have been able to describe the bulk air saturation and general process of air sparging but they cannot efficiently represent the details of air distribution such as air channeling (Thomson & Johnson, 2000). A new approach will have to be found before accurate predictions of field performance can be made based on a reasonable amount of field data.

1.2.2. Contaminant Removal

The effectiveness of air sparging at removing contaminants from the subsurface is dependant on transferring mass between the aqueous and the gaseous phases. This is true for both volatilization and aerobic biodegradation (Ahlfeld et al, 1994). Due to the high air velocities and potentially short air flow paths in air sparging, it is unlikely that equilibrium will be reached between the gaseous and aqueous phases. This results in difficulties in determining mass transfer rates. Also complicating matters is whether or not the aqueous concentration at the air/water interface is representative of the bulk water concentration. This is unlikely, especially when there are significant distances between air channels, because the volatilization occurring at the air/water interface drives the aqueous concentration down locally. As a result, the overall rate of mass transfer will quickly be dominated by diffusion and advection of contaminants towards the air/water interface. Diffusion and advection are significantly slower than volatilization so many small air channels are preferable to a few large ones. Remediation times will be further increased if NAPL is present and not directly contacted by air channels. This is due to the fact that NAPL has to first dissolve into the aqueous phase before moving by diffusion and advection towards the air/water interface (Ahlfeld et al, 1994). Johnson (1998) presents evidence based on theoretical analysis that the evaporation of water by flowing air can have a significant impact if the resulting velocity towards the air channel is greater than two cm/day. This would result in contaminant concentrations moving towards the channel primarily through advection rather than diffusion.

During the early phases of air sparging, volatilization is the dominant mechanism of contaminant removal. As long as there is NAPL in contact with air channels volatilization will occur. Once all of the NAPL in contact with air channels has been removed as well as the high aqueous concentrations near air channels, advection and diffusion will control mass removal rates. When there is a sufficiently high permeability contrast between layers and the less permeable layer is underlain or surrounded by the higher permeability layer, air will not enter the less permeable layer. As a result, contaminants in the low permeability layer will only be removed by diffusion and advection which will take a long time (Reddy & Adams, 2001).

Benner et al (2002) analyzed data from five field sites and used numerical simulations in an attempt to understand the important factors effecting remediation time and cost for actual sites. They found that contaminant type, pulsed sparging operation, number of wells, maximum biodecay rate, total porosity and aquifer organic carbon content all had significant impacts. Aquifer organic carbon content affects the removal efficiency because many contaminants sorb to organic matter. The factors mentioned above are important considerations when designing air sparging systems but they are not necessarily the physical, chemical or biological factors directly controlling removal efficiency. Benner et al (2002) inferred that each of the identified design factors were based on a combination of subsurface coverage of the sparged air, sparged air residence time, system contaminant equilibrium, contaminant phase distributions, oxygen availability for microbes and contaminant volatility. Design factors having little to moderate impact were depth of the sparge point below the water table, air injection rate/pressure, horizontal air conductivity and anisotropy ratio.

Air sparging has been applied to remove a range of contaminants from different types of subsurface environments with varying levels of success. Successful applications include Johnston et al (2002) where 65% of the mass of weathered gasoline removed from a sand aquifer through a combined air sparging/SVE system was attributable to sparging and Gordon (1998) where concentrations of several VOCs including TCE and PCE in a shallow sand aquifer were significantly reduced as a result of air sparging. However, results from the application of air sparging at gasoline contaminated sites with lower permeabilities (Kirtland et al, 2001; Hall et al, 2000) did not prove successful. Bass et al (2000) provide a good review of air sparging case studies and noted that rebound frequently occurs at sites where NAPL was initially present as either free phase or residuals (and likely still present after remediation). This is not unexpected due to air sparging's limitations in removing NAPL. So after the remediation is stopped, the remaining NAPL will continue to partition into the aqueous phase potentially resulting in unacceptably high aqueous concentrations (Waduge et al, 2004).

1.2.3. Contribution of Biodegradation

Air sparging can promote aerobic biodegradation in the saturated zone by providing oxygen (Johnson et al, 1993). Johnson (1998) evaluated the contribution of aerobic biodegradation through a theoretical analysis of the mechanisms and factors involved in air sparging and determined that aerobic biodegradation is only significant when dissolved contaminant concentrations are less than one mg/l.

Adams and Reddy (2003) evaluated the contribution of aerobic biodegradation to the overall mass removal in the laboratory during biosparging. Biosparging is a variation of air sparging where air is injected at a high rate for a short period of time and then stopped for a long period of time. During the time of no air injection, the air trapped as bubbles when the system was shut of will gradually collapse and release oxygen into the aqueous phase. Their experiment studied benzene removal from a laboratory column and found that volatilization was still the dominant mechanism but that biodegradation could

account for a substantial portion of the mass removal, especially when the system was designed to maximize oxygen transfer to the aqueous phase.

Field studies by Johnston et al (1998) and Aelion & Kirtland (2000) confirm that volatilization is the dominant mechanism of removal during air sparging. Johnston reported that volatilization accounted for at least an order of magnitude more mass removal than aerobic biodegradation while Aelion and Kirtland reported 77 times more mass was removed by volatilization.

1.2.4. Pulsed Air Sparging

The goal of pulsed air sparging is to induce more mixing in the subsurface than is possible through continuous injection (Johnson et al, 1993). Mixing occurs because when sparging begins the injected air displaces groundwater resulting in localized groundwater mounding around the injection well. Over time, minutes to days depending on soil grain size, the mound dissipates. The opposite happens when injection is stopped, air pathways collapse and a depression is created around the well. By pulsing air injection, groundwater mixing can be induced by creating pressure gradients. This mixing will redistribute contaminant concentrations relative to air channel locations reducing dependence on diffusion to move aqueous phase contaminants towards air channels (Kirtand & Aelion, 2000).

Studies at field sites by Kirtland and Aelion (2000) and Yang et al (2005) showed clear evidence of increased contaminant removal rates when air sparging was pulsed compared to continuous operation. A review of case studies by Bass et al (2000) also showed that pulsing tended to provide better results than continuous operation. Gordon (1998) used a novel application of pulsing to help prevent offsite migration of contaminants. Rows of sparging wells were aligned perpendicular to groundwater flow and operated in sequence starting with the most down-gradient row to "comb" groundwater up-gradient. There was no evidence that this approach had an impact on the remediation efficiency, but at the very least it prevented off-site migration due to mounding as had been feared during the design of the project.

1.3. Soil Vapour Extraction

Many NAPLs, including gasoline, are quite volatile allowing them to be removed from the unsaturated zone by flowing air (Figure 1.2). Initially, applying a vacuum at wells screened in the unsaturated zone near the contaminated area will result in the removal of soil gas that was in equilibrium with the NAPL. Over time, air will be drawn across the contaminated area and the contaminants will be transferred from the NAPL, aqueous and sorbed phases to the vapour phase in an attempt to re-establish equilibrium conditions (Baehr et al, 1989). Eventually the overall concentration of NAPL in the unsaturated zone will decrease, ideally to levels that meet the criteria for the site.

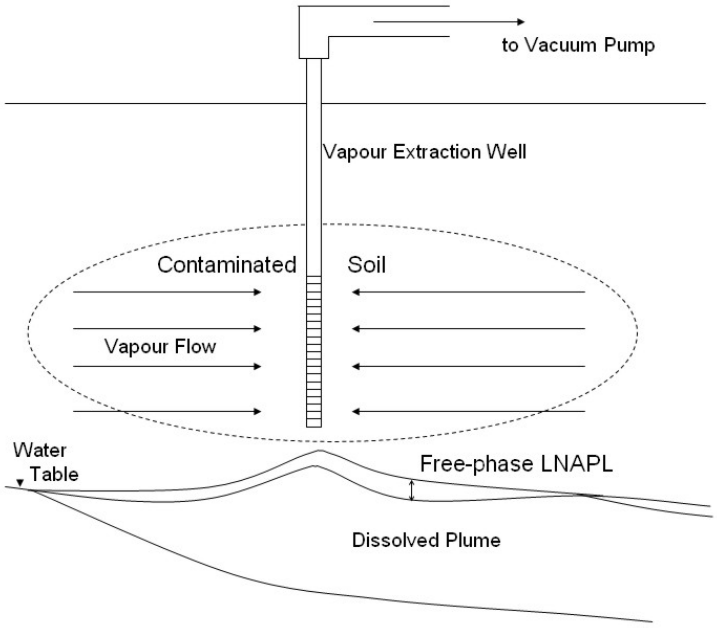

Figure 1.2 Conceptual model of the application of SVE at a site contaminated with residuals in the soil, free phase LNAPL and a dissolved plume.

The three main factors affecting the performance and applicability of SVE are: chemical composition of the contaminant (primarily its volatility, or the volatility of the compounds of concern if it is a mixture), vapour flow rates through the unsaturated zone and vapour flow paths (whether or not they contact the contaminants) (Johnson et al, 1990). The main challenge is inducing flow paths that will intersect the zones of contamination. If the contamination is concentrated in areas of higher water content, which gas flow will preferentially avoid, then mass removal is limited by aqueous phase diffusion to areas with access to gas flow (Thomson & Flynn, 2000). The impact of this preferential flow was considerable in a field study where the subsurface is fairly homogeneous sand so it would be even more significant at real word sites that generally have more complex subsurface stratigraphy (Thomson & Flynn, 2000). When there is good contact between the flowing air and areas of high contamination, removal rates are dependant on the volatility of the contaminant (or its components) (Baehr et al, 1989).

In addition to volatilization, SVE has been found to enhance biodegradation of some contaminants due to the supply of oxygen provided by the flow of surface air into the subsurface (Capuano & Johnson, 1996). Coupling SVE with air sparging can increase the amount of oxygen provided for biodegradation (Aelion & Kirtland, 2000; Kirtland et al, 2001).

In many cases SVE has proven to be a cost effective remediation option in part because the system can be easily built and the extracted vapour may not have to be treated (Johnson et al, 1990).

1.4. Dual Phase Extraction

Dual phase extraction (DPE) systems work by applying a large vacuum that allows the removal of both soil vapour and groundwater through the same pipe or hose. The pipe or hose is placed at or near the water table so that it extracts the desired combination of air and water without creating a drawdown cone (Figure 1.3). If a drawdown cone is desired, a submersible pump can be used to draw down the water level in the well before the extraction is begun. The pipe or hose is then positioned near the lowered water table and extraction is begun and the submersible pump is shut off (O'Melia & Parson, 1996). Alternatively, a submersible pump can be used to remove groundwater while the vacuum is applied at the top of the well head to remove soil vapour exclusively (Kirschner et al, 1996). If a there is free phase LNAPL at the water table, the DPE system will remove it as well, through volatilization and free phase extraction (O'Melia & Parson, 1996). DPE can be considered to combine pump and treat with soil vapour extraction in one remediation system with additional advantages described below. In addition to the advantages of requiring less infrastructure, DPE systems may be capable of higher groundwater and soil vapour extraction rates than conventional pumping systems in low permeability soils (O'Melia & Parson, 1996).

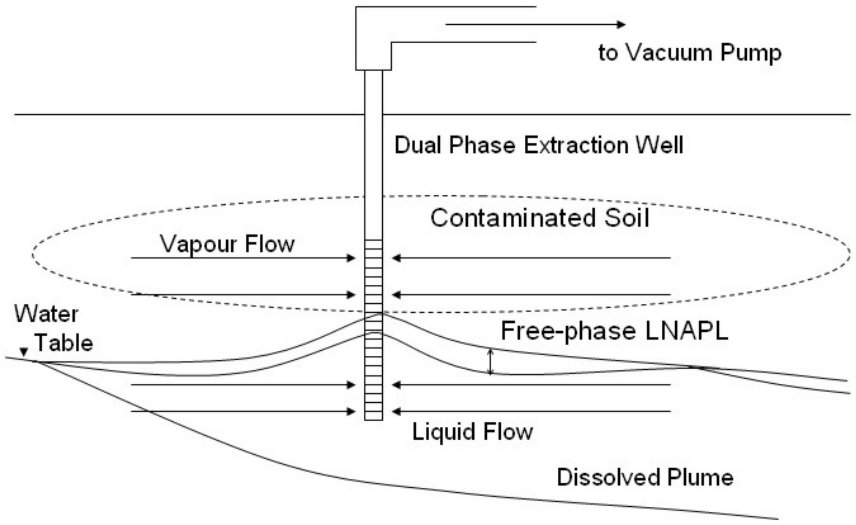

Figure 1.3 Conceptual model of the application of DPE at a site contaminated with residuals in the soil, free phase NAPL and a dissolved plume.

In addition to the removal mechanisms mentioned above, biodegradation can be significant hydrocarbon removal mechanism (Kirshner et al, 1996). This is due to air being drawn into the subsurface by the applied vacuum. This air will have higher levels of oxygen which promotes biodegradation. To enhance this effect, and to volatilize dissolved and residual NAPL below the water table, air sparging can be used in conjunction with DPE (Kirshner et al, 1996).

DPE also removes capillary fringe water, which is not impacted by most conventional remediation systems (Edwards et al, 2002). Successful remedial applications include case studies described by Yen et al (2003) and Kirshner et al (1996).

1.5. Gas inFusion™ Principles

For supersaturated water injection (SWI) to be a viable groundwater remediation method there needs to be a continuous supply of carbonated water to the subsurface at high levels of saturation and flow rate. Through a proprietary technology, the *Gas inFusion* (GI) generator can provide this. The saturated concentration is the highest concentration of dissolved gas thermodynamically stable in water for a given temperature and pressure. For a given temperature, the saturation concentration, or equilibrium concentration, of a dissolved gas is given by Henry's Law:

$$x_i = \frac{P_i}{H} \qquad \textbf{Equation 1.1}$$

Where x_i is the mole fraction of the dissolved gas in the liquid, P_i is the partial gas pressure and H is the Henry's coefficient. Since the Henry's coefficient stays constant for a given temperature, if the pressure is increased, then the equilibrium mole fraction of the solute will also increase. This results in a higher concentration of the dissolved gas in the liquid. If the pressure is then decreased, the solution will no longer be in equilibrium and the system is said to be supersaturated with the gas. This condition will not last long, gas bubbles will nucleate and gas will be released until a new equilibrium is established with a lower concentration of gas in the liquid. However, this does not happen instantaneously, there is a period of time over which these bubbles form.

SWI with the GI generator works by combining water and gas (CO_2 in this project) under pressure to create high concentrations of CO_2 in the water. This carbonated water is then pumped into the subsurface where the pressure drops to the hydrostatic pressure at that point in the subsurface which will be significantly less than the pressure in the GI generator. As a result, the carbonated water will no longer be in thermodynamic equilibrium and bubbles of CO_2 will begin to form. Since the water is being injected into the aquifer at a fairly high flow rate and the carbonated water does not immediately return to equilibrium, bubbles will continue to nucleate as the water flows outwards from the injection well.

Most current systems of dissolving gas into water are inefficient and are typically too large to be transported to contaminated sites. The most common method of dissolving a gas into water is by sparging gas into a column of water. However, the rising bubbles provide a limited interface for mass transfer and most of the gas reaches the top of the column before it can dissolve and must be recycled.

Gas inFusion is a patented technology (patent no. 6,209,855) that efficiently dissolves gas into water at elevated pressures. The interface across which mass transfer occurs is thousands of hydrophobic micro-hollow fibers (Figure 1.4). CO_2 enters these fibers under pressure and flows through the fibers along the length of the GI generator (Figure 1.5). Pressurized water enters the GI generator and then into and out of a radially perforated pipe that is surrounded by the gas-filled micro-hollow fibers. Since the micro-hollow fibers are hydrophobic, water will not enter them and as a result mass transfer occurs all over the surface area of the fibers. There are thousands of these fibers inside each GI generator (Figure 1.6) which allows high levels of concentration to be reached even with relatively high water flow rates. The pressure of the system, and as a result the level of concentration (for a given water flow rate), is determined by the pressure of the water supply.

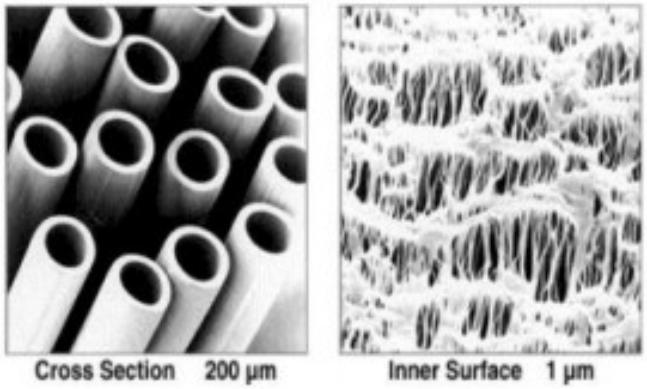

Figure 1.4 Magnified photos of the hydrophobic micro-hollow fibres that are the basis of the *Gas inFusion* technology (Li, 2004).

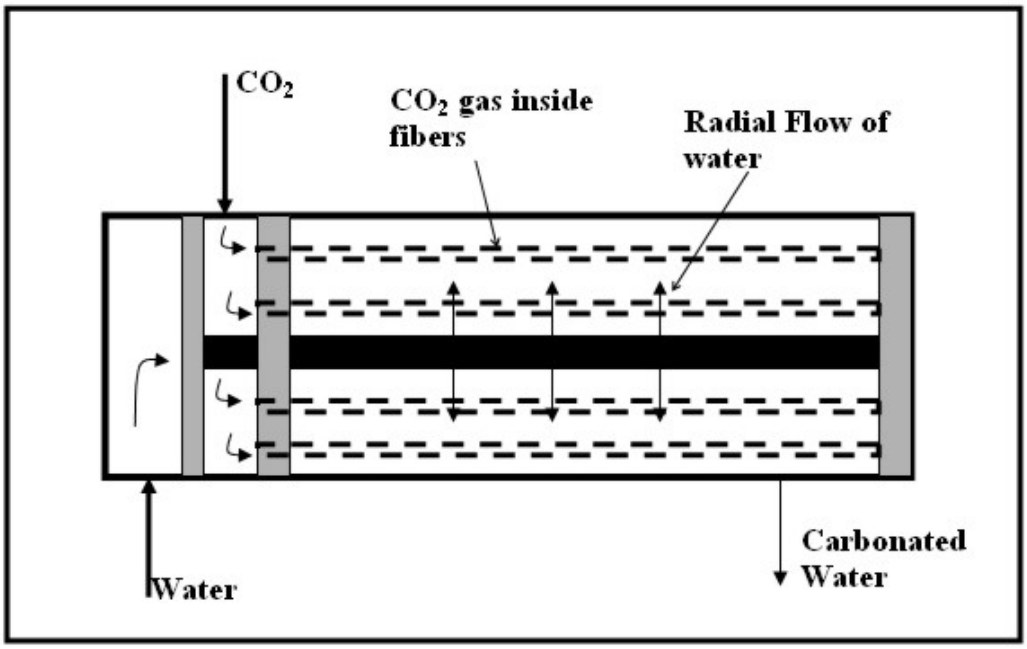

Figure 1.5 Schematic of the *Gas inFusion* generator showing direction of gas and water flow (Li, 2004).

Figure 1.6 Photograph of the GI generator used in phase II of the remediation.

1.6. Remediation Conceptual Model

Once water containing elevated concentrations of CO_2 under pressure leaves the GI generator it flows to an injection well. The screen of this injection will be located below the residual NAPL (Figure 1.7). When the carbonated water exits the well screen the pressure will drop and the amount of CO_2 in the water will no longer be thermodynamically stable; the water will be supersaturated with CO_2. Supersaturation will not last long though and immediately CO_2 bubbles will begin nucleating as the supersaturated water flows radially out from the well. Doughty (2006) found that bubbles continued to nucleate until the injected water had flowed several meters from the injection point (the distance will be dependant on many factors including water injection,

water pressure and the hydraulic conductivity of the porous medium). The newly formed CO_2 bubbles will rise up though the porous medium or become trapped in a pore. Some of the bubbles that continue to rise will come into contact with residual NAPL ganglia.

If the NAPL is volatile, the contact between the CO_2 bubble and the NAPL will result in the NAPL being volatilized and incorporated into the bubble (Li, 2004). This bubble that now contains CO_2 and volatilized NAPL will continue to rise and will reach the unsaturated zone if it does not become trapped in a pore. Once the CO_2 and volatilized NAPL reach the unsaturated zone they will be drawn into the extraction well by the applied vacuum and removed from the subsurface.

If the NAPL is non volatile, the contact between the CO_2 bubble and the NAPL will result in the NAPL spreading around the bubble and forming a film that surrounds the bubble (Li, 2004). The bubble, and its film of NAPL, will continue to rise until reaches the water table unless it becomes trapped in a pore. At the water table the non volatile NAPL will be deposited. If enough non volatile NAPL collects at the water table it will form a free phase will be drawn into the extraction well by the applied vacuum and removed from the subsurface. The applied vacuum will also remove groundwater which will contain small amounts of dissolved NAPL. However, since NAPLs are by definition insoluble in water the amount of NAPL removed by this mechanism will be insignificant.

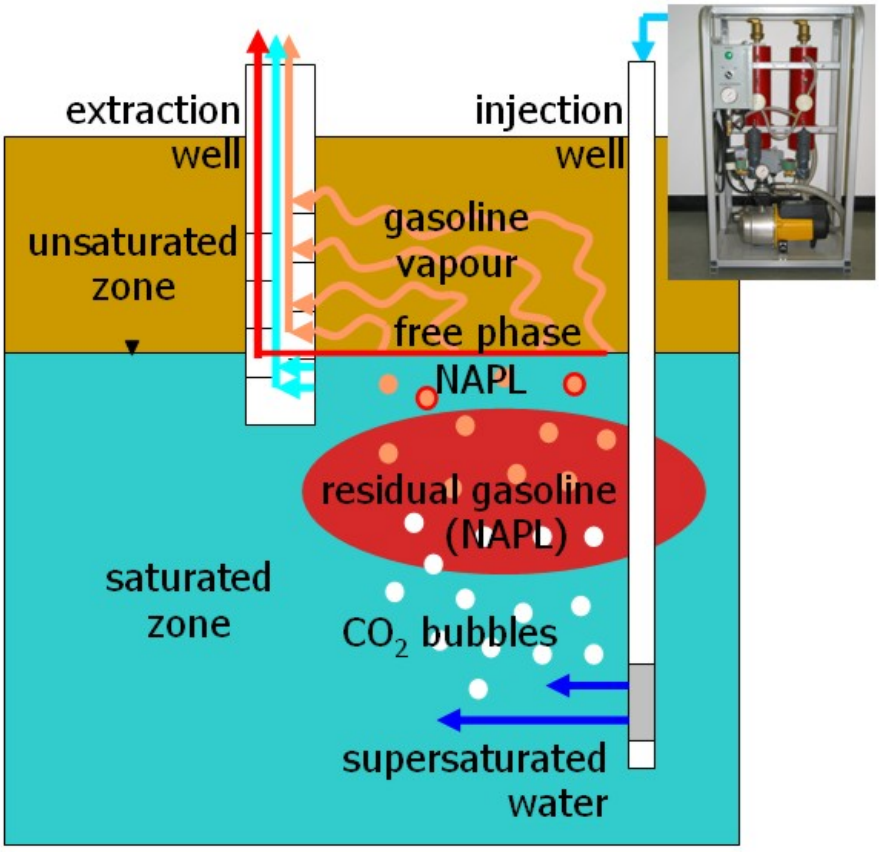

Figure 1.7. The conceptual model of remediation of a residual LNAPL source zone below the water table.

1.7. Previous Lab Studies (Li, 2004)

The SWI process was first evaluated in lab scale tests to ensure that the basic principles behind the application of this technology to groundwater remediation were valid. The first experiment involved the volatilization of residual NAPL ganglia by bubbles of CO_2 nucleated in the pore spaces of an etched glass micro-model. The micro-model allowed the processes of bubble growth and NAPL volatilization to be directly observed. The next step was to attempt to recover residual NAPL from a sand packed column. Hexane and octane were emplaced at residual concentrations in a water saturated column. Supersaturated water was injected into the bottom the column and CO_2 bubbles nucleated in the column before flowing upwards, volatilizing and mobilizing residual NAPL. The mobilization of the residual NAPL was not anticipated but it accounted for a significant amount of the NAPL removed (Table 1.1). Mobilization occurred when NAPL formed a liquid film around a rising bubble. Octane, which is less volatile (Table 1.1) was more likely to be removed by mobilization than hexane.

	Hexane	Octane
Initial mass	33.6 g	17.4 g
Mass removed by volatilization	19.2 g	5.7 g
Mass removed by mobilization	3.2 g	3.5 g
Total mass removed	22.4 g	9.2 g
NAPL remaining in column	1.2 g	2.3 g
% NAPL unaccounted for	29.8 %	33.1 %
Vapour pressure	20.2 kPa *	1.8 kPa *

Table 1.1 Results of the laboratory NAPL recovery experiment (Li, 2004). * (MacKay et al, 1992)

The final experiment attempted to estimate a zone of influence for the technology. A box filled with sand saturated with water was used to visualize bubble evolution. In addition, the gas flux out of the top of the box was measured at several locations over time. The zone of influence extended beyond the end of the box used in the experiment. These lab results successfully demonstrated the ability of SWI to recover residual NAPL. In addition, mathematical models for liquid-gas mass transfer were developed to study the nucleation and growth of bubbles in a single pore and increase of gas saturation in a macroscopic two dimensional domain.

1.8. Previous Field Studies (Doughty, 2006)

Since the zone of influence could not be determined in the lab due to spatial restrictions, a field study was undertaken to determine the zone of influence and to begin to evaluate the effectiveness of SWI at the field scale. Determining the zone of influence in the field was also advantageous because it would more closely represent conditions at contaminated sites. To measure the zone of influence, geophysical surveys (surface ground penetrating radar (GPR), cross borehole GPR and neutron measurements) were combined with groundwater monitoring of CO_2 partial pressure (pCO_2).

Based on the monitoring of pCO_2, the radius of the area where there is potential for evolution of bubbles is between 5.5 and 7.0 meters. Figures 1.8 and 1.9 show the results of pCO_2 monitoring undertaken six days after injection had begun. The small black circle in the center is the location of the injection well and each grid square in one meter by one meter.

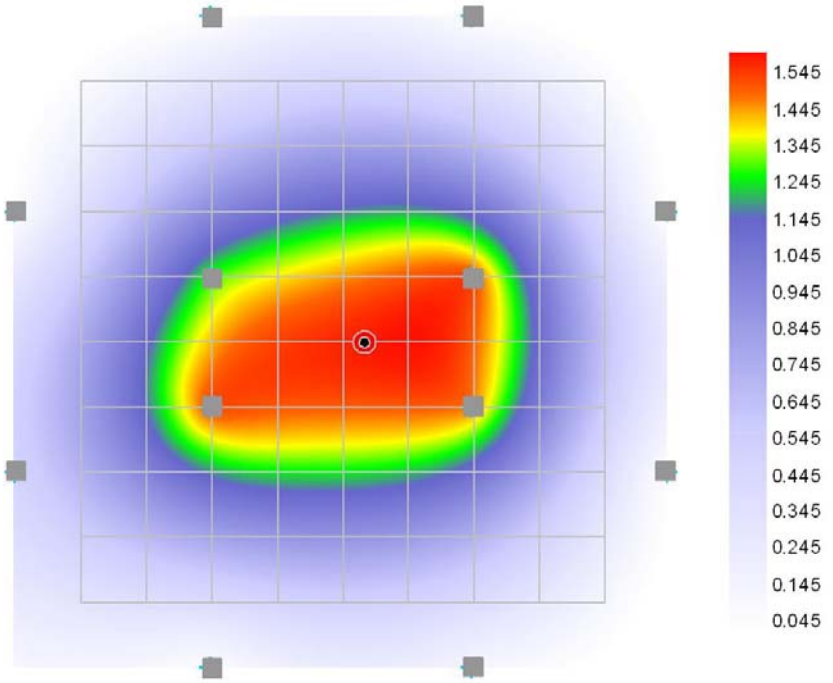

Figure 1.8 pCO_2 levels (atm) in groundwater at 2.5 meters below ground surface.

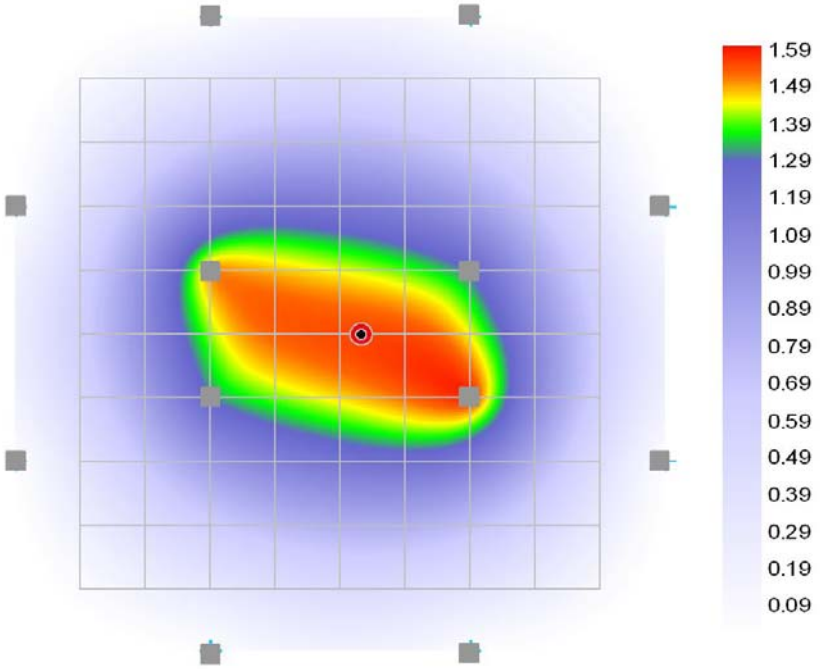

Figure 1.9 pCO_2 levels (atm) in groundwater at 4.0 meters below ground surface (the depth of SWI injection).

Based on the results of the geophysical surveys, the radius of the zone in which a measurable gas phase developed is greater than 5.3 meters. Cross-borehole GPR allows the change in water content with depth to be calculated. Figure 1.10 shows the maximum change in water content for one of the profiles near the injection point. The greatest decrease in water content (which is the greatest increase in gas content) occurs near three meters below ground surface.

The Borden aquifer is composed of medium to fine sand with fairly minor horizontal bedding (Mackay et al, 1986). After the experiment was completed, soil cores were taken and hydraulic conductivity measurements were made. It was found that there are variations in hydraulic conductivity with depth so the increased gas content is likely due to a low hydraulic conductivity layer resisting vertical migration of gas bubbles. A similar phenomenon has been reported for air sparging at Borden (Tomlinson et al, 2003), at other field sites (Hall et al, 2000) and in laboratory experiments (Reddy & Adams, 2001).

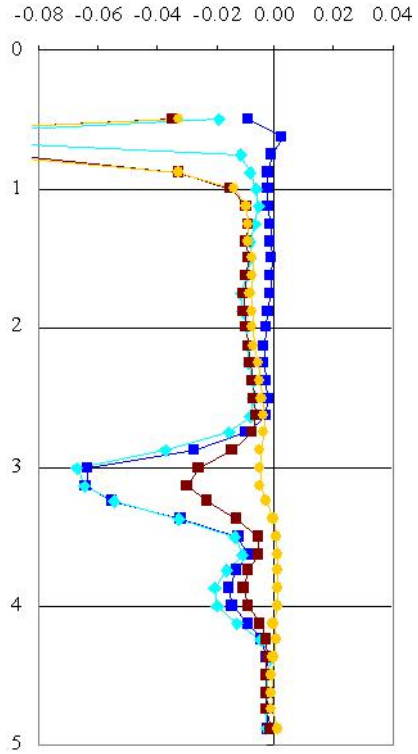

Figure 1.10. Change in water content with depth below ground surface (meters) for a cross-borehole GPR survey near the SWI injection point.

A comparison of the results from this experiment was made to the results of an experiment conducted by Tomlinson et al (2003) on air sparging at Borden (Table 1.2).

Parameter	SWI	Air Sparging
Total Running Time (days)	5.2	7
Gas	CO_2	Air
Total Volume of Gas (m^3)	122	1400
Total Volume of Water (L)	57,247	NA
Gas Saturation (%)	2-16	15 – 60
Approximate Gas Saturation Distance from Injection/Sparge Point [Geophysics] (m)	≥ 5.3	≥ 2.5
Approximate Distance from Injection/Sparge Point with Potential to Release Gas [Groundwater Data]	≥ 5.5 – 7	NA

Table 1.2 Comparison of supersaturated water injection (SWI) (Doughty, 2006) and air sparging (Tomlinson et al, 2003).

The main points of comparison are the greater zone of influence for SWI and the greater gas saturation for air sparging.

1.9. Project Objectives

Laboratory studies (Li, 2004) demonstrated that CO_2 gas bubbles will evolve from solution during flow of supersaturated water through medium sand. These bubbles will then flow upwards through the saturated zone, volatilizing and mobilizing residual NAPL that they contact. The next step in evaluating the effectiveness of this new remediation technology was to apply it in a field setting. To do so, a mixture of volatile and nonvolatile hydrocarbons was emplaced below the water table at residual concentrations. Supersaturated water injection was then employed in an attempt to remediate the area. The amount of hydrocarbons removed from the cell will be calculated based on monitoring and sampling of both the vapour and aqueous phases as they are removed from the cell. The mass removed will be compared to the mass emplaced to determine the effectiveness of this remediation method. Other considerations such as the distribution of hydrocarbons in the subsurface before and after the remediation will also be taken into account in the performance evaluation.

1.10. Site Location and Description

The study cell is located in an abandoned sand pit on Canadian Forces Base (CFB) Borden which is 20 kilometers west of Barrie, Ontario, Canada (Figure 1.11). The interior of the cell consists of the local aquifer, comprised of Borden sand that extends from the ground surface to approximately seven meters below ground surface (mbgs) at this location. The aquifer is composed of fairly homogeneous clean, well-sorted, medium- to fine-grained sand that exhibits horizontal and parallel bedding (Mackay et al,

1986). It is underlain by a thick silty clay deposit, which forms the bottom boundary of the cell. The walls of the cell were constructed of sealable-joint steel sheet piling to prevent migration of contaminants out of the cell.

Figure 1.11 Location of CFB Borden and study site.

2. Methods

2.1. Field Installations

2.1.1. Cell Construction

In order to contain the contaminants, a cell was constructed using Waterloo Barrier sealable-joint steel sheet piling (Starr et al, 1992). The sheet piles were driven down seven meters and into the silty clay layer that acts as the bottom of the cell. The joints between the sheet piles were specifically designed to minimize the amount of leakage into or out of the cell. Once the sheet piles were in place, the joints were cleared and a grout was injected into the joint to create a seal between the two sheet piles. The constructed cell is 4.5 meters x 4.5 meters by seven meters deep.

A layer of coarse, angular, gravel-sized crushed rock (referred to as the gravel layer) sixty centimeters thick was placed over the native sand to provide a layer that would easily conduct air flow during the experiment. Above the gravel a sheet of geotextile fabric was placed to prevent fine bentonite clay (Figure 2.1) from falling down into the gravel and clogging the pore spaces. On top of the geotextile a layer of bentonite clay fifteen centimeters thick was placed. This was accomplished by pouring a layer of bentonite pellets on top of the geotextile and then spraying the pellets with water which caused them to swell and form a layer that is very resistant to air flow. As a result the cell is sealed from the atmosphere and volatilized contaminants cannot escape. To protect the clay layer while working in the cell, another layer of geotextile and a fifteen centimeter layer of sand were placed over the clay.

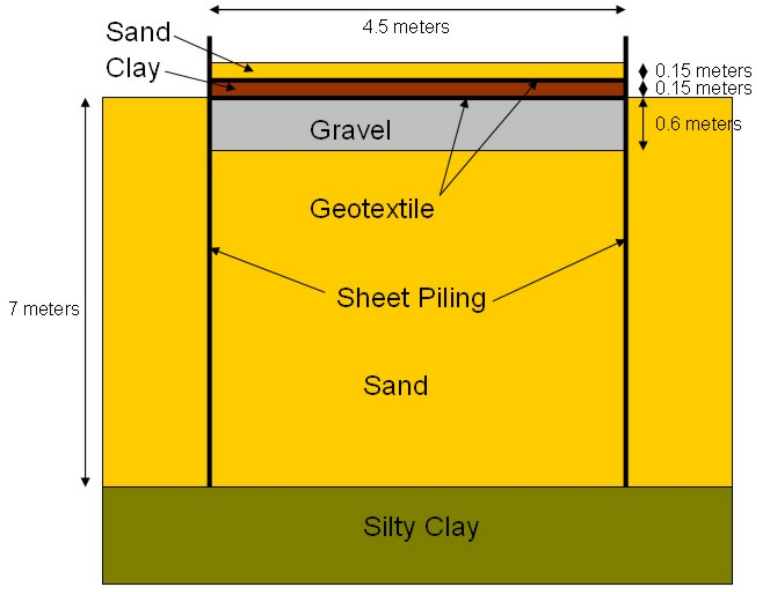

Figure 2.1. Cross section of completed cell (not to scale).

2.1.2. Wells

2.1.2.1 Vent Wells

Vent wells were installed near the edge of the cell to allow air to enter the cell when the dual phase extraction system was running and more air was being extracted than CO_2 was being added. They were constructed of five centimeter diameter schedule 40 PVC. The wells are two meters in length, the top thirty centimeters (cm) were riser pipe and the bottom 170 cm were slot ten well screen (Figure 2.2). Sixteen wells were installed near the edge of the cell, four per side at approximately 15 cm from the sheet piling (Figure 2.3). Vent wells are designated by the prefix V on all figures.

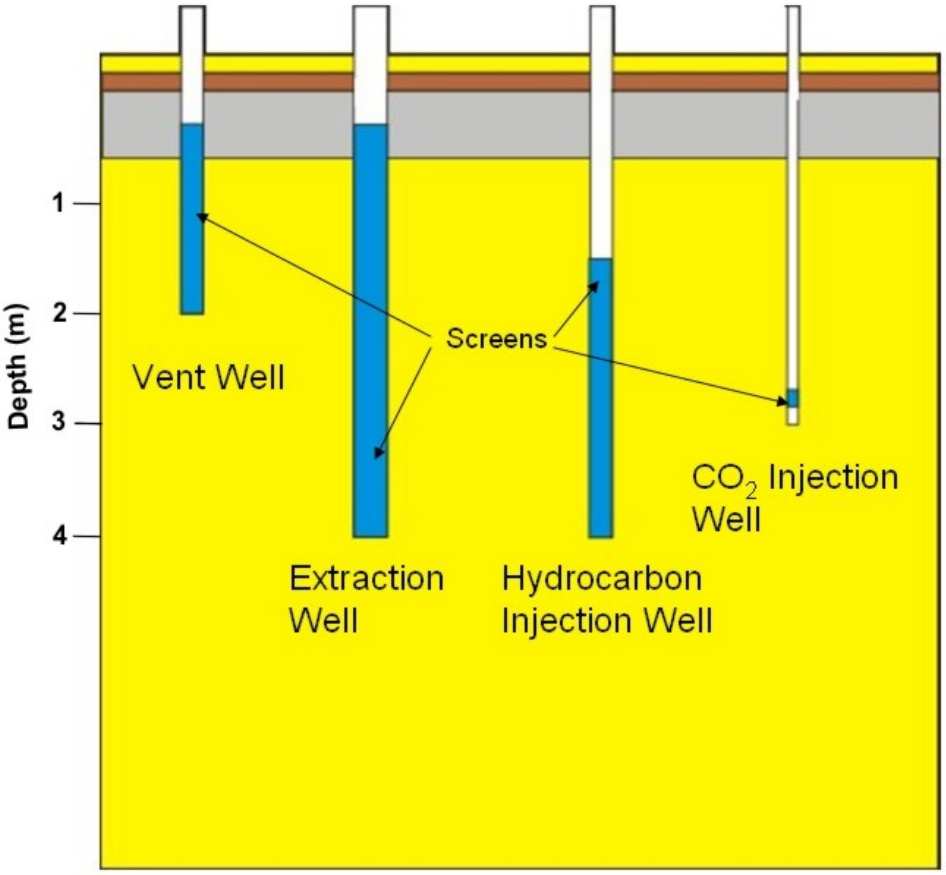

Figure 2.2 Well and screen depths. Note that the water table was drawn down to about 300 cmbgs before and during hydrocarbon injection.

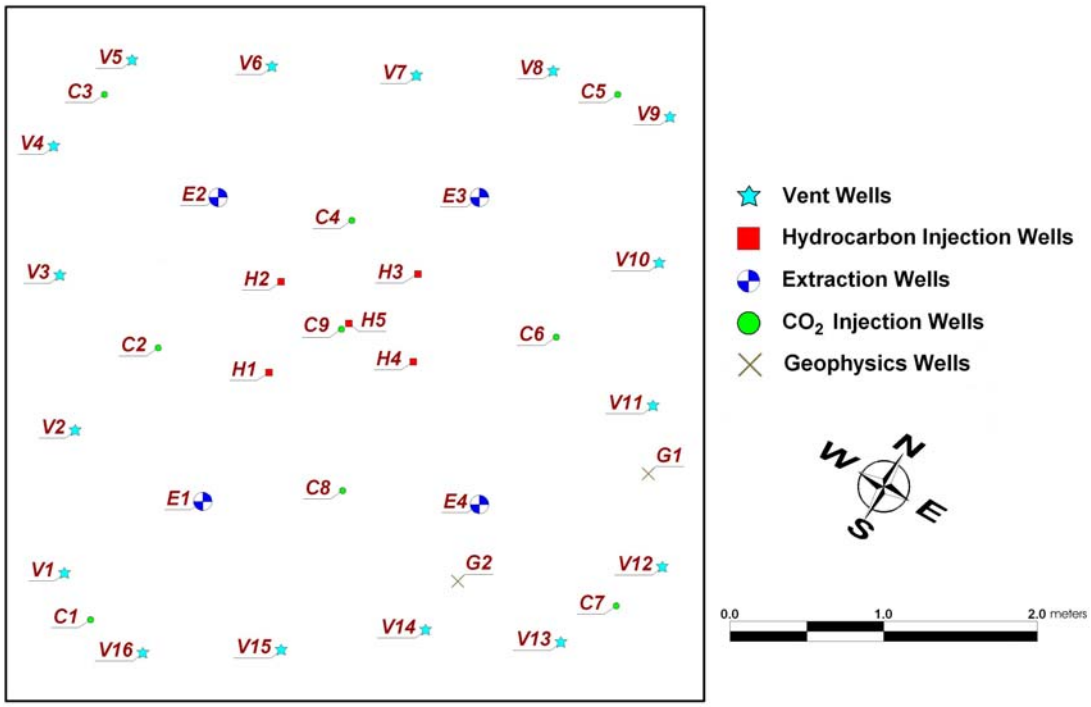

Figure 2.3. Well Locations.

2.1.2.2 Contaminant Injection Wells

Contaminant injection wells were installed in the central area of the cell ("H" wells in Figure 2.3). These wells were used to inject the hydrocarbon mixture into the subsurface. Five wells were installed but only four (H1, H2, H3 and H4) were used. These four wells were installed in a rectangular pattern, with approximately one meter between wells. The fifth well was used to measure water levels and was located in the middle of the rectangle formed by the other four wells. Each well was constructed of five cm diameter schedule 40 PVC well materials. The wells are four meters in length, the top 150 centimeters are riser pipe and the bottom 250 cm are slot 10 well screen (Figure 2.2).

2.1.2.3 Extraction Wells

The extraction wells were also installed in a rectangular arrangement but with approximately 2 meters between them. If the cell were to be divided up into quadrants, each extraction well would be near the centre of a quadrant. Each well was constructed of schedule 40 PVC well materials; three inch diameter during phase I and four inch diameter during phase II. The wells are four meters in length, the top 30 centimeters are riser pipe and the bottom 370 cm are slot 10 well screen (Figure 2). The wells were designed with long screens so that both water and air could be drawn into the well. Extraction wells are designated by the prefix E on all figures.

2.1.2.4 CO_2 Injection Wells

The CO_2 injection wells were installed in triangular configurations around extraction wells. The CO_2 injection wells are designated by the prefix C on all figures. These configurations were arranged so that CO_2 injection wells located between extraction wells could be used when either extraction well was being used (Figure 2.3). Each well was constructed of 2.5 cm diameter schedule 40 PVC well materials. The wells are three meters in length and made entirely of riser pipe (Figure 2.2).

For phase I, a CO_2 injection well screen was made by drilling sixteen 0.8 mm diameter holes in the riser pipe. Four holes were equally spaced around the circumference of the pipe in each of four rows, the bottom most row was 15 cm from the bottom of the well and there was approximately 5 cm between rows (Figure 2.4). For phase II the screen was made by drilling forty-eight 0.8 mm holes in six rows of eight equally spaced holes. Once again the bottom row was 15 cm from the bottom of the well and the rows were 15 cm apart. The approximate quantity and size of the holes was based on the testing by Doughty (2006). Field testing verified that these numbers of holes achieved the desired combination of water pressure and flow of seven liters per minute and sixty pounds per square inch respectively.

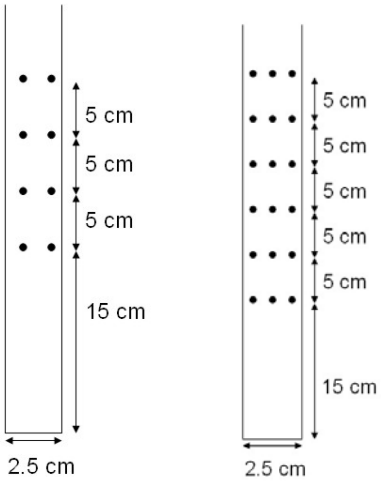

Figure 2.4. CO_2 injection point well for a) phase I; b) phase II.

2.1.2.5 Geophysics Access Tubes

Geophysics access tubes (G1 and G2) were installed in the E4 quadrant of the cell (Figure 2.3) so that cross-borehole ground penetrating radar (GPR) antennas could be lowered into the subsurface and a survey could be completed. Using the two access tubes (G1 and G2) and well H3 three geophysical cross sections could be completed. Each access tube was constructed of 5 cm diameter schedule 40 PVC riser pipe sealed at the bottom to prevent water or sand entry. The tubes were four meters in length.

2.1.3. Well Installation

The vent, hydrocarbon and phase one extraction wells were installed using a four inch inside diameter hollow stem auger. At the time of installation the layers of clay and geotextile had not yet been installed so the augers could drill from the ground surface to the desired depth. To allow well installation, a cap was placed on the bottom of the lead auger and drilling began. More augers were added above the lead auger as the drilling progressed until the desired depth was reached. At this point, the augers were lifted a few centimeters and the cap was dislodged from the lead auger. The well was then lowered into the hollow stem of the augers and the augers were pulled out leaving the well in the ground, the bottom of it resting on the cap.

The CO_2 injection wells (phases I and II) and the geophysics access tubes were installed by pushing a steel casing to the desired depth with a jackhammer (Figure 2.5). While the casing was being driven in, water was jetted into the casing to remove sediment from inside the casing. Once the casing was driven to the appropriate depth and the sand jetted out from the casing's interior, the well was inserted into the casing and pushed down until it sat at the desired depth. The casing was then removed by jacking it up, which allowed the sand to collapse around the well.

Figure 2.5. Photograph of use of jackhammer to push steel casing for installation of CO_2 injection wells.

During the experiment performed by Doughty (2006) the aquifer was excavated down to the water table near the CO_2 injection well and it was observed that most of the bubbles reaching the water surface were within a few centimeters of the well. This is partly due to the disturbed area around the injection well. In order to minimize this area of

disturbance, the inner diameter of the steel casing used was only approximately four millimeters greater than the outer diameter of the CO_2 injection well.

2.1.4. Bailing and Soil Vapour Extraction – Preliminary Phase

After the contaminant spill there was a layer of free phase NAPL on the water table in some areas of the cell and in several of the contaminant injection and extraction wells. Since the objective of this experiment was to test SWI's ability to remove residual NAPL from below the water table this free phase NAPL had to be removed. The first step was to remove as much as possible from the wells by bailing them with a commercial bailer. After each round of bailing the volume of NAPL removed from each of the wells was recorded. Several rounds were required because after the NAPL was removed from the well, NAPL from in the surrounding aquifer would flow into the well. Once significant volumes of NAPL were no longer entering the wells, the free phase NAPL in aquifer was targeted. In order to remove this free phase NAPL soil vapour extraction was used. To do this the phase I dual phase extraction system (Section 2.1.5) was used but the extraction hose was positioned at the top of the well so that only vapour was removed from the cell. The contaminant concentrations in the extracted air were monitored by the photo-ionization detector (PID) and vapour samples were taken to be analyzed by gas chromatograph in Waterloo. The extraction rate was also monitored so that the mass removed by SVE could be calculated. Once the contaminant concentrations were approaching non-detect the system was shut down and phase I could begin.

2.1.5. Dual Phase Extraction System – Phase I

The dual phase extraction system used in phase I (Figure 2.6) removes vapour, water and NAPL (if present) from one of the 7.5 cm ID extraction wells through a 2.5 cm ID hose that is inserted into the well and positioned just above the static water table. It was provided as a unit by SCG Industries of Saint John, New Brunswick who also set up the system. An adapter at the top of the well provides a seal between the hose and the well head maintaining the applied vacuum (Figure 2.7). The 2.5 cm ID hose is connected to a 7.5 cm ID hose that has a knockout canister attached that allows the collection of water samples. From there the gas and water flow into a liquid gas separator which separates the liquid (water, dissolved NAPL, non-volatile free phase NAPL) from the gas (air, CO_2 and volatilized NAPL).

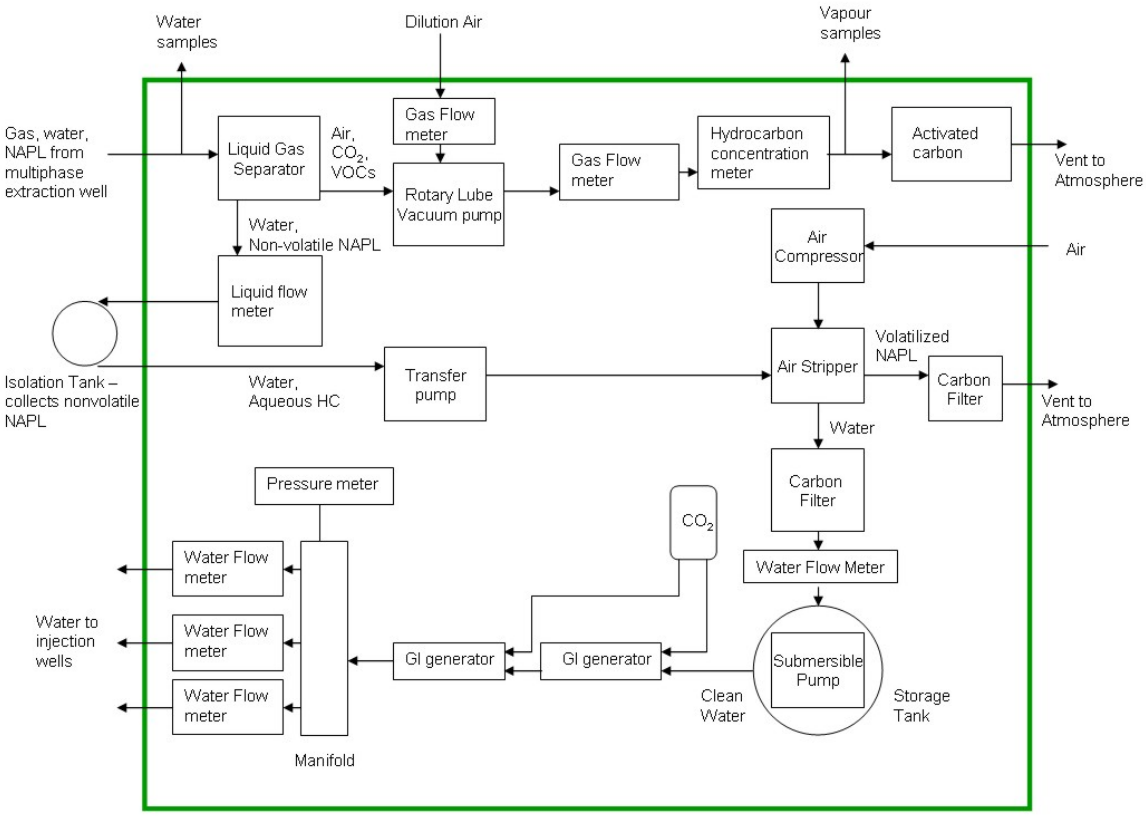

Figure 2.6 Flow diagram of the dual phase extraction (phase I) and gas infusion injection system.

Figure 2.7 Photograph of well head adapter with dual-phase extraction hose.

In order for the vacuum pump to maintain the desired vacuum in the cell, additional air must be drawn into the pump from the atmosphere. The flow rate of this dilution air is metered before it arrives at the pump. After the gas from the cell mixes with the dilution air in the pump it flows through a four inch ID PVC pipe past a flow meter, a photo-ionization detector (PID) and a gas sampling port. At the end of this pipe is a container containing 180 kg of activated carbon. After passing through this activated carbon filter, the clean air is discharged through a four inch ID PVC pipe to the atmosphere.

Liquid collects in a chamber attached to the liquid gas separator and once a certain volume has collected the liquid is pumped through a three inch ID hose past a liquid flow meter and into an isolation tank where any LNAPL present will float to the top where it can be measured and collected. Once the liquid in the tank nears the top a pump is activated and liquid is removed from the tank through a three inch ID hose attached to the tank near its bottom. The water is then passed through an air stripper where any dissolved hydrocarbons are transferred to the vapour phase.

The air added by the stripper and any volatilized hydrocarbons are passed through an activated carbon filter before being vented to the atmosphere. After passing through the air stripper the water flows through two activated carbon filters attached in series before flowing through a flow meter and into the large water storage tank.

2.1.6. Dual Phase Extraction System – Phase II

The dual phase extraction system used in phase II (Figure 2.8) does essentially the same functions that the phase I system did, but was assembled on site. It proved to be more efficient than the phase I system and less prone to mechanical break-down. Since very little mass was removed in the aqueous phase in phase I, a water sampling apparatus was not included in the design. In addition, the activated carbon analysis did not provide good quality data during phase I (Section 3.2.3) so activated carbon filters were not used in phase II. The major drawback of this system is the drawdown created around the extraction well by the submersible pump. This drawdown cone may have exposed residual NAPL to air flow resulting in its removal by volatilization which is not the removal mechanism we are evaluating. However, soil sampling between phase I and phase II indicated that there is little NAPL remaining near extraction wells (section 3.2.4.1) so it has been assumed that no significant contaminant mass is removed by this mechanism.

In this system the water and vapour extraction systems are separate. An adapter at the top of the well provides a seal between water extraction hose and the well head maintaining the applied vacuum. A 2.5 cm ID water extraction hose runs from a submersible pump, through the adapter on top of the well to two filters connected in series. These filters (30 μm and 5 μm) remove sand and silt. They were primarily used in the first half an hour after the pump started up. After passing through the filters the water runs through a flow meter and into the storage tank.

The vapour is extracted by a blower that is attached to the well head adapter by a three inch ID hose. The vapour moves form the cell, up the well and then through the adapter, three inch hose and into the blower. On the other side of the blower, the vapour moves through a short hose and then a short length of three inch PVC pipe before discharging to the atmosphere. Attached to the PVC pipe is a thermometer, a manometer, and vapour sampling port while a PID sat right at the end of the pipe.

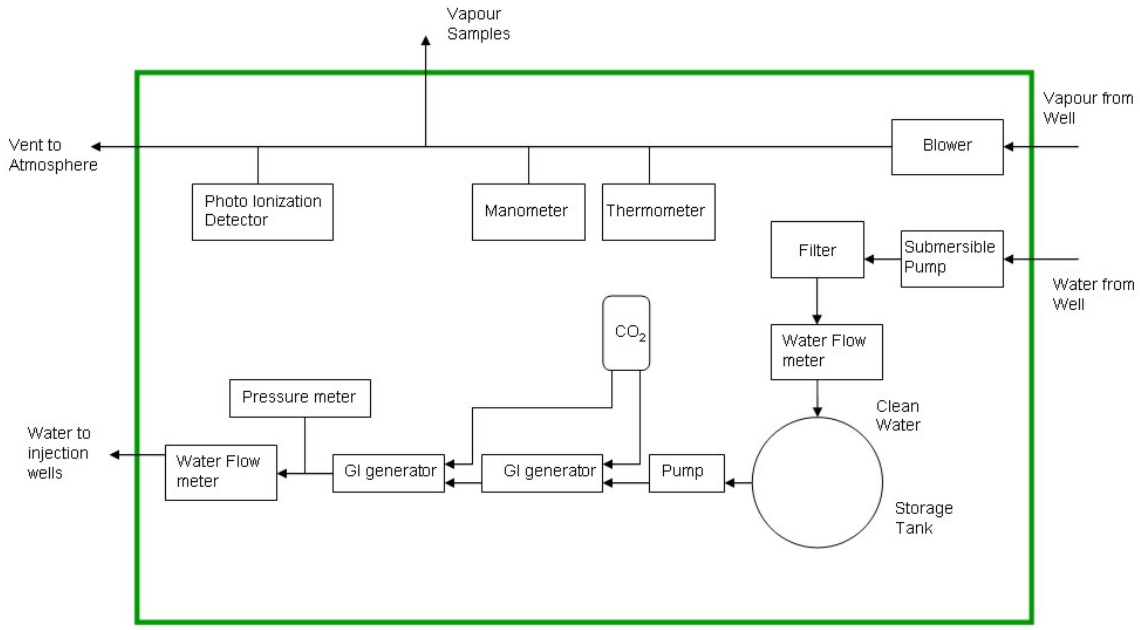

Figure 2.8. Flow diagram of the dual phase extraction (phase II) and gas infusion system.

2.1.7. Gas InFusion System

A submersible pump in the water storage tank (phase I) or a rotary pump (phase II) provided water to the first of two gas infusion (GI) generators connected in series. A large CO_2 tank provides pressurized CO_2 gas to each of the GI generators. Water saturated with CO_2 under pressure flows from the first GI generator to the second where more CO_2 is added and the desired level of saturation is reached. The pressurized, CO_2-saturated water flows from the second GI generator through 2.5 cm hose to a manifold that has a pressure meter attached. During phase I the flow of water split at the manifold and then flows to the injection well heads. After splitting, each of the streams passes through a water flow meter and then through a two cm inch before reaching one of the well heads (Figure 2.9). During phase II only one injection well is used so the manifold does not split the flow of water. After the manifold the water passes through a water flow meter and then through a two cm hose before reaching the well head.

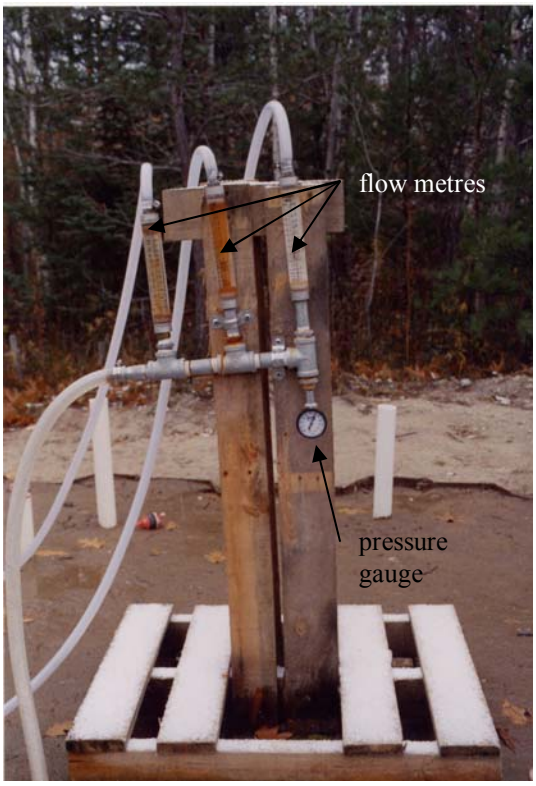

Figure 2.9. Photograph of injection manifold (phase I).

2.2. Contaminant Emplacement

The goal of the contaminant emplacement was to produce a source zone at residual concentrations below the water table. The spill consisted of 200 liters of hydrocarbons: 80 liters of pentane, 80 liters of hexane and 40 liters of Soltrol 130. The pentane and hexane were chosen to be representative of volatile hydrocarbons while Soltrol 130 is representative of nonvolatile hydrocarbons. Soltrol 130 is a mixture of decane, undecane, dodecane and tridecane (Chevron Phillips, 2002). All of the hydrocarbons have very low solubility (Table 2.1) in water and will exist as a non aqueous phase liquid (NAPL). The hydrocarbons are common in commercial gasoline, making this emplacement fairly representative of a residual gasoline source (Kreamer & Stetzenbach, 1990).

Compound	Aqueous Solubility* (mg/L)
Pentane	38.5
Hexane	12.3
Decane	0.052
Undecane	0.0042
Dodecane	0.0037

Table 2.1 The aqueous solubility of compounds in simulated gasoline NAPL mixture. *(Mackay et al, 1992)

In order to emplace the gasoline below the water table at residual concentrations the water table was lowered, the contaminants injected and allowed to flow across the lowered water table. Then the water able was allowed to rise "smearing" the contaminants across the aquifer at residual concentration. This method simulates the effect of seasonal water table fluctuations which can cause the emplacement of residual sources of gasoline constituents at contaminated sites (Ryan & Dhir, 1993). This method was based upon the work of Barbaro (1999) and Oliveira (1997) both of whom emplaced similar source zones at Borden.

Oliveira (1997) found that gasoline residuals occupied 12% of the pore volume of Borden sand. Mackay et al., 1986 determined that the porosity of Borden sand is 0.33, so the residuals would have occupied 4% of the total volume. If it is assumed that the injected contaminants will spread laterally to an extent of 10 m^2, which is a reasonable assumption based upon Oliveira (1997), then the drawdown required was calculated as follows. The height required would be the volume of NAPL (0.2 m^3) divided by the lateral extent (10 m^2) divided by the volume fraction occupied by residuals (0.04). This calculation gives a height of 0.5 m over which the NAPL would have to be smeared. However, the presence of trapped gas in the area of the spill as the water table rises would result in lower residual NAPL saturation than the value calculated above. So as a factor of safety, the water table was to be drawn down 1.0 m to allow for this and other factors that may arise in the field.

In order to keep the injected contaminants from pooling in the well and forming a layer of free product, packers were used to isolate a 10 cm vertical section of the injection well

through which the contaminants were injected (Figure 2.10). The bottom of this section was 30 cm above the elevation of the water table in the well because that is the height of the capillary fringe in Borden sand (Nwankor et al, 1984). The injection was above the capillary fringe so that there was as much air filled porosity as possible.

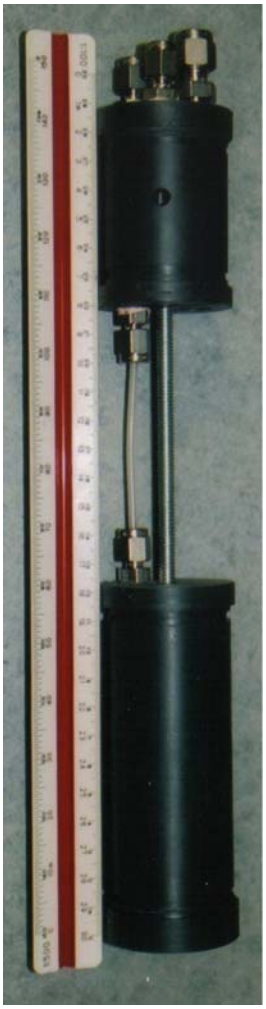

Figure 2.10. Packer, before placement of rubber sleeves.

The initial plan was for the injection to occur over two days. This plan required that the cell be completely hydraulically isolated from the surrounding aquifer. Unfortunately that is not the case and the only way to draw down the water table sufficiently was by continuously withdrawing water. As a result, drawdown cones were created around the wells used for extraction and the resulting residual source zone will not be as evenly distributed as hoped.

The only wells suitable for extracting water are the extraction wells so water was continuously extracted from wells E-1 to E-4 (Figure 2.11) during the gasoline injection. One pump was used to extract from all four wells by splitting the intake, and then splitting each of those lines (Figure 2.12). The hose from each well had a valve which allowed the flow to be regulated and the draw down in each well equalized.

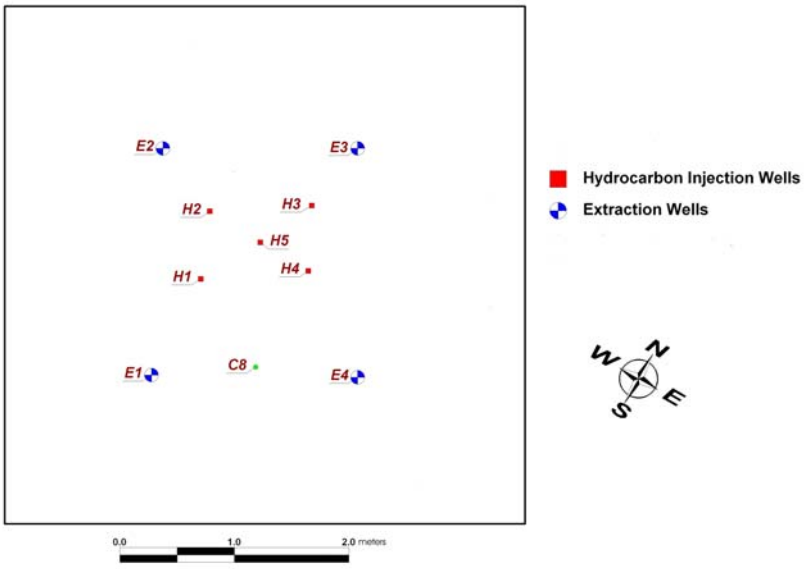

Figure 2.11. Location of hydrocarbon injection wells and extraction wells.

Figure 2.12. Photograph of injection infrastructure, showing both the contaminant injection system and the groundwater extraction system.

The injection occurred into two wells simultaneously. The contaminants were stored in two large high density polyethylene garbage containers that had one cm connections screwed into the bottom of the container. The connections were sealed with hydrocarbon resistant sealant. One meter of one cm ID hose was attached to each connection at the bottom of the container. This length of hose had a valve near the other end that allowed the flow to be controlled. An adapter connected the one cm hose from the garbage container to a three mm ID hose that ran to the top of the packer. This allowed any container to be connected to any packer. An in-line flow meter could also the connected between the two hoses to measure flow rates.

The contaminant mixture was created on-site by combining 40 liters of pentane (EMD Chemicals), 40 liters of hexane (EMD Chemicals) and 20 liters of Soltrol 130 (Chempoint.com) with Oil Red O (Sigma-Aldrich Inc.), a non-volatile organic soluble dye (Figure 2.13). Oil Red O has a negligible effect on contaminant and mass transfer properties (Wilkins et al, 1995). The components were combined in the container and then manually mixed until the dye was completely dissolved. During the injection process the lids were kept on the containers to minimize volatilization.

Figure 2.13. Photograph of the dyed contaminant mixture in high density polyethylene container prior to injection.

Once the draw down was stabilized at 2.95 meters below ground surface (mbgs) the contaminant injection began. In the first stage, fifty liters of the hydrocarbon mixture was fed by gravity into H1 and H3 (25 liters per well) at approximately 700 ml/min per well. In the second stage, fifty liters was injected into H2 and H4 by gravity feed at ~700 ml/min.

At the beginning of stage one the total water withdrawal rate from all four wells was 16.2 l/min. As the hydrocarbon mixture was added the withdrawal rate had to be decreased a few times to keep the level of drawdown constant so that by the end of the second stage it was 11.7 l/min.

For the third stage, the injection was into H1 and H3 again. Before the injection began it was discovered that the rubber on the packers had burst. So from that point on the injection was through the packer apparatus but the packer was not inflated. Between the second and third stages the packer placed into H1 became clogged so no gasoline was injected into H1 during round three. Injection into H3 was at approximately the same rate as in round one (~650 ml/min).

The final stage began with injection into H4. Once that injection was progressing, the packer from H2 was placed into H1 and injection into H1 began. Injection into H4 finished after the expected duration, followed by the injection into H1. Finally the packer from H1 was returned to H2 and the final 25 liters was injected. The flow rates were not calculated during the final stages but they did not take significantly longer than the earlier stages.

After the injection was completed, the extraction from the E- wells was stopped. However, to slow the recovery a submersible pump was placed into H5 and water was extracted at approximately seven liters per minute.

Despite some difficulties, fifty liters of the contaminant mixture was injected into each of the four hydrocarbon injection wells. Unfortunately an accumulation of free product in each of the hydrocarbon injection wells occurred. In addition, the drawdown cones in the extraction wells resulted in the migration of free product into well E3 during the injection and into E1 and E2 by the next day.

2.3. Data Collection Methods

2.3.1. Vapour Sampling

The effluent vapour was sampled by creating a "T" joint on the conduit between the rotary lube vacuum pump and the activated carbon filter (Figure 2.14). During phase II the T joint was between the blower and the end of the pipe where the vapour is discharged to the atmosphere. At this joint 4 mm ID copper tubing was attached to the PVC pipe. A ball valve controlled the amount of flow (if any) that was diverted to the sampling apparatus. The copper tubing was connected to a 1 mm Teflon tube which was in turn attached to a 1 mm needle.

Vapour samples were collected in 40 ml VOA vials (Figure 2.14) by water displacement as follows. Immediately before sampling these vials were submerged in distilled water in a plastic container. While submerged they were filled with water and then positioned vertically with the opening at the bottom (Figure 2.15). The vials were then raised until the rim of the vials was 1 mm below the water level in the container. At this point the vial is filled with water but most of it was above the water level.

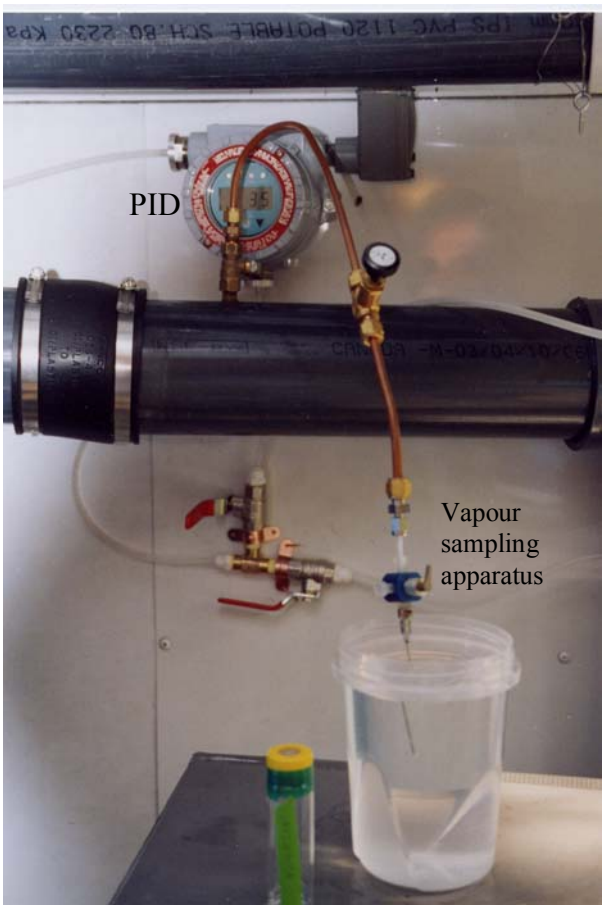

Figure 2.14. Photograph of vapour sampling apparatus and PID.

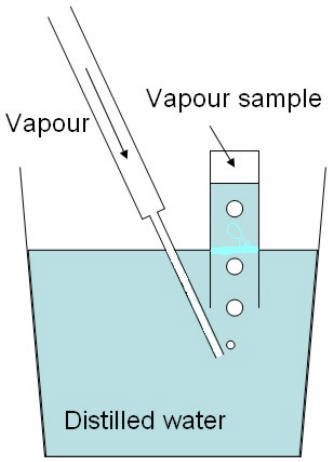

Figure 2.15. Vapour sampling method.

The ball valve was then opened so that vapour was flowing through the tubing and out the needle. The end of the needle was then submerged in the water and maneuvered so that the bubbles of vapour exiting the end of the needle would enter the vial. Once the bubbles entered the vial they rose upwards, displacing the distilled water. Once water

was entirely displaced by the vapour, usually after 10 seconds, the vial was sealed underwater with a plastic cap containing a Teflon septum. The ball valve was then closed and the needle removed from the water.

Samples were taken in triplicate during phase I and in duplicate during phase II. The vials were transported to Waterloo for analysis within seventy two hours.

2.3.2. Water Sampling

To sample the extracted water a ball valve above the knockout can was opened and the can was allowed to fill with water (Figure 2.16). This usually took 5 seconds. The can was then removed and a water sample taken by immersing a forty mL VOA vial in the water and quickly capping the vial with a plastic cap and Teflon septum. Samples were taken in duplicate. The vials were transported to Waterloo for analysis within seventy two hours.

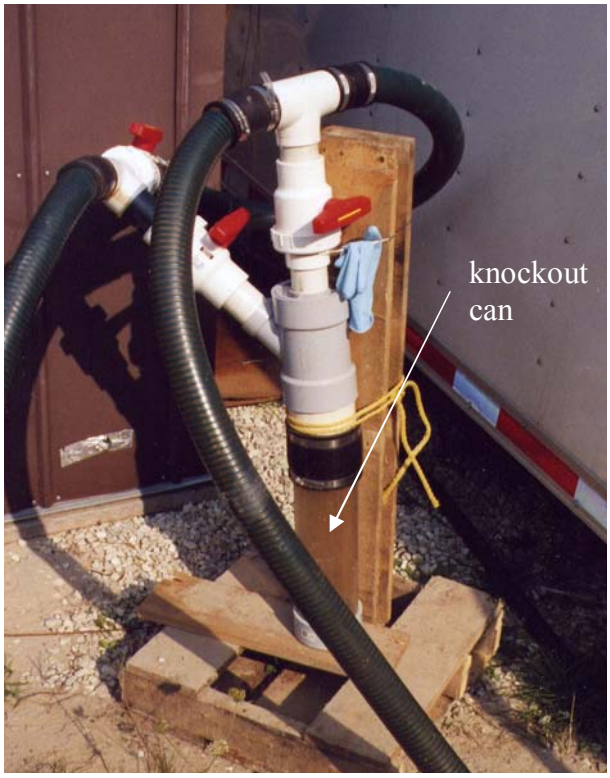

Figure 2.16. Photograph of water sampling apparatus.

2.3.3. Activated Carbon

In order to sample the activated carbon, it was removed from the filter box and placed in twenty liter high density polyethylene containers. To homogenize the activated carbon, the carbon from two of the containers (forty liters) was placed into a cement mixer (Figure 2.17) and mixed for forty-five minutes. The opening of the mixer was covered

with plastic to minimize the amount of fine carbon from escaping. Once the mixer had stopped, five grab samples were taken from the mass of carbon in the mixer. Samples were taken by filling 40 mL VOA vials with carbon and capping the vial with a plastic lid and Teflon lined septum. That day the samples were transported to Waterloo. The remaining carbon was put back into the containers, sealed and stored for potential future analysis.

Figure 2.17. Photograph of cement mixer used to homogenize activated carbon and high density polyethylene containers filled with activated carbon.

2.3.4. Soil Sampling

Soil cores were taken to determine the concentration of gasoline components remaining in the cell after phase I of remediation. The method of Starr and Ingleton (1992) was used to collect the soil cores. This method involves driving the sampler through the sample interval (the top of the sand to ~ 310 cmbgs) and then withdrawing the sampler with the sample inside. The sampler was driven with a jackhammer and withdrawn with a slip ring and jack.

Once the core had been recovered it was cut into two or three equal sections which varied in length from 45 to 88 cm depending on the total length of the recovered core. During the sampling following phase I, a four cm wide strip was longitudinally removed from the wall of the first section of core to allow sampling immediately (Figure 2.18). During the sampling following phase II, two cm diameter holes were drilled in the wall immediately before sampling and samples were removed through these holes (Figure 2.19). During both sampling events low density polyethylene caps were placed on the ends of the other two sections to minimize volatilization while the first section was sampled.

Figure 2.18. Photograph of soil sampling procedure (phase I).

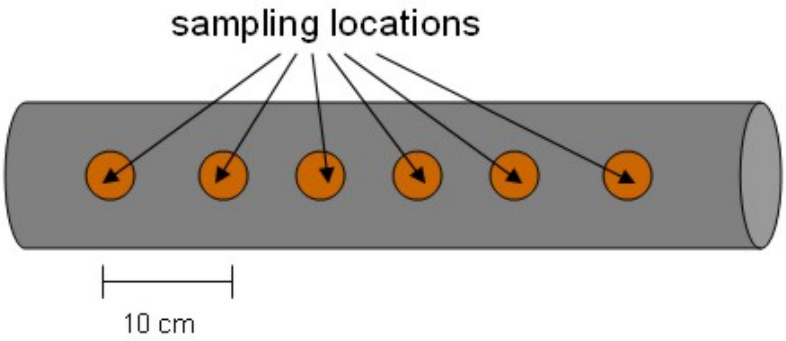

Figure 2.19. Diagram of sampling locations along the soil cores taken after phase II.

Samples were taken from the core using methods similar to Hewitt's (1996) and Schumacher and Minnich's (2000). A three ml plastic syringe with the tip removed was inserted into the exposed area of the soil core until there was two ml of soil in the syringe (Figure 2.18). The syringe was then removed with the sub-sample intact in the barrel. The syringe containing the sub-sample was then inserted into the mouth of a 40 ml VOA vial that had been pre-filled with a known mass (eight grams) of either water or carbon disulphide. Care was taken not to get any soil on the vial rim during this transfer to allow for a tight seal. The plunger was then depressed, and the sub-sample deposited into the vial. Once the sub-sample was in the vial a cap with a Teflon septum was sealed to the rim of the vial using a crimper.

This procedure was completed as quickly as possible to minimize volatilization losses. Three people were involved in the sampling so that the whole procedure took less than

five minutes per section of core. The samples were immediately brought to the lab in Waterloo where they were weighed to determine the sub-sample mass and prepared for analysis.

2.3.5. Data Logging

In phase I several operational parameters were logged on a laptop computer at the site. These parameters were: pressure differential across the air outlet (inches of water column), pressure differential across the dilution air inlet (inches of water column), system vacuum (inches of mercury) and photo-ionization detector (RAEGuard, RAE Systems Inc.) reading (ppm of isobutylene equivalents), water injection flow (gallons/minute) and water system discharge flow (gallons/minute). Unfortunately the water flow sensors were calibrated at incorrect ranges and did not provide any useful data. The sampling frequency varied between once every four seconds to once every ten seconds. This sampling frequency provided an unmanageable amount of data so it was pared down to one sample every minute.

In addition, several parameters were manually recorded every hour or two, usually corresponding to a sampling event, and included activated carbon filter back pressure (inches of water), pump temperature (degrees C), air stripper back pressure (inches of water), outside temperature (degrees C), CO_2 tank pressure differential (inches of water), GI generator water and CO_2 pressure (pounds per square inch (psi)), temperature inside GI generator shed (degrees Celsius) and injection flow rate (liters per minute) and pressure (psi).

In phase II the only parameter that was automatically data logged was the photo-ionization detector (MultiRAE Plus, RAE Systems, Inc.) reading (ppm of isobutylene equivalents). It was logged by the PID at an interval of once every minute. Since the extraction system was different for phase II, different parameters were manually logged, but the interval was still once every hour or two, usually at the same time as a sampling event. In this phase the parameters logged were injection flow rate (liters per minute) and pressure (psi), height of water in storage tank (cm), pressure differential across the exhaust air outlet (inches of water column), exhaust air outlet temperature (degrees C), CO_2 tank pressure differential (inches of water), GI generator water and CO_2 pressure (psi), water extraction rate (litres per minute), water filter back pressure (psi) and water table depth in well E1 (centimeters below top of casing). The pressure differential across the exhaust air outlet was measured with a Series 475 Mark III digital manometer from Dwyer Instruments Inc.

2.4. Geophysics

Cross borehole ground-penetrating radar (GPR) surveys were carried out in quadrant 4 of the cell to determine the water content of the aquifer before and during SWI. During each survey two methods were used, zero offset profiles (ZOPs) and multiple offset gathers (MOGs). The principle advantage of MOGs is that they provide two dimensional data across a plane between the two wells used (depth and distance) while the data provided by ZOPs is only one dimensional (depth). However, ZOPs take considerably less time to complete. The objective of the surveys was to determine if the water content (and therefore the air content) changes during SWI. On each of the two days, surveys were completed between G1-G2, S4-G1 and S4-G2 (Figure 19). Appendix A contains full details on the methodology.

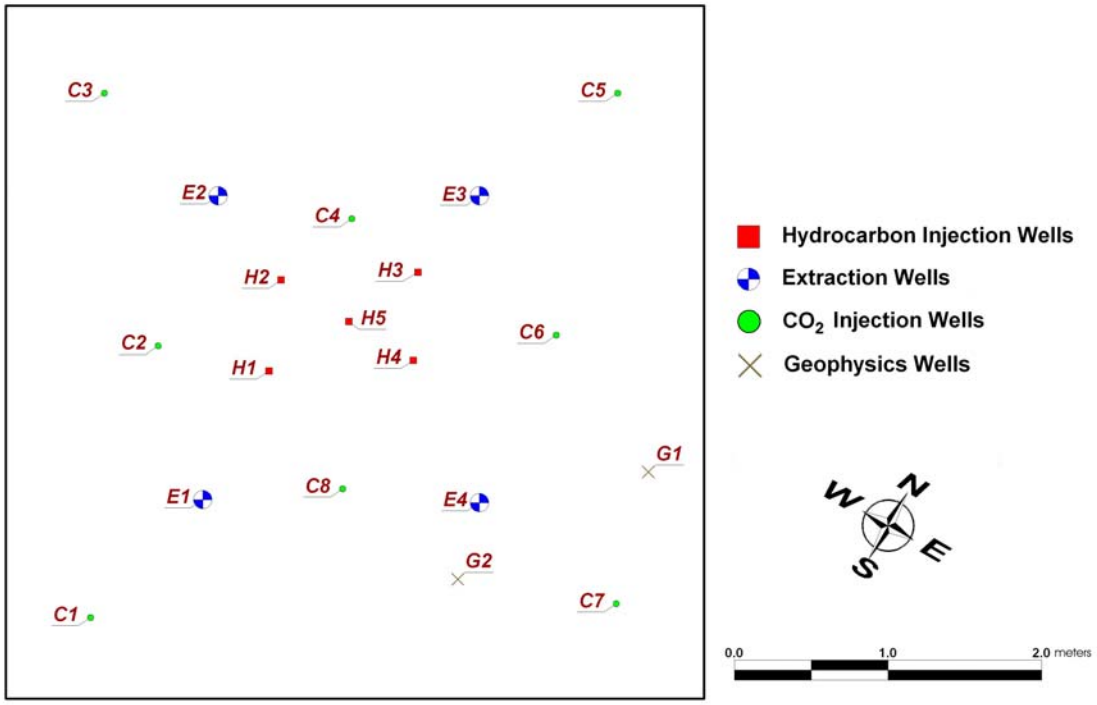

Figure 2.20. Location of geophysical access tubes.

2.5. Modeling

Visual MODFLOW was used to model the flow in the cell under a) phase I conditions and b) conditions for several potential phase II scenarios. Aquifer properties used are given in Table 2.2.

Parameter	Value	Source
Horizontal Hydraulic Conductivity	$7x10^{-5}$ m/s	MacKay et al, 1986
Vertical Hydraulic Conductivity	$7x10^{-6}$ m/s	
Specific Storage	$3.25x10^{-4}$ m^{-1}	Nwankwor et al, 1984
Specific Yield	0.3	Nwankwor et al, 1984
Effective Porosity	0.3	MacKay et al, 1986
Injection Rate (per well)	8.64 m^3/day (past scenarios) 6.48 m^3/day (box scenarios) 12.96 m^3/day (sweeping scenarios)	

Table 2.2. Values used in MODFLOW model.

Simulations were run at steady state and to eight hours of operation for all of the scenarios. Eight hours was chosen as the amount of time over which significant amounts of CO_2 would evolve in the aquifer. Simulations were run for conditions during extraction from each of the extraction wells used in phase I. The simulations for potential phase II scenarios were grouped into two groups, box scenarios and sweep scenarios. Box scenarios involved either, injecting into a four outer injection wells and extracting from one well in the centre, or injecting into one well in the centre and extracting from one of the outer extraction wells. Sweep scenarios involved injecting on one side of the cell and extracting from the other side. The exact well configurations are presented in the results section.

Since water table levels were not recorded, it was not possible to calibrate the model. However, the aquifer parameters at Borden are quite well defined as a result of the many studies performed there.

2.6. Laboratory Analysis

All of the laboratory analysis of samples collected in the field was conducted at the Organic Geochemistry Lab at the University of Waterloo. The analysis methodology for pentane and hexane in vapour is presented in Appendix J, the methodology for pentane and hexane in water is in Appendix K, the methodology for Soltrol 130 in water is in Appendix L and the methodology for pentane and hexane in soil samples is in Appendix M. Appendix N contains the methodology for desorbing and analyzing pentane and hexane from activated carbon.

3. Results

3.1. Preliminary Phase

The presence of a layer of free phase non-aqueous phase liquid (NAPL) on the water table after the injection of the gasoline contaminants necessitated an attempt to remove as much of it as possible. The purpose of this entire experiment was to evaluate the performance of the remediation of a residual source so removing any free phase NAPL before the remediation began was necessary. For the purposes of the analysis in the following sections, the initial amount of NAPL is considered to be the amount spilled (200 liters) minus the amount removed by bailing and soil vapour extraction. The original amount is the amount spilled, 200 liters.

3.1.1. Bailing

After the contaminant injection, there was a layer of free phase NAPL in several of the wells. A bailer was used on several occasions to remove free product from the wells. Repeating the process several times was necessary because after a well was bailed free product in the surrounding soil would flow into the well. Table 3.1 presents the results of these bailing sessions.

Well	Date				Total
	Sept. 7	Sept. 8	Sept. 19	Sept. 24	
E1	125	80	200	40	445
E2	1355	225	900	220	2700
E3	490	70		10	570
H1	820	15	150	50	1035
H2	450	10		30	490
H3	310	35		50	395
H4	400	10		20	430
Total	3950	445	1250	420	6065

Table 3.1 Volume of NAPL (mL) removed by bailing from each well during the preliminary phase.

The bailing removed a total of 6065 ml of NAPL from the cell. If it is assumed that the NAPL was still 40% pentane, 40% hexane and 20% Soltrol by volume, and there is no reason to believe it had changed significantly, then 2426 ml of each pentane and hexane were removed. Given densities of 0.626 g/ml and 0.658 g/ml for pentane and hexane respectively; the baling removed 1.52 kg of pentane and 1.60 kg of hexane.

3.1.2. Soil Vapour Extraction

Once bailing was no longer producing significant volumes of NAPL, soil vapour extraction (SVE) was used in an attempt to remove as much of the remaining free phase NAPL as possible. Figure 3.1 shows the concentration of both pentane and hexane over time based on vapour samples that were analyzed by gas chromatograph (GC) in the laboratory and based on the photo-ionization detector (PID) readings.

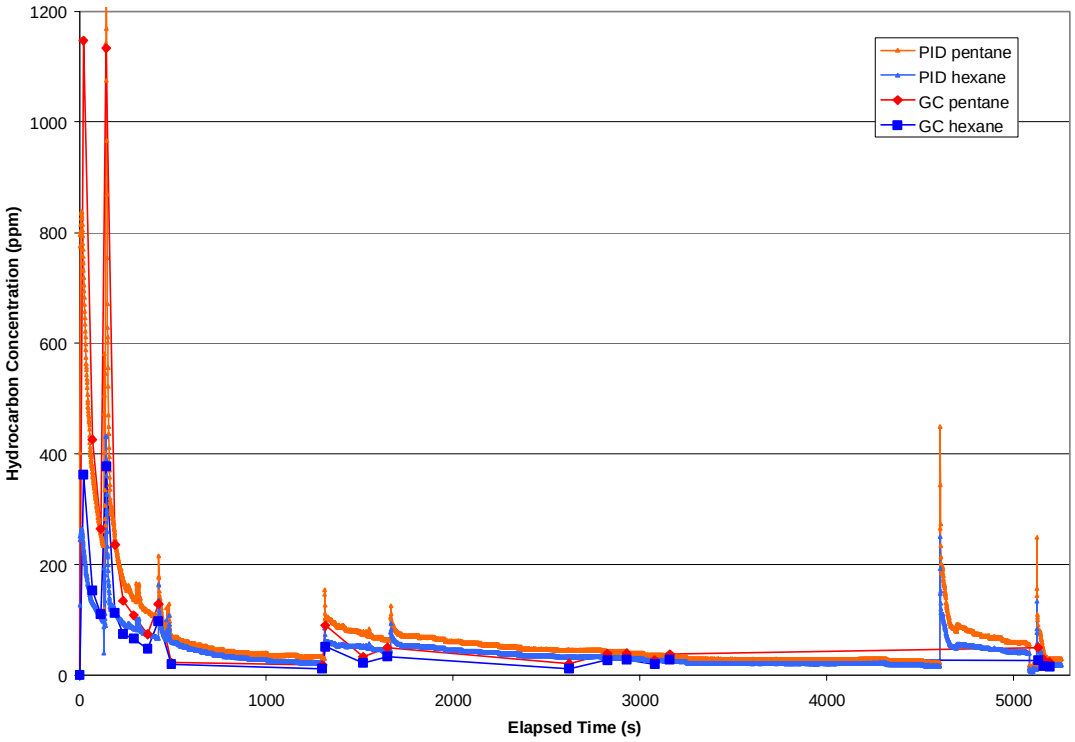

Figure 3.1 Concentration of pentane and hexane versus time during SVE in the preliminary phase.

The concentrations are very high at the beginning of the soil vapour extraction when the air moving through the cell contacts and volatilizes easily accessible NAPL. The concentrations quickly taper off and then decrease slightly over time until the system was shut down. However, when a new extraction well is used the concentrations spike upwards initially before tapering off in a similar manner for each well. There is good agreement between the lab-analyzed samples and the PID, especially considering that the vapour sampling protocol was still being established during this preliminary phase. Due to the variation in vapour sampling protocols, the PID concentrations are assumed to be the most representative. Some samples, including those taken at ~400, ~1400 and ~2600 minutes are anomalously low, potentially due to losses during sampling, shipping or storage of these highly volatile compounds.

The total mass removed was determined to be 5.9 kg of pentane and 4.3 kg of hexane (Figure 3.2). The shape of the contaminant concentration curves is consistent with the

results from SVE lab studies (Baehr et al, 1989) and implementation at contaminated sites (Mills et al, 1996). After three and a half days of SVE operation it was decided that most of the easily accessible free phase NAPL mass had been removed from the cell. Since most of the free phase NAPL had been removed and due to time constraints it was decided to stop the SVE phase after three and a half days of operational time.

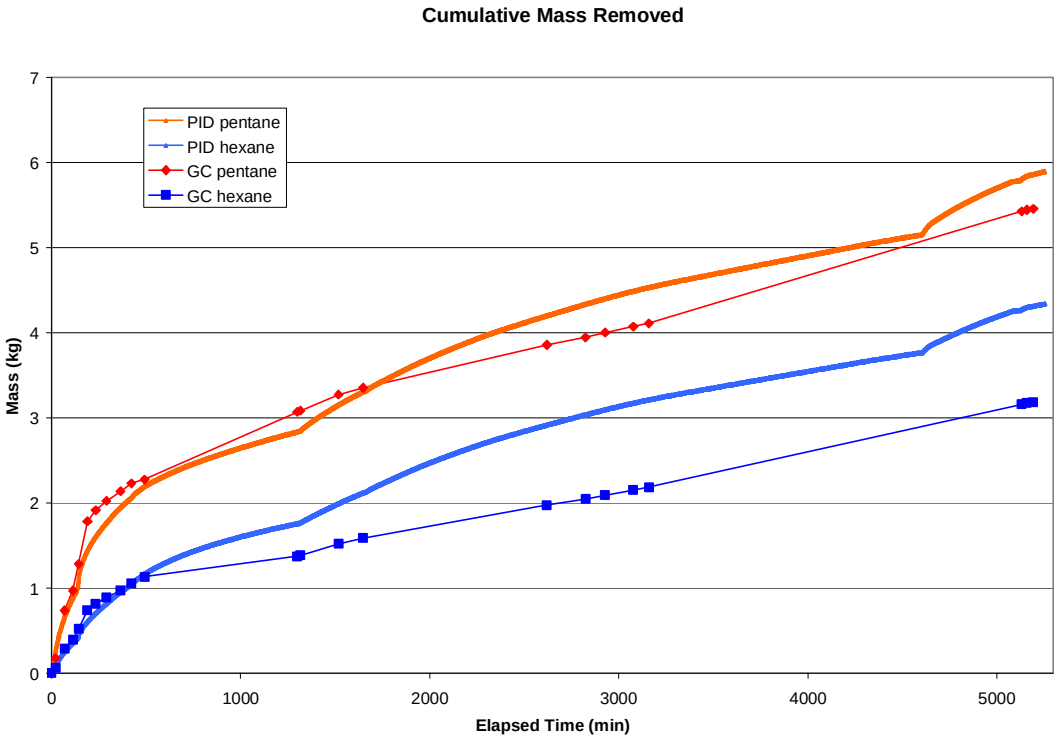

Figure 3.2. Cumulative mass of pentane and hexane removed over time during the preliminary stage.

3.2. Phase I

3.2.1. Vapour Sampling and PID

Based on the work of Li (2004) it was expected that the majority of the pentane and hexane removed would be in the vapour phase. As a result, samples were taken of the vapour extracted from the cell and submitted to the lab in Waterloo for analysis and a photo-ionization detector continuously monitored the concentration of volatile organic compounds in the vapour stream. The results of these two monitoring methods are presented in this section.

3.2.1.1 E2

Since more than half of the mass removed by bailing was removed from the wells in quadrant two (H2 and E2) it was decided to begin the experiment in that quadrant. Remediating quadrant two involves injecting water from the GIs through wells C2, C3 and C4 while extracting from well E2 (Figure 3.3).

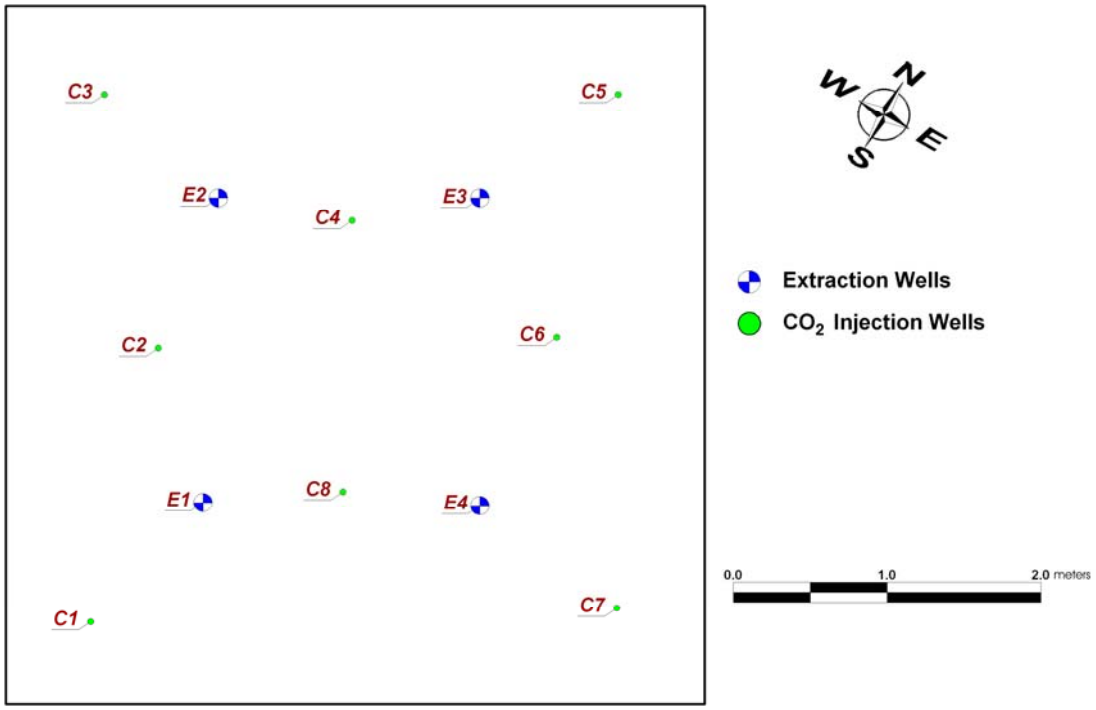

Figure 3.3. Site layout showing extraction wells and CO_2 injection wells.

Quadrant two was remediated for 128 hours (5.3 days) of total operation time. However there were several interruptions in the remediation due to mechanical and electrical problems. The occurrence of these stops and starts is apparent in Figure 3.4. Immediately after start-up the concentrations are at their highest and tail off as time progresses. The times that the system was operational are displayed in Figure 3.5. The spikes likely occur because the CO_2 bubbles continue to migrate upwards through the aquifer volatilizing NAPL ganglia after the system has been shut-off. During the time that the system is shut-off CO_2 and volatilized hydrocarbons will collect at the top of the cell and when the system is restarted this vapour with elevated hydrocarbon concentrations will be removed first.

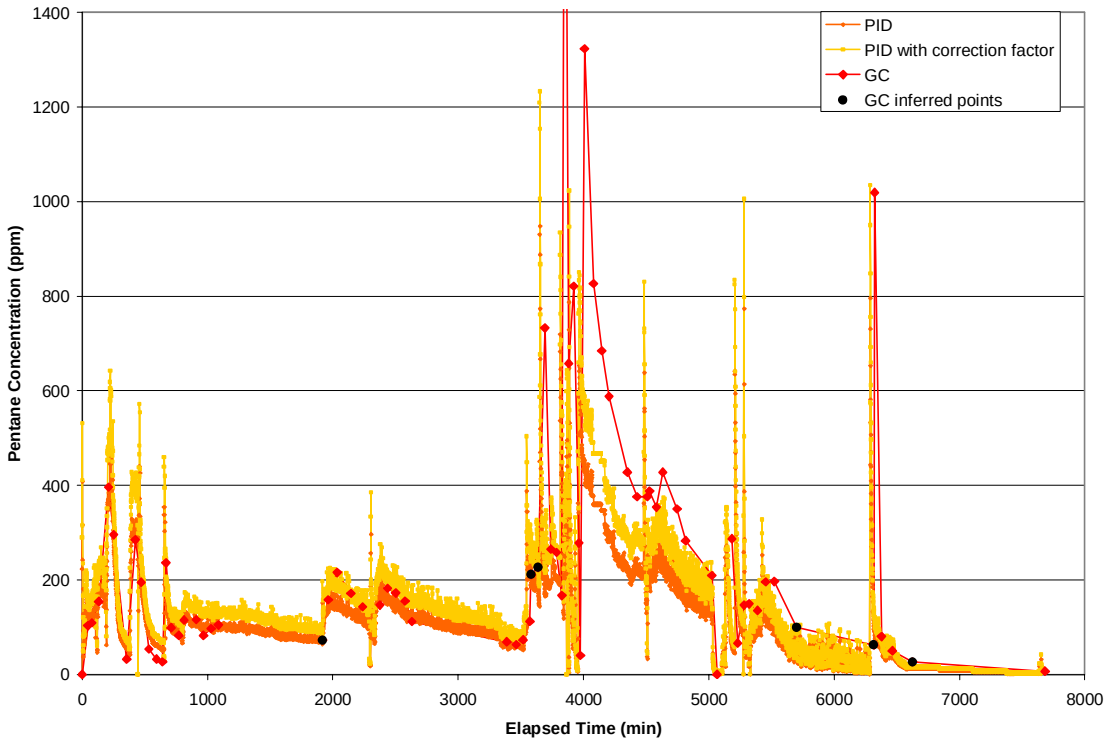

Figure 3.4. Pentane and hexane vapour concentrations in the air extracted from E2 over time during phase I.

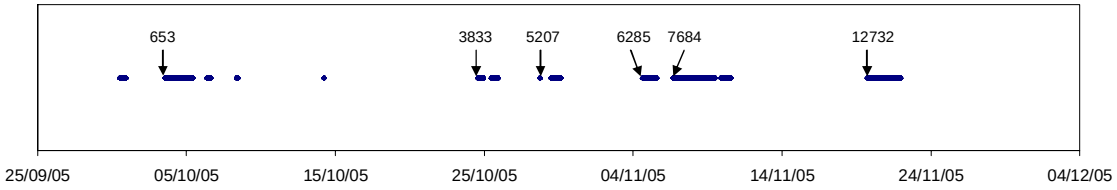

Figure 3.5. The intervals over which the system was operational (indicated by blue dots) during phase I. The numbers on the figure indicate the elapsed operational time (in minutes) at that point.

The PID results did not exactly match the results from the samples analyzed by the GC in the lab. The trends match, but the values are not the same. This may be due to several factors. The PID reading is affected by temperature, humidity and dirt on to the sensor. However, the vapour temperature and humidity were not known for that point in the system so accurate correction factors could not be used. All of the factors will cause the PID to read lower than the actual value (Haag & Wrenn, 2002). To test the response of the PID, a canister containing a known concentration of isobutylene (102 ppm) was also connected to the PID and the PID's response was measured (Figure 3.6). After the PID reading had stabilized, the isobutylene canister was removed and a canister containing a known concentration of hexane (404 ppm) was connected (Figure 3.6). The isobutylene was connected from 2.3 minutes to 9.7 minutes while the hexane was connected from 10.3 to 14 minutes. The isobutylene response was higher than it should have been; the PID was calibrated to isobutylene so the PID reading should have been 102 as opposed to

114 which was the actual reading. The hexane response on the other hand was lower than it should have been. 404 ppm of hexane should give a reading of 94 based on the correction factor of 4.3 provided in Haag & Wrenn (2002) (Equation 3.1) but the PID reading was 71.

$$R = Conc./CF \qquad \textbf{Equation 3.1}$$

R is the PID response (ppm isobutylene equivalents), Conc. is the concentration of hexane (ppm) and CF is the correction factor. Based on this data a correction factor was calculated for the PID based on the ratio of the expected hexane response to the actual hexane response. This correction factor has a value of 1.32 and applying it to the PID data results in the "PID with correction factor" values in Figure 3.4.

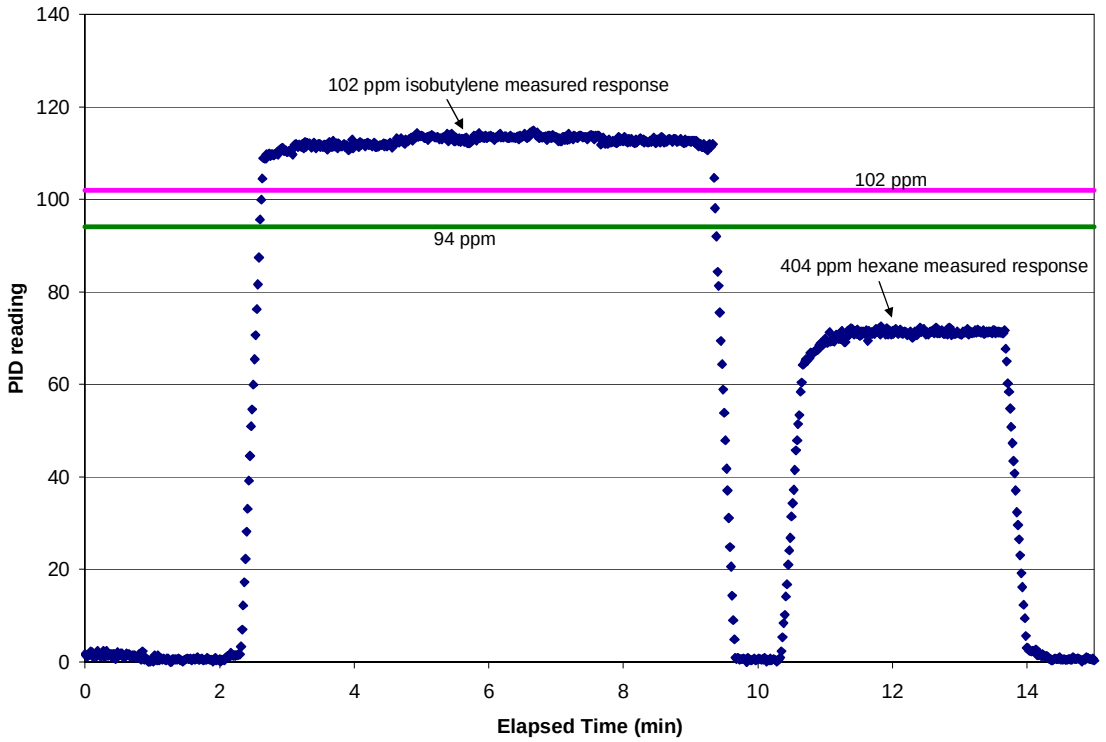

Figure 3.6. Results of testing PID response to known concentrations of isobutylene and hexane from commercial gas cylinders.

However, this correction factor does not account for the effects of temperature and humidity because the hexane came from a canister. The vapour extracted from the cell would have a higher temperature (from flowing through the vacuum pump, which usually had a temperature around forty degrees Celsius) and higher humidity (from being in contact with the extracted water in the hoses between the well and the liquid-gas separator).

Adding the correction factor to the PID data does not result in a match with the GC data. Overall the fit is better but it is still far from perfect. As a result, the PID data will only be used to evaluate trends in the data because the trends were consistent with the trends in the GC results.

The mass removal estimates for quadrant E2 are presented in Figure 3.7. Estimates for the PID, GC and PID with correction factor methods described above provide significantly different totals. Since the GC results are the most accurate they can be used as a basis for a new method. The primary problem with using just the GC results is that sampling may miss significant changes in concentration. For example, at ~1900 minutes the power at the site was interrupted and the injection and extraction stopped. This occurred in the early morning so there had been no samples taken since the previous night. A sample was taken after the system was restarted but the concentration in this sample would be elevated relative to samples taken when the system had been running for a long time. So using the last sample from the previous night and sample from right after restart to represent concentrations during the night would result in an overestimation. To correct for this, the data from the PID is used to infer a value for the time before the power shut off. Several other data points were inferred using this method for other similar circumstances. By adding these points to the GC results, a new estimate is arrived at, GC with inferred points (Figure 3.7).

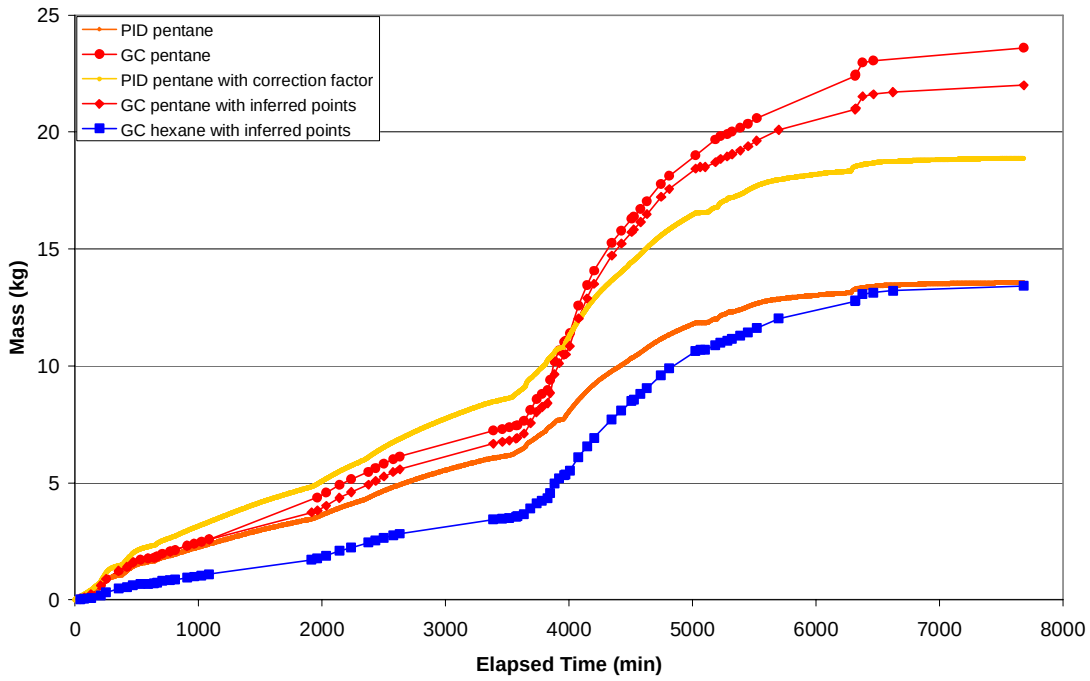

Figure 3.7. Cumulative mass of pentane and hexane removed in the vapour phase during phase I. The most representative data is given by the PID with inferred points data sets for both pentane and hexane.

One interesting finding of this experiment is that the highest contaminant concentration in the effluent stream was not recorded immediately after start-up. Field studies of air

sparging systems consistently report having the highest concentrations immediately following start-up (Gordon, 1998; Kirtland & Aelion, 2000; Benner et al, 2002; Johnston et al, 2002). Using supersaturated water injection resulted in the highest concentrations occurring a few days of operational time after start-up. This is most likely due to the location of the injection wells relative to the emplaced source (see Section 3.2.6 for a description of the likely location of the emplaced source). Supersaturated water and CO_2 bubbles will each likely flow more slowly than injected air, resulting in more residence time in the aquifer and delayed arrival at the extraction well. In addition, initially much of the CO_2 will evolve and flow upwards very close to the injection well. However, over time trapped bubbles of CO_2 will decrease the permeability of this area (Christiansen, 1944) diverting supersaturated water and CO_2 bubbles away from the well. Since there is likely more contamination at a distance from the well, the highest concentrations are a result of CO_2 bubbles reaching more highly contaminated areas of the subsurface.

3.2.1.2 Other Quadrants

The other quadrants (E1, E4 and E3) did not produce much contaminant mass. E1 (Figure 3.8a) and E3 produced their highest concentrations initially (similar to air sparging) while E4 (Figure 3.8b) had its highest concentrations after the system had been operating for a while (similar to E2).

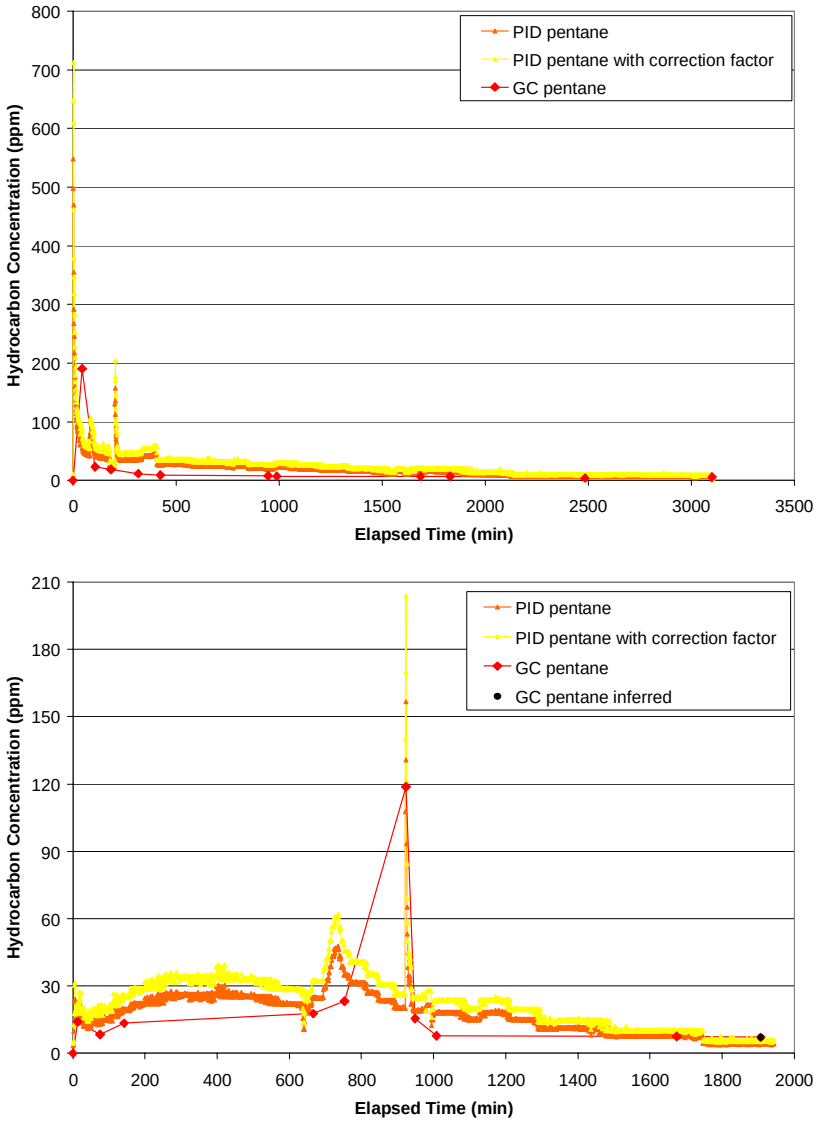

Figure 3.8. Pentane and hexane vapour concentrations in the air extracted from E1 (a) and E4 (b) during phase I.

3.2.1.3 Summary

Phase I of the remediation removed 24.2 kg of pentane and 15.1 kg of hexane which represents 57% of the initial pentane and 32% of the initial hexane. The higher volatility of pentane relative to hexane likely accounts for the difference in the amounts removed. This result matches the observation of Johnston et al (1998) that compounds with higher Henry's Law constants (higher volatility) will be preferentially removed by volatilization. Figure 3.9 presents the cumulative mass removed over time and illustrates the fact that most of the mass removed was from well E2. All of the data from the GC analysis is provided in Appendix B.

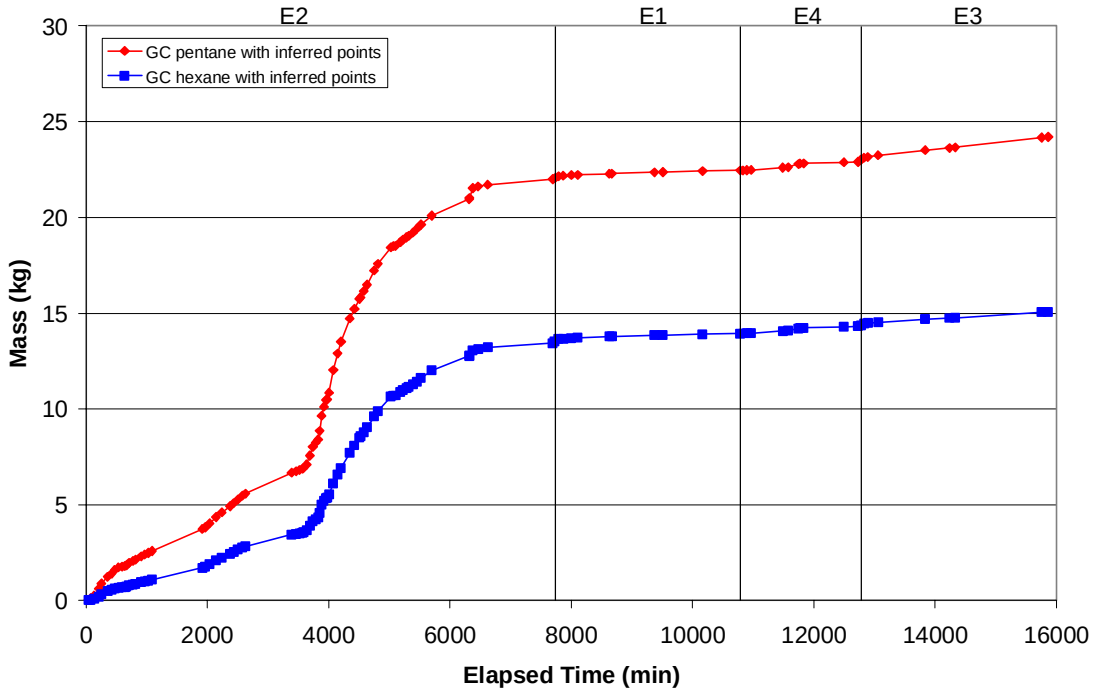

Figure 3.9. Cumulative mass of pentane and hexane removed in the vapour phase during phase I.

3.2.2. Water Sampling

Pentane, hexane and Soltrol 130 all have very low solubility in water. The manufacturers of Soltrol 130 report its solubility as "negligible" while lab studies have determined the solubility of pentane to be 38.5 mg/L (Mackay et al, 1992) and that of hexane to be 12.3 mg/L (Leinonen & Mackay, 1973). However, in a mixture the solubility of each component of the mixture will be lower and proportional to its mole fraction in the mixture (Leinonen & Mackay, 1973). The solubility of each component in a mixture is its effective solubility. Effective solubility can be calculated by using Raoult's Law:

$$S_e = XS \qquad \textbf{Equation 3.2}$$

S_e is the effective solubility, X is the mole fraction of the compound in the mixture and S is the pure phase solubility of the compound. Since the mixture originally contained 40% pentane, 40% hexane and 20% Soltrol 130, the effective solubility of pentane was 17.8 mg/L and that of hexane was 5.1 mg/L.

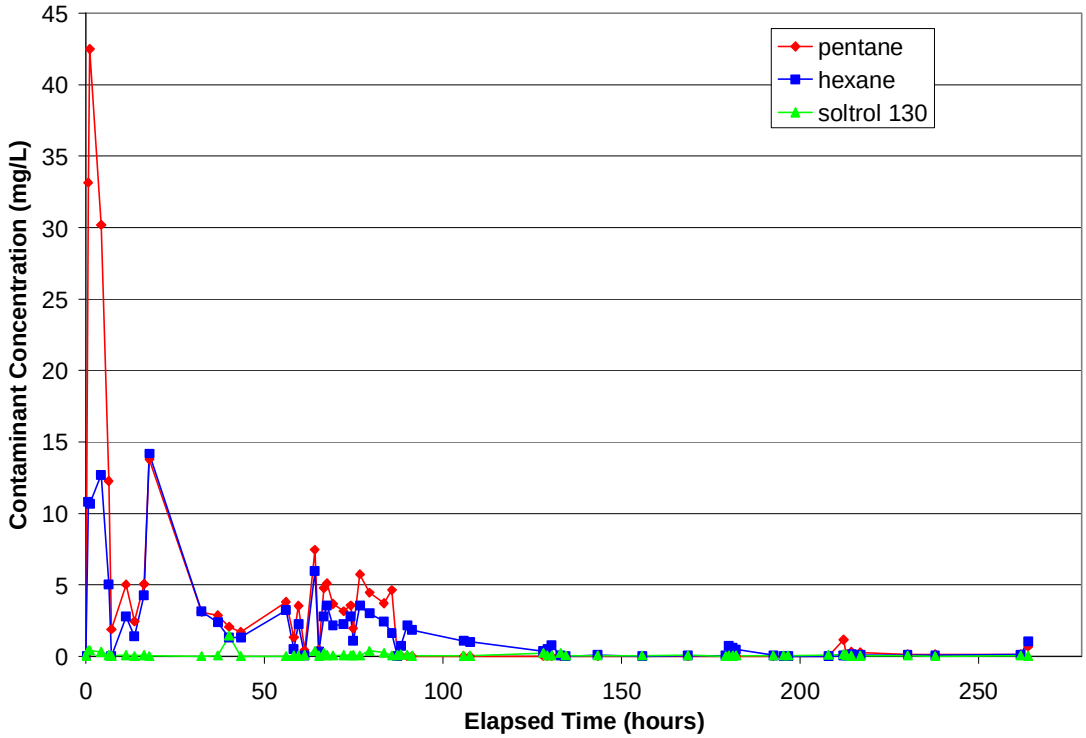

Figure 3.10. Aqueous concentrations of pentane and hexane over time during phase I.

The highest concentrations, with some at or above the effective solubility, were found near the beginning of the experiment and generally decrease with time as more of the NAPL is removed (Figure 3.10). Concentrations above the effective solubility could be due to the presence of NAPL in the sample (perhaps as a NAPL in water emulsion) or variable NAPL composition at different locations in the cell resulting in a different effective solubility for each component of the NAPL. For example, based on Raoult's Law (Equation 3.2), if the NAPL composition changes so that it is comprised of more hexane than pentane, the effective solubility of hexane will increase while that of pentane will decrease. However, it should be noted that no evidence for the recovery of NAPL was ever observed. There is some variability in the data and some of that variability may be attributable to a rebound effect after the system was shut down. Equilibrium is not usually attained between flowing groundwater and NAPL (Sahloul et al, 2002). However, during times that the system was shut down, groundwater flow within the cell would be negligible and there would be time for local equilibrium to be established between the water and NAPL. When the system was restarted, water that had attained equilibrium with the NAPL, as well as water from other areas, would be removed and sampled. Over time concentrations would decrease until the system was shut off again and the process would repeat itself. However each time there would be less NAPL and therefore the concentrations near start-up would be less because there would be less water in contact with NAPL during the time the system was shut down. Full results for the water sampling can be found in Appendix C.

A similar phenomenon occurred each time a new extraction well was used. Concentrations would be higher to begin and decrease with time. New extraction wells were used beginning at 7750, 10800 and 12740 minutes of elapsed running time.

The remediation process preferentially removes the more volatile compound, pentane. As a result over time the mole fraction of pentane in the NAPL will decrease and those of hexane and Soltrol will increase. This will have an impact on the relative solubility of the compounds, decreasing that of pentane and increasing those of hexane and Soltrol. The impact of the changing composition of the NAPL is not evident in the sampling data; there is no obvious change in the relative amounts of pentane, hexane and Soltrol over time.

Due to the relative insolubility of each compound, a very small fraction of contamination was removed in the aqueous phase. The totals are presented below in Table 3.2 and Figure 3.11. Almost all of the mass that was removed in the aqueous phase was removed in the first 130 hours (five and a half days) which is a slightly shorter time frame than the one over which most of the contamination was removed in the vapour phase.

Contaminant	Mass Removed (g)	% of Initial Mass
Pentane	57	0.13
Hexane	40	0.08
Soltrol 130	2.8	0.003

Table 3.2. Masses of hydrocarbons removed in the aqueous phase during phase I.

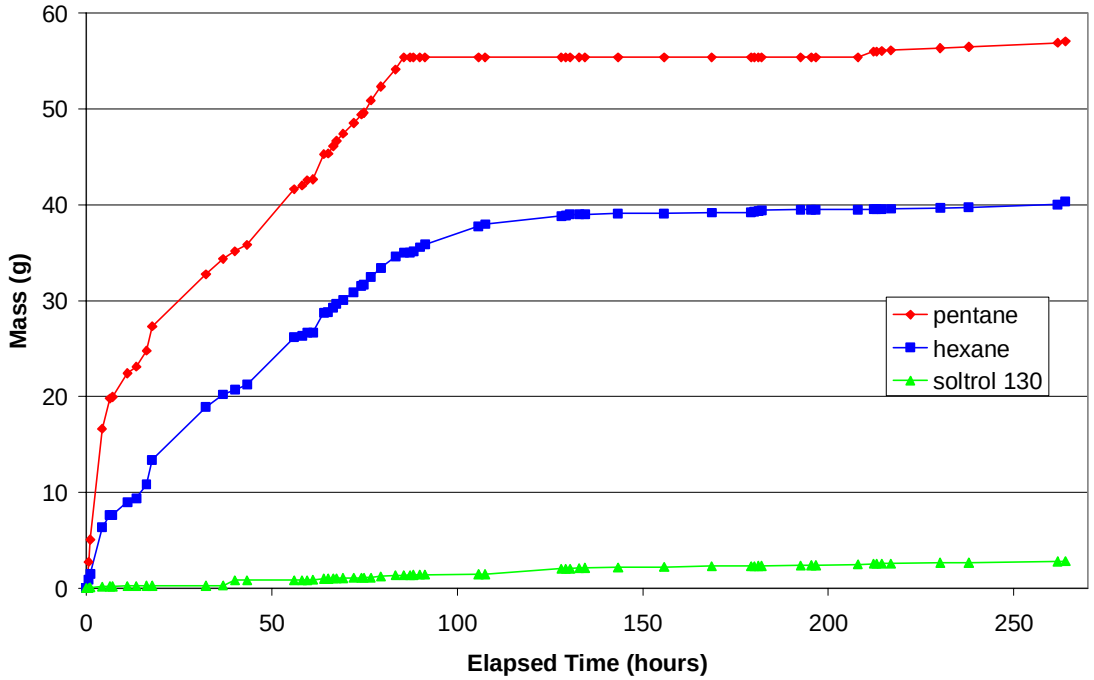

Figure 3.11. Cumulative mass removed for pentane, hexane and Soltrol 130 in the aqueous phase during phase I.

A lab experiment by Li (2004) identified NAPL mobilization as a mechanism for remediation by SWI. In order to test the remediation potential of SWI, hexane and octane were emplaced in a sand box and removed using SWI. Mobilization occurred when the NAPL formed a film around CO_2 bubbles which then rose through the sand carrying the NAPL film along with them. This mechanism was further investigated with the use of a micro-model experiment which confirmed that SWI mobilized NAPL in a lab setting. There are no reports of this phenomenon in the groundwater remediation literature for similar remediation technologies but a similar phenomenon has been reported in the oil production literature during a lab experiment by Grattoni & Dawe (2003).

In Li's experiment 14% of the hexane removed was removed by mobilization while 62% of the octane removed was by mobilization. This mechanism was not observed during this field experiment. NAPL was never observed in the oil-water separator and there was no evidence of dye staining the walls of the oil water separator during the phase I of the remediation. During phase II of remediation a sheen of hydrocarbons was observed on top of the water in the storage tank but it was of negligible mass.

3.2.3. Activated Carbon

During phase I of the remediation all of the effluent streams passed through granular activated carbon filters before being discharged to the atmosphere (vapour) or flowing into the storage tank (water) (Figure 3.12). There were two vapour filters, one that filtered vapour extracted from the cell and one that filtered vapour from the air stripper.

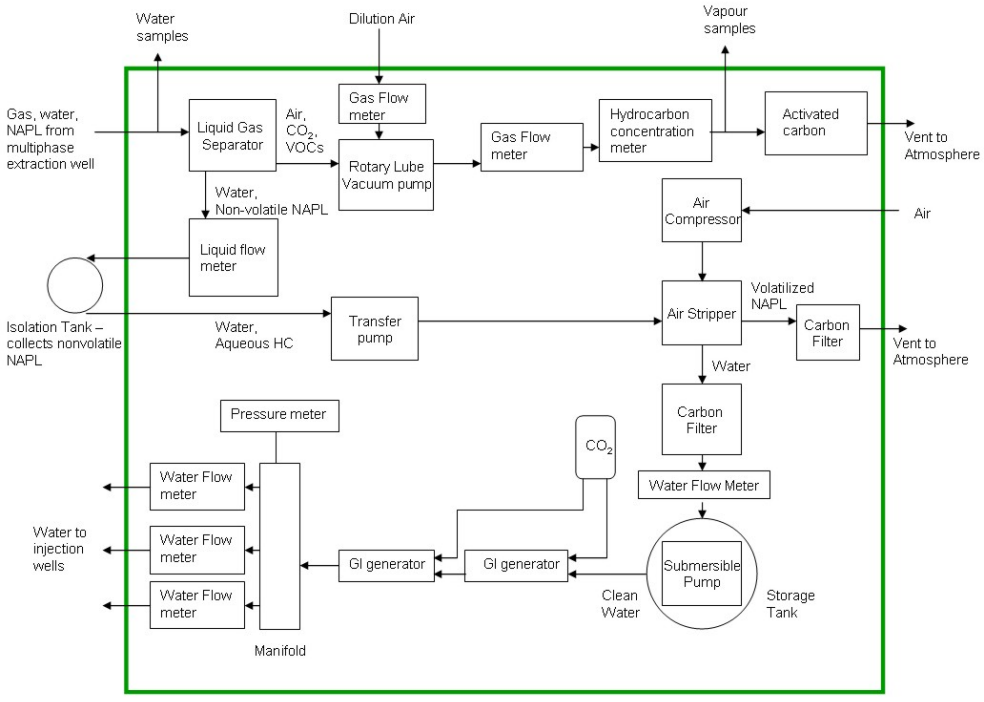

Figure 3.12. Process and instrumentation diagram for phase I of the remediation.

Granular activated carbon is widely used to remove hydrocarbons and other toxic substances from both water (Giffin & Davis, 1998) and vapour (Adams & Reddy, 1999). Activated carbon was chosen for two reasons: it has a high adsorption capacity (Do & Do, 2002) and that adsorption can be reversed allowing the mass of adsorbed hydrocarbons to be extracted and determined (Adams & Reddy, 2003; Brooks et al, 2004).

3.2.3.1 Vapour

The vapour flowing directly from the cell had a much higher concentration of hexane and pentane than the vapour from the air stripper. Consequently the cell filter was much larger than the stripper filter and the activated carbon had to be replaced once during phase I. Table 3.3 contains data from the first batch of carbon used in the cell filter. This carbon was removed once vapour samples taken from a sampling port located after the filter showed detectable concentrations of pentane. Since the volume of the filter was so large (it had a mass of 180kg) the entire volume could not be homogenized in one batch. The activated carbon was removed in layers, with composite sample A1 taken from the top layer (nearest the filter outlet) and composite sample A4 taken from the bottom layer (nearest the filter inlet).

Composite Sample	Concentration (g/kg)		Pentane: Hexane Ratio
	Pentane	Hexane	
A1	61.0	0.0	-
A2	60.1	0.974	62
A3	36.9	41.4	.89
A4	37.5	84.4	.44
Total			1.5

Table 3.3. Sample results for hexane and pentane on the first batch of granular activated carbon in the cell filter during phase I.

Each concentration value presented in Table 3.3 is an average of five samples taken after the layer had been homogenized. The concentrations were quite consistent (Appendix D) indicating that the layer was well homogenized. It is interesting to note the progression in the pentane: hexane ratio between the layers (Figure 3.13). Hexane, the heavier molecule, is concentrated in the lower two layers while pentane is concentrated in the upper two layers. The results indicate that the hexane is replacing the pentane near the bottom forcing the pentane off the carbon and into the vapour and that later the pentane is reabsorbed higher up the filter.

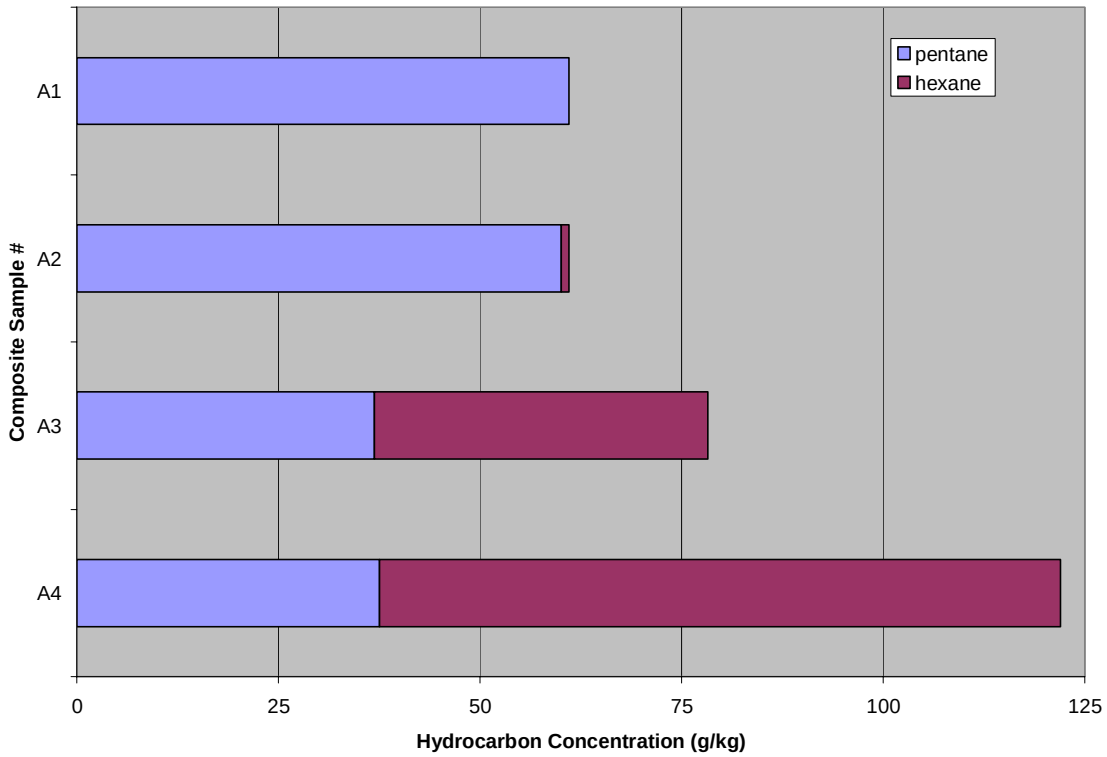

Figure 3.13. Concentrations of pentane and hexane with height in the cell filter.

At the end of phase I, the carbon from both the cell filter and the stripper filter were sampled and analyzed. The results are presented in Table 3.4. The trend identified in the first batch is also evident in this batch; although because composite sample B1 is entirely from the stripper filter and composite sample B2 is partially from the stripper filter and partially from the cell filter the trend is not as evident. Sampling was done in the same manner as for batch one and the samples were as consistent (Appendix D). Lab analysis indicated that there was some Soltrol 130 present in composite sample B6 but it was not quantified.

Composite Sample	Concentration (g/kg)		Pentane: Hexane Ratio
	Pentane	Hexane	
B1	0.549	0.0271	20
B2	5.77	0.628	9.1
B3	50.8	0.579	88
B4	21.4	42.6	0.50
B5	9.45	78.6	0.12
B6	9.08	68.7	0.13
Total			0.60

Table 3.4. Sample results for hexane and pentane on the second batch of granular activated carbon in the cell filter during phase I.

3.2.3.2 Water

The filters on the water stream did not have to be changed so they were only sampled once, after the completion of phase I. However, they did clog up over time with a red colored precipitate (likely iron based on the colouration) (Figure 3.14) and the presence of this precipitate may have impacted the laboratory analysis. The sampling was complicated by the fact that it was done in the winter when the temperatures were below zero degrees Celsius causing some freezing of the water in the filters, especially near the walls of the filter. As a result it was not possible to remove all of the carbon from the filters, although visually it was estimated that more than ninety percent was removed. The carbon in the water filters was not removed as systematically as in the vapour filters due to the difficulty in removing it. As a result there is no pattern in the data (Table 3.5; Appendix E). Samples were taken after the water filter and neither pentane nor hexane was ever detected, so there was no evidence of breakthrough.

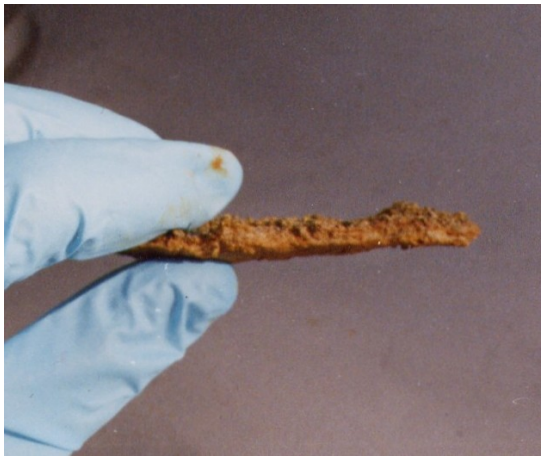

Figure 3.14. Photograph showing colour and thickness of precipitate formed in water filter.

Composite Sample	Concentration (mg/kg)		Pentane: Hexane Ratio
	Pentane	Hexane	
W1	17.6	14.3	1.2
W2	25.4	13.7	1.9
W3	6.39	13.6	0.47
W4	10.2	15.8	0.65
Total			1.0

Table 3.5. Sample results for hexane and pentane on the granular activated carbon in the water filter during phase I.

3.2.3.3 Mass Captured

Table 3.6 presents the total mass desorbed from the carbon filters on all three streams. The percentage of spilled mass is presented because the filters were on line during the SVE phase. As a result, the filters contained hydrocarbon mass that was removed from the cell before the supersaturated water injection began. This mass is not incorporated into the analysis when vapour and water sampling and the PID were used. However,

there is no simple way to differentiate between mass removed in the SVE phase and phase I in the filters. It was not considered financially prudent to replace the filters after the SVE phase and venting high concentrations of hydrocarbons directly to the atmosphere was not desirable.

Composite Sample	Mass (kg)		
	Carbon	Pentane	Hexane
A1	45	2.74	0.0
A2	45	2.70	0.0438
A3	45	1.66	1.86
A4	45	1.69	3.80
B1	45	0.0247	0.00122
B2	45	0.260	0.0283
B3	45	2.29	0.0260
B4	45	0.963	1.92
B5	45	0.425	3.54
B6	20	0.182	1.37
Vapour Total	**425**	**13**	**13**
W1	20	3.51×10^{-5}	2.85×10^{-5}
W2	20	5.08×10^{-5}	2.73×10^{-5}
W3	20	1.27×10^{-5}	2.71×10^{-5}
W4	20	2.04×10^{-5}	3.16×10^{-5}
Water Total	**80**	$\mathbf{1.19 \times 10^{-4}}$	$\mathbf{1.15 \times 10^{-4}}$
Total	**505**	**13**	**13**
% of Spilled Mass		**27**	**25**

Table 3.6. Total masses of hydrocarbons retained by the filters during phase I.

As is evident in Table 3.6, the mass captured on the water filter contributed a negligible amount of mass to the total. This is not surprising considering the low solubility of the contaminants in water and the fact that water entering the filter had already passed through an air stripper.

The estimation of the mass removed from the cell based on this method is significantly less than the estimation based on vapour and water sampling and the PID. There are several possible explanations for this. One is that there was breakthrough of pentane through the cell filter part way through phase I. The impact of this breakthrough on the results is evident when the ratio of pentane to hexane is compared. Based on the carbon data, the ratio is 1:1 while for the sampling/PID method it is 1.6:1. So the carbon method has relatively less pentane, indicating that some of the pentane was lost.

However, pentane breakthrough does not fully explain the discrepancy between the sampling methods because there was less hexane estimated by the carbon method than the sampling/PID method and there is no evidence of hexane breakthrough.

The homogenization process also may have resulted in desorbtion while mixing occurred. However, the temperature was very likely cooler during the homogenization process than

when vapour was passing through the filter so there would have been little thermodynamic driving force to desorb the contaminants. Other issues related to the logistics of handling, sampling and transporting such a large quantity of carbon may have contributed to some minor desorbtion.

Incomplete desorbtion of contaminants from the carbon during lab analysis is also a potential source of error because the carbon used in the laboratory to prepare standards was from a different batch than the carbon used in the filters. Other researchers (Adams & Reddy, 1999) have also encountered problems matching desorbed activated carbon data with data from sampling. The discrepancy that Adams and Reddy reported was less than the one found in the experiment and they attributed it to breakthrough when contaminant concentrations were very high.

3.2.4. Soil Sampling

Five soil cores were taken from the cell after phase one of the remediation to determine areas that still contained high concentrations of contaminants. High contaminant concentrations would indicate locations not impacted by remediation. Low and non-detected concentrations would indicate that the location had been remediated or that the location had not been contaminated during the emplacement. The locations of these cores are presented in Figure 3.15. The concentrations reported are in milligrams of pentane or hexane per kilogram of wet soil. The scales on the figures are not always the same due to the wide range in concentrations. Appendix F contains all of the soil sampling lab results.

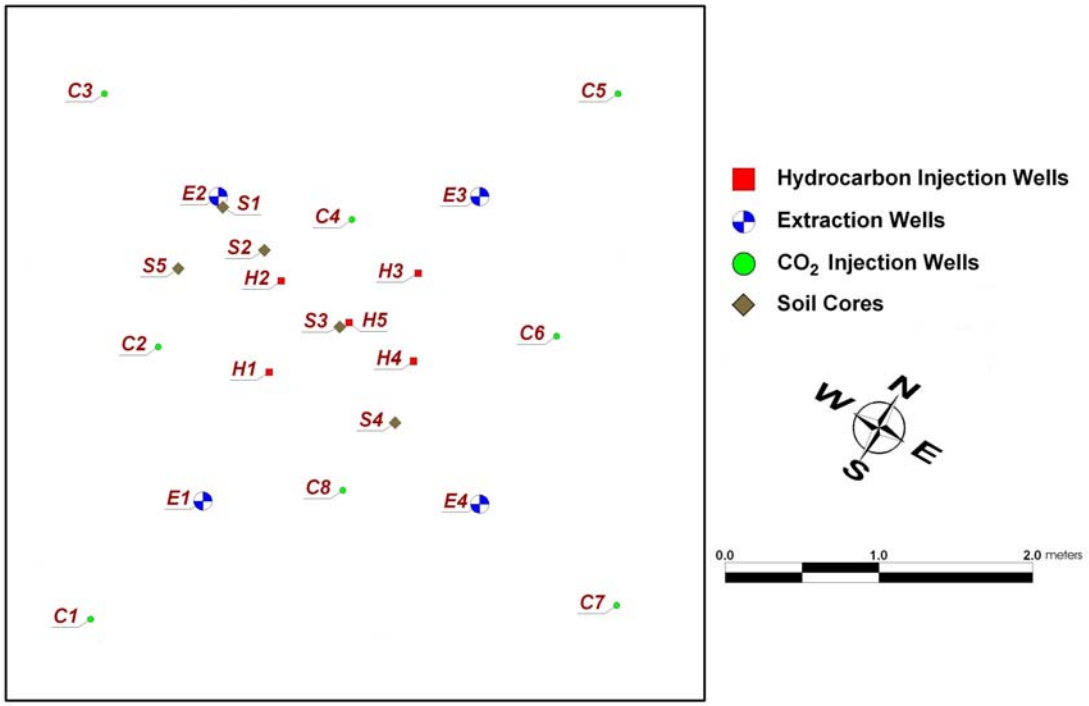

Figure 3.15. Location of Soil Cores.

Concentrations greater than the yellow vertical lines labeled "no NAPL max" indicate the presence of NAPL in the sample based on the method described by Feenstra et al (1991). The method assumes that there is no NAPL present and that all of the contaminant mass is partitioned at equilibrium between the solid, pore water and soil gas phases. If the measured concentration of contaminant is greater than can be accounted for in those three phases, a NAPL phase must be present. Equation 3.3 gives the maximum total concentration possible without there being a NAPL phase present.

$$C_t = C_w(K_d \rho_b + \phi_w + H_c \phi_a)/\rho_b \qquad \textbf{Equation 3.3}$$

The following abbreviations are used in the calculations:

C_t Total soil contaminant concentration (mg/kg)
C_w Contaminant concentration in the pore water (mg/L)
K_d Partition coefficient between pore water and soil solids (cm^3/g)
ϕ_w Water filled porosity (volume fraction)
H_c Henry's Law Constant (dimensionless)
ϕ_a Air filled porosity (volume fraction)
ρ_b Bulk density of the soil sample (g/cm^3)
K_{oc} Partition coefficient between pore water and organic carbon
f_{oc} Organic carbon fraction
S_i^e Effective solubility (mg/L)
X_i Mole fraction
S_i Pure phase solubility (mg/L)

See Table 3.7 for the values of these parameters for pentane, hexane and Borden sand. For hexane the maximum total concentration possible without a NAPL phase is 41 mg/kg and for pentane it is 353 mg/kg. Since pentane has a higher value it is shown on the figures and it is used in the sample calculation shown below. The K_d value for pentane can be calculated using the following formula:

$$K_d = K_{oc} f_{oc} \qquad \textbf{Equation 3.4}$$

This approximation is valid provided that f_{oc} is greater than 0.01 (Karickhoff, 1984). Since the emplaced contamination is a mixture, the solubility of the components, such as pentane, will be affected. In this case the effective solubility must be used and it can be calculated through Raoult's Law (Equation 2 in Section 3.2.2). For pentane, K_{oc} is 982 (Gustafson et al, 1997) and the f_{oc} of Borden sand is 0.02 (MacKay et al, 1986). Substituting into Equation 3.4, the K_d of pentane at Borden is 19.6. The solubility of pentane is 38.5 (MacKay et al, 1992) and the mole fraction of pentane in the original mixture is 0.46 so substituting into Equation 3.2 gives an effective solubility of 17.8 mg/L.

To calculate the maximum total concentration possible without a NAPL phase the values in Table 3.7 are substituted into Equation 3.3 and the effective solubility is used as the pore water concentration (C_w).

Parameter	Value	Reference
C_w	17.7 mg/L	Calculated above
K_d	19.6	Calculated above
ρ_b	1.81 g/cm^3	MacKay et al, 1986
ϕ_w	0.33	MacKay et al, 1986
H_c	51.9	Yaws et al, 1991
ϕ_a	0.00	Assumed

Table 3.7. Physical and chemical properties for pentane and Borden sand.

Since all of the samples were taken from below the water table, there is no air filled porosity and Equation 3.3 simplifies slightly to:

$$C_t = C_w(K_d\rho_b + \phi_w)/\rho_b \qquad \textbf{Equation 3.5}$$

Substituting the values from Table 3.7 into Equation 3.5 we get a maximum pentane concentration of 353 mg/kg without there being a NAPL phase present. This value is converted to 0.57 mL/kg presented on Figures 3.16 to 3.20 as the line labelled "no NAPL max". The concentration is expressed as a volume per mass because equal volumes of each contaminant were emplaced (not equal masses) so the NAPL originally had equal volumes of each contaminant. If the NAPL was only partial volatilized during remediation there would be a higher concentration of hexane because the pentane was preferentially removed.

3.2.4.1 Core S1

This core was taken near well E2, a water and vapour extraction well. The majority of the contaminant mass removed during the experiment was removed from this well. The only area of the core showing contamination is above 180 centimeters (Figure 3.16). This may be due to contaminant migration occurring during the winter after the system was shut off. Since migration of free phase LNAPL would happen at the water table, it is a better explanation for the NAPL at 100 cm than the NAPL lower in the core. The samples that had NAPL had significantly more hexane than pentane indicating some remediation because the pentane is more volatile than hexane and it would be preferentially removed by volatilization during remediation.

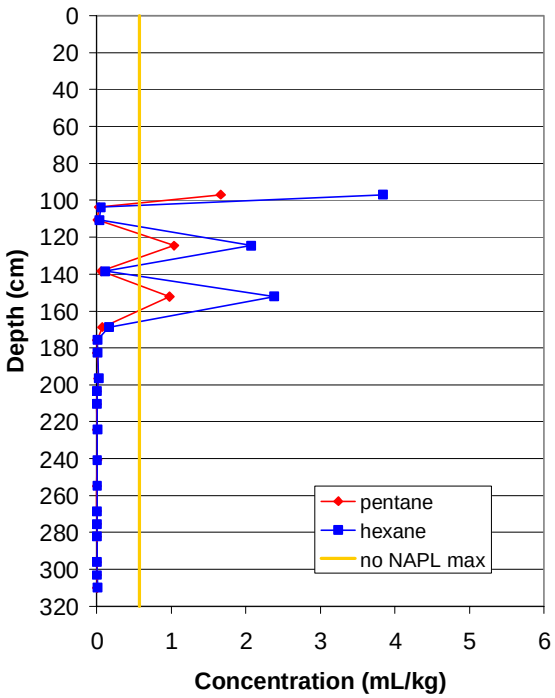

Figure 3.16. Soil Core S1.

3.2.4.2 Core S2

Core S2 was taken between wells E2 (extraction) and H2 (contaminant injection). There were many locations of high pentane and hexane concentration in this core, with two areas of particularly high concentrations around 220 and 285 cm (Figure 3.17). There was also a smaller peak around 190 cm. This high variability is to be expected and has been reported by researchers at Borden (Feenstra, 2005) and other sites (Schumacher & Minnich, 2000; West et al, 1995). The high concentrations of hexane and pentane and the fact that the concentrations are very similar, usually within sampling/analytical uncertainty, indicates that little or no remediation was done in the area this core was taken from. The concentration of pentane is higher than that of hexane in the uppermost samples which may indicate some remediation but on the whole, the remediation efforts did not impact this location.

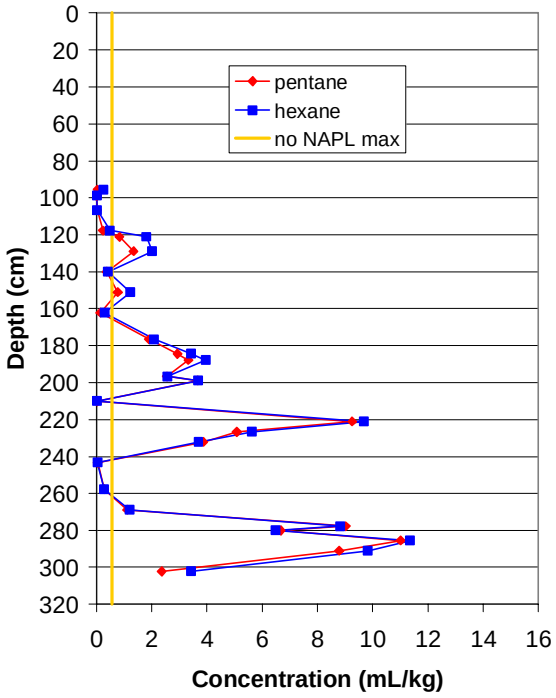

Figure 3.17. Soil Core S2

3.2.4.3 Core S3

Core S3 was taken near the middle of the cell. Along with core S2 it had the highest concentrations of hexane and pentane (Figure 3.18). There were two peaks, a large one between 190 and 280cm and a smaller one nearer the surface between 110 and 150cm. It is likely that none of the CO_2 reached this area of the cell and the hydrocarbons are as originally emplaced or redistributed by movement of free-phase NAPL at the water table (between 110 and 150cm). The pentane concentration is higher than the hexane concentration for most locations between 160 and 250cm but based on the high magnitude of the concentrations this is not due to remediation. The high concentrations mean that this area was not remediated during the first phase.

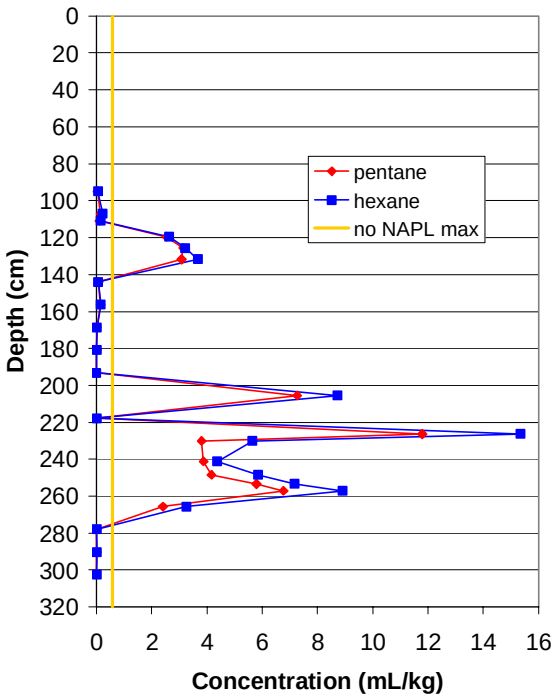

Figure 3.18. Soil Core S3

3.2.4.4 Core S4

Core S4 was located between wells E2 (extraction) and C2 (CO_2 injection). It had the lowest concentrations of all the cores sampled after phase I (Figure 3.19). This may be due to effective remediation due to its proximity to a CO_2 injection point or because there wasn't much contamination in this area to begin with. All of the hexane and pentane was found above 180 cm in relatively small peaks at 125 cm and 170 cm. The elevated concentrations of hexane relative to pentane, especially considering the relatively low contaminant concentrations, indicate that the hydrocarbons present were impacted by remediation. There is no way to definitively tell if there ever was substantial contamination in this area but the low concentrations and the relationship between the pentane and hexane concentrations indicate that the area was remediated. The higher concentrations above 150 cm may be due to a lower conductivity layer at that elevation impeding vertical migration of CO_2 bubbles. There is no direct evidence for a low permeability layer, however, Mackay et al (1986) observed horizontal bedding features in Borden sand and Doughty (2004) found that layers with lower hydraulic conductivity influenced vertical migration of CO_2 bubbles at Borden.

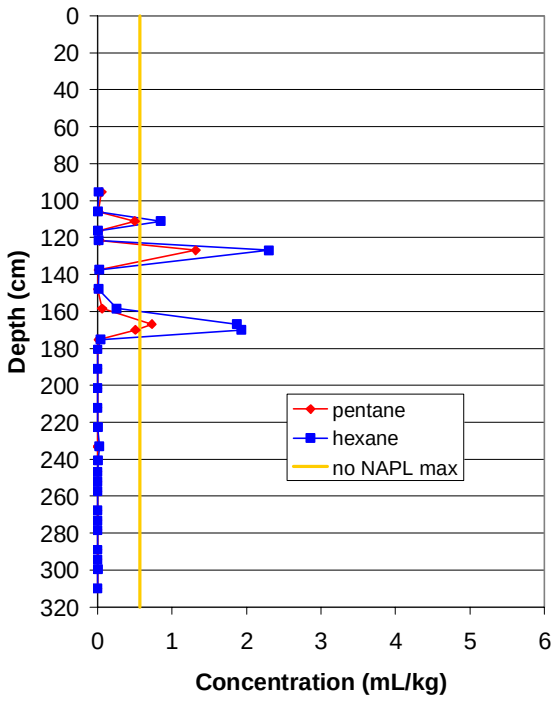

Figure 3.19. Soil Core S4

3.2.4.5 Core 5

Core 5 was taken near H4 (hydrocarbon injection), between H4 and E4 (water and vapour extraction). The location was similar to that of core S2 although more mass was removed from the extraction well near core S2 (well E2) than through E4. Core S5 had lower concentrations than core S2 indicating that a much larger volume of contamination was initially present in the vicinity of E2 (Figure 3.20). There is NAPL present at several depths in this core however it is quite variable below 200cm. Below 200cm there is evidence of remediation but above 150cm there is a significant amount of pentane and hexane remaining with no indication of remediation. Below 200 the pentane concentrations are high and double the hexane concentrations indicating minor volatilization. The high, and similar, concentrations centered on 150 cm indicate that this area was not remediated at all, possibly due to a low permeability layer centered on 190cm preventing the vertical migration of CO_2 bubbles. As in core 4 there is no direct evidence of this layer so the interpretation is based on the findings of previous researchers at Borden.

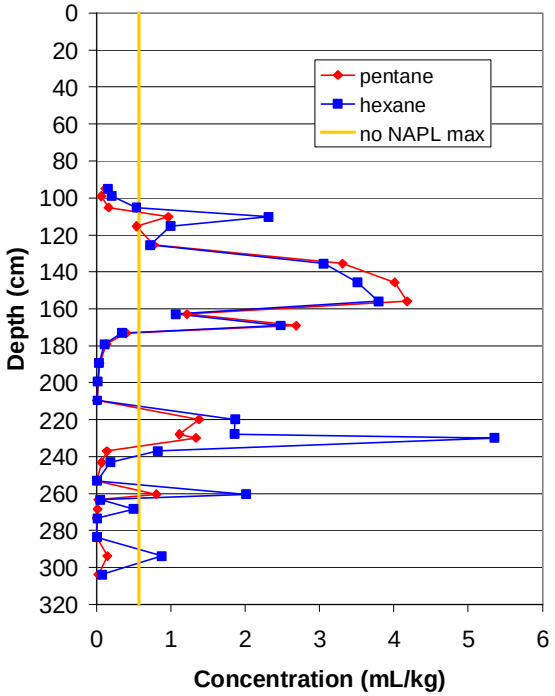

Figure 3.20. Soil Core S5.

3.2.4.6 Summary

The cores containing the lowest concentrations were located either beside an extraction well (S1) or directly between a CO_2 injection well and an extraction well (S2). The cores with higher contaminant concentrations were located near the center of the cell.

Two controls on the hydrocarbon content of core are recognized: the NAPL movement during and after emplacement and the remediation which in turn may reflect either/both the distribution of CO_2 infused water and the distribution of CO_2 bubbles rising from the infused water. The two controls are not mutually exclusive however and the results presented here show elements of both factors. The highest initial contaminant concentrations were likely in the middle of the cell but there are indications of remediation in several of the cores, especially those nearest CO_2 injection and water and vapour extraction wells, but not in the centre of the cell. This indicates that the remediation system design did not target the center of the cell where a significant amount of contamination was emplaced.

3.2.5. Geophysical Surveys

Doughty (2006) found cross-borehole GPR to be the most effective geophysical method of determining changes in water and air saturation and hence the presence of CO_2 bubbles in the Borden aquifer. As a result a cross-borehole GPR survey was carried out to identify areas receiving CO_2 bubbles.

The initial survey was conducted on November 3, 2005 before SWI was begun in quadrant four. Three surveys were completed: H4-G1, G1-G2 and G2-H4. They form a triangle around the extraction well E4 (Figure 3.21). On November 10, 2005 while the SWI system was remediating quadrant four, another survey was completed.

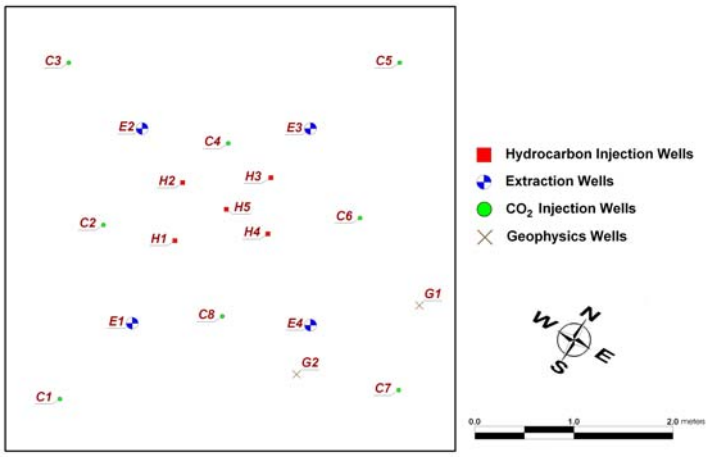

Figure 3.21. Location of geophysics access tubes.

Each survey consisted of two different methods, ZOPs (zero offset profiles) and MOGs (multiple offset gathers). Both methods provide water saturations but ZOPs are taken when both antennas are at the same depth while MOGs are taken when the antennas are at varying depths (see Appendix A for more details). The consequence is that ZOPs provide one dimensional data (depth) while MOGs provide two dimensional data (depth and distance between antennas).

By comparing the water saturations before and during SWI the volume and location of areas with increased air saturation can be determined. Figures 3.22 and 3.23 show the results of the survey conducted between G1 and G2. There is good agreement between the two methods and the decrease in water content is between one and two percent of the total volume of the aquifer. These results show fairly minor variation with depth. This is in contrast to the results reported by Doughty (2006) where strong variation with depth was evident in most of the profiles that had observable levels of gas saturation. This variation with depth was attributed to the presence of lower conductivity layers which resulted in the accumulation of gas below the layer and little to no gas above it. It is possible that low conductivity layers are not present at this site or are not influencing the vertical flow of bubbles in the same manner. The magnitude of water content change of up to two percent is consistent with the results reported by Doughty (2006).

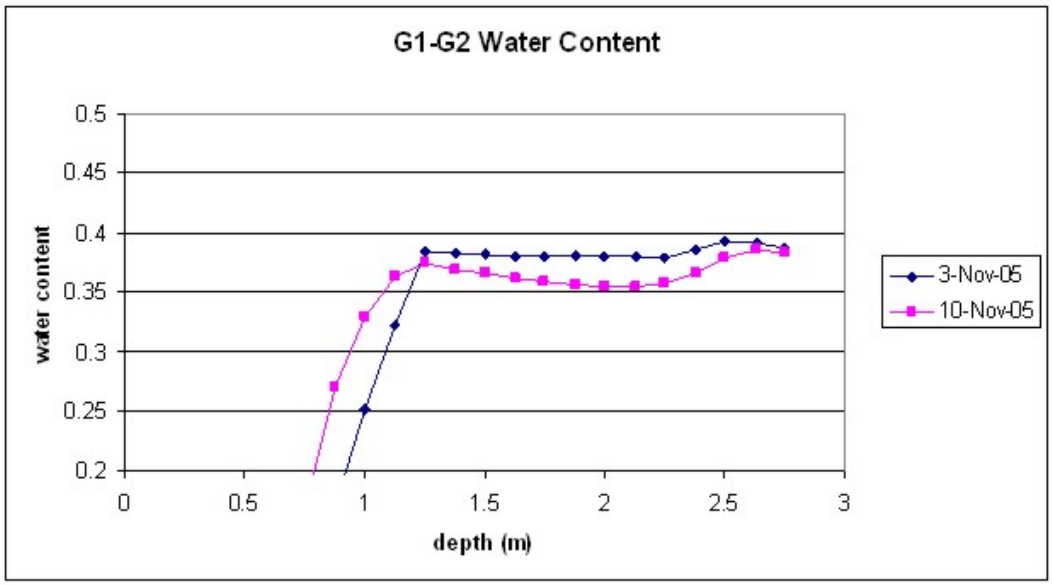

Figure 3.22. Water content between G1 and G2 based on ZOP data.

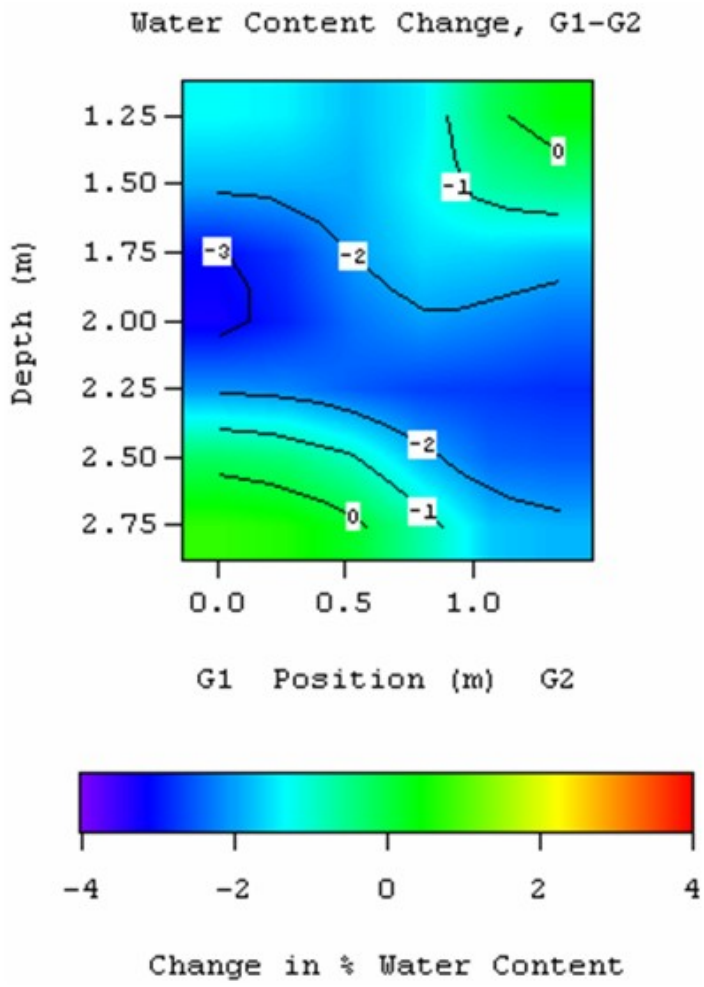

Figure 3.23. Change in water content between G1 and G2 based on MOG data.

The results for H4-G1 (Figure 3.24) and H4-G2 (Figure 3.25) are significantly different than those for G1-G2. The results show that the water content increased after SWI began. This is not physically possible in the saturated zone if only water and CO_2 gas are present. However, the presence of residual NAPL in the subsurface during the background survey and the removal of some of it by the time the second survey was done may explain this finding.

Gasoline has a dielectric constant of 1.95 (Musil & Zacek, 1986) which is much closer to that of a CO_2 bubble (1) than water (80). As a result, the apparent increase in water content may be due to a decrease in NAPL content. After emplacement, the residual saturation of gasoline NAPL in the Borden aquifer is expected to be two or three percent (Section 2.2). So completely removing a NAPL that was homogeneously distributed would result in at most a three percent increase in water saturation which matches the observed increased water saturation of between two and three percent (Figures 3.24 & 3.25).

However, all of the NAPL was not removed and the soil core (S5) removed from this area indicated the continued presence of NAPL. Based on the amount of NAPL actually removed, the increase in water saturation should be at most one percent and it should not be evenly distributed with depth.

In addition, the results from G1-G2 indicate that CO_2 bubbles decrease the water content by one or two percent. So even if the there had been a uniformly distributed NAPL at three percent saturation that was totally removed, that accounts for the entire increase in water content. It does not account for the presence of CO_2 bubbles that should have decreased the water content by one or two percent.

The only way to account for the increase in water content between the two surveys is by the removal of residual NAPL from the subsurface. However, the magnitude and even distribution of the increase in water content does not match the observations of the impacts of NAPL distribution, NAPL removal and CO_2 injection. For complete geophysics results please see Appendix A.

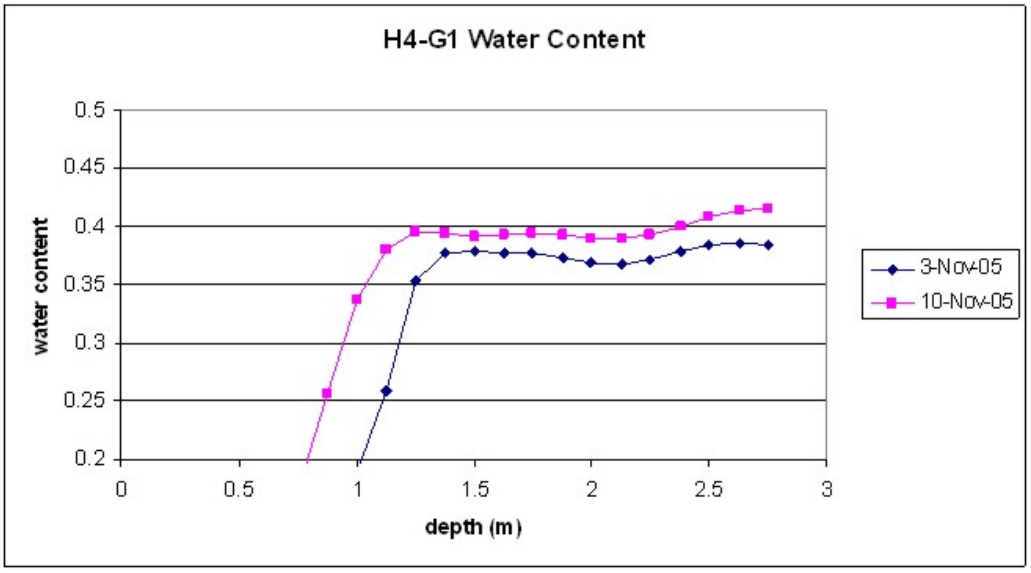

Figure 3.24 Water content between H4 and G2 based on ZOP data.

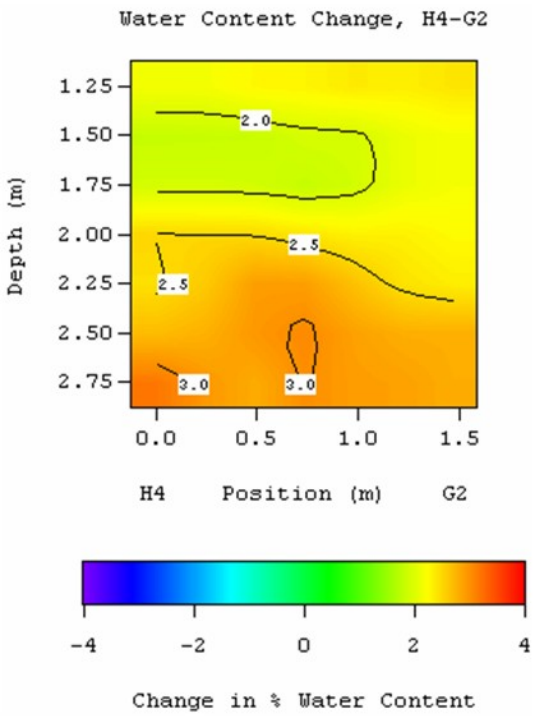

Figure 3.25 Change in water content between G1 and G2 based on MOG data.

3.2.6. Modeling

The amount of contaminant mass removed during phase I, which was less than anticipated, and the high levels of contaminant concentration in the soil cores taken after phase I was complete lead to questions about the whether or not the injected water and the resulting CO_2 bubbles reached the center of the cell. Based on the soil sampling results it was evident that there were still high concentrations of NAPL in the center of the cell and that the majority of the contaminant mass may not have migrated away from the center of the cell during the contaminant injection. As a result, MODFLOW was used to model the flow of injected water in the cell under the conditions present during phase I. Since it was known that the CO_2 comes out of solution fairly quickly, a time period of eight hours was chosen to determine the area that would be reached by water capable of producing CO_2 bubbles. Appendix G contains the results of the model for other time spans.

The majority of the mass removed during phase I was removed through E2 while injection was through C2, C3 and C4. The modeling of that scenario (Figure 3.26) shows strong control of the flow lines by the extraction of water through E2.. This supports the hypothesis that injected water capable of releasing CO_2 bubbles did not reach the center of the cell. The model results also support the results of the soil sampling; S1 and S5 are within areas predicted to have received water capable of releasing CO_2 bubbles while S3 is not. S2 is in a location close to the modeled flow lines but due to its imprecision, the model is not useful in predicting whether or not this exact location would have been remediated or not. The results of the soil sampling indicate that it was not remediated.

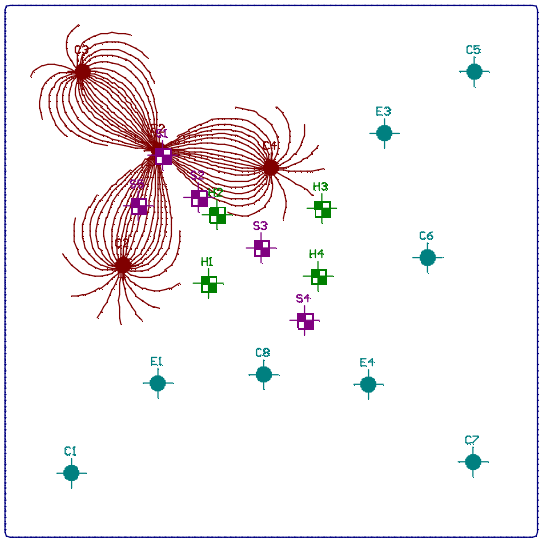

Figure 3.26. Modeled flow paths after eight hours of SWI injection through C2, C3 & C4 with extraction through E2 during phase I.

The modeling of the other quadrants (Appendix G) resulted in very similar flow patterns. For example, the modeling of E4 (Figure 3.27) is very similar and shows that soil core S4 was likely at the edge of the area that was remediated. The contaminant concentrations in the soil core indicate that the location was slightly impacted by remediation efforts.

The model clearly shows that during phase I injected water capable of producing CO_2 bubbles did not reach the middle of the cell. Combined with the soil sampling evidence that there were significant amounts of contamination left in the center of the cell it is not surprising that phase I removed 40% of the initial mass.

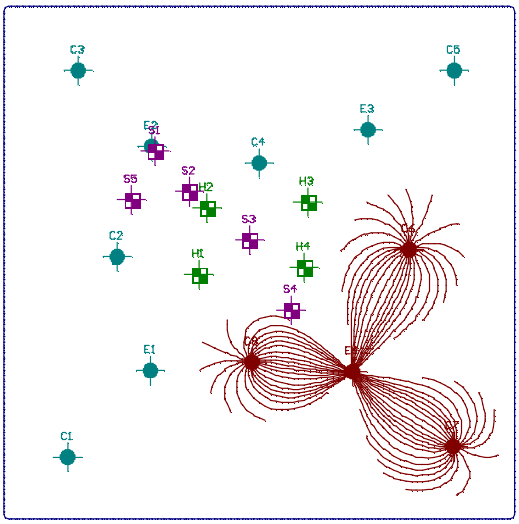

Figure 3.27. Modeled flow paths after eight hours of SWI water injection through C6, C7 & C8 with extraction through E4 during phase I.

Based on the evidence that there was a significant amount of mass still in the cell that was not impacted by the remediation activities in phase I it was decided to design a second phase of remediation to target the center of the cell where most of the remaining mass was believed to be located. It was decided that the best way to target the middle of the cell was to place a single CO_2 injection well in the center of the cell and reuse the existing extraction wells. The extraction wells would be used one at a time to draw the injected water towards each of the four corners of the cell. For example if the water was extracted through E2, the water flow lines would look similar to Figure 3.28. By injecting right in the center of the cell the injected water would reach most of the central area of the cell that was missed in phase I. In addition, the area between C2 and C4 that contains S2 (Figure 3.26) and was not impacted in phase I would also be remediated. Due to the symmetry of the cell, extracting from other E- wells would impact similar areas in each quadrant. Other injection and extraction well configurations were evaluated (Appendix G) but injecting into one central point was chosen due to the areas that it would impact and the minimal amount of disturbance to the cell that would be entailed through the installation of only one new well.

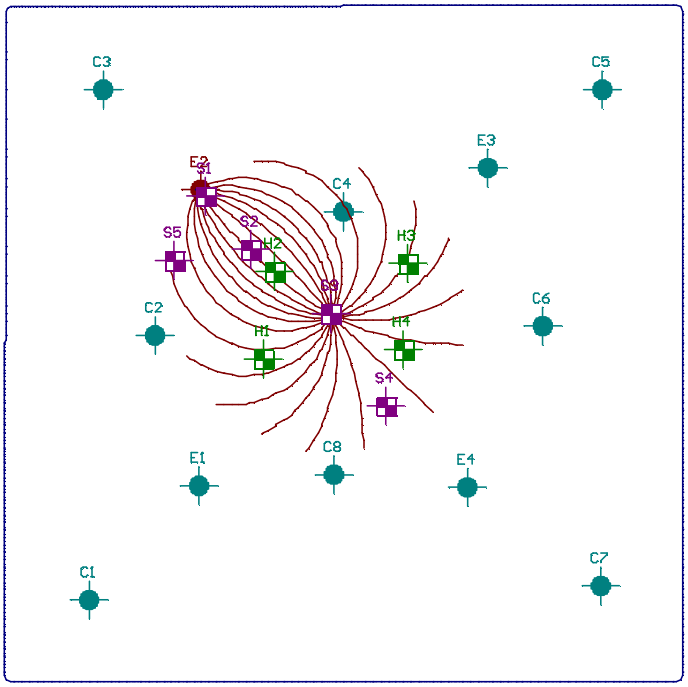

Figure 3.28. Modeled flow paths after eight hours of SWI water injection through C9 and extracted through E2 during phase II.

3.3. Phase II

Based on the results of the first round of soil sampling and the modeling, it was decided that another phase of remediation would be beneficial. In this second phase the centre of the cell would be targeted because it was not adequately reached during phase I and there were likely still large concentrations of contaminants there. In order to get supersaturated water into the centre of the cell, an injection well (C9) was installed in the centre of the cell at the location of soil sample S3 (Figure 3.29). Water from the GIs was injected through C9 below the contamination at 15 to 20 liters per minute under 50 to 60 pounds per square inch of pressure for a total of eleven days. Water and vapour were extracted from one of E1-E4 at different times.

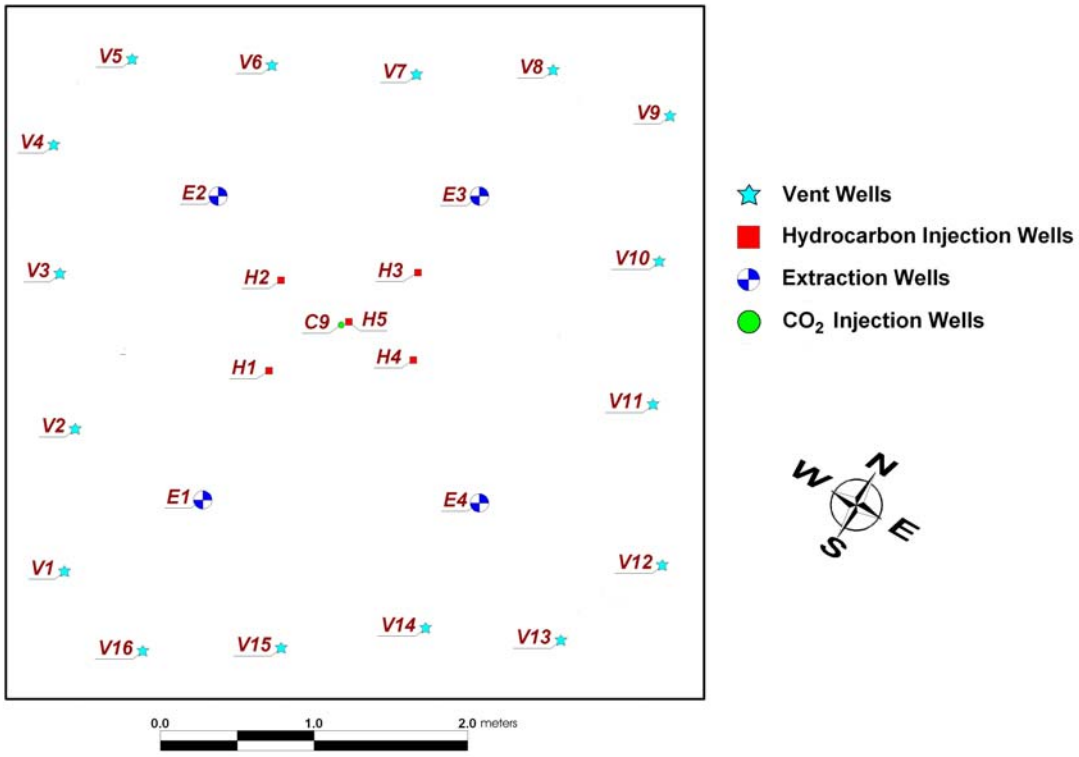

Figure 3.29 Location of wells during phase II.

3.3.1. Vapour Sampling and PID

During phase II, the concentration of hexane and pentane in the air extracted from the cell remained fairly constant until 12000 minutes when a gradual decline began (Figure 3.30). This differs from the phase I experience where the concentrations steadily decreased over time at each extraction well. It is not obvious why this is the case but may be related to the distribution of NAPL in the subsurface. The fairly constant concentrations may be due to CO_2 bubbles continuously following new pathways through the pore spaces in the

aquifer. As the bubbles flow through new pore spaces, they may contact residual NAPL and volatilize it. They may also become immobile when there is not sufficient force to enter the next pore throat. The mobility of bubbles is conversely correlated with hydraulic conductivity. As CO_2 bubbles nucleate in the pore space the conductivity of the soil is reduced, diverting the flow of carbonated water into other pathways resulting in more contacted NAPL. As the bubbles nucleate, grow and mobilize towards the surface residual NAPL is also mobilized allowing it to be more readily available for recovery. Since most of the bubbles nucleate near the injection well, that area will be remediated first. As bubbles become entrapped, the hydraulic conductivity near the well will decrease and bubbles will be forced to travel radially outwards from the well, slowly expanding the area that has been remediated. This process would explain the fairly constant concentrations because the CO_2 bubbles would be continually reaching new areas with residual NAPL and volatilizing it. Eventually, the CO_2 bubbles would have contacted most of the accessible residual NAPL in the well's area of influence and the concentrations would decrease. Full results of the vapour sampling can be found in Appendix H.

As in phase I, the spikes in concentration were due to system re-starts (Figure 3.30) and represent the elevated concentrations that built up in the unsaturated zone of the cell during the time the extraction was not occurring. After ~9250 minutes of running time, the operation of the system was modified slightly. Up to that point, the extraction water pump would shut off unexpectedly, especially after running for 24 to 36 hours, and not start up for several hours. So it was decided to "pulse" the SWI injection (alternate between periods of injection and no injection) so that the extraction pump would not have to run for extended periods of time. The impacts of this pulsing are apparent in the PID data in Figure 3.30 from 9250 to 1400 minutes. The cyclical nature of the increases and decrease in concentration coincide with the intervals that SWI injection was operated. The intervals when the concentration was increasing correspond to times when SWI injection was occurring (with some amount of lag time for the CO_2 bubbles to travel through the cell).

The frequency of vapour sampling events was much higher during phase II than during phase I. As a result, when the total mass removed was calculated, fewer points inferred from the PID results were required (Figure 3.32). As in phase I, the trends in the lab analyzed (GC) results and the PID results matched well but the magnitudes did not always match well. This was especially the case during the first ~9250 minutes. The sampling procedures did not change; however, the alignment of the intake on the PID relative to the exhaust stream was changed several times over the course of the experiment. After ~9250 minutes, the agreement between the GC samples and the PID readings was consistently excellent.

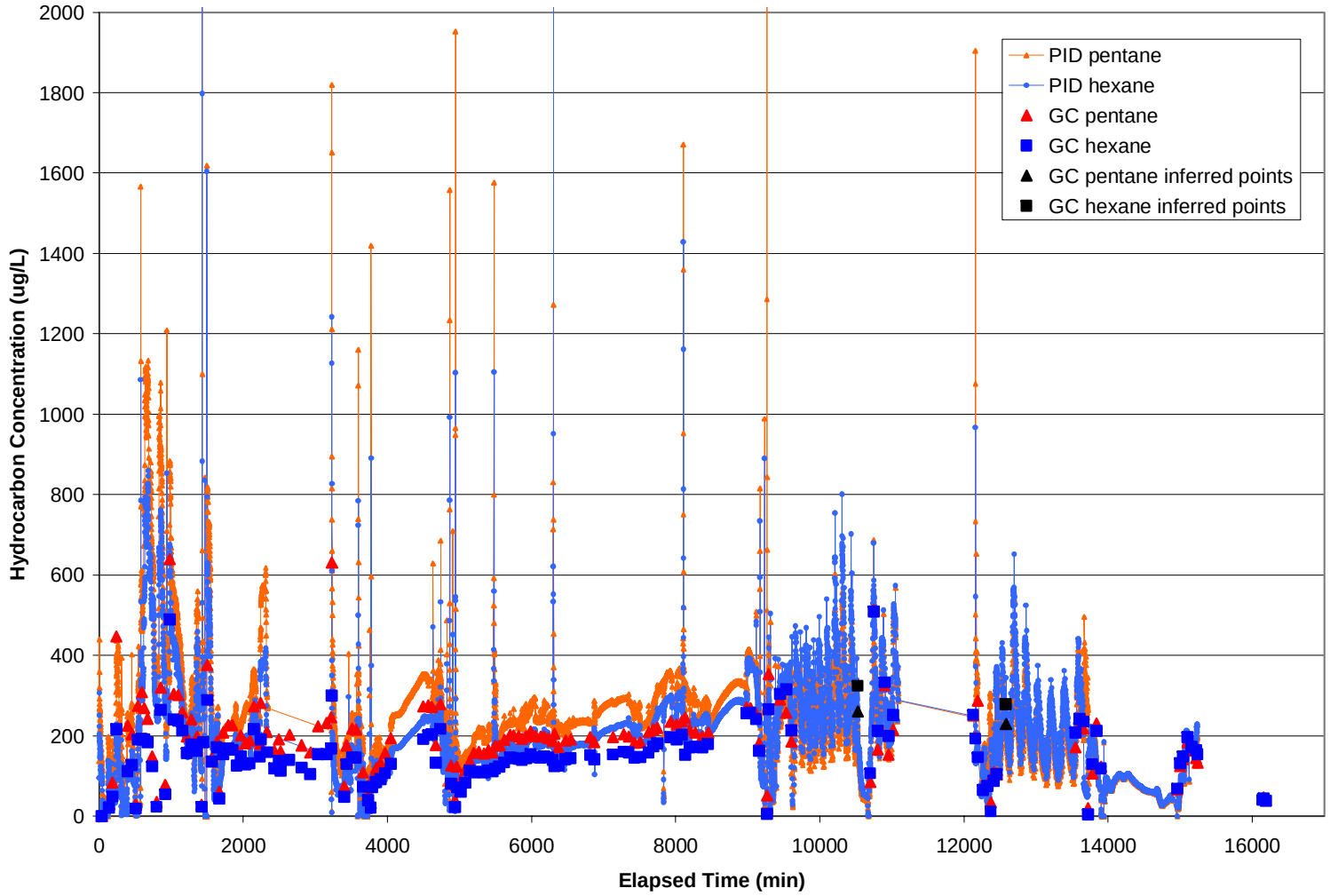

Figure 3.30. Concentration of pentane and hexane in the air extracted from the cell during phase II based on photo-ionization detector readings (PID), samples analyzed on a gas chromatograph (GC) and points inferred based on PID readings (GC inferred).

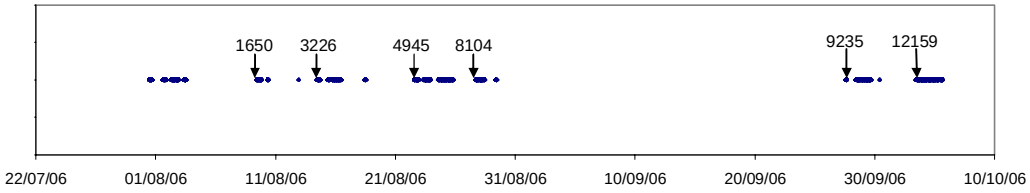

Figure 3.31. The intervals over which the system was operational (indicated by blue dots) during phase II. The numbers on the figure indicate the elapsed operational time (in minutes) at that point.

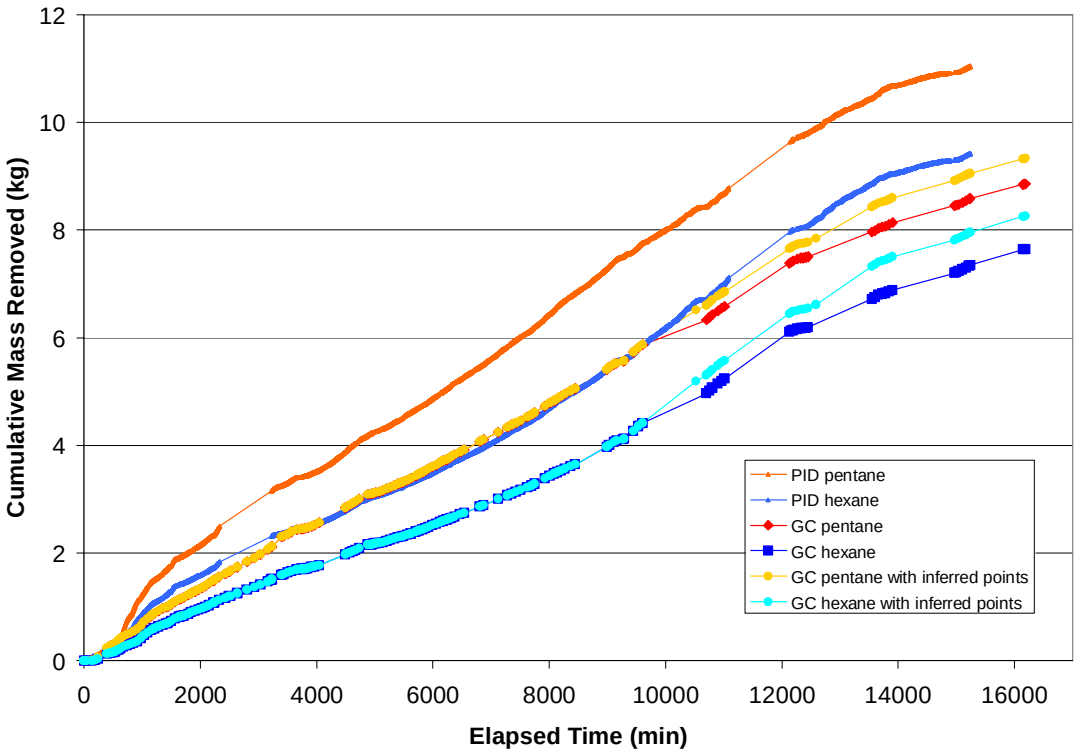

Figure 3.32 Cumulative masses of pentane and hexane removed from the cell in the vapour phase based on photo-ionization detector readings (PID), samples analyzed on a gas chromatograph (GC) and GC samples and points inferred from the PID readings (GC inferred)

Since the hydrocarbon concentrations in the exhaust were fairly consistent for most of the experiment, the cumulative mass removed versus time plots as a fairly straight line for the duration of phase II.

Pentane is more volatile than hexane so it was expected that initially the extracted vapour would be enriched with pentane relative to hexane. Johnston et al (1998) reported that the more volatile constituents of gasoline were preferentially removed during air sparging at an actual contaminated site. This general trend was observed in the data from this experiment as well (Figure 3.33). The trend is particularly clear between 5000 and 8000 minutes. In general the pentane to hexane ratio decreased from 1.4 (40% more pentane than hexane) near the beginning to 1 (equal amounts of pentane and hexane) near the end. The ratio presented here is based on mass while the original NAPL mixture had equal

volumes of each hydrocarbon. Since hexane is denser than pentane, on a mass basis the original NAPL consisted of 38% hexane and 40% pentane.

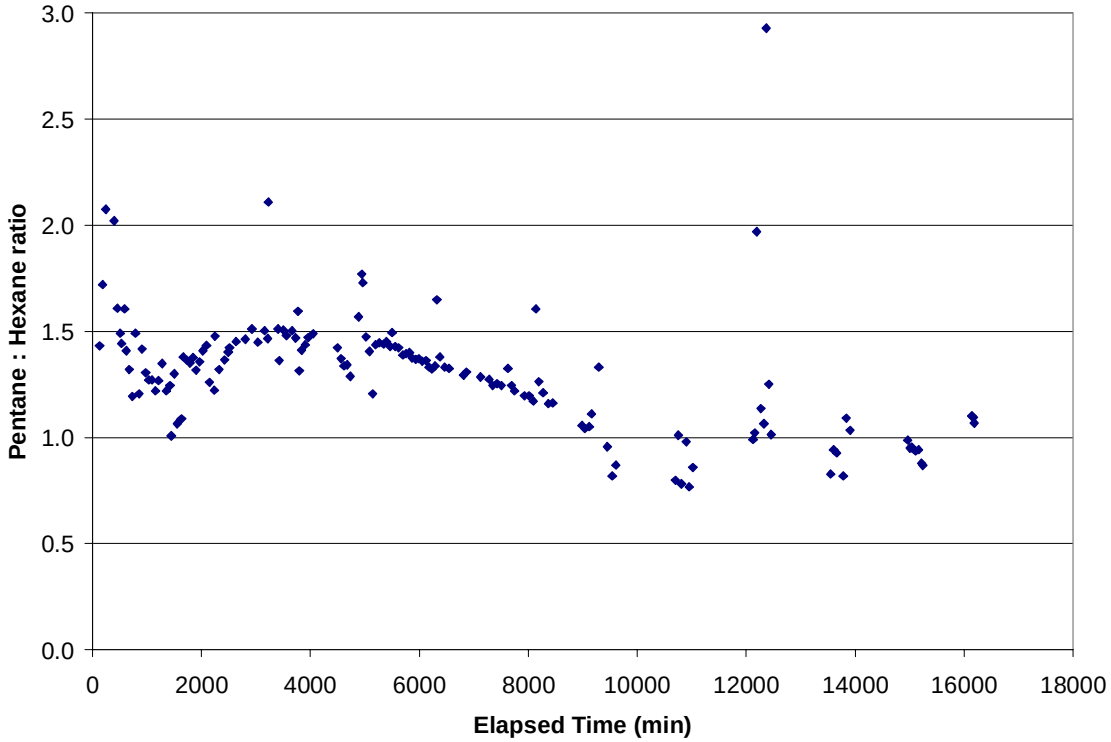

Figure 3.33 The ratio of pentane to hexane in the samples analyzed on the GC.

3.3.2. Soil Sampling

After phase II of the remediation was completed more soil sampling was done (full results in Appendix I) to determine the impact on contaminant concentration and distribution in the cell. The locations for coring were chosen based on proximity to the cores taken after phase I (S6, S7 and S8) or to examine an area that had not been previously cored (S9). However, the locations were limited by the fact that the removal of previous cores would impact the soil structure in the area. As a result, the locations selected in this round were at least 30 cm from previous locations (Figure 3.34). Due to equipment restrictions, the cores were only sampled every 10 centimeters during this sampling round. In the previous round samples were also taken at locations where there was visible red NAPL. However since the core was only exposed at the sampling locations during this round, this additional sampling was not possible. Since the additional samples targeted locations of visible NAPL, the cores from the first round of sampling would tend to have more locations with high contaminant concentrations.

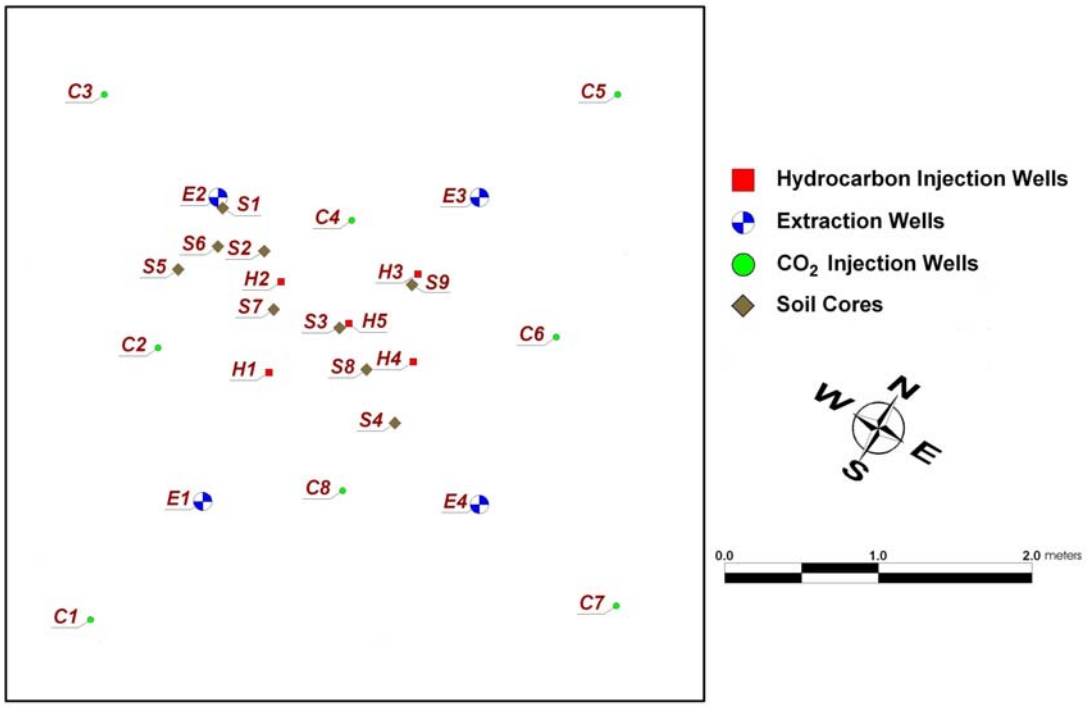

Figure 3.34 Location of soil cores taken after phase II.

3.3.2.1 S6, S7 & S8

Soil cores S6, S7 and S8 (Figure 3.34) were taken along a line nearly parallel to, and slightly south of, a line formed by the cores S1, S2, S3 and S4 which were extracted after phase I was completed. This allows a comparison to be made between the contaminant concentrations before and after phase II of the remediation. In general the contaminant concentrations indicate that there is little NAPL remaining in this area (Figures 3.35, 3.36 & 3.37). There are isolated areas where concentrations indicate the presence of NAPL, usually near the water table but in general the concentrations are low. In addition, the concentration of pentane is almost always less than that of hexane despite the fact that equal volumes of each were emplaced. Pentane is more volatile than hexane so it would be preferentially removed so these results indicate the impact of remediation in this area.

S6's location likely received CO_2 bubbles during both phases of remediation, based on the modeling (Figures 3.26 and 3.28). So despite the fact that it is close to S2, which had high contaminant concentrations, it is not unexpected that there is little evidence of NAPL remaining after phase II (Figure 3.35).

Based on the modeling (Figure 3.26) and the manner in which the hydrocarbon injection was carried out, it is likely that high contaminant concentrations would have existed at location S7 after phase I was completed. The predictive modeling of phase II (Figure 3.28) indicated that this location would receive CO_2 bubbles and based on the soil sampling results; it did (Figure 3.36). Considering its proximity to S2 and S3, the cores

with the highest contaminant concentrations after phase I, it is remarkable to little contamination was found in S7.

S8 is in a similar location to S7 in that it likely had a lot of NAPL initially and was only remediated during phase II. Like S7, it had low contaminant concentrations (Figure 3.37) indicating only small areas containing small amounts of NAPL.

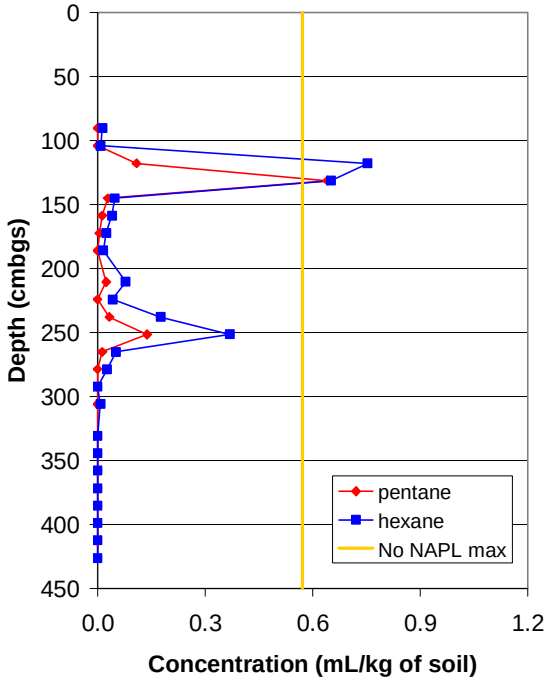

Figure 3.35. Concentration of pentane and hexane in soil samples from soil core S6.

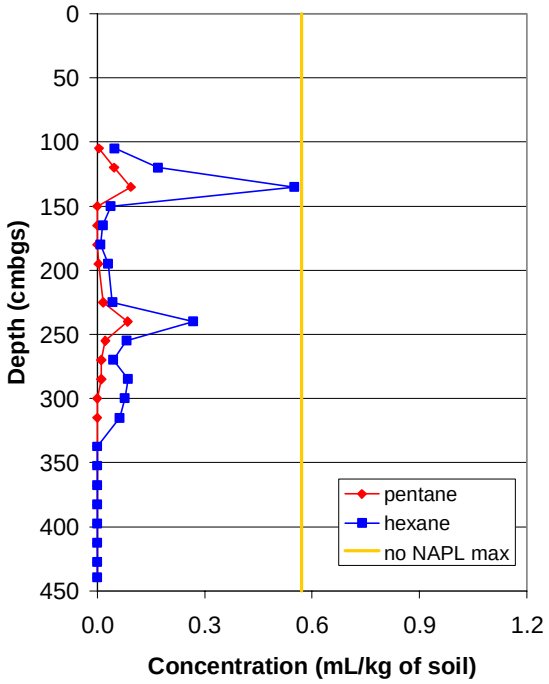

Figure 3.36 Concentration of pentane and hexane in soil samples from soil core S7.

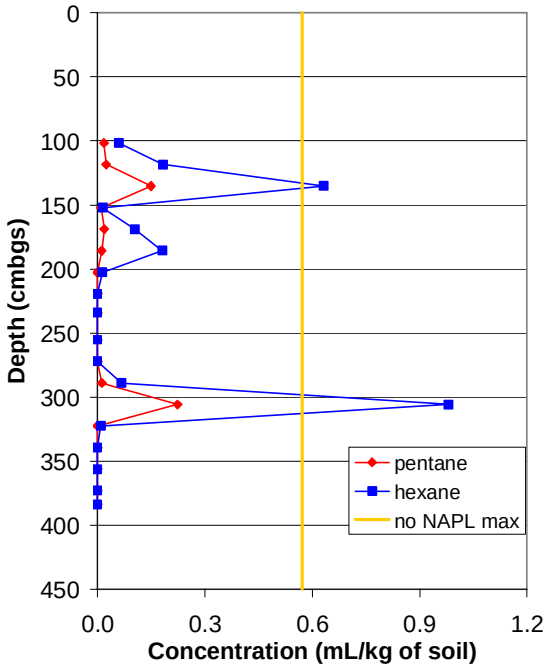

Figure 3.37 Concentration of pentane and hexane in soil samples from soil core S8.

3.3.2.2 S9

Soil core S9 had by far the highest concentrations of contaminants from this round of soil sampling (Figure 3.38). However, they are lower than the concentrations in cores S2 and S3 which were taken between phase I and phase II. Concentrations indicating the presence of NAPL were found between 200 cm and 270 cm as well as between 110 cm and 150 cm. The higher concentrations of hexane than pentane indicate that the area has been impacted by remedial efforts despite the continued presence of NAPL. Even though little contaminant mass was recovered from the quadrant, this location would likely have been impacted by CO_2 bubbles during phase II when extraction was occurring from any of the wells, for example E2 (Figure 3.28).

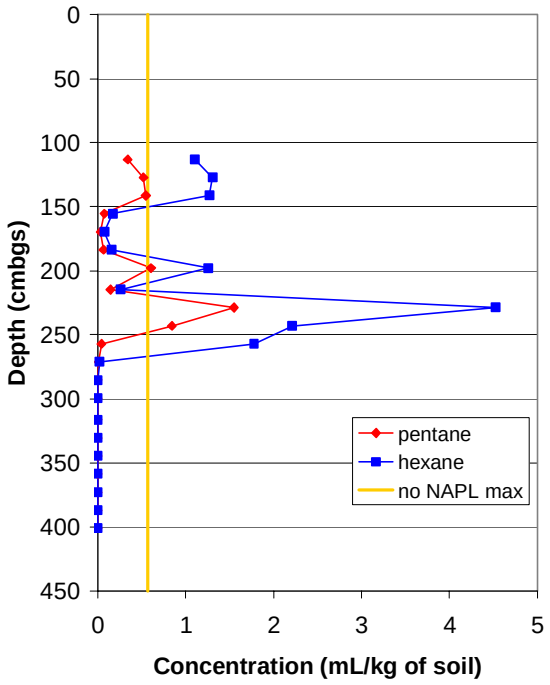

Figure 3.38 Concentration of pentane and hexane in soil samples from soil core S9.

4. Interpretation and Summary of Results

4.1. Removal of NAPL and Dissolved Components

As shown in section 3.2.2, the mass of contaminants removed in the aqueous phase was negligible in comparison to the mass removed in the vapour phase. The mass of both pentane and hexane removed in the aqueous phase was 0.1% of the initial mass. Considering the very low solubility of each of the contaminants this was expected.

Li (2004) reported that mobilization was a significant removal mechanism during SWI experiments at the laboratory scale, especially for less volatile contaminants. In those experiments mobilization occurred when the contaminant formed a film of NAPL around the CO_2 bubble after the bubble contacted residual NAPL ganglia. This film stayed in place around the bubble as it rose through the sand and formed a layer of NAPL at the water table before being removed. However, during this experiment there was no evidence of significant NAPL mass being removed from the cell. During phase I, any extracted LNAPL would have formed a layer in the isolation tank; no presence or evidence of NAPL was ever recorded during inspections of the tank. During phase II, a sheen of what appeared to be hydrocarbons was observed several times floating on top of the water in the storage. The sheen, however, would have comprised a negligible amount of mass.

However, the soil cores taken after phase II all have much higher concentrations of hexane near the water table than in most of the rest of the core (although there are some locations deeper in the core that also have elevated concentrations). The hexane concentrations near the water table are very close to the concentration that would indicate the presence of NAPL. This indicates that there may or may not be NAPL at this elevation but there is not a high enough to form a free phase. The exact concentration required for a free phase to be possible was not determined but it would be significantly higher than the concentration required for the presence of NAPL.

This elevated concentration of hexane near the water table could indicate that mobilization is occurring but the quantities mobilized are not large enough to form a layer of free phase at the water table that could be drawn into an extraction well. Unfortunately Soltrol concentrations were not analyzed in the soil samples so the presence of Soltrol at elevated concentrations near the water table can not be verified. However, it is possible that Soltrol has been mobilized and has been concentrated near the water table but not at high enough concentrations to form a free phase that could be drawn into an extraction well. This may explain why virtually no Soltrol was recovered by the extraction system. The fact that a significant amount (the actual amount was not determined because not enough was mobilized in this experiment) of contaminant must be mobilized to the water table before an extraction system can remove them from the subsurface will likely be a limitation on the mobilization component of this remediation technique.

4.2. Evaluation of Efficacy

In previous sections, and in much of the published literature, one of the main parameters used to evaluate performance is the concentration of contaminant in the air extracted from the subsurface. Figure 4.1 presents concentration of pentane and hexane in the extraction air for samples analyzed with a gas chromatograph over the entire experiment. However, these concentrations are highly dependant on the amount of air that is drawn into the cell by the dual phase extraction system. In this experiment the extracted air consisted of less than ten percent carbon dioxide from the SWI system (Figure 4.2). The remaining air was either atmospheric air that was drawn through the gravel layer of the cell after entering through one of the vent wells or dilution air drawn into the vacuum pump to keep it from overheating (phase I).

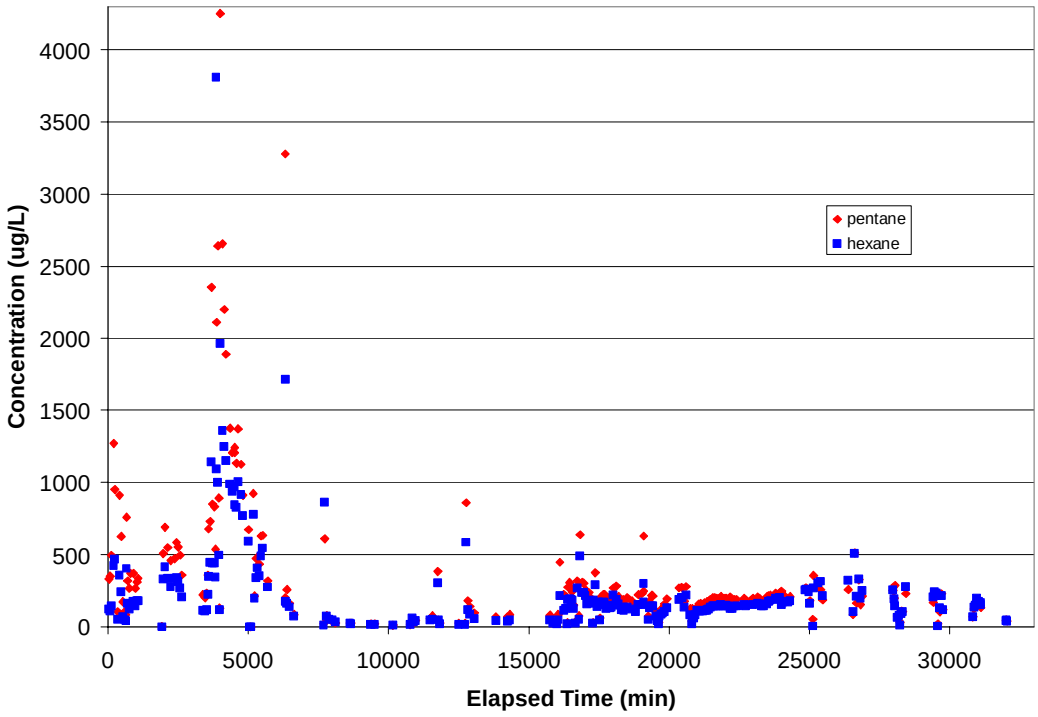

Figure 4.1 The concentration of pentane and hexane in the extracted air in samples analyzed with a gas chromatograph.

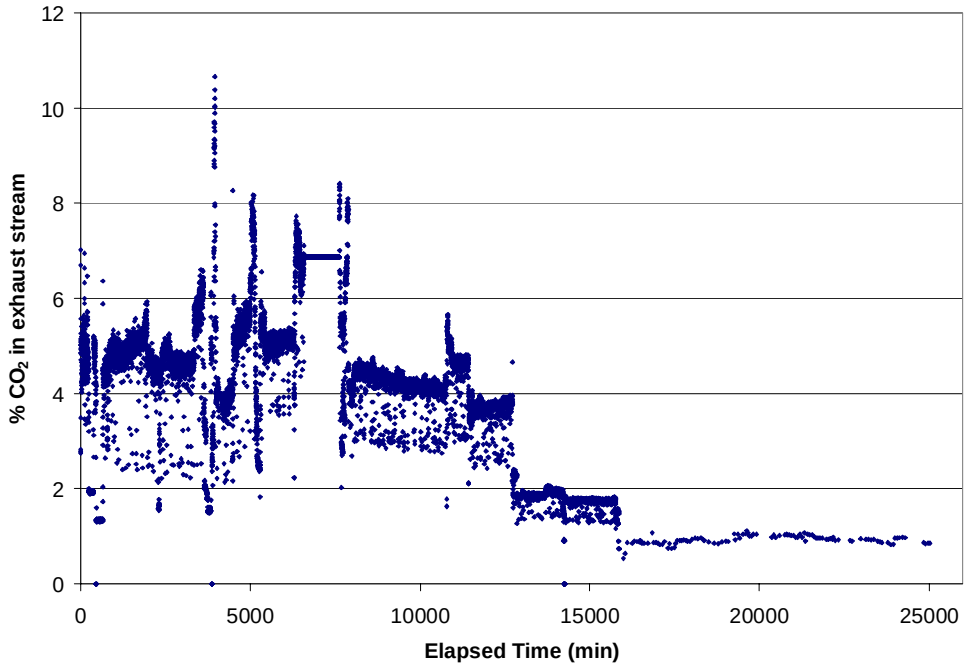

Figure 4.2 The percentage of the extracted air that was carbon dioxide injected with the SWI system, on a volume basis.

The percentage of CO_2 in the extracted air was primarily dependant on how the system was operated. The decrease from four percent to two percent at 13000 minutes was due to one of the injection points breaking, so from 13000 minutes to 16000 minutes the injection was through two wells instead of three. Phase II began at 16000 and the extraction system used from then on extracted air at a higher rate resulting in the CO_2 comprising a smaller percentage of the total gas extracted.

The amount of CO_2 injected was calculated based on logged values of the water pressure in the GI generator and the CO_2 saturated water injection rate. The maximum concentration of CO_2 in water (C_0) is dependant upon the water pressure (P_l) and can be calculated with Henry's Law:

$$C_0 = \frac{P_l}{H} \qquad \textbf{Equation 4.1}$$

H is the Henry's coefficient and for CO_2 in water at 10 C it is 1227 atm/mol fraction CO_2. However, since the water is flowing through the GI generator there is not sufficient time to reach equilibrium concentrations of CO_2 in water due to mass transfer limitations. Based on laboratory results, the GI generator will provide a CO_2 concentration of 4.3 g/L at a flow rate of 18 liters per minute and 52 pounds per square inch of pressure at 15 C. The equilibrium concentration for those conditions is 9.0 g/L. Since those conditions are similar to those in this experiment, a correction factor of 0.48 (4.3/9) was applied to the equilibrium concentrations to estimate the CO_2 concentration in the injected water. The water flow rates were logged in the field enabling the CO_2 flow rate to be calculated.

As mentioned above, the contaminant concentration in the extracted air may not be the best way to evaluate the performance of a remediation system. A potentially more useful measure of effectiveness is the contaminant mass removed per volume of injected gas phase, which is CO_2 in this case (Figure 4.3). This has been called the remediation efficiency by other authors (e.g. Thomson & Flynn, 2000). The trends in the Figure 4.1 and Figure 4.3 are quite similar as expected but the magnitude of the concentrations in Figure 4.3 are two orders of magnitude higher in general. This is also to be expected because the injected CO_2 comprises between one and ten percent of the extracted air.

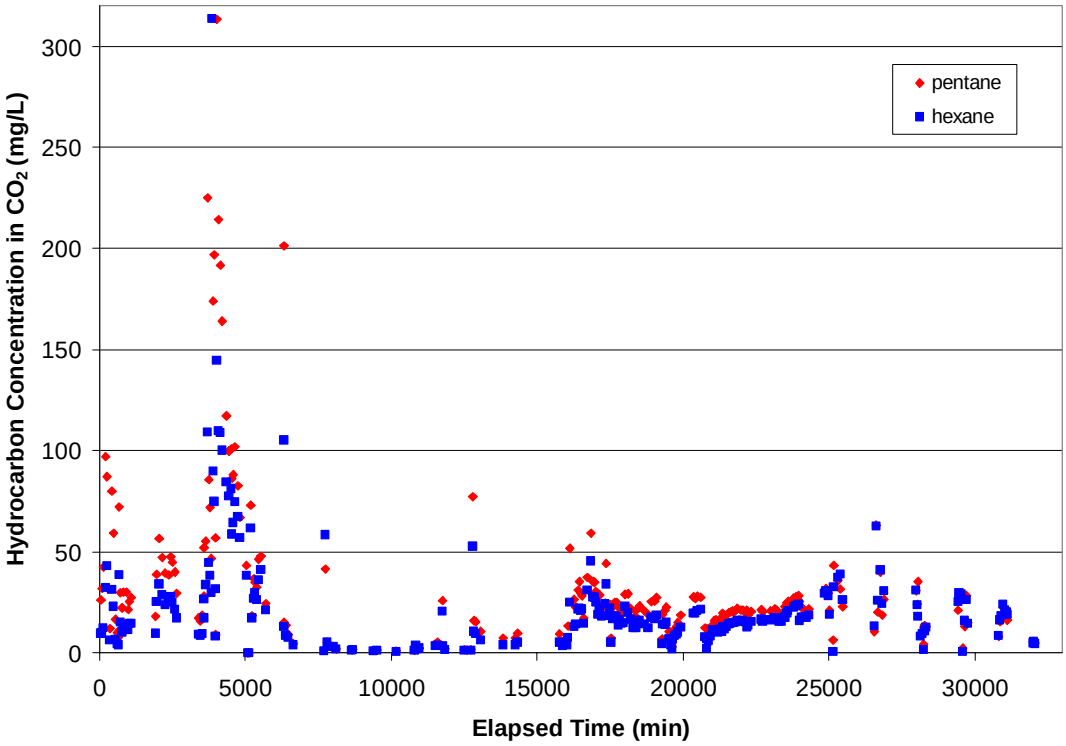

Figure 4.3 Calculated concentration of pentane and hexane in the CO_2.

To take this analysis a step further, the percent saturation of each hydrocarbon in the CO_2 can be evaluated as another measure of efficiency. In order to calculate the percent saturation in the CO_2, the composition of the NAPL in contact with the CO_2 must be known. Since the initial masses of the components of the NAPL are known as is the amount removed at each sampling time, the composition of the remaining NAPL can be calculated at each sampling time. To do this it has been assumed that the mass of Soltrol 130 does not decrease over the duration of the experiment because only a negligible amount of mass was removed (Section 4.1). Figure 5.4 shows the changing composition of the NAPL over time with the pentane becoming depleted and the hexane and Soltrol becoming enriched over time.

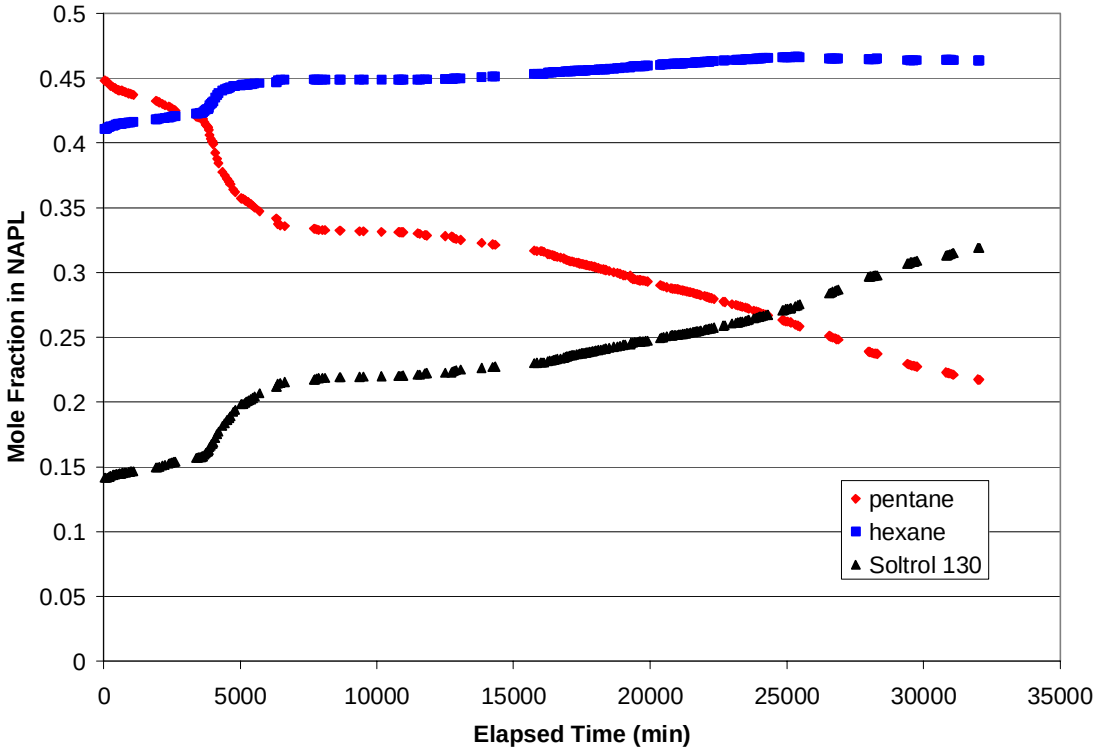

Figure 4.4 The mole fraction remaining in the NAPL over time of each of the three hydrocarbon components based on the mass of each component removed in the vapour phase.

Using this data, we can calculate the maximum concentration in the CO_2 in equilibrium with the NAPL from Raoult's Law, which can be expressed as:

$$C = \frac{m_w pX}{RT} \qquad \textbf{Equation 4.2}$$

Where C is the concentration of the contaminant in equilibrium with the NAPL, m_w is the molecular weight, p is the vapour pressure, X is the mole fraction in the NAPL, R is the universal gas constant (8314.427 L Pa K^{-1} mol^{-1}) and T is the temperature (293 K). This assumes that the activity coefficient is one. The values used are presented in Table 5.1.

Contaminant	**w (g/mol)**	**p (Pa)***
Pentane	72.5	68330
Hexane	86.6	20164
Soltrol 130+	163	16

Table 4.1 Table of contaminant characteristics for calculating the concentration in equilibrium with the remaining NAPL. + Molecular weight (w) is an average of the hydrocarbons in Soltrol 130 and the vapour pressure (p) is that of dodecane. * (Mackay et al, 1992).

Using the above data a graph of the percent saturation of the CO_2 for each contaminant can be constructed (Figure 4.5). The temporal trends are very close to the trends in the concentrations in the extracted air (Figure 4.1) and in the CO_2 (Figure 4.3). The most

notable aspect is the fact that the hexane concentrations are closer to saturation than the pentane concentrations despite the pentane concentrations being higher.

Also notable is the fact that the level of saturation is almost always less than 40% and usually less than 20% for both pentane and hexane. Based on the rate that CO_2 was introduced into the subsurface, which is significantly lower than the air injection rate in air sparging, it is interesting to note that the levels of saturation are so low. The lower injection rate and the resulting increased residence time would be expected to increase the levels of saturation. However, the experimental design may be at least part of the reason that the CO_2 is not close to being saturated with contaminants. During phase I, four of the injection wells (C1, C3, C5 and C7) were located in areas where the CO_2 injected through them likely never reached contaminated regions. Due to the way that the system was operated, these wells accounted for approximately one third of the total injection flow at any time during phase I. However, even if it were assumed that all of the extracted hydrocarbons were removed in the CO_2 from two injection wells (as opposed to three) the saturation level would only increase by fifty percent. Also, in phase II there was only one injection point and it was located in the center of the area that was still contaminated. Or, it may be that channeling is occurring, despite previous laboratory evidence to the contrary, and the low saturation levels are due to the majority of the CO_2 rising through the saturated zone in channels. However, there is no direct evidence of channeling occurring.

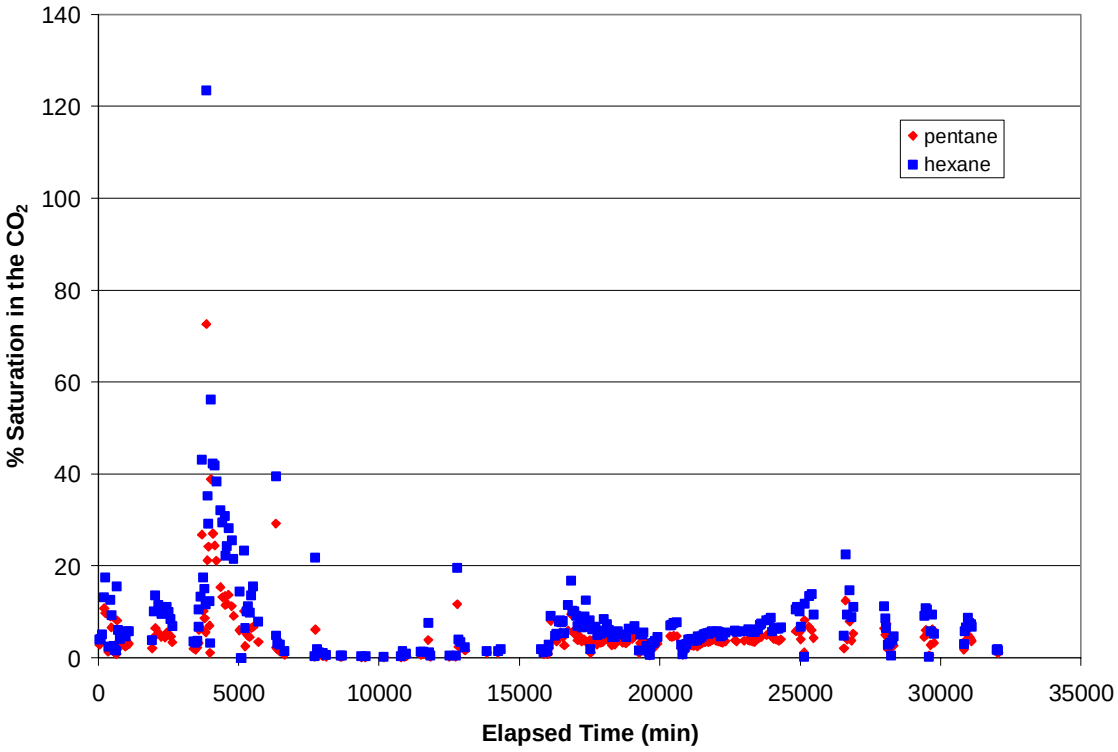

Figure 4.5 The percent saturation of pentane and hexane in the CO_2 injected by the SWI system.

The most likely explanation for levels of saturation around ten percent is that a significant number of the CO_2 bubbles are flowing through areas that do not contain residual NAPL. Whether this is due to the relatively small amount of contamination present or due to the formation of preferential pathways is unclear. One preferential pathway present in the cell is the area directly around the wells that was disturbed during the well installation. Doughty (2006) observed that the majority of bubbles reaching the water table did so within a few centimeters of the injection well. The injection wells used in this experiment were installed in a manner such that the disturbance was minimized but the fact that most of the CO_2 comes out of solution very soon after it enters the aquifer means that it will be very difficult if not impossible to prevent significant amounts of CO_2 from flowing upwards near the injection well. The fact that the CO_2 injection well used in phase II was installed at the same location as a soil core was removed means that the soil in that area was disturbed twice.

At different times during both phases different extraction wells (and as a result different CO_2 injection wells) were used. In both phases the majority of the mass removed was removed through E2. In phase I the reason for this appears to be that a lot of the contaminants ended up in the area near E2. The modeling of the flow paths for injected water (Figure 3.26) indicate that when E2 was being used as the extraction well, the injected water stayed in the E2 quadrant. As a result only contamination in that quadrant would have been removed during that period. In addition, during the preliminary phase when NAPL was being removed from the water table more was removed from E2 than any other well (Table 3.1) indicating that during the contaminant injection more NAPL ended up in that quadrant than the others. In phase II the primary reason that most of the mass removed was removed from E2 was that E2 was used for a longer period of time than any other well. This was primarily due to logistical reasons. The concentration in the effluent vapour was fairly constant over most of phase II (Figure 3.30), no matter which well was used. This supports the hypothesis that most of the NAPL remaining in the cell after phase I was in the center of the cell and would have been remediated no matter which extraction well was used.

	Phase I				Phase II			
	E1	E2	E3	E4	E1	E2	E3	E4
Pentane	0.54	22	1.2	0.44	0.40	6.4	-	1.9
Hexane	0.62	13	0.71	0.36	0.43	5.9	-	2.5
Total	1.3	35	1.9	0.80	0.83	12	-	4.4

Table 4.2. The masses (in kg) of the volatile compounds removed through each extraction well.

When the results of the vapour sampling, PID measurements and air extraction rate monitoring are combined, a graph of the cumulative mass removed in the vapour phase over time can be created (Figure 4.6) and the total mass removed in the vapour phase calculated (Table 4.3). By the end of the experiment, 64% of the initial mass of volatiles (pentane and hexane) had been removed. 77% of the pentane, which is the more volatile of the two, and 53% of the hexane were removed. More contaminant mass was removed in phase I (39.3 kg) than in phase II (17.6 kg) and there was much more pentane than hexane removed. In phase II nearly as much hexane was removed as pentane, 8.3 kg and

9.3 kg respectively. It should be noted that the slopes in Figure 4.6 had not leveled off by the end of the experiment and that more mass would have been removed if the experiment had continued.

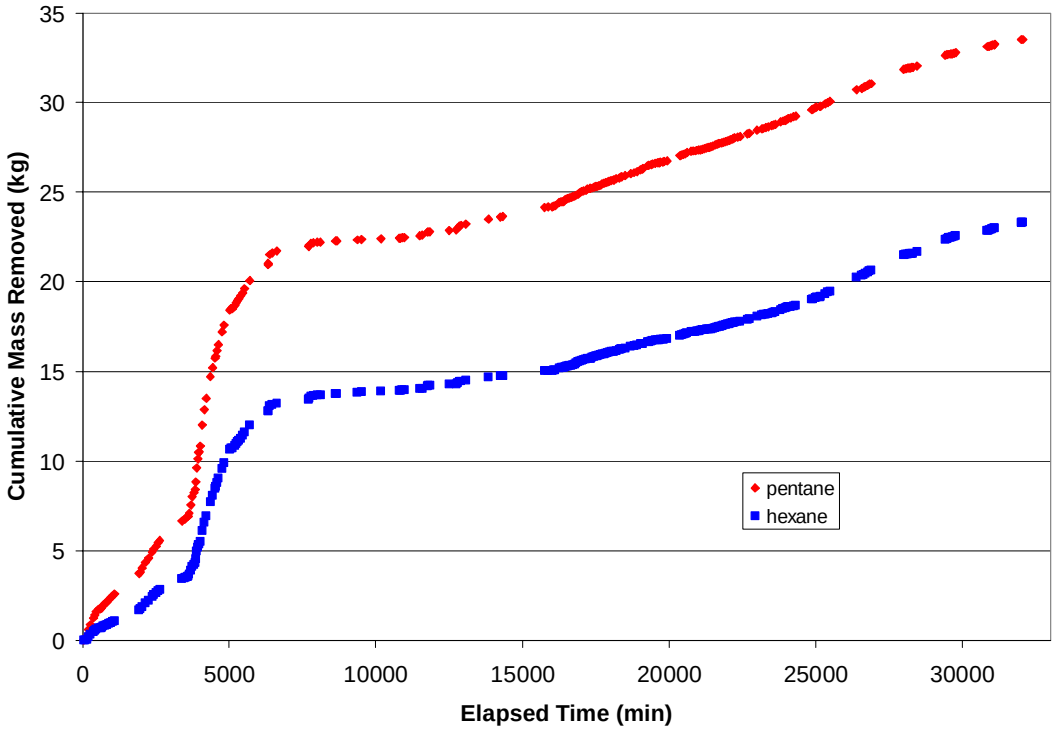

Figure 4.6 Cumulative masses of pentane and hexane removed from the cell in the vapour phase over the entire experiment.

	Pentane		Hexane		Total	
	Mass (kg)	**%**	**Mass (kg)**	**%**	**Mass (kg)**	**%**
Phase I	24	57	15	35	39	44
Phase II	9.3	20	8.3	18	17	20
Total	33	77	23	53	57	64

Table 4.3 Total masses of pentane and hexane removed in the vapour phase during the entire experiment. The percentages removed are based on the initial masses (the mass in the subsurface after the use of soil vapour extraction); 42.7 kg of pentane and 46.7 kg of hexane.

4.3. Mass Quantification using Soil Sampling

Two rounds of soil sampling were conducted; one following the completion of phase I and the other following the completion of phase II. The objective was to determine the concentration and distribution of NAPL in the subsurface. To allow for comparison between the two rounds, and to help assess the effectiveness of phase II, the cores were taken from similar locations during each round (Figure 4.7). Several of the cores were taken in a line, allowing cross-sections through the cell to be constructed from the

concentration data. Cross-section A-A' is comprised of cores taken after phase I (S1, S2, S3 and S4) while cross-section B-B' is comprised of cores taken after phase II (S6, S7 and S8). The cores taken after phase II were located at least 30 cm from where cores were removed after phase I.

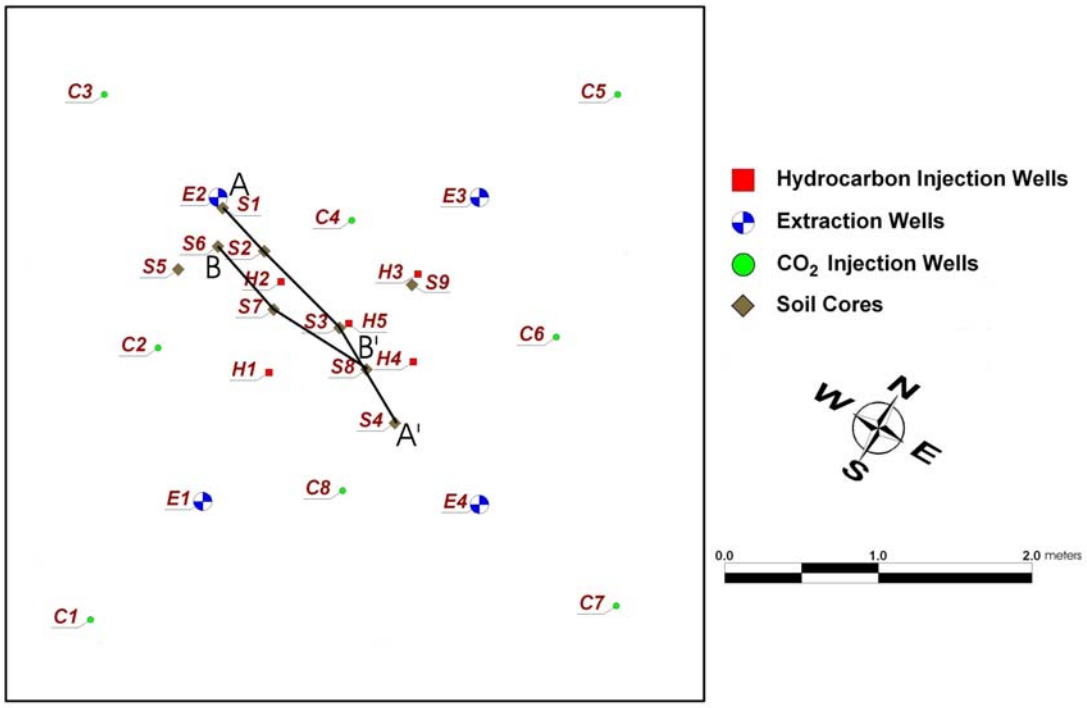

Figure 4.7. Location of the soil sampling cross-sections.

This attempt at quantification assumes that the NAPL distribution between adjacent cores can be interpolated by the results from the cores. Due to the heterogeneity of the aquifer the NAPL distribution will vary greatly over very short distances and therefore the results will only be an approximation. It is also assumed that the two cross-sections are from comparable locations. Once again, the heterogeneity of the aquifer may cause difficulties in comparing two cross sections, even though the cores used to construct the cross sections were taken from locations that are as close together as possible.

The decrease in contamination between the sampling events as a result of remediation during phase II is well represented in Figure 4.8a for pentane and Figure 4.8b for hexane. It should be noted that for the sampling event after phase one (cross-section A-A') only the data from the samples taken at regular intervals (not the data from the samples taken from areas that showed significant amounts of red dye present) is presented here to make the comparison more representative.

The impacts are most obvious for pentane where significant areas of the aquifer with contamination following Phase I have been completely remediated after phase II. Decreases up to two orders of magnitude seem to exist for a significant amount of the

cross-section. However, it should be noted that the distribution of NAPL in the subsurface is very heterogeneous (Feenstra, 2003) and as a result it is possible to miss areas of NAPL concentration. Two zones of significant pentane contamination are evident at 1.5 and 2.5 meters in both sampling events but appear to be more pronounced after phase II. This may be due to the subtle stratigraphic bedding features in the Borden sand (Mackay et al, 1986; Doughty, 2006) exhibiting some control on CO_2 bubble migration or the initial contaminant distribution. The decrease in hexane concentration is not quite as great as that of pentane which is not surprising given that significantly more pentane was removed from the cell.

Another way to evaluate the soil sampling data is to determine areas where the sampled concentrations are high enough to indicate the presence of NAPL. For pentane, concentrations above 353 mg/kg indicate the presence of NAPL while for hexane the threshold concentration is only 41 mg/kg (see Section 3.2.4 for the calculation of the concentrations). The areas with the inferred presence of NAPL are indicated in red in Figure 5.9. The fact that hexane is less soluble in water and less volatile than pentane results in the presence of hexane NAPL at lower sampled concentrations. The impact of these properties is made evident in Figure 4.9b where nearly the entire cross-section is interpreted to have the presence of NAPL after phase I. Conversely, Figure 4.9a indicates that there is little to no remaining pentane NAPL in the cross-section after phase II while there are two layers where hexane NAPL still remains (Figure 4.9b).

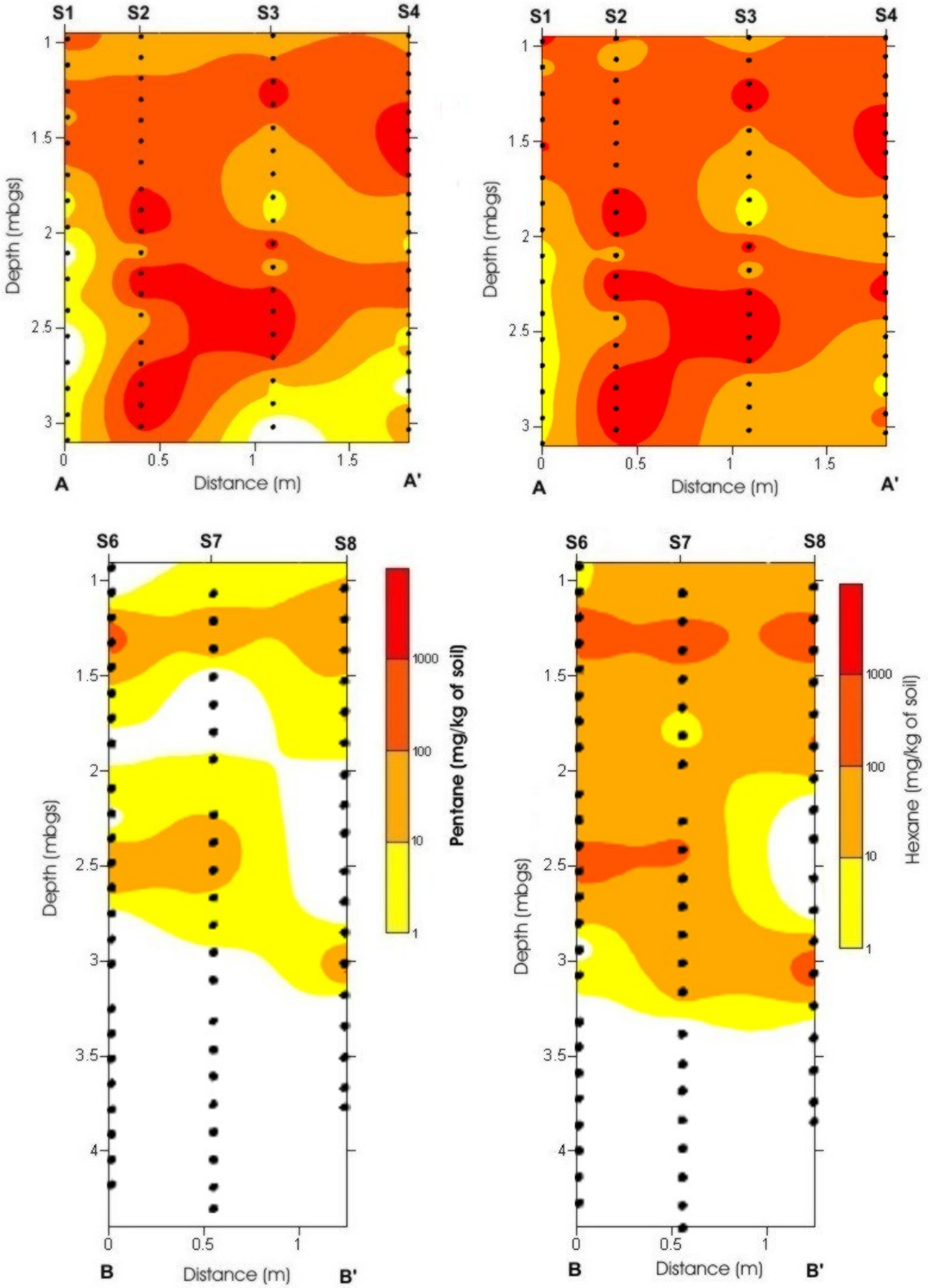

Figure 4.8. Interpolated concentrations of pentane (a) and hexane (b) in the soil sampling cross-sections (the water table during the late summer and fall would be between 1.00 and 1.50 mbgs).

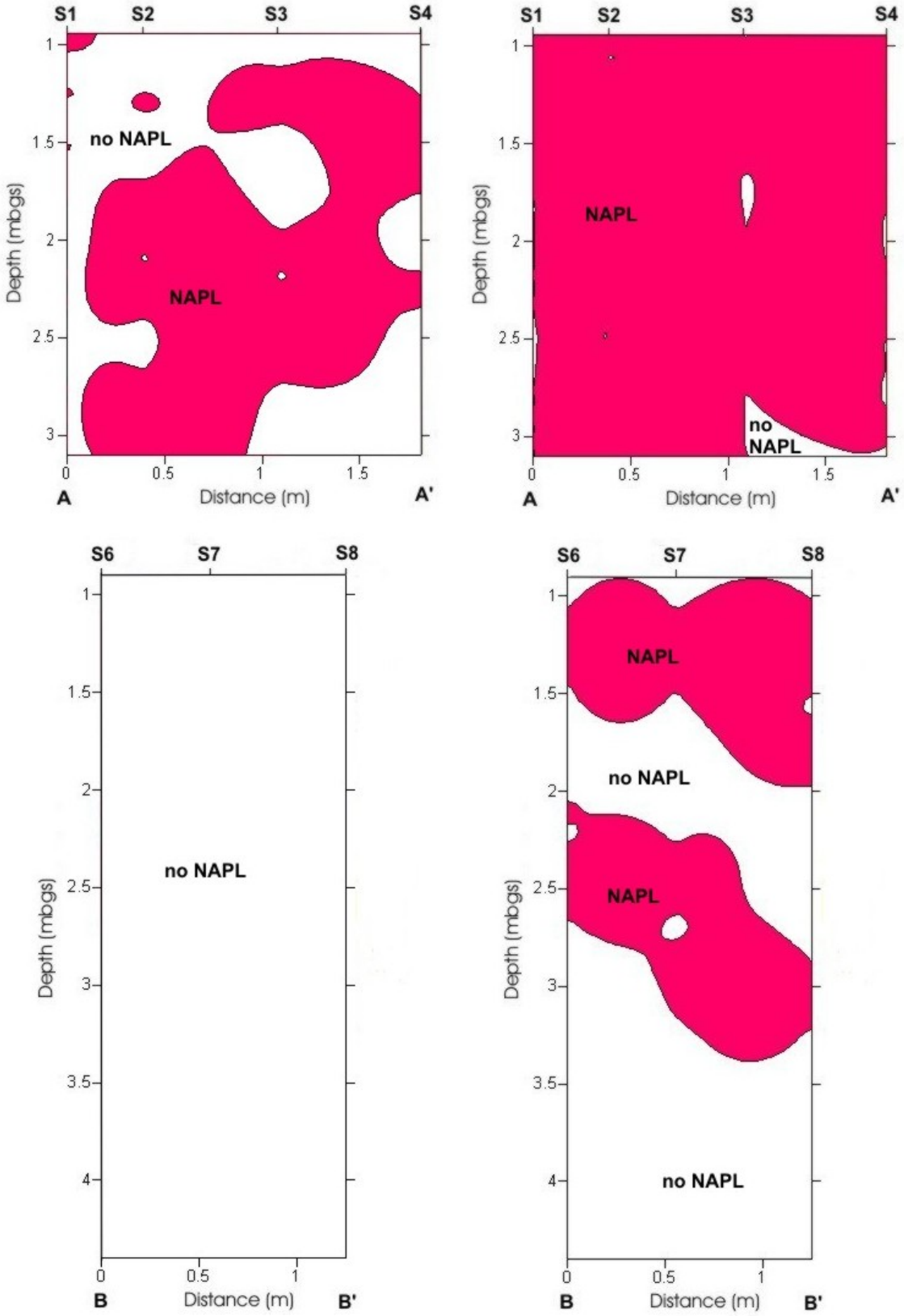

Figure 4.9. Locations of NAPL based on soil sampling concentrations for pentane (a) and hexane (b) (the water table during the late summer and fall would be between 1.00 and 1.50 mbgs).

The soil sampling results can also be used to approximate the amount of contamination remaining in the cell after each phase. The uncertainties involved in soil sampling are compounded when an attempt is made to interpolate the mass distribution throughout the cell based on a few soil cores. However an attempt to do so may provide a useful comparison to the vapour sampling and PID data. In order to estimate the mass in the cell, the volume of the aquifer impacted by the contaminants must be estimated. The horizontal extent of the spill will be estimated with a circle centered on the center of the cell (H5) with a radius equal to the distance between H5 and the extraction wells. Since the extraction wells were used to extract water during the spill, it is unlikely that any contaminants migrated significantly beyond the extraction wells. In fact, it is likely that the drawdown cones around extraction wells resulted in the area containing contaminants to have the form of a fat "X" centered on H5 with the arms extending to the extraction wells. However, there is no direct evidence of the contaminant distribution, other than the presence of free product in several wells after the spill, so a circle will be used to estimate the limits of contaminant migration (Figure 4.10).

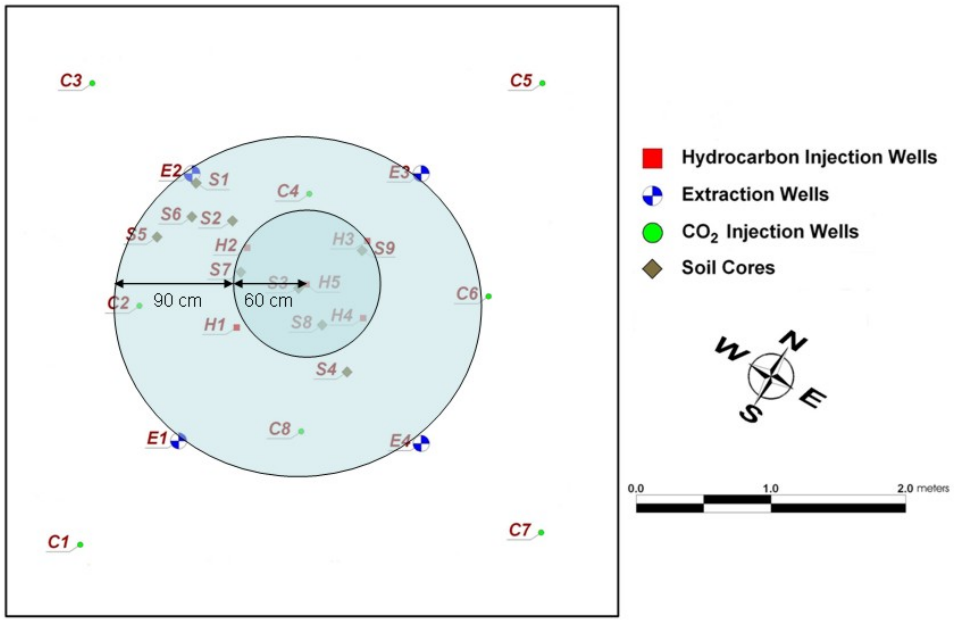

Figure 4.10. Location of zones for the purposes of an estimate of the mass remaining in the cell.

Since the center of the cell generally had higher contaminant concentrations after phase I, the interpreted zone of contamination has been divided in two, an inner zone with a radius of sixty centimeters (the distance between H5 and the other contaminant injection wells) and an outer zone consisting of the rest of the interpreted contamination zone (Figure 4.10). In order to arrive at a representative value for each soil core, the following formula was used:

$$C_s = C\rho_b d \qquad \textbf{Equation 4.3}$$

Where C_s is the surface concentration (which is the average mass of contaminant per unit of cell surface area), C is the concentration of contamination in the soil, ρ_b is the bulk density (1.8 g/cm^3 for Borden sand (Mackay et al, 1986)) and d is the length of the soil core. This formula was used to account for the fact that each soil core was a different length (Table 4.4). Once a surface concentration had been calculated for each soil core, all of the cores in each of the zones were averaged together and multiplied by the surface area of the zone to arrive at the total contaminant mass in the zone (Table 4.5).

Soil Core	C (mg/kg)		d (cm)	C_s (mg/cm^2)	
	Pentane	Hexane		Pentane	Hexane
S1	151	306	213	58	117
S2	1445	1705	206	536	632
S3	1011	1326	208	379	496
S4	562	751	199	201	269
S5	751	562	209	282	211
S6	26	63	335	16	38
S7	8	46	335	5	28
S8	16	82	282	8	42
S9	142	445	282	72	226

Table 4.4. Concentrations of hexane and pentane in soil cores.

Contaminant	Phase I			Phase II			Total Removed Mass (%)
	Remaining Mass (kg)	Removed Mass		Remaining Mass (kg)	Removed Mass		
		(kg)	(%)		(kg)	(%)	
Pentane	20	22	53	1.3	19	45	97
Hexane	24	23	49	3.4	20	44	93
Total	44	55	51	4.6	40	44	95

Table 4.5. Masses removed from the cell based on soil sampling data.

The soil sampling conducted after phase I matches the vapour sampling and PID data well considering the uncertainties involved. Overall it overestimates the total mass removed and the mass of hexane removed but it underestimates the mass of pentane removed, compared to the vapour/PID results. The relative volatilities of pentane and hexane indicate that pentane should be preferentially removed and so on that basis, the vapour/PID results are more credible. For phase II the results from the soil sampling indicate substantially more mass removal than the vapour/PID results. This is likely due to the cores being taken from locations that are not representative of the cell as a whole. Three of the cores (S6, S7 & S8) were taken from areas that would have been significantly impacted by CO_2 bubbles during extraction from E2 which is the area that received most of the attention during both phases. The low contaminant concentrations in this area, especially in comparison to the high concentrations in the area following phase II, indicate that the remediation was very effective in the target area but that those cores are not necessarily indicative of conditions in other areas of the cell. Finally, the overall mass removal based on the soil cores, which is approaching 100%, is too high to be credible based on the vapour/PID results, Li's (2004) lab results for SWI and the results for SVE at Borden (Thomson & Flynn, 2000).

4.4. Comparison to Other Remediation Methods

Unfortunately, there are no field studies in the literature where air sparging was used to remediate an emplaced source of known mass. However, other technologies have been tested in settings similar to this experiment but they used DNAPLs as the contaminant. Thomson and Flynn (2000) evaluated SVE in a test cell at Borden and recovered 63% of the available mass of perchloroethylene (PCE). It should be noted that SVE would usually be used as a complimentary technology to SWI, as it often is with air sparging. Two studies that have been reported in the literature were conducted in cells at Dover Air Force Base in Delaware. The subsurface at Dover consists of layers of sand and silty sand (Brooke et al, 2004), and so significantly more stratified and heterogeneous than Borden. Brooks et al (2004) used cosolvent flushing with ethanol to remove 64% of the 91.7 liters emplaced PCE in 40 days, although they believed that more mass would have been recovered if it would have been possible to continue. Childs et al (2006) used surfactant flooding to remove 68% of the 77.9 liters of PCE emplaced without allowing downward migration of the mobilized DNAPL.

The field studies of air sparging in the literature were conducted at contaminated sites that have significantly more than 200 liters of contamination. This makes it difficult to compare masses removed or remediation efficiencies (defined as the mass of contaminant per volume of gas injected). The most applicable comparison is with a pilot scale test by Johnston et al (2002) that calculated the concentration of VOCs in the sparged air at a heavily contaminated site. They determined that the concentration of VOCs in the sparge air was near saturation for the first five days of operation. However, after the test, soil sampling revealed that concentrations of those VOCs had not significantly decreased because contamination from other areas of the site was continuously migrating to the area they were remediating. In a hydraulically isolated cell there is little migration of contaminants into remediated areas. The difficulty in comparing these two studies is further exacerbated by the locations of the CO_2 injection points in relation to the location that the contaminants ended up in this experiment. For example, injection points C1, C3, C5 and C7 were well removed from the center of the cell where the contamination was apparently concentrated, so that the CO_2 injected through them likely never contacted any contaminants. As a result this CO_2 essentially dilutes the CO_2 that did contact and volatilize NAPL and decreases the remediation efficiency. At the site used by Johnston et al the continued influx of NAPL resulted in a high remediation efficiency and a large amount of mass removed for the scale and duration of the test.

One disadvantage of SWI is that it will likely cost more than air sparging. Most of the equipment costs are the same but SWI requires GI generators and tanks of CO_2. For this experiment the tank delivery cost $1,000, the tank rental was $350 per month and the price of CO_2 was $0.34 per pound. The cost of the dual phase recovery system was xxx. The operating labour costs were estimated as xxx. They are high due to the frequent system upsets and restarts. All prices are in Canadian dollars.

In comparison to the evaluations of the flushing remediation technologies at Dover mentioned above, this study removed a comparable percentage of the initial mass. This is some encouragement for further testing of the SWI.

5. Conclusions

SWI with CO_2 was successful in removing nearly two thirds (64%) of the initial mass of volatile hydrocarbon NAPL (pentane and hexane) from a hydraulically isolated section of the Borden aquifer. The removal was greater for pentane which is the more volatile of the two. 34 kg of pentane were removed, which represents 77% of the initial mass while 22 kg of hexane were removed and this represents 53% of the initial mass. The remediation system operated for 22.25 days over an experimental period of three months, reflecting technical difficulties. Soil sampling indicated significant reductions in NAPL concentrations due to removal by volatilization.

Only a negligible amount of the original mass of non-volatile NAPL (Soltrol 130) was recovered. In laboratory experiment Li (2004) was able to mobilize and collect non-volatile NAPL but there was little evidence of this removal mechanism operating effectively during this experiment.

The success of this trial, and the previous laboratory and modeling work, indicate that this remediation technology likely has viable applications at actual contaminated sites. However, further evaluation of the operational limitations and economics should be investigated at the pilot scale first.

6. Recommendations

- In order to verify the mobilization of Soltrol to the water table soil cores should be from the cell and analyzed for the presence of Soltrol. These cores would not have to be as deep as the ones removed after phase I and phase II, a depth of 1.75 meters below the ground surface should suffice.

- The next step is to employ the SWI method at an actual contaminated site to determine how well the method scales up. Based on the positive results described here for a controlled site the prospects are promising for pilot- and full-scale operations.

- In order for this method to be widely applied the economics of need to be evaluated, if they have not been already.

- Horizontal wells may be a more effective way to inject CO_2 saturated water. Morgan (1992), Unger et al (1995) and Plummer et al (1997) have shown that there are advantages to horizontal wells for air sparging and those advantages may apply to SWI as well. An additional benefit would be that the disturbed area around the well from installation activities would no longer be vertically oriented and therefore would not form a preferential pathway to the surface. If horizontal wells are not used, it would be beneficial to explore other installation methods for the CO_2 injection wells that minimize disturbance to the surrounding soil.

- During this work and that of Doughty (2006) the CO_2 injection points were built by hand and the design finalized by field testing. Before this technology can be advanced, a better way of manufacturing the points must be found. This may result in points made with small holes (similar to the ones used here) or a screen or some other configuration. In addition, a method of correlating the size and number of holes or the size of the screen and mesh size or whichever variables control the water pressure and flow rate and the water pressure and flow rate needs to be developed. This method will have to incorporate the effects of the aquifer on pressure and flow as well, and these effects may be different for different aquifer materials.

- The use of packers to inject at different depths may also be beneficial. For example, low hydraulic conductivity layers may impede vertical migration of bubbles so being able to apply SWI above and below such a layer at the same or at different times may shorten the time required to remediate a site. Near the end of phase I one of the CO_2 injection points was manually raised to determine if this had any impact on the concentrations of contaminants in the extracted vapour. Unfortunately the action of raising the injection well caused the holes in the injection point to become clogged so no results were obtained.

Bibliography

Adams, J.A and K.R. Reddy. 1999. Laboratory Study of Air Sparging of TCE-Contaminated Saturated Soils and Ground Water. *Ground Water Monitoring & Remediation. 19(3)*: 182-190.

Adams, J.A. and K.R. Reddy. 2003. Extent of Benzene Biodegradation in Saturated Soil Column During Air Sparging. *Ground Water Monitoring and Remediation. 23(3)*: 85-94.

Aelion, C.M. and B.C. Kirtland. 2000. Physical versus Biological Hydrocarbon Removal during Air Sparging and Soil Vapour Extraction. *Environmental Science & Technology. 34*: 3167-3173.

Ahlfeld, D.P., A. Dahmani, and W. Ji. 1994. A Conceptual Model of Field Behavior of Air Sparging and Its Implications for Application. *Ground Water Monitoring and Remediation. 14(4)*: 132-139.

Baehr, A.L., G.E. Hoag and M.C. Marley. 1989. Removing Volatile Contaminants from the Unsaturated Zone by Inducing Advective Air-Phase Transport. *Journal of Contaminant Hydrology. 4*: 1-26.

Barbaro, J.R. 1999. *Enhanced Bioremediation of Dissolved Aromatic Hydrocarbons within a Gasoline Source Area Using Nitrate and Oxygen as Electron Acceptors.* Ph.D. Thesis. University of Waterloo.

Bass, D.H., N.A. Hasting, and R.A. Brown. 2000. Performance of Air Sparging Systems: A Review of Case Studies. *Journal of Hazardous Materials. 72*:101-119.

Benner, M.L., R.H. Mohtar and L.S. Lee. 2002. Factors Affecting Air Sparging Remediation Systems Using Field Data and Numerical Simulations. *Journal of Hazardous Materials. B95*: 305-329.

Brooks, M.C., W.R. Wise and M.D. Annable. 1999. Fundamental Changes in In Situ Air Sparging Flow Patterns. *Groundwater Monitoring and Remediation. 19 (2)*: 105-113.

Brooks, M.C., M.D. Annable, P.S.C. Rao, K Hatfield, J.W. Jawitz, W.R. Wise, A.L. Wood and C.G. Enfield. 2004.Controlled release, blind test of DNAPL remediation by ethanol flushing. *Journal of Contaminant Hydrology. 69:*281-297.

Capuano, R.M. and M.A. Johnson. 1996. Geochemical Reactions During Biodegradation/Vapor-Extraction Remediation of Petroleum Contamination in the Vadose Zone

Chevron Phillips Chemical Company LP. 2002. *Material Safety Data Sheet – Soltrol 130 Isoparaffin Solvent*. The Woodlands, Texas.

Childs, J., E. Acosta, M.D. Annable, M.C. Brooks, C.G. Enfield, J.H. Harwell, M. Hasegawa, R.C. Knox, P.S.C. Rao, D.A. Sabatini, B. Shiau, E. Szekeres and A.L. Wood. 2006. Field Demonstration of Surfactant-Enhanced Solubilization of DNAPL at Dover Air Force Base, Delaware. *Journal of Contaminant Hydrology. 82*: 1-22.

Christiansen, J.E. 1944. Effect of Entrapped Air Upon the Permeability of Soils. *Soil Science. 58:* 355-365.

Clayton, W.S. 1998. A Field and Laboratory Investigation of Air Fingering During Air Sparging. *Ground Water Monitoring & Remediation. 18(3)*:134-145.

Do, D.D. and H.D. Do, 2002. Effects of Adsorbate-Adsorbate Interaction in the Description of Adsorption Isotherm of Hydrocarbons in Micro-Mesoporous Carbonaceous Materials. *Applied Surface Science. 196*: 13-29.

Doughty, C. 2006. *NAPL Recovery Using CO_2-Supersaturated Water Injection: Distribution of the CO_2 Gas Phase.* M.Sc. Thesis. University of Waterloo.

Edwards, D.A., J.W. Little, W. Lanik and P.A. Hajali. 2002. Calibration of a Model for Volatile Organic Campound Mass Removal by Multiphase Extraction. *Journal of Environmental Engineering. 128 (5)*: 472-475.

Feenstra, S., D.M. Mackay and J.A. Cherry. 1991. A Method for Assessing Residual NAPL Based on Organic Chemical Concentrations in Soil Samples. *Ground Water Monitoring & Remediation. 11(2)*:128-136.

Feenstra, S. 2003. Spatial Variability of Non-Aqueous Phase Liquid Chemicals in Soil - Implications for Source Zone Mass Estimates. *Environmental & Engineering Geoscience. 9(1)*: 19-23.

Feenstra, S. 2005. Soil Sampling in NAPL Source Zones: Challenges to Representativeness. *Environmental Forensics. 6*: 57-63.

Giffin, S.D. and A.P. Davis. 1998. Prediction of Carbon BTEX Adsorption Capacity Using Field Monitoring Data. *Journal of Environmental Engineering. 124 (10)*: 921-931.

Gordon, M.J. 1998. Case History of a Large-Scale Air Sparging/Soil Vapor Extraction System for Remediation of Chlorinated Volatile Organic Compounds in Ground Water. *Ground Water Monitoring & Remediation. 18(2):* 137-149.

Grattoni, C.A. & R.A. Dawe. 2003. Gas and Oil Production from Waterflood Residual Oil: Effects of Wettability and Oil Spreading Characteristics. *Journal of Petroleum Science and Engineeting. 39*: 297-308.

Gustafson, J.B., J.G. Tell and D. Orem. 1997. *Total Petroleum Hydrocarbon Criteria Working Group Series: Volume 3: Selection of Representative TPH Fractions Based on Fate and Transport Considerations.* Amherst, Massachusetts: Amherst Scientific Publishers.

Haag, W. and C. Wrenn. 2002. *Theory and Applications of Direct-Reading Photoionization Detectors (PIDs).* Sunnydale, CA: RAE Systems.

Hall, B.L., T.E. Lachmar and R.R. Dupont. 2000. Field Monitoring and Performance of an In Situ Air Sparging System at a Gasoline-Contaminated Site. *Journal of Hazardous Materials. B74*: 165-186.

Hewitt, A.D. 1996. Effect of Collection and Handling Practices on Concentrations of Volatile Organic Compounds Detected in Soil Subsamples. In *Volatile Organic Compounds in the Environment, ASTM STP 1261.* Philadelphia, Pennsylvania: American Society for Testing and Materials. p. 170-180.

Ji, W., A. Dahmani, D. Ahlfeld, J.D. Lin and E. Hill III. 1993. Laboratory Study of Air Sparging: Air Flow Visualization. *Ground Water Monitoring and Remediation. 23(4)*: 115-126.

Johnson, P.C. 1998. Assessment of Contributions of Volatilization and Biodegradation to In Situ Air Sparging Performance. *Environmental Science & Technology. 32(2)*: 276-281.

Johnson, P.C., C.C. Stanley, M.W. Kemblowski, D.L. Byers and J.D. Colhart. 1990. A Practical Approach to the Design, Operation, and Monitoring of In Situ Soil-Venting Systems. *Ground Water Monitoring and Remediation. 10(2)*: 159-178.

Johnson, R.L., P.C. Johnson, D.B. McWorter, R.E. Hinchee and I. Goodman. 1993. An Overview of In Situ Air Sparging. *Ground Water Monitoring and Remediation. 13(4)*: 127-135.

Johnston, C.D., J.L. Rayner, B.M. Patterson and G.B. Davis.1998. Volatilization and biodegradation during air sparging of dissolved BTEX-contaminated groundwater. *Journal of Contaminant Hydrology. 33*: 377-404.

Johnston, C.D., J.L. Rayner and D. Briegel. 2002. Effectiveness of in situ air sparging for removing NAPL gasoline from a sandy aquifer near Perth, Western Australia. *Journal of Contaminant Hydrology. 59*: 87-111.

Karickhoff, S. 1984. Organic Pollutant Sorption in Aquatic Systems. *Journal of Hydraulic Engineering. 110(6)*: 707-735.

Kent, B. and G.C. Bianchi Mosquera. 2001. Remediation of NAPL-contaminated aquifers: is the cure worth the cost? *Journal of Environmental Science and Health. A36(8):* 1559-1569.

Khan, F.I., T. Husain and R. Hejazi. 2004. An Overview and Analysis of Site Remediation Technologies. *Journal of Environmental Management. 71*: 95-122.

Kirshner, M., N.C. Pressly and R.J. Roth. 1996. In Situ Remediation of Jet A in Soil and Groundwater by High Vacuum, Dual Phase Extraction. *Ground Water Monitoring & Remediation. 16(4):* 73-79.

Kirtand, B.C. and C.M. Aelion. 2000. Petroleum Mass Removal from Low Permeability Sediment Using Air Sparging/Soil Vapour Extraction: Impact of Continuous or Pulsed Operation. *Journal of Contaminant Hydrology. 41*: 367-383.

Kirtland, B.C. C.M. Aelion and M.A. Widdowson. 2001. Long-Term AS/SVE for Petroleum Removal in Low-Permeability Piedmont Saprolite. *Journal of Environmental Engineering. 127 (2)*: 134-144.

Kreamer, D.K. and K.J. Stetzenbach. 1990. Development of a Standard, Pure Compound Base Gasoline Mixture for Use as a Reference in Field and Laboratory Experiments. *Ground Water Monitoring & Remediation. 10(2):* 135-145.

Leinonen, P.J. & D. Mackay. 1973. The Multicomponent Solubility of Hydrocarbons in Water. *The Canadian Journal of Chemical Engineering. 51*: 230-233.

Li, T.M.W. 2004. *Recovery of Source Non-Aqueous Phase Liquids from Groundwater Using Supersaturated Water Injection.* M.A.Sc. Thesis. University of Waterloo.

Mackay, D.M., D.L. Freyburg, P.V. Roberts and J.A. Cherry. 1986. A Natural Gradient Experiment on Solute Transport in a Sand Aquifer: 1. Approach and Overview of Plume Movement. *Water Resources Research. 22(13)*: 2017-2029.

Mackay, D., W.Y. Shiu and K.C. Ma. 1992. *Illustrated Handbook of Physical-Chemical Properties and Environmental Fate for Organic Chemicals, vol. III.* Boca Raton: Lewis Publishers.

Mills, W.B., K.M. Johnson, S Liu, J.Y. Loh and C.S. Lew. 1996. Multimedia Risk-Based Soil Cleanup at a Gasoline-Contaminated Site Using Vapor Extraction. *Ground Water Monitoring & Remediation. 16(3)*: 168-178.

Morgan, J.H. 1992. Horizontal Drilling Applications of Petroleum Technologies for Environmental Purposes. *Ground Water Monitoring & Remediation. 12(3)*: 98-102.

Musil, J. and F. Zacek. 1986. *Microwave measurements of complex permittivity by free space methods and their application*. Amsterdam: Elsevier.

Nwankor, G.I., J.A. Cherry, R.W. Gillham. 1984. A Comparitive Study of Specific Yield Determinations for a Shallow Sand Aquifer. *Ground Water. 22 (6)*: 764-772.

O'Melia, B.C. and D.R. Parson. 1996. Dual-Phase Vacuum Extraction Technology for Soil and Ground-Water Remediation: A Case Study. In *Volatile Organic Compounds in the Environment, ASTM STP 1261.* Philadelphia, Pennsylvania: American Society for Testing and Materials. p. 272-286.

Oliveira, E. 1997. *Ethanol Flushing of Gasoline Residuals – Microscale and Field Scale Experiments.* Ph.D. Thesis. University of Waterloo.

Plummer, C.R., J.D. Nelson and G.S. Zumwalt. 1997. Horizontal and Vertical Well Comparison for In Situ Air Sparging. *Ground Water Monitoring & Remediation. 17(1): 91-96.*

Reddy, K.R. and J.A. Adams. 2001. Effects of Soil Heterogeneity on Airflow Patterns and Hydrocarbon Removal during In Situ Air Sparging. *Journal of Geotechnical and Geoenvironmental Engineering. 127(3)*: 234-247.

Ryan, R.G., and V.K. Dhir. 1993. The Effect of Soil-Particle Size on Hydrocarbon Entrapment Near a Dynamic Water Table. *Journal of Soil Contamination. 2(1)*: 1-35.

Sahloul, N.A., M.A. Ioannidis and I Chatzis. 2002. Dissolution of residual non-aqueous phase liquids in porous media: pore-scale mechanisms and mass transfer rates. *Advances in Water Resources. 25*: 33-49.

Schumacher, B.A. and M.M. Minnich. 2000. Extreme Short-Range Variability in VOC-Contaminated Soils. *Environmental Science and Technology. 34*: 3611-3616.

Soga, K., J.W.E. Page, T.H. Illangasekare. 2004. A Review of NAPL Source Zone Remediation Efficiency and the Mass Flux Approach. *Journal of Hazardous Materials. 110*: 13-27.

Starr, R.C. and R.A. Ingleton. 1992. A New Method for Collecting Core Samples Without a Drilling Rig. *Ground Water Monitoring and Remediation. 12(1)*: 91-95.
Starr et al, 1992

Starr, R.C., J.A. Cherry and E.S. Vales. 1992. A New Type of Steel Sheet Piling With Sealed Joints For Groundwater Pollution Control. *Proceedings, 45th Canadian Geotechnical Conference, Toronto, Ontario, October 26-28.*

Thomson, N. and D.J. Flynn. 2000. Soil Vacuum Extraction of Perchloroethylene from the Borden Aquifer. *Ground Water. 38*: 673-688.

Thomson, N.R. and R.L. Johnson. 2000. Air Distribution During In Situ Air Sparging: An Overview of Mathematical Modeling. *Journal of Hazardous Materials. 72*: 265-282.

Tomlinson, D.W., N.R. Thomson, R.L. Johnson, and J.D. Redman. 2003. Air Distribution in the Borden Aquifer during In Situ Air Sparging. *Journal of Contaminant Hydrology. 67*: 113-132.

Unger, A.J.A., E.A. Sudicky and P.A. Forsyth. 1995. Mechanisms Controlling Vacuum Extraction Coupled with Air Sparging for Remediation of Heterogeneous Formations Contaminated by Dense Nonaqueous Phase Liquids. *Water Resources Research. 31(8)*: 1913-1925.

Waduge, W.A.P., K. Soga and J. Kawabata. 2004. Effect of NAPL Entrapment Conditions on Air Sparging Remediation Efficiency. *Journal of Hazardous Materials. 100*: 173-183.

West, O.R., R.L. Siegrist, T.J. Mitchell and R.A. Jenkins. 1995. Measurement Error and Spatial Variability Effects on Characterization of Volatile Organics in the Subsurface. *Environemntal Science and Technology. 29*: 647-656.

Wilkins, M.D., L.M. Abriola and K.D. Pennell. 1995. An Experimantal Investigation of Rate-Limited Nonaqueous Phase Liquid Volatilization in Unsaturated Porous Media: Steady State Mass Transfer. *Water Resources Research. 31 (9)*: 2159-2172.

Yang, X., D. Beckmann, S. Fiorenza and C. Neidermeier. 2005. Field Study of Pulsed Air Sparging for Remediation of Petroleum Hydrocarbon Contaminated Soil and Groundwater. *Environmental Science & Technology. 39*: 7279-7286.

Yen, H.K., N.B Chang and T.F. Lin. 2003. Bioslurping Model for Assessing Light Hydrocarbon Recovery in Contaminated Unconfined Aquifer. I: Simulation Analysis. *Practice Periodical of Hazardous, Toxic and Radioactive Waste Management. 7 (2)*: 114-130.

Appendix A

Geophysics Report

Cross-borehole ground penetrating radar measurements at Gas Infusion Test Site, CFB Borden, November 2005

Environmental Geophysics Facility
Department of Earth Sciences

prepared by Scott Piggott

for Leif Nelson

November 2006

Cross-borehole ground penetrating radar measurements at Gas Infusion Test Site, CFB Borden, November 2005

INTRODUCTION

This report presents the results of cross-borehole ground penetrating radar (GPR) surveys performed to measure changes in water content during experimental testing of a gas infusion system. Measurements were done between boreholes H4, G1 and G2 as shown in the lower right of the site layout in Figure 1 on the next page. All of the wells used as access tubes were 2 inch PVC wells.

Well H4 was previously used as a hydrocarbon injection well. The antenna lowered down this well was first wrapped in plastic to avoid contaminating the antenna. Wells G1 and G2 were installed exclusively for the borehole GPR surveys. Wells C6, C7 and C8 were used to inject carbonated water from the gas infusion generators while fluids were extracted from well E4.

Surveys were performed on November 3 and November 10, 2005 so as to be before and after water content changes caused by the operation of the gas infusion system. Measurements were attempted on Oct. 7 and Oct. 20 2005. On these dates the equipment malfunctioned and needed repairs and valid measurements were not obtained.

Borehole GPR

Borehole GPR has become a useful method for measuring the distribution of subsurface physical properties between boreholes as shown by previous studies (e.g. Parkin et al., 2000, Gilson, 1996 and Gilson et al., 1996). Electromagnetic (EM) wave propagation from one borehole to another is controlled by the velocity and the attenuation of the material between the holes. The velocity and attenuation are directly determined by measuring the travel time and amplitude respectively, of radar waves passing from one borehole to another. The velocity can be used to obtain a measure of the water content and the attenuation can be used to estimate the electrical conductivity. In these surveys, the method was used to determine the water content.

In normal practice, the average value of the EM wave velocity is measured for the ray path between the location of a transmitter in one borehole and a receiver in another borehole a known distance away. The velocity is obtained by dividing the known distance by the measured travel time. From the velocity, the average water content along the ray path can be calculated as follows.

The water content is obtained from the measured velocity (V) by first calculating the relative dielectric permittivity (also known as the dielectric constant) K:

$$K = \frac{c^2}{V^2} \qquad (1)$$

where c is the velocity of the EM wave in free space (0.3 m/ns). The volumetric water content (θ) is calculated from the relative permittivity (K) using the empirical relationship developed by Topp et al. (1980).

$$\theta = -5.3\times10^{-2} + 2.92\times10^{-2}K - 5.5\times10^{-4}K^2 + 4.3\times10^{-6}K^3 \qquad (2)$$

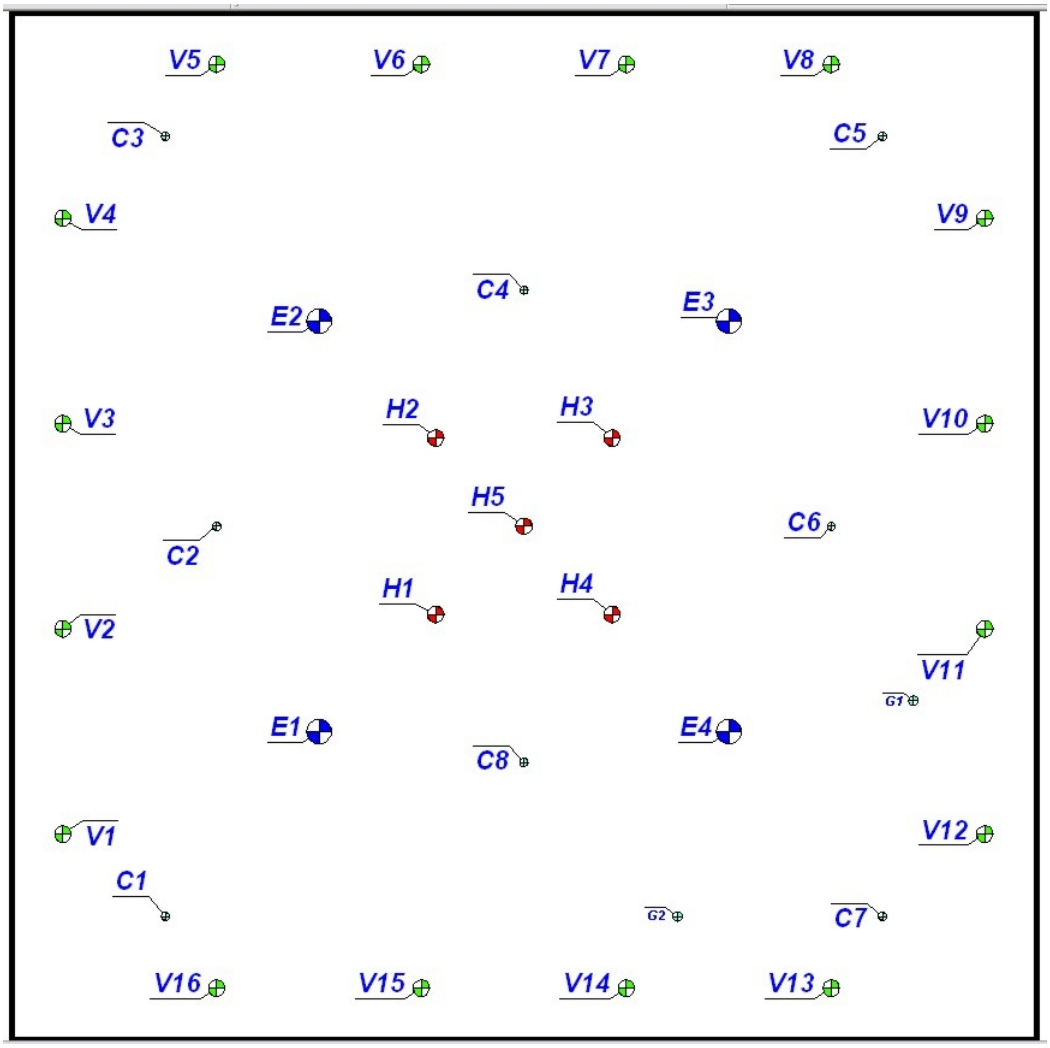

Figure 1. Site Layout, borehole GPR measurements were done between H4, G1 and G2 only, in the bottom right area of the figure

GPR Equipment and Data Collection Parameters

The borehole GPR data were acquired using a pulseEKKO 100 borehole GPR system with 200 MHz antennas. The following is a brief discussion of the equipment and collection parameters used.

The system can be used with a 400 V transmitter or 1000 V transmitter to create the transmit pulse. The data presented in this report were collected with a 400 V transmitter.

Before a GPR trace is stored to disk, a number of full data traces are collected rapidly and averaged to create the data trace that is stored. This process is known as stacking. The number of traces that go into each average is called the number of stacks. A higher number of stacks takes longer to collect but improves the signal to noise ratio. The data presented in this report contain 16 stacks.

The time window (the length in nanoseconds of each trace) was 75 ns. The sampling interval (time between successive points along each trace) for all the data was 0.1 ns.

Data Collection Procedures

Two survey modes were used to collect the data, the zero offset profile (ZOP) mode and the multiple offset gather (MOG) mode (see Figure 2). The ZOP mode is used to obtain a one dimensional profile, along the length of the boreholes, of the average water content between corresponding points from one borehole to the other. The MOG mode is used to generate a two-dimensional image of the water content in the plane between the boreholes.

Zero Offset Profiles

In the zero offset profile (ZOP) mode, a series of 19 radar traces was recorded while both antennas were moved downward at equal steps of 0.125 m within each hole with the transmitter and receiver antennas always at the same depth. Analysis of such a data set provides a profile with depth, of the average volumetric water content between the holes. The ZOP water content profiles extend from 0.5 m to 2.75 m depth (relative to top of casing) for each well pair.

Each ZOP survey took approximately 2-3 minutes to complete. Each ZOP survey was performed at least four times to evaluate the repeatability of the results. The ZOP surveys were performed as shown in Table 1.

Multiple Offset Gathers

Each multiple offset gather (MOG) was collected by fixing the transmitter antenna at a specific position (starting at 0.5 m depth below top of casing) in one of the tubes and collecting data as the receiver antenna is lowered step-wise down a different tube at intervals of 0.25 m, a radar trace being collected at each of the 10 receiver positions from 0.5 m to 2.75 m below the top of casing. This process was repeated for each of the 10 transmitter positions also spaced 0.25 m apart.

The travel times measured for the ray paths between the various transmitter and receiver depths are used to produce a two dimensional image of the water content between the access tubes. The MOG surveys were performed as listed in Table 1.

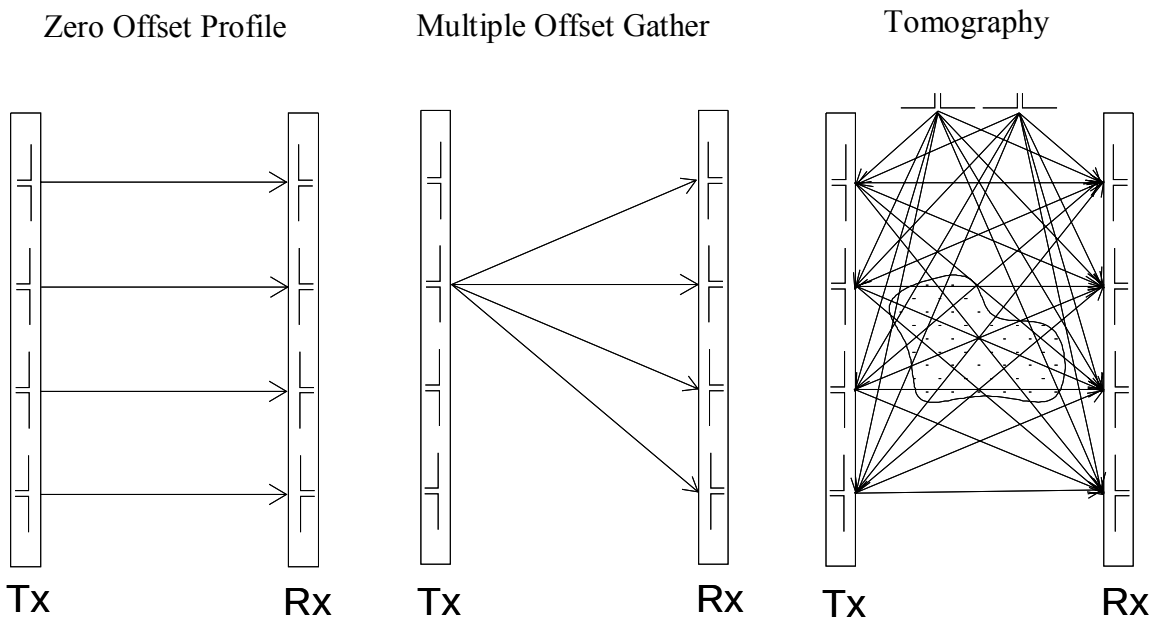

Figure 2. Borehole radar data acquisition modes showing typical ray path patterns between transmitter (Tx) and receiver (Rx) positions.

Table 1. List of borehole GPR surveys

Tx=transmitter, Rx=receiver

Zero Offset Profiles (ZOPs)

Nov. 3, 2005

Survey Type	Tx	Rx	Filename	Separation (m)	Cal File #	Date
ZOP	H4	G2	zopa4	1.458	11	03-Nov-05
ZOP	H4	G2	zopa5	1.458	12	03-Nov-05
ZOP	H4	G2	zopa6	1.458	13	03-Nov-05
ZOP	H4	G2	zopa7	1.458	14	03-Nov-05
ZOP	H4	G2	zopa8	1.458	15	03-Nov-05
ZOP	H4	G2	zopa9	1.458	16	03-Nov-05
ZOP	H4	G2	zopa10	1.458	17	03-Nov-05
ZOP	H4	G1	zopa11	1.617	20	03-Nov-05
ZOP	H4	G1	zopa12	1.617	21	03-Nov-05
ZOP	H4	G1	zopa13	1.617	24	03-Nov-05
ZOP	H4	G1	zopa14	1.617	25	03-Nov-05
ZOP	G1	G2	zopa5	1.328	10	03-Nov-05
ZOP	G1	G2	zopa6	1.328	12	03-Nov-05
ZOP	G1	G2	zopa7	1.328	13	03-Nov-05
ZOP	G1	G2	zopa8	1.328	14	03-Nov-05

Nov. 10, 2005

Survey Type	Tx	Rx	Filename	Separation (m)	Cal File #	Date
ZOP	H4	G2	zopb1	1.458	15	10-Nov-05
ZOP	H4	G2	zopb2	1.458	16	10-Nov-05
ZOP	H4	G2	zopb3	1.458	18	10-Nov-05
ZOP	H4	G2	zopb4	1.458	19	10-Nov-05
ZOP	H4	G2	zopb5	1.458	20	10-Nov-05
ZOP	H4	G1	zopb6	1.617	22	10-Nov-05
ZOP	H4	G1	zopb7	1.617	23	10-Nov-05
ZOP	H4	G1	zopb8	1.617	24	10-Nov-05
ZOP	H4	G1	zopb9	1.617	25	10-Nov-05
ZOP	G1	G2	zopb10	1.328	26	10-Nov-05
ZOP	G1	G2	zopb11	1.328	28	10-Nov-05
ZOP	G1	G2	zopb12	1.328	30	10-Nov-05
ZOP	G1	G2	zopb13	1.328	31	10-Nov-05
ZOP	G1	G2	zopb14	1.328	32	10-Nov-05

Multiple Offset Gathers (MOGs)

Filename	Survey Type	Tx	Rx	Separation (m)	Cal File #	Date
mog1a1 to mog1a10	MOG	H4	G2	1.458	18	03-Nov-05
mog2a1 to mog2a10	MOG	H4	G1	1.617	1	03-Nov-05
mog3a1 to mog3a10	MOG	G1	G2	1.328	3	03-Nov-05
mog1b1 to mog1b10	MOG	H4	G2	1.458	1	10-Nov-05
mog2b1 to mog2b10	MOG	H4	G1	1.617	2	10-Nov-05
mog3b1 to mog3b10	MOG	G1	G2	1.328	1	10-Nov-05

Results and Discussion

The ZOP results are shown in Figure 3 as water content plotted vs. depth for the three well pairs. Note that the unsaturated zone affects the measured water content readings down to a depth of approximately 1.25 m. We will consider only the depths greater than or equal to 1.25 m within the saturated zone.

It should be noted that the borehole GPR readings will underestimate the water content in the upper part of the saturated zone because of wave refraction up into the unsaturated zone and should not be relied on to indicate the top of the saturated zone accurately.

During the processing of the MOGs, only the data from transmitter and receiver positions from 1.25 m to 2.75 m were used to produce the water content images in Figure 4.

The MOG results show the measured water content distribution and water content change over the two-dimensional plane between two boreholes. The ZOP results display only the average water content measured between two boreholes as a function of depth. The following interpretation will focus on the basic indications of the ZOP results only. The MOG results can be viewed to obtain an indication of the two dimensional water content distribution and water content changes between each pair of boreholes.

Zero Offset Profiles

Figures 3 a, b and c show the ZOP results. For each well pair (H4-G2, H4-G1 or G1-G2), the water content profiles of Nov. 3 and Nov. 10 are plotted and the difference from Nov. 3 to Nov. 10 is plotted directly below.

It was expected that the gas infusion system would emplace carbon dioxide bubbles in the saturated zone which would cause a decrease in the volumetric water content (volume of water divided by total volume). A decrease in water content was indeed observed between wells G1 and G2 but in the other two well pairs the (H4-G2 and H4-G1) an increase in the water content was recorded as shown in Figure 3 a and b.

For the well pair G1-G2, the one that showed the expected water content decrease, the decrease is a maximum at approximately 2 m depth and the curve is roughly symmetrical about that depth with less water content change above and below 2m. This result is consistent with what we expected.

For the other two well pairs (H4-G2 and H4-G1), the ones that show an increase in water content, a trend is observed, in which the water content increase is larger at increasing depth. The water content change increases from approximately 0.015 at 1.5 m depth to just over 0.03 near the bottom of the wells at approximately 2.75 m deep. These measurement results were not as expected. We can speculate on the reasons for the measured increase in water content at H4-G2 and H4-G1.

Gasoline removal?

Symmetrically, the well pairs H4-G2 and H4-G1 bear the same spatial relationship to the hydrocarbon injection well H4 and extraction well E4 so it makes sense that the water content change between the well pairs H4-G2 and H4-G1 are similar. The planes between these two well pairs will be more influenced by the presence of hydrocarbon, since H4 was a hydrocarbon injection well. We would expect that if the gasoline injection had any effect on the borehole GPR results, it would be greatest in H4-G2 and H4-G1 and less so or nonexistent in G1-G2. It is proposed that the gasoline injection at H4 has affected the results in the two H4 well pairs (H4-G2 and H4-G1).

Since the water content measurement depends on the dielectric constant and since the dielectric constant of gasoline is 1.95 compared to 80 for water and 1 for air, the replacement of water with gasoline, during the hydrocarbon injection should also cause the measured water content to decrease. It is proposed that gasoline was then removed at H4-G2 and H4-G1 resulting in higher water content measurements there.

To test this hypothesis, we can review other information gathered from the site. The residual hydrocarbon saturation has been estimated to be about 10% of the porosity, approximately 3 % of the total volume before use of the GI technique. From Leif's coring and monitoring of the extracted vapour and water during GI use it has been estimated that at least half of the hydrocarbon is still in the cell. Without knowing the distribution of the remaining half of the hydrocarbon it is difficult to say whether this information is consistent with the borehole GPR results. However the measured water content increases of as high as 3 % of total volume at H4-G2 and H4-G1 seem unrealistically high especially considering that some carbon dioxide bubbles may have been emplaced which would counteract the effect from removal of gasoline.

It remains unclear whether or not the measured increase in water content was caused by removal of gasoline or from some systematic error in the borehole GPR measurements.

Precision (Repeatability) and Accuracy of Measurements

All of the individual ZOP measurements are shown on pages 16-18 (Figure 5). As can be seen, the repeatability or precision of the measurements is quite good. The poorest repeatability is shown in the data between G1 and G2 on Nov. 3. The four repeated water content measurements between G1 and G2 vary by no more than ± 0.007 from the average of the four measurements.

In comparison, the water content changes calculated to have occurred from Nov. 3 to Nov 10 during GI operation, between all three well pairs is, for the most part, between 0.01 and 0.03 as shown in figures 3 a,b and c.

As for the accuracy of the measurements (i.e. whether the measurements of water content are truly and accurately representative of the actual water content), it seems that water content measurements at Borden, using this method, indicate a unrealistically high porosity in the saturated zone. Values as high as 0.43 were measured between H4 and G2

and similarly high measurements have been obtained at other sites at Borden. Previous studies at sites at Borden have reported porosities of 0.38 (MacFarlane et al., 1983) and 0.36 (Greenhouse et al. 1993). Nonetheless, such a systematic error in the accuracy of the water content should not affect the calculation of the water content change since this systematic error will be approximately the same for all measurements and as such, will cancel during the difference calculation.

Conclusions and Recommendations

Borehole GPR measurements were performed before and after use of gas infusion flushing. A decrease in water content was measured between G1 and G2 as expected, presumably from emplacement of CO_2 bubbles. Unexpectedly, an increase in water content was observed between H4 and G1 and between H4 and G2.

The hypothesis is that water content increases were measured (H4-G1 and H4-G2) because of removal of hydrocarbon by the GI system between these well pairs. However, the increases in water content that were measured seem unusually high, considering the volume of hydrocarbon that was introduced and that which has been estimated to have been removed from coring and monitoring of the extracted fluids and considering that CO_2 bubbles were also likely emplaced between these well pairs too.

The borehole GPR measurements of water content have good repeatability and seem of good quality, so the discrepancy remains unexplained. In hindsight, it would have been good to take borehole GPR measurements before and after hydrocarbon injection to determine the effects of the hydrocarbon on the water content measurements.

References

Greenhouse, J., Brewster, M., Schneider, G., Redman, D., Annan, P., Olhoeft, G., Lucius, J, Sander, K., Mazzella, A., 1993. Geophysics and solvents: The Borden experiment, The Leading Edge, April, 1993, pp. 261-267

MacFarlane, D.D., Cherry, J.A., Gillham, R.W., Sudicky, E.A., 1983. Migration of contaminants in groundwater at a landfill: A case study, 1. Groundwater flow and plume delineation, Journal of Hydrology, v. 63, pp. 1-29

Figure 3a. Zero Offset Profile (ZOP) results for well pair H4-G2.

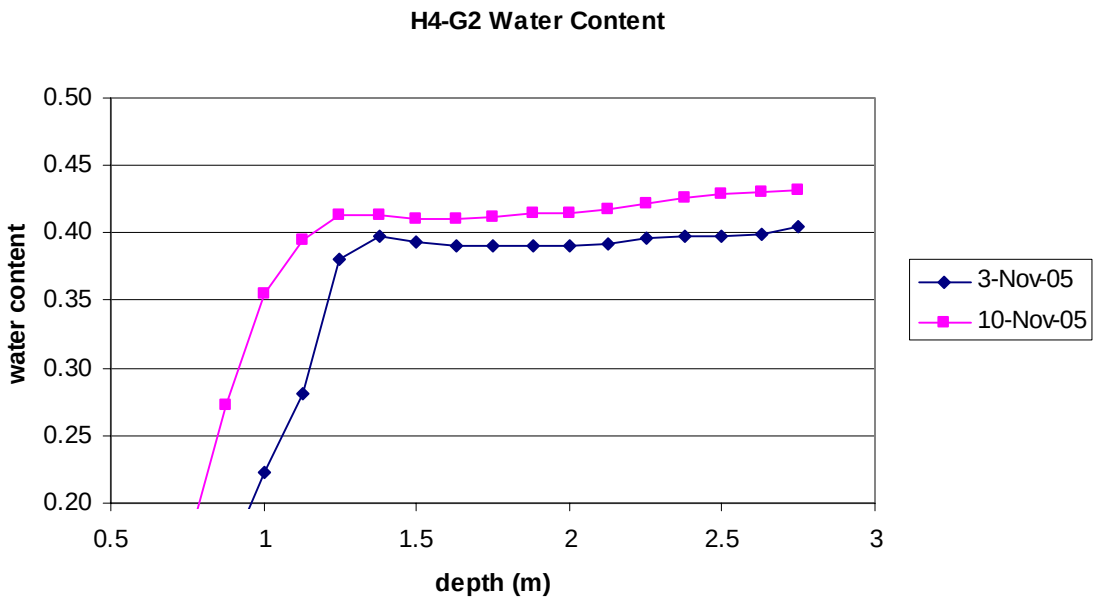

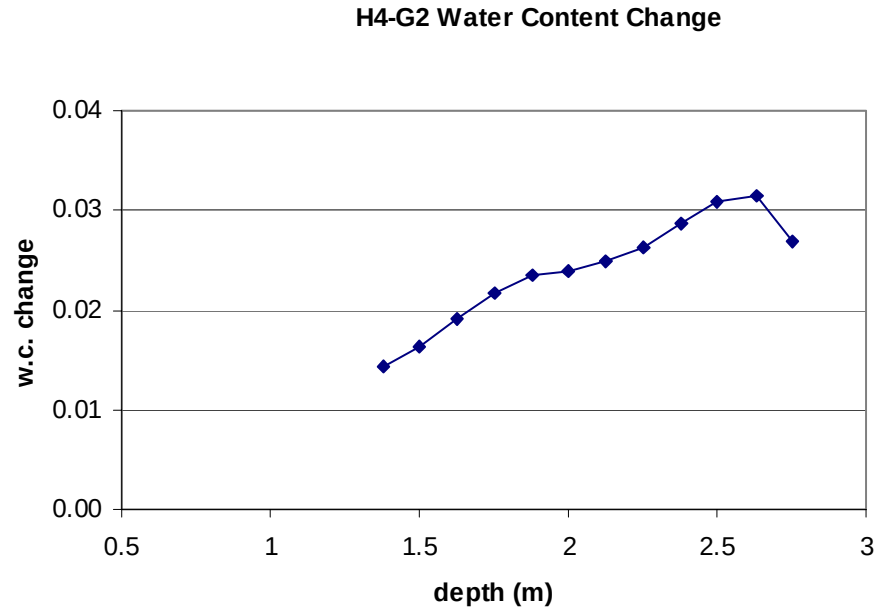

Figure 3b. Zero Offset Profile (ZOP) results for well pair H4-G1.

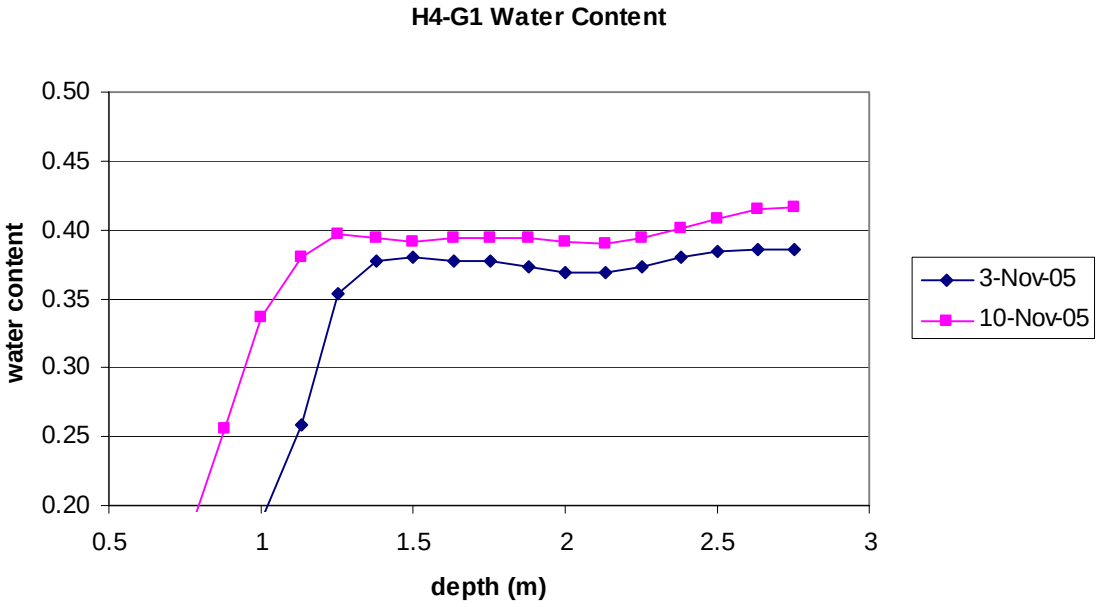

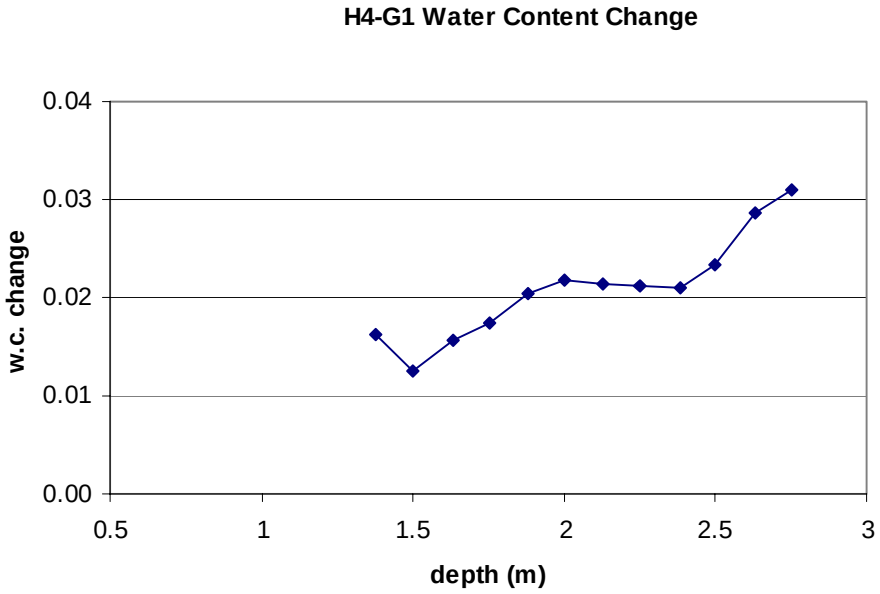

Figure 3c. Zero Offset Profile (ZOP) results for well pair G1-G2.

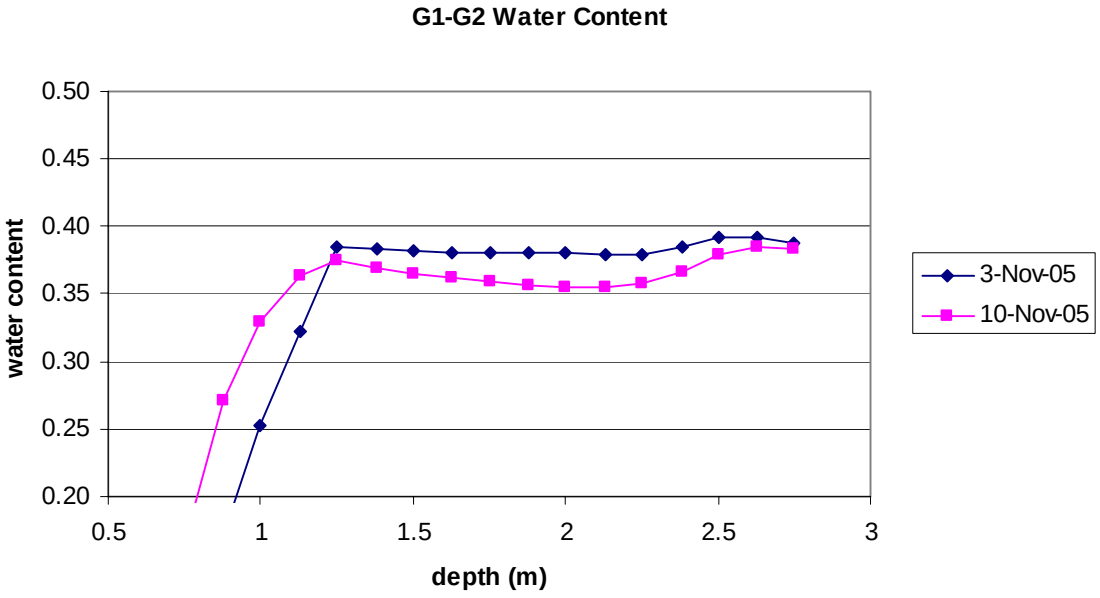

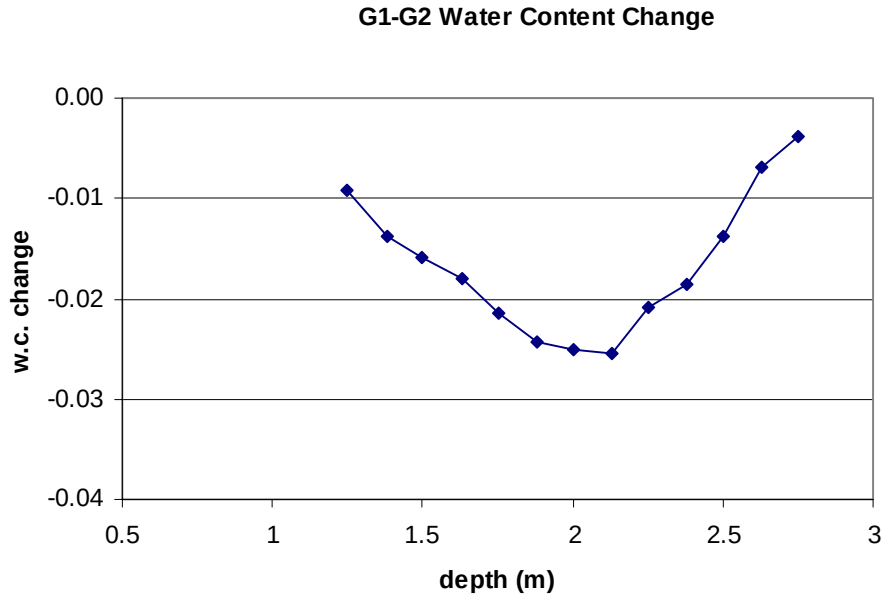

Figure 4a. Multiple Offset Gather (MOG) results between wells H4 and G2.

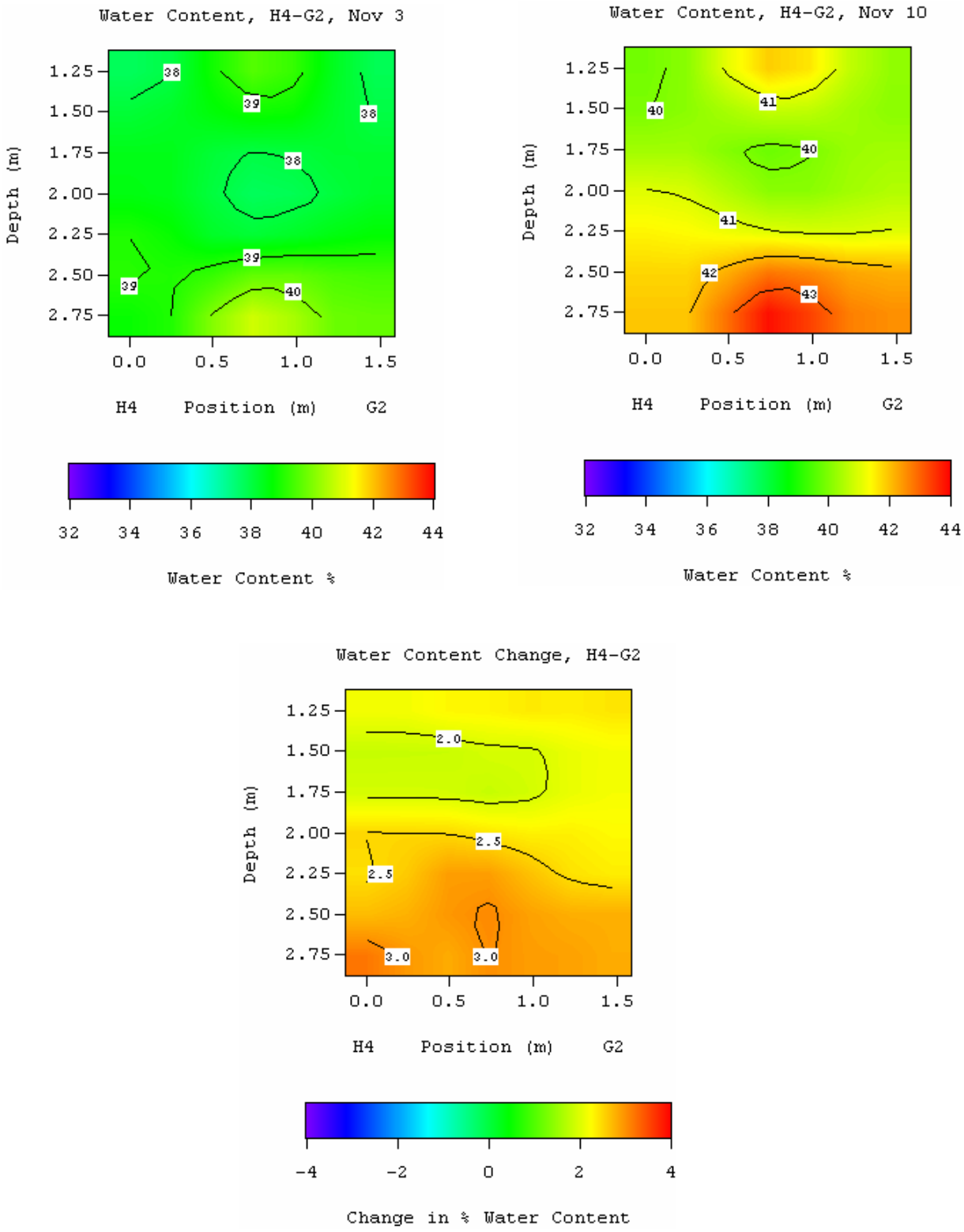

Figure 4b. Multiple Offset Gather (MOG) results between wells H4 and G1.

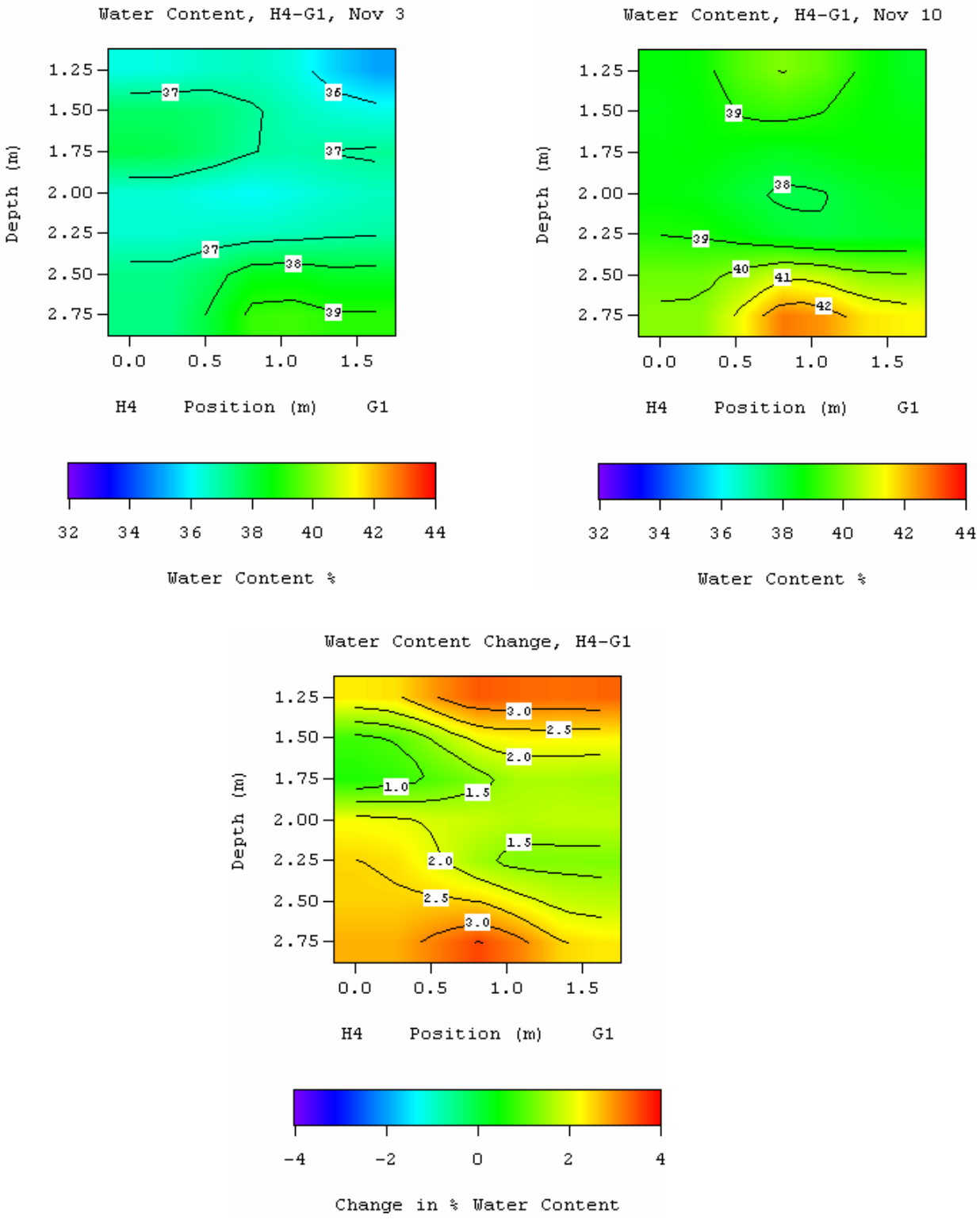

Figure 4c. Multiple Offset Gather (MOG) results between wells G1 and G2.

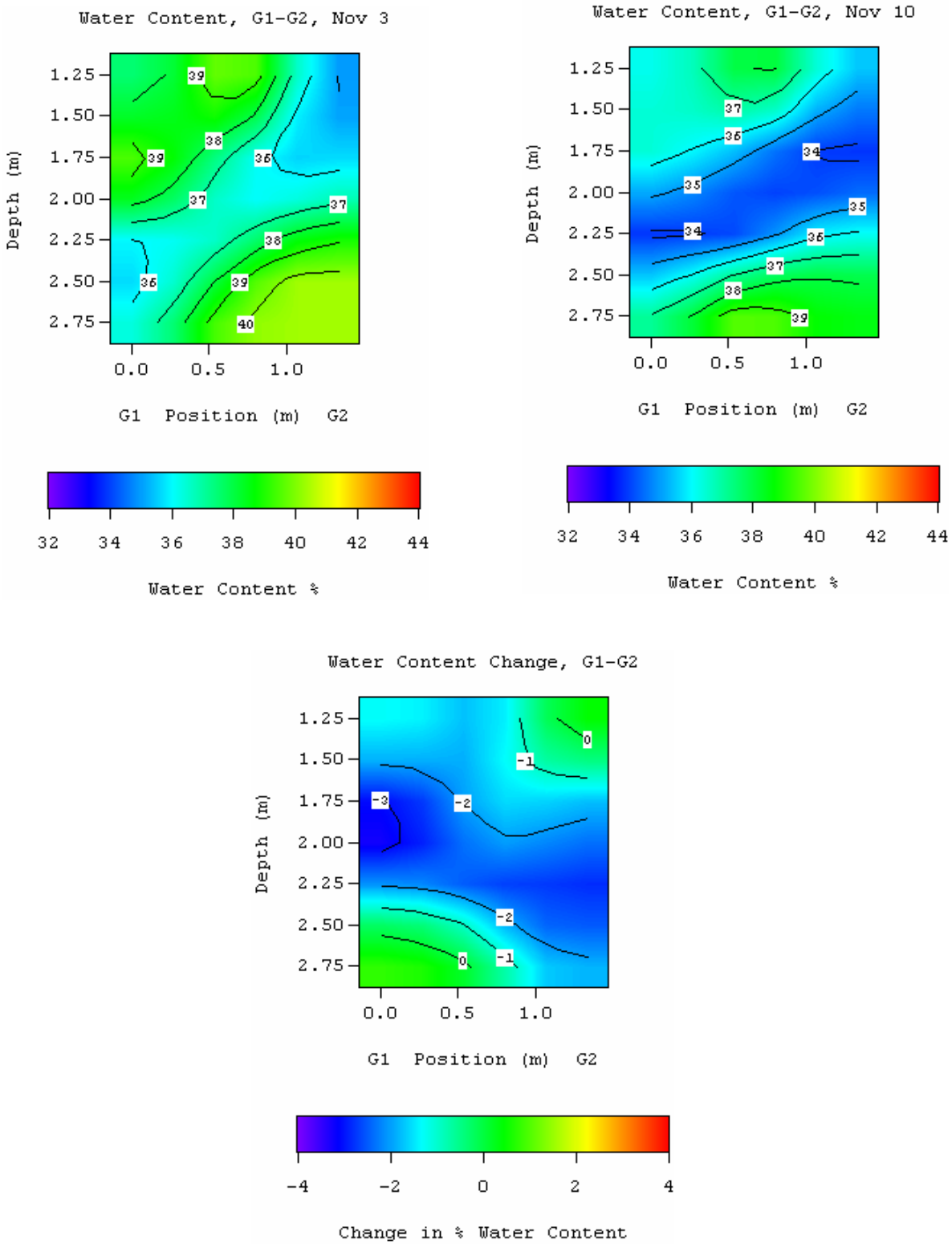

Figure 5. Individual ZOP Measurements

H4-G2

	Water Content	Water Content	Water Content	Water Content	
Depth	zopa7	zopa8	zopa9	zopa10	3-Nov-05
0.5	0.103	0.101	0.099	0.100	0.101
0.63	0.106	0.105	0.103	0.104	0.105
0.75	0.124	0.122	0.117	0.122	0.121
0.88	0.159	0.155	0.152	0.156	0.156
1	0.226	0.224	0.221	0.224	0.223
1.13	0.281	0.281	0.283	0.279	0.281
1.25	0.384	0.380	0.380	0.380	0.381
1.38	0.401	0.398	0.396	0.398	0.398
1.5	0.397	0.393	0.392	0.394	0.394
1.63	0.393	0.391	0.387	0.392	0.391
1.75	0.393	0.388	0.386	0.392	0.390
1.88	0.393	0.389	0.388	0.393	0.391
2	0.394	0.388	0.389	0.393	0.391
2.13	0.395	0.391	0.390	0.394	0.393
2.25	0.398	0.394	0.394	0.397	0.396
2.38	0.400	0.397	0.396	0.398	0.398
2.5	0.401	0.397	0.396	0.398	0.398
2.63	0.402	0.398	0.399	0.399	0.399
2.75	0.406	0.403	0.404	0.404	0.405

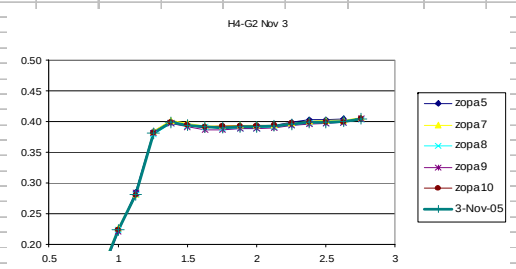

	Water Content	Water Content	Water Content	
Depth	zopb2	zopb4	zopb5	10-Nov-05
0.5	0.117	0.118	0.115	0.117
0.63	0.123	0.123	0.122	0.123
0.75	0.169	0.170	0.168	0.169
0.88	0.270	0.275	0.272	0.272
1	0.356	0.354	0.354	0.355
1.13	0.395	0.395	0.392	0.394
1.25	0.413	0.413	0.412	0.413
1.38	0.413	0.413	0.412	0.413
1.5	0.410	0.410	0.410	0.410
1.63	0.410	0.409	0.409	0.410
1.75	0.412	0.411	0.411	0.411
1.88	0.416	0.413	0.413	0.414
2	0.416	0.415	0.414	0.415
2.13	0.418	0.418	0.417	0.418
2.25	0.423	0.421	0.421	0.422
2.38	0.428	0.426	0.426	0.427
2.5	0.430	0.429	0.428	0.429
2.63	0.432	0.430	0.430	0.431
2.75	0.432	0.431	0.430	0.431

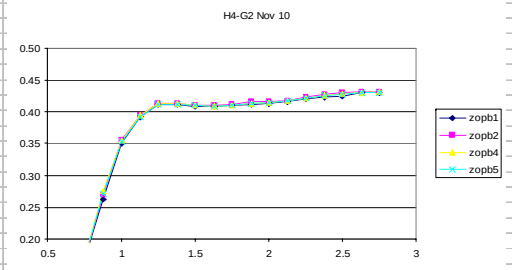

Final Results H4-G2

Depth	3-Nov-05	10-Nov-05	Difference
0.5	0.101	0.117	0.016
0.63	0.105	0.123	0.018
0.75	0.121	0.169	0.048
0.88	0.156	0.272	0.117
1	0.223	0.355	0.131
1.13	0.281	0.394	0.113
1.25	0.381	0.413	0.032
1.38	0.398	0.413	0.014
1.5	0.394	0.410	0.016
1.63	0.391	0.410	0.019
1.75	0.390	0.411	0.022
1.88	0.391	0.414	0.023
2	0.391	0.415	0.024
2.13	0.393	0.418	0.025
2.25	0.396	0.422	0.026
2.38	0.398	0.427	0.029
2.5	0.398	0.429	0.031
2.63	0.399	0.431	0.031
2.75	0.405	0.431	0.027

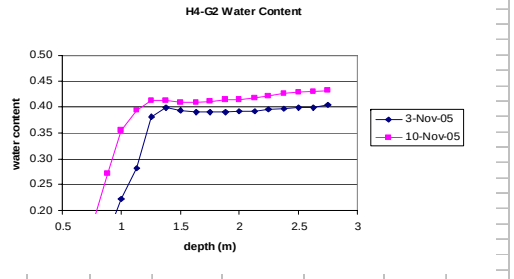

Figure 5. Individual ZOP Measurements

H4-G1

Depth	Water Content zopa12	Water Content zopa13	Water Content zopa14	**Average 3-Nov-05**
0.5	0.084	0.084	0.087	0.085
0.63	0.086	0.086	0.089	0.087
0.75	0.098	0.098	0.098	0.098
0.88	0.126	0.124	0.127	0.126
1	0.186	0.188	0.190	0.188
1.13	0.261	0.257	0.258	0.259
1.25	0.354	0.352	0.355	0.354
1.38	0.377	0.377	0.379	0.377
1.5	0.379	0.379	0.380	0.379
1.63	0.378	0.378	0.378	0.378
1.75	0.377	0.377	0.378	0.377
1.88	0.373	0.373	0.374	0.373
2	0.369	0.369	0.370	0.369
2.13	0.368	0.368	0.369	0.368
2.25	0.372	0.372	0.373	0.372
2.38	0.379	0.379	0.380	0.379
2.5	0.384	0.385	0.385	0.385
2.63	0.385	0.386	0.386	0.386
2.75	0.385	0.385	0.386	0.385

Depth	Water Content zopb6	Water Content zopb7	Water Content zopb8	Water Content zopb9	**Average 10-Nov-05**
0.5	0.132	0.131	0.129	0.131	0.131
0.63	0.133	0.134	0.132	0.135	0.134
0.75	0.172	0.176	0.171	0.172	0.173
0.88	0.254	0.256	0.258	0.257	0.256
1	0.336	0.336	0.336	0.340	0.337
1.13	0.379	0.379	0.379	0.382	0.380
1.25	0.396	0.394	0.397	0.398	0.396
1.38	0.393	0.392	0.394	0.396	0.394
1.5	0.392	0.389	0.392	0.394	0.392
1.63	0.393	0.391	0.394	0.396	0.393
1.75	0.394	0.392	0.395	0.397	0.394
1.88	0.393	0.392	0.394	0.395	0.394
2	0.391	0.389	0.391	0.392	0.391
2.13	0.388	0.390	0.390	0.390	0.390
2.25	0.392	0.395	0.394	0.394	0.394
2.38	0.398	0.402	0.400	0.401	0.400
2.5	0.406	0.409	0.408	0.409	0.408
2.63	0.413	0.415	0.413	0.416	0.414
2.75	0.415	0.415	0.416	0.417	0.416

Final Results H4-G1

Depth	**3-Nov-05**	**10-Nov-05**	Difference
0.5	0.085	0.131	0.046
0.63	0.087	0.134	0.046
0.75	0.098	0.173	0.075
0.88	0.126	0.256	0.131
1	0.188	0.337	0.149
1.13	0.259	0.380	0.121
1.25	0.354	0.396	0.043
1.38	0.377	0.394	0.016
1.5	0.379	0.392	0.012
1.63	0.378	0.393	0.016
1.75	0.377	0.394	0.017
1.88	0.373	0.394	0.020
2	0.369	0.391	0.022
2.13	0.368	0.390	0.021
2.25	0.372	0.394	0.021
2.38	0.379	0.400	0.021
2.5	0.385	0.408	0.023
2.63	0.386	0.414	0.029
2.75	0.385	0.416	0.031

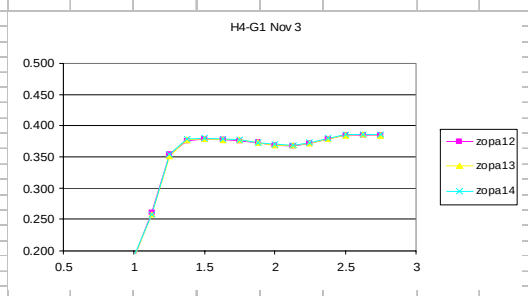

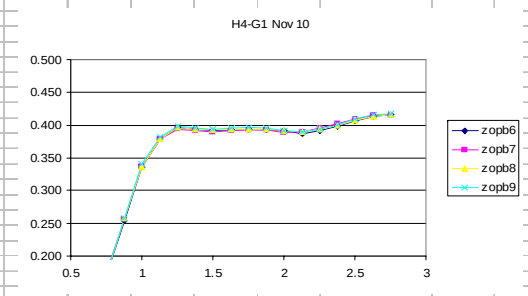

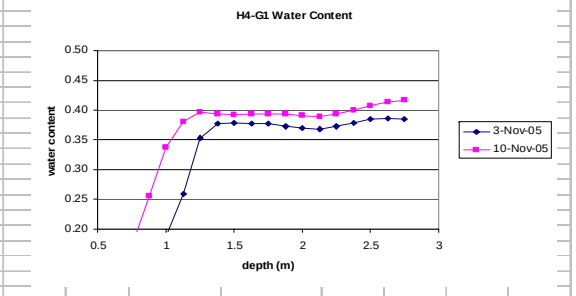

Figure 5. Individual ZOP Measurements

G1-G2

Depth	Water Content zopa5	Water Content zopa6	Water Content zopa7	Water Content zopa8	Average 3-Nov-05
0.50	0.096	0.099	0.096	0.101	0.098
0.63	0.100	0.103	0.099	0.104	0.102
0.75	0.121	0.125	0.118	0.125	0.122
0.88	0.169	0.173	0.168	0.174	0.171
1.00	0.255	0.255	0.242	0.259	0.253
1.13	0.323	0.323	0.322	0.325	0.323
1.25	0.384	0.387	0.384	0.383	0.384
1.38	0.383	0.385	0.383	0.383	0.383
1.50	0.381	0.383	0.380	0.382	0.382
1.63	0.379	0.383	0.379	0.381	0.381
1.75	0.378	0.384	0.379	0.381	0.381
1.88	0.377	0.384	0.379	0.382	0.381
2.00	0.377	0.384	0.379	0.381	0.380
2.13	0.373	0.384	0.380	0.382	0.380
2.25	0.376	0.383	0.377	0.379	0.379
2.38	0.380	0.390	0.385	0.387	0.385
2.50	0.387	0.396	0.391	0.395	0.392
2.63	0.387	0.396	0.391	0.394	0.392
2.75	0.384	0.390	0.386	0.389	0.387

Depth	Water Content zopb11	Water Content zopb12	Water Content zopb13	Water Content zopb14	Average 10-Nov-05
0.5	0.117	0.118	0.116	0.116	0.117
0.63	0.126	0.130	0.130	0.131	0.129
0.75	0.165	0.166	0.171	0.166	0.167
0.88	0.268	0.273	0.270	0.272	0.271
1	0.328	0.326	0.329	0.333	0.329
1.13	0.363	0.359	0.365	0.366	0.363
1.25	0.376	0.373	0.376	0.376	0.375
1.38	0.372	0.367	0.369	0.371	0.370
1.5	0.366	0.364	0.365	0.367	0.366
1.63	0.363	0.363	0.361	0.363	0.362
1.75	0.359	0.359	0.359	0.360	0.359
1.88	0.356	0.358	0.355	0.357	0.356
2	0.356	0.356	0.354	0.355	0.355
2.13	0.352	0.357	0.353	0.355	0.354
2.25	0.357	0.360	0.357	0.358	0.358
2.38	0.365	0.368	0.366	0.367	0.367
2.5	0.378	0.380	0.378	0.378	0.379
2.63	0.385	0.387	0.384	0.386	0.385
2.75	0.383	0.386	0.382	0.383	0.384

Final Results G1-G2

Depth	3-Nov-05	10-Nov-05	Difference
0.5	0.098	0.117	0.019
0.63	0.102	0.129	0.028
0.75	0.122	0.167	0.045
0.88	0.171	0.271	0.100
1	0.253	0.329	0.076
1.13	0.323	0.363	0.040
1.25	0.384	0.375	-0.009
1.38	0.383	0.370	-0.014
1.5	0.382	0.366	-0.016
1.63	0.381	0.362	-0.018
1.75	0.381	0.359	-0.022
1.88	0.381	0.356	-0.024
2	0.380	0.355	-0.025
2.13	0.380	0.354	-0.025
2.25	0.379	0.358	-0.021
2.38	0.385	0.367	-0.019
2.5	0.392	0.379	-0.014
2.63	0.392	0.385	-0.007
2.75	0.387	0.384	-0.004

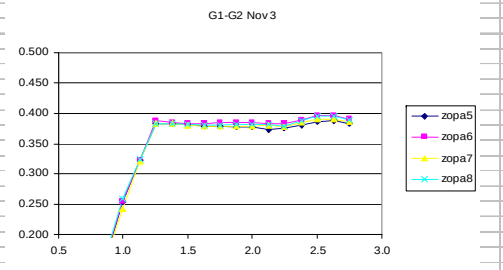

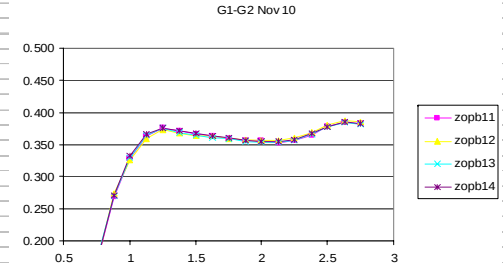

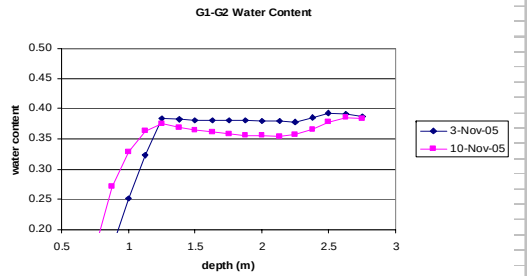

Appendix B

Phase I GC Vapour Sampling Results

Date	Time	Elapsed Time (min)	Air Pressure Differential (inches of water)	Outlet Flow (m^3/min)	Sample #	Pentane (ug/L)	Hexane (ug/L)	Pentane Removed (kg)	Hexane Removed (kg)
30-Sep-05	12:57:01	45	0.37	6.151	LNV093001A	331.84	122.57	0.05	0.02
30-Sep-05	13:29:01	77	0.35	5.960	LNV093002A	350.02	110.42	0.11	0.04
30-Sep-05	14:25:01	133	0.34	5.914	LNV093003A	494.93	145.33	0.25	0.08
30-Sep-05	15:40:33	209	0.27	5.277	LNV093004A	1273.15	423.33	0.62	0.20
30-Sep-05	16:25:01	253	0.39	6.336	LNV093005A	951.27	468.50	0.90	0.31
30-Sep-05	18:08:01	356	0.39	6.354	LNV093006A	104.20	53.93	1.24	0.48
30-Sep-05	19:15:01	423	0.23	4.852	LNV093007A	913.50	356.33	1.41	0.55
30-Sep-05	20:02:01	470	0.27	5.213	LNV093008A	627.79	243.23	1.60	0.62
30-Sep-05	21:05:01	533	0.27	5.254	LNV093009B	173.60	68.65	1.73	0.68
30-Sep-05	22:06:01	594	0.27	5.247	LNV093010A	103.63	47.39	1.77	0.69
30-Sep-05	22:54:01	642	0.26	5.206	LNV093011A	83.80	40.77	1.80	0.71
3-Oct-05	13:32:32	666	0.30	5.552	LNV100301A	758.25	402.99	1.85	0.73
3-Oct-05	14:16:00	709	0.24	4.995	LNV100302A	317.47	162.01	1.98	0.80
3-Oct-05	15:19:00	772	0.24	4.995	LNV100303A	265.49	120.73	2.07	0.84
3-Oct-05	16:00:00	813	0.24	4.951	LNV100304A	369.56	155.35	2.13	0.87
3-Oct-05	17:35:32	909	0.24	4.916	LNV100305A	373.33	173.28	2.31	0.95
3-Oct-05	18:34:00	967	0.24	4.908	LNV100306A	266.51	142.35	2.40	1.00
3-Oct-05	19:35:00	1028	0.23	4.896	LNV100307A	311.03	179.07	2.49	1.04
3-Oct-05	20:35:08	1088	0.24	4.940	LNV100308A	335.58	175.87	2.58	1.10
4-Oct-05	11:11:28	1965	0.23	4.819	LNV100401A	507.78	331.48	4.38	2.18
4-Oct-05	12:22:00	2035	0.24	4.951	LNV100402A	691.98	415.10	4.59	2.31
4-Oct-05	14:10:00	2143	0.24	4.951	LNV100403A	550.81	334.54	4.92	2.51
4-Oct-05	15:46:00	2239	0.24	4.991	LNV100404A	460.89	277.50	5.16	2.65
4-Oct-05	18:04:00	2377	0.25	5.026	LNV100405A	470.41	333.11	5.48	2.86
4-Oct-05	19:04:00	2437	0.24	4.987	LNV100406B	585.90	340.62	5.64	2.96
4-Oct-05	20:10:00	2503	0.24	4.991	LNV100407A	554.28	309.72	5.83	3.07
4-Oct-05	21:24:20	2577	0.24	4.991	LNV100408A	498.36	264.95	6.02	3.18
4-Oct-05	22:17:40	2631	0.26	5.126	LNV100409A	357.84	207.87	6.14	3.24
6-Oct-05	8:51:30	3388	0.23	4.815	LNV100601A	220.84	114.75	7.24	3.85

Date	Time	Elapsed Time (min)	Air Pressure Differential (inches of water)	Outlet Flow (m^3/min)	Sample #	Pentane (ug/L)	Hexane (ug/L)	Pentane Removed (kg)	Hexane Removed (kg)
6-Oct-05	10:04:58	3462	0.22	4.799	LNV100602A	203.68	107.60	7.31	3.89
6-Oct-05	11:01:58	3519	0.22	4.791	LNV100603A	235.96	116.63	7.37	3.92
6-Oct-05	11:54:18	3572	0.22	4.700	LNV100604A	361.35	221.41	7.45	3.97
6-Oct-05	13:49:18	3584	0.22	4.762	LNV100605A	678.84	345.37	7.48	3.98
6-Oct-05	14:42:58	3638	0.22	4.708	LNV100606A	729.27	442.47	7.66	4.08
8-Oct-05	8:37:28	3691	0.34	5.937	LNV100801A	2355.73	1140.85	8.12	4.32
8-Oct-05	9:25:48	3739	0.38	6.242	LNV100802A	852.54	441.67	8.58	4.55
8-Oct-05	10:10:32	3784	0.28	5.365	LNV100804A	830.15	441.81	8.80	4.66
8-Oct-05	10:55:00	3828	0.28	5.376	LNV100805A	537.51	342.08	8.96	4.75
14-Oct-05	5:12:20	3850	0.26	5.119	LNV101402A	7291.64	3808.12	9.40	4.99
14-Oct-05	5:44:48	3883	0.26	5.115	LNV101404A	2113.46	1092.29	10.20	5.40
24-Oct-05	13:18:38	3922	0.26	5.168	LNV102401A	2638.94	1001.90	10.68	5.61
24-Oct-05	13:58:38	3962	0.19	4.407	LNV102402A	893.70	497.77	11.03	5.76
24-Oct-05	14:11:38	3975	0.22	4.787	LNV102403A	129.56	118.67	11.06	5.78
24-Oct-05	14:44:50	4008	0.22	4.754	LNV102404A	4252.69	1962.02	11.40	5.94
24-Oct-05	15:55:10	4078	0.26	5.164	LNV102405A	2656.86	1359.21	12.59	6.51
24-Oct-05	17:04:18	4147	0.26	5.162	LNV102406A	2198.46	1248.94	13.45	6.98
24-Oct-05	18:01:38	4205	0.26	5.145	LNV102407A	1889.85	1151.82	14.06	7.34
24-Oct-05	20:26:30	4349	0.26	5.134	LNV102408A	1375.04	989.86	15.27	8.13
24-Oct-05	21:43:10	4426	0.25	5.061	LNV102409A	1207.02	937.18	15.78	8.51
24-Oct-05	23:05:38	4509	0.25	5.080	LNV102410A	1206.97	969.28	16.29	8.91
25-Oct-05	11:05:08	4526	0.20	4.569	LNV102501A	1245.25	844.02	16.39	8.98
25-Oct-05	12:00:20	4582	0.26	5.149	LNV102502A	1135.48	827.57	16.71	9.21
25-Oct-05	12:51:40	4633	0.26	5.172	LNV102503A	1373.73	1004.40	17.04	9.45
25-Oct-05	14:47:28	4748	0.26	5.161	LNV102504A	1125.81	916.83	17.78	10.02
25-Oct-05	15:52:40	4813	0.26	5.164	LNV102505A	910.47	771.51	18.13	10.31
25-Oct-05	19:23:48	5025	0.26	5.138	LNV102506A	673.51	594.85	18.99	11.05
25-Oct-05	22:05:20	5186	0.29	5.481	LNV102507A	923.93	779.19	19.68	11.64
25-Oct-05	22:47:48	5229	0.35	5.960	LNV102508A	213.73	199.02	19.81	11.76

Date	Time	Elapsed Time (min)	Air Pressure Differential (inches of water)	Outlet Flow (m^3/min)	Sample #	Pentane (ug/L)	Hexane (ug/L)	Pentane Removed (kg)	Hexane Removed (kg)
28-Oct-05	18:10:58	5283	0.31	5.601	LNV102801A	470.85	341.07	19.92	11.84
29-Oct-05	11:08:00	5322	0.26	5.187	LNV102901A	480.19	408.49	20.02	11.92
29-Oct-05	12:14:50	5388	0.28	5.369	LNV102902A	434.49	349.66	20.18	12.05
29-Oct-05	13:18:20	5452	0.28	5.310	LNV102903A	629.86	490.42	20.36	12.20
29-Oct-05	14:28:10	5522	0.29	5.427	LNV102904A	632.60	544.91	20.60	12.39
4-Nov-05	14:52:20	6324	0.29	5.427	LNV110401A	3277.08	1714.23	29.11	17.31
4-Nov-05	15:45:00	6377	0.23	4.880	LNV110402A	258.18	162.63	29.61	17.58
4-Nov-05	17:14:30	6466	0.24	4.943	LNV110403A	162.32	137.32	29.70	17.64
5-Nov-05	13:43:50	7696	0.24	4.920	LNV110501A	21.85	11.45	30.26	18.09
6-Nov-05	16:07:10	7728	0.23	4.884	LNV110601A	611.65	862.87	30.31	18.16
6-Nov-05	17:00:50	7791	0.24	4.935	LNV110602A	74.77	73.99	30.42	18.31
6-Nov-05	18:26:10	7867	0.23	4.835	LNV110603A	59.97	51.13	30.44	18.33
6-Nov-05	20:38:50	8000	0.19	4.407	LNV110604A	36.99	48.42	30.47	18.36
6-Nov-05	22:26:40	8108	0.17	4.161	LNV110605A	29.18	31.76	30.49	18.38
7-Nov-05	7:09:20	8630	0.17	4.132	LNV110701A	26.06	22.86	30.55	18.44
7-Nov-05	7:51:30	8673	0.22	4.716	LNV110702A	22.27	20.91	30.55	18.44
7-Nov-05	19:28:10	9369	0.17	4.146	LNV110703A	21.76	17.86	30.62	18.50
7-Nov-05	21:52:10	9513	0.17	4.137	LNV110704A	21.60	17.99	30.63	18.51
8-Nov-05	8:46:20	10167	0.17	4.170	LNV110801A	13.18	11.80	30.68	18.55
8-Nov-05	19:02:30	10784	0.17	4.203	LNV110802A	17.79	17.66	30.72	18.59
8-Nov-05	20:21:30	10836	0.20	4.577	LNV110803A	45.38	60.19	30.73	18.60
8-Nov-05	21:23:20	10898	0.16	4.027	LNV110804A	26.93	31.83	30.74	18.61
8-Nov-05	22:30:10	10965	0.15	3.983	LNV110805A	43.21	42.02	30.75	18.62
9-Nov-05	8:06:30	11490	0.20	4.478	LNV110901A	56.91	45.76	30.86	18.72
9-Nov-05	9:31:50	11576	0.18	4.272	LNV110902A	74.82	52.76	30.88	18.74
9-Nov-05	20:55:40	11746	0.17	4.189	LNV110903A	381.78	300.97	31.05	18.87
9-Nov-05	21:21:40	11772	0.17	4.175	LNV110904A	50.18	49.22	31.07	18.88
9-Nov-05	22:20:30	11831	0.17	4.132	LNV110905A	25.22	20.88	31.08	18.89
10-Nov-05	9:26:30	12497	0.17	4.137	LNV111001A	24.18	17.88	31.15	18.95

Date	Time	Elapsed Time (min)	Air Pressure Differential (inches of water)	Outlet Flow (m^3/min)	Sample #	Pentane (ug/L)	Hexane (ug/L)	Pentane Removed (kg)	Hexane Removed (kg)
19-Nov-05	17:25:20	12778	0.19	4.376	LNV111901A	858.38	584.19	31.69	19.32
19-Nov-05	18:16:10	12829	0.18	4.295	LNV111902A	180.44	118.84	31.80	19.39
19-Nov-05	19:20:10	12893	0.18	4.286	LNV111903A	141.36	85.60	31.85	19.42
19-Nov-05	22:08:20	13061	0.18	4.235	LNV111904A	97.51	58.38	31.93	19.47
20-Nov-05	13:07:50	13835	0.17	4.226	LNV112001A	68.61	38.42	32.21	19.63
20-Nov-05	19:47:40	14235	0.18	4.249	LNV112002A	67.79	36.19	32.32	19.70
20-Nov-05	21:29:00	14331	0.18	4.336	LNV112003A	83.52	44.97	32.35	19.71
21-Nov-05	21:13:50	15756	0.18	4.309	LNV112101A	81.93	45.82	32.86	19.99
21-Nov-05	23:00:30	15863	0.24	4.955	LNV112102A	40.44	25.12	32.89	20.01

Appendix C

Phase I GC Water Sampling Results

Date	Time	Sample #	Pentane (ug/L)	Hexane (ug/L)
30-Sep-05	12:53:00	LNW093001A	3315.5	1079.1
30-Sep-05	13:20:00	LNW093002A	4251.0	1066.3
30-Sep-05	16:30:00	LNW093003A	3019.3	1269.2
30-Sep-05	18:37:00	LNW093004A	1226.0	503.6
30-Sep-05	19:22:00	LNW093005A	187.8	0.0
3-Oct-05	13:39:00	LNW100301A	502.2	277.0
3-Oct-05	16:03:00	LNW100303A	242.9	138.2
3-Oct-05	18:45:00	LNW100304A	506.0	427.7
3-Oct-05	20:16:00	LNW100305A	1379.1	1418.8
4-Oct-05	11:22:00	LNW100401A	308.0	312.3
4-Oct-05	15:57:30	LNW100402A	287.9	236.7
4-Oct-05	19:10:00	LNW100403A	206.9	130.1
4-Oct-05	22:25:00	LNW100405A	168.6	131.1
5-Oct-05	11:00:00	LNW100501A	116.4	76.4
5-Oct-05	12:00:00	LNW100502A	113.6	60.4
5-Oct-05	13:00:00	LNW100503A	125.2	76.7
5-Oct-05	14:00:00	LNW100504A	145.0	77.4
6-Oct-05	09:03:00	LNW100601A	379.9	320.7
6-Oct-05	11:13:00	LNW100602A	131.6	48.2
6-Oct-05	14:14:00	LNW100603A	352.8	223.4
8-Oct-05	08:53:00	LNW100801A	41.9	4.8
14-Oct-05	17:43:00	LNW101401A	746.7	593.9
23-Oct-05	12:45:00	LNW102301A	684.7	396.0
24-Oct-05	13:49:00	LNW102401A	46.1	29.9
24-Oct-05	15:11:00	LNW102402A	477.0	278.9
24-Oct-05	16:02:00	LNW102403A	511.1	355.4
24-Oct-05	17:45:00	LNW102404A	366.7	214.6
24-Oct-05	20:39:00	LNW102405A	315.3	222.5
24-Oct-05	22:43:00	LNW102406A	355.8	277.0
25-Oct-05	11:07:00	LNW102501A	194.6	109.3
25-Oct-05	12:59:00	LNW102502A	572.6	353.6
25-Oct-05	15:41:00	LNW102503A	444.5	298.4
25-Oct-05	19:37:00	LNW102504A	370.3	243.1
25-Oct-05	21:54:00	LNW102505A	462.6	160.0
28-Oct-05	18:00:00	LNW102801A	0.0	0.0
29-Oct-05	11:15:00	LNW102901A	0.0	72.1
29-Oct-05	13:00:00	LNW102902A	0.0	214.4
29-Oct-05	14:21:00	LNW102903A	0.0	184.3
4-Nov-05	15:51:00	LNW110401A	0.0	107.6
4-Nov-05	17:37:00	LNW110402A	0.0	100.1
6-Nov-05	16:00:00	LNW110601A	0.0	34.8
6-Nov-05	17:10:00	LNW110602A	0.0	50.6
6-Nov-05	18:20:00	LNW110603A	0.0	75.5
6-Nov-05	20:48:00	LNW110604A	0.0	2.2
6-Nov-05	22:21:00	LNW110605B	0.0	0.0
7-Nov-05	07:14:00	LNW110701A	0.0	7.6
7-Nov-05	19:41:00	LNW110703A	0.0	0.0

Date	Time	Sample #	Pentane (ug/L)	Hexane (ug/L)
8-Nov-05	08:30:00	LNW110801A	0.0	4.5
8-Nov-05	19:08:00	LNW110803A	0.0	3.8
8-Nov-05	20:25:00	LNW110804A	0.0	72.4
8-Nov-05	21:32:00	LNW110805A	0.0	58.4
8-Nov-05	22:26:00	LNW110806A	0.0	47.3
9-Nov-05	09:45:00	LNW110901A	0.0	6.0
9-Nov-05	21:10:00	LNW110902A	0.0	0.0
9-Nov-05	22:24:00	LNW110904A	0.0	0.0
10-Nov-05	09:43:00	LNW111002A	0.0	0.0
19-Nov-05	16:51:00	LNW111901A	114.5	3.7
19-Nov-05	18:03:00	LNW111902A	14.9	4.6
19-Nov-05	19:29:00	LNW111903A	30.7	12.5
19-Nov-05	21:59:00	LNW111904A	25.6	7.8
20-Nov-05	13:17:00	LNW112001A	13.8	6.9
20-Nov-05	21:06:00	LNW112002A	13.4	5.6
21-Nov-05	21:02:00	LNW112101A	14.5	10.7
21-Nov-05	23:09:00	LNW112102A	68.6	105.0

Appendix D

Phase I Granular Activated Carbon Sampling Results (Vapour)

Composite Sample	Sample ID	Date	Pentane (mg/kg)	Hexane (mg/kg)
A1	LNC102812A	28-Oct-05	64939.46	0.00
A1	LNC102812B	28-Oct-05	67652.71	0.00
A1	LNC102812C	28-Oct-05	56024.30	0.00
A1	LNC102812D	28-Oct-05	55512.68	0.00
A2	LNC102834A	28-Oct-05	59733.07	850.52
A2	LNC102834B	28-Oct-05	62138.30	519.05
A2	LNC102834C	28-Oct-05	57450.63	1931.18
A2	LNC102834D	28-Oct-05	60921.93	596.74
A3	LNC102856A	28-Oct-05	36381.72	41090.13
A3	LNC102856B	28-Oct-05	38700.70	42366.99
A3	LNC102856C	28-Oct-05	38170.93	44671.41
A3	LNC102856D	28-Oct-05	34219.40	37393.86
A4	LNC102878A	28-Oct-05	29121.60	66312.45
A4	LNC102878B	28-Oct-05	40337.54	90120.00
A4	LNC102878C	28-Oct-05	42079.20	91651.25
A4	LNC102878D	28-Oct-05	38513.40	89679.36
B1	LNC12010910A	1-Dec-05	546.95	45.48
B1	LNC12010910B	1-Dec-05	564.42	19.33
B1	LNC12010910C	1-Dec-05	646.05	7.70
B1	LNC12010910D	1-Dec-05	439.74	35.89
B2	LNC12011112A	1-Dec-05	4790.37	566.36
B2	LNC12011112B	1-Dec-05	5699.56	472.29
B2	LNC12011112C	1-Dec-05	8199.91	860.52
B2	LNC12011112D	1-Dec-05	4387.91	616.39
B3	LNC12011314A	1-Dec-05	50010.93	62.48
B3	LNC12011314B	1-Dec-05	54607.66	1489.10
B3	LNC12011314C	1-Dec-05	49390.26	685.20
B3	LNC12011314D	1-Dec-05	49190.12	77.39
B4	LNC12011516A	1-Dec-05	23944.94	47084.80
B4	LNC12011516B	1-Dec-05	25994.76	42382.31
B4	LNC12011516C	1-Dec-05	18550.46	42338.36
B4	LNC12011516D	1-Dec-05	17133.61	38679.18
B5	LNC12021718A	2-Dec-05	9259.55	75837.59
B5	LNC12021718B	2-Dec-05	10375.00	86892.35
B5	LNC12021718C	2-Dec-05	9496.07	78966.30
B5	LNC12021718D	2-Dec-05	8688.58	72849.23
B6	LNC120219A	2-Dec-05	10053.29	75317.07
B6	LNC120219B	2-Dec-05	9258.45	66255.49
B6	LNC120219C	2-Dec-05	7936.83	68216.07
B6	LNC120219D	2-Dec-05	9062.62	65161.00

Appendix E

Phase I Granular Activated Carbon Sampling Results (Water)

Composite Sample	Sample ID	Date	Pentane (mg/ kg)	Hexane (mg/Kg)
W1	LNC121301A	13-Dec-05	12.23	10.46
W1	LNC121301B	13-Dec-05	23.40	17.34
W1	LNC121301C	13-Dec-05	17.08	15.10
W2	LNC121302A	13-Dec-05	26.66	15.69
W2	LNC121302B	13-Dec-05	23.98	11.67
W2	LNC121302C	13-Dec-05	25.58	13.60
W3	LNC121303A	13-Dec-05	6.79	11.52
W3	LNC121303B	13-Dec-05	5.76	12.53
W3	LNC121303C	13-Dec-05	6.60	16.75
W4	LNC121304A	13-Dec-05	9.49	15.97
W4	LNC121304B	13-Dec-05	12.22	18.02
W4	LNC121304C	13-Dec-05	8.90	13.44

Appendix F

Phase I Soil Sampling Results

Core	Depth (cm)	Sample #	Colouration	Pentane (mg/kg)	Hexane (mg/kg)	Pentane (mL/kg)	Hexane (mL/kg)	% Pentane	% Hexane
1	97	101	pink	1033	2538	1.663	3.844	30	70
1	104	102	clear	18	39	0.029	0.059	33	67
1	111	103	clear	7	24	0.011	0.036	23	77
1	125	104	slight pink	645	1370	1.038	2.076	33	67
1	138	105	clear	38	79	0.061	0.119	34	66
1	152	106	pink	606	1575	0.976	2.385	29	71
1	169	107	clear	45	109	0.073	0.165	31	69
1	176	112	clear	3	6	0.005	0.010	33	67
1	183	108	clear	4	9	0.007	0.014	32	68
1	197	109	clear	13	18	0.021	0.028	43	57
1	203	113	clear	2	4	0.003	0.006	37	63
1	210	110	clear	0	3	0.000	0.005	0	100
1	224	111	clear	4	6	0.007	0.010	40	60
1	241	114	clear	6	6	0.010	0.009	53	47
1	255	115	clear	0	5	0.000	0.008	0	100
1	268	116	clear	0	2	0.000	0.004	0	100
1	275	121	clear	2	4	0.003	0.005	36	64
1	282	117	clear	2	4	0.004	0.006	38	62
1	296	118	clear	3	4	0.004	0.005	43	57
1	303	123	clear	2	3	0.004	0.004	46	54
1	310	119	clear	4	9	0.006	0.014	30	70
2	96	124	pink	25	159	0.040	0.240	14	86
2	99	132	clear	5	9	0.007	0.014	35	65
2	107	125	clear	12	20	0.019	0.031	38	62
2	118	126	slight pink	148	321	0.238	0.486	33	67
2	121	131	slight pink	517	1190	0.832	1.803	32	68
2	129	127	slight pink	834	1334	1.341	2.021	40	60
2	140	128	clear	228	283	0.367	0.428	46	54
2	151	129	slight pink	480	808	0.772	1.224	39	61
2	162	130	clear	91	193	0.147	0.293	33	67
2	177	133	slight pink	1180	1373	1.900	2.080	48	52
2	184	140	pink	1823	2266	2.933	3.432	46	54
2	188	134	pink	2067	2609	3.327	3.951	46	54
2	197	141	pink	1584	1703	2.549	2.579	50	50
2	199	135	pink	2275	2428	3.661	3.678	50	50
2	210	136	clear	16	14	0.026	0.021	55	45
2	221	137	very pink	5753	6394	9.258	9.683	49	51
2	227	142	pink	3156	3716	5.078	5.628	47	53
2	232	138	slight pink	2401	2436	3.865	3.689	51	49
2	243	139	clear	25	26	0.041	0.039	51	49
2	258	143	clear	173	185	0.279	0.279	50	50
2	269	144	clear	689	799	1.108	1.210	48	52
2	278	149	very pink	5602	5823	9.015	8.819	51	49
2	280	145	very pink	4142	4288	6.666	6.494	51	49
2	286	148	very pink	6843	7494	11.013	11.350	49	51
2	291	146	very pink	5458	6481	8.784	9.815	47	53

Core	Depth (cm)	Sample #	Colouration	Pentane (mg/kg)	Hexane (mg/kg)	Pentane (mL/kg)	Hexane (mL/kg)	% Pentane	% Hexane
2	302	147	slight pink	1468	2261	2.362	3.424	41	59
3	95	5	clear	33	38	0.052	0.058	48	52
3	107	4	clear	96	157	0.154	0.238	39	61
3	111	7	clear	72	105	0.115	0.158	42	58
3	119	3	slight pink	1576	1744	2.536	2.641	49	51
3	126	6	slight pink	1946	2122	3.131	3.213	49	51
3	132	2	pink	1917	2423	3.085	3.670	46	54
3	144	1	clear	48	48	0.077	0.073	52	48
3	156	150	clear	91	109	0.146	0.165	47	53
3	169	8	clear	13	13	0.021	0.019	52	48
3	181	9	clear	9	8	0.014	0.012	54	46
3	193	10	clear	4	3	0.007	0.004	63	37
3	206	11	pink	4514	5766	7.264	8.733	45	55
3	218	12	clear	12	11	0.019	0.016	54	46
3	226	14	very pink	7325	10139	11.788	15.355	43	57
3	230	13	pink	2366	3731	3.807	5.651	40	60
3	241	15	slight pink	2413	2892	3.884	4.380	47	53
3	249	22	pink	2590	3870	4.168	5.861	42	58
3	253	16	pink	3599	4741	5.792	7.181	45	55
3	257	21	pink	4210	5884	6.775	8.912	43	57
3	266	17	slight pink	1497	2151	2.410	3.257	43	57
3	278	18	clear	8	9	0.013	0.014	47	53
3	290	19	clear	9	12	0.014	0.019	43	57
3	303	20	clear	0	10	0.000	0.016	0	100
4	95	23	clear	35	13	0.056	0.020	73	27
4	106	24	clear	10	6	0.016	0.009	65	35
4	111	30	slight pink	312	563	0.502	0.853	37	63
4	116	25	clear	8	10	0.012	0.015	46	54
4	122	31	clear	21	12	0.034	0.018	65	35
4	127	26	slight pink	820	1522	1.320	2.305	36	64
4	137	27	clear	10	17	0.016	0.025	39	61
4	148	28	clear	5	10	0.008	0.016	35	65
4	158	29	clear	41	170	0.065	0.258	20	80
4	167	39	slight pink	454	1239	0.731	1.876	28	72
4	170	32	slight pink	317	1275	0.510	1.931	21	79
4	175	41	clear	9	29	0.015	0.044	26	74
4	181	33	clear	0	3	0.000	0.005	0	100
4	191	34	clear	0	2	0.000	0.003	0	100
4	202	35	clear	0	2	0.000	0.004	0	100
4	212	36	clear	0	2	0.000	0.003	0	100
4	223	37	clear	0	6	0.000	0.009	0	100
4	233	38	clear	0	19	0.000	0.029	0	100
4	241	40	clear	0	8	0.000	0.012	0	100
4	247	42	clear	0	0	0.000	0.000		
4	252	49	clear	0	0	0.000	0.000		
4	257	43	clear	0	0	0.000	0.000		

Core	Depth (cm)	Sample #	Colouration	Pentane (mg/kg)	Hexane (mg/kg)	Pentane (mL/kg)	Hexane (mL/kg)	% Pentane	% Hexane
4	268	44	clear	0	0	0.000	0.000		
4	273	50	clear	0	0	0.000	0.000		
4	278	45	clear	0	0	0.000	0.000		
4	289	46	clear	0	0	0.000	0.000		
4	294	51	clear	0	1	0.000	0.002	0	100
4	299	47	clear	0	5	0.000	0.007	0	100
4	310	48	clear	0	2	0.000	0.002	0	100
5	95	52	clear	78	105	0.126	0.159	44	56
5	99	59	clear	42	139	0.068	0.210	24	76
5	105	53	pink	101	355	0.163	0.537	23	77
5	110	60	pink	602	1529	0.968	2.315	29	71
5	115	54	clear	335	658	0.540	0.997	35	65
5	125	55	clear	480	479	0.773	0.725	52	48
5	136	56	slight pink	2056	2020	3.309	3.060	52	48
5	146	57	pink	2492	2318	4.011	3.510	53	47
5	156	58	pink	2596	2505	4.178	3.794	52	48
5	163	61	slight pink	758	706	1.220	1.069	53	47
5	169	62	slight pink	1669	1634	2.686	2.474	52	48
5	173	71	clear	249	226	0.401	0.343	54	46
5	179	63	clear	82	72	0.133	0.110	55	45
5	189	64	clear	27	23	0.044	0.035	55	45
5	199	65	clear	11	14	0.018	0.021	45	55
5	210	66	clear	7	9	0.011	0.014	46	54
5	220	67	clear	859	1232	1.383	1.866	43	57
5	228	70	slight pink	694	1227	1.117	1.858	38	62
5	230	68	pink	834	3536	1.342	5.355	20	80
5	237	69	clear	88	545	0.142	0.825	15	85
5	243	72	clear	44	124	0.071	0.188	28	72
5	253	73	clear	4	7	0.006	0.010	39	61
5	260	80	slight pink	501	1329	0.807	2.013	29	71
5	263	74	clear	17	35	0.028	0.053	35	65
5	268	75	slight pink	9	331	0.015	0.502	3	97
5	274	76	clear	2	9	0.002	0.014	15	85
5	284	77	clear	0	4	0.000	0.006	0	100
5	294	78	slight pink	91	579	0.146	0.878	14	86
5	304	79	clear	18	50	0.028	0.075	27	73

Appendix G

Modeled Scenarios

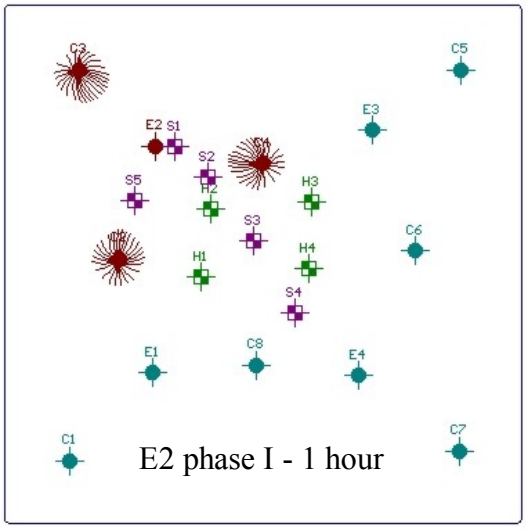
E2 phase I - 1 hour

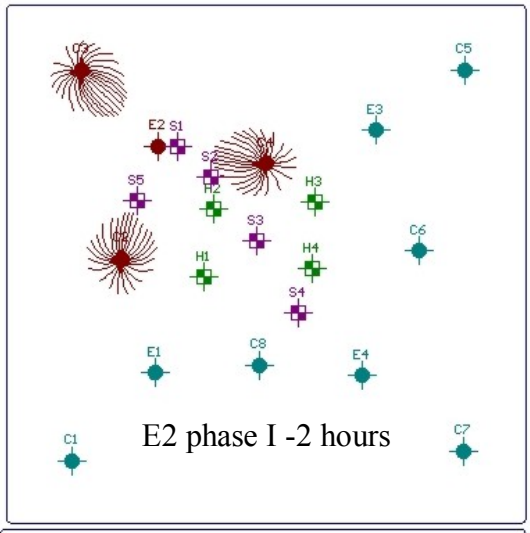
E2 phase I -2 hours

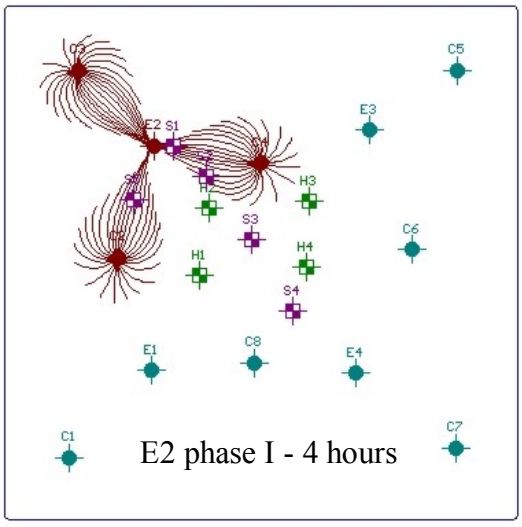
E2 phase I - 4 hours

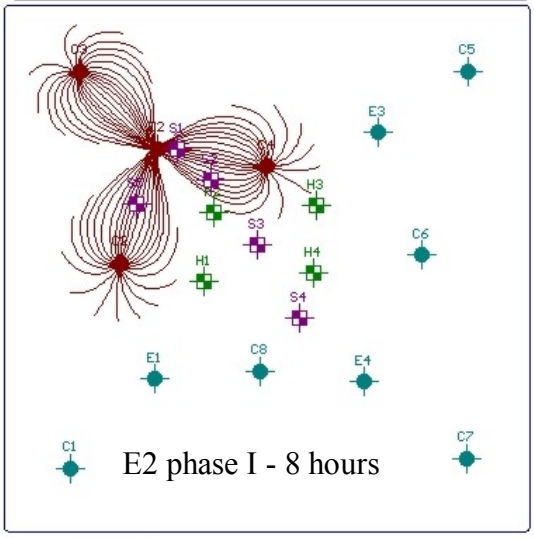
E2 phase I - 8 hours

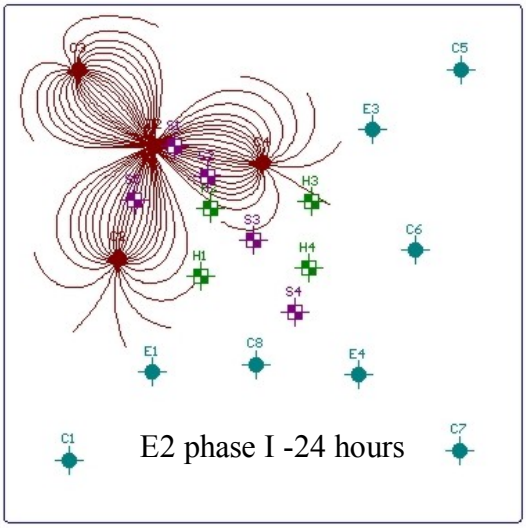
E2 phase I -24 hours

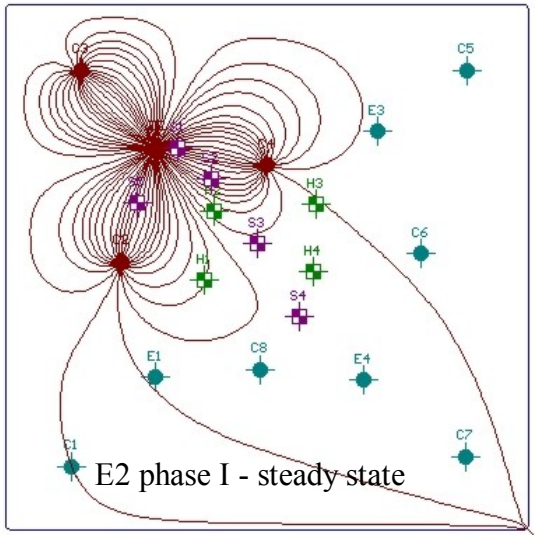
E2 phase I - steady state

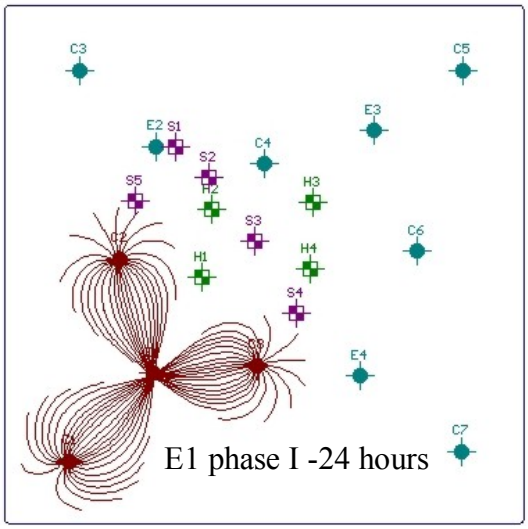

E1 phase I -24 hours

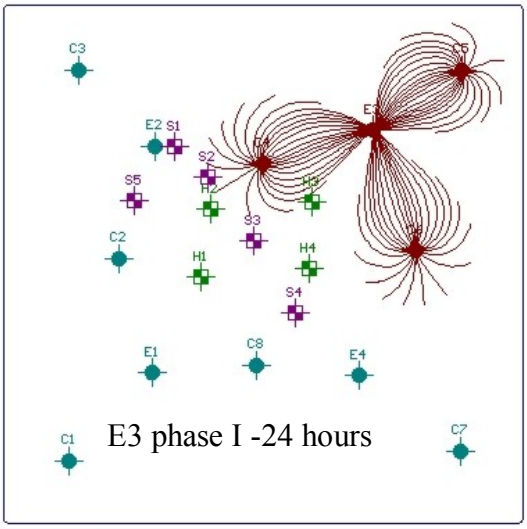

E3 phase I -24 hours

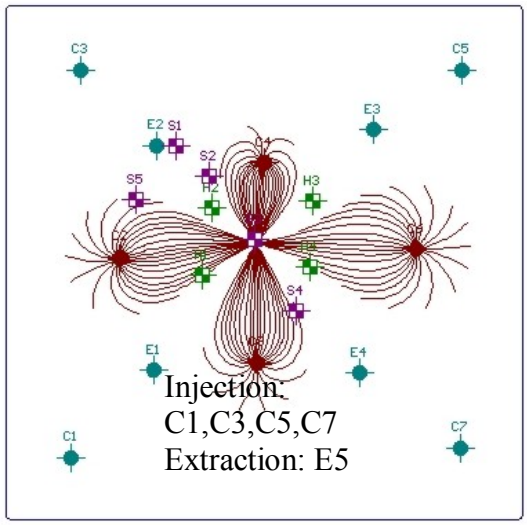

Injection:
C1,C3,C5,C7
Extraction: E5

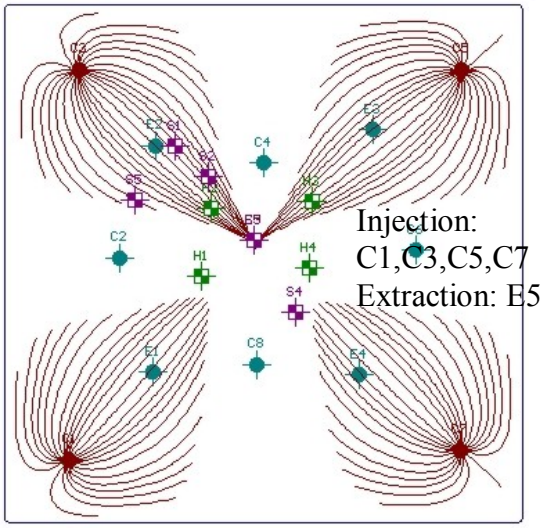

Injection:
C1,C3,C5,C7
Extraction: E5

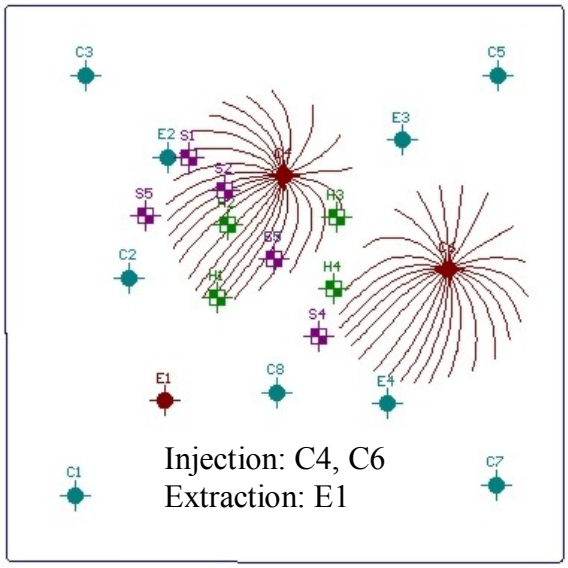

Injection: C4, C6
Extraction: E1

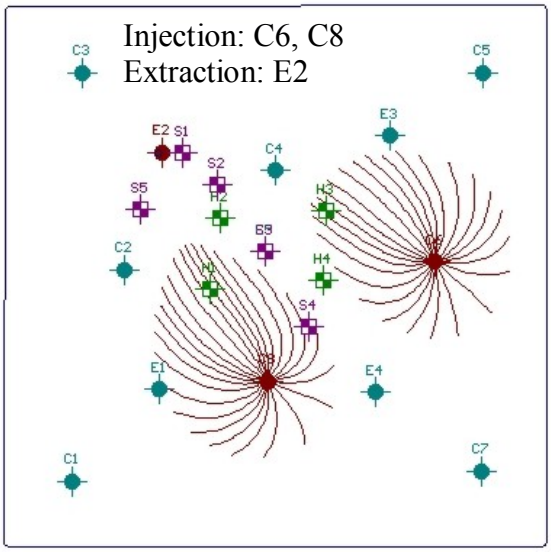

Injection: C6, C8
Extraction: E2

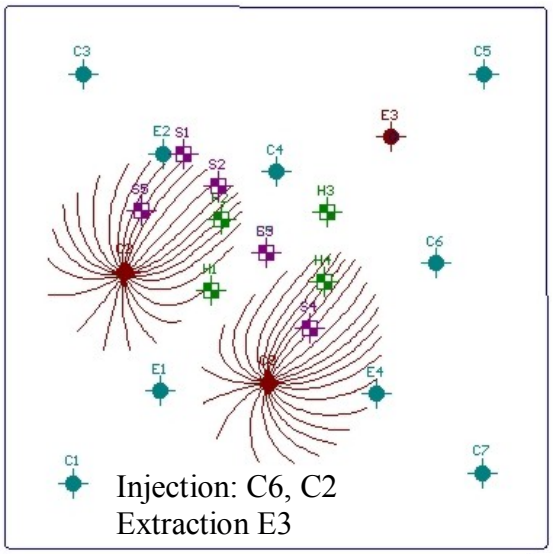

Injection: C6, C2
Extraction E3

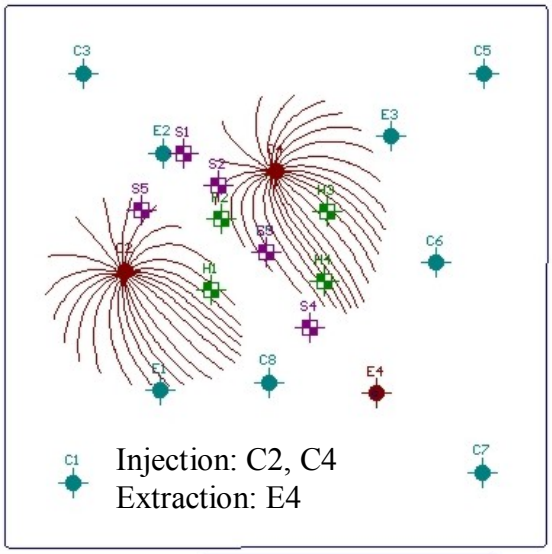

Injection: C2, C4
Extraction: E4

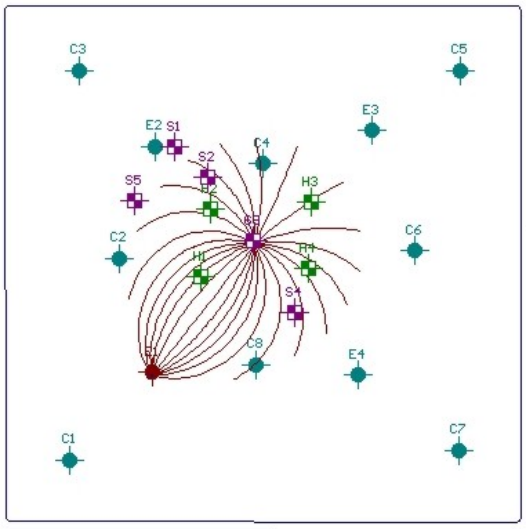

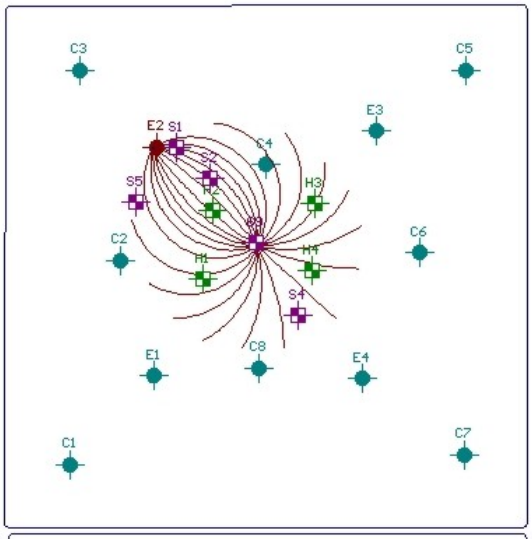

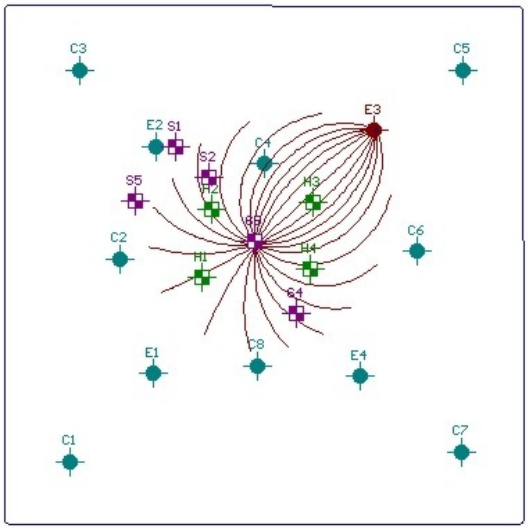

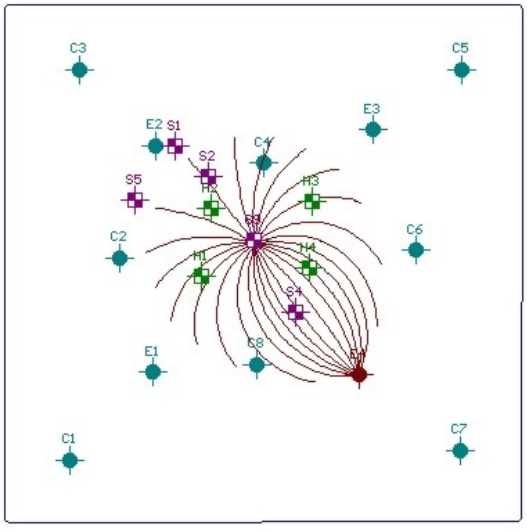

Appendix H

Phase II GC Vapour Sampling Results

Elapsed Time (min)	Date	Extraction P differential (in wc)	Extraction Flow cubic metres/min	Sample #	Pentane ug/L	Hexane ug/L	Pentane Removed (kg)	Hexane Removed (kg)
39	7/31/2006 11:35	-0.46	3.780	073101	0	0	0.00	0.00
139	7/31/2006 13:15	-0.47	3.821	073102	30.65	21.42	0.01	0.00
184	7/31/2006 14:00	-0.33	3.202	073103	83.67	48.65	0.01	0.01
243	7/31/2006 14:59	-0.35	3.297	073104	447.08	215.43	0.07	0.03
396	8/1/2006 16:14	-0.38	3.436	080101	225.61	111.63	0.24	0.12
456	8/1/2006 17:14	-0.34	3.250	080102	204.01	126.81	0.28	0.14
509	8/1/2006 18:07	-0.35	3.297	080103	27.95	18.75	0.30	0.16
539	8/1/2006 20:19	-0.38	3.436	080104	274.68	190.39	0.32	0.17
592	8/2/2006 7:38	-0.38	3.436	080201	308.65	192.19	0.37	0.20
627	8/2/2006 8:13	-0.37	3.390	080202	268.83	190.92	0.40	0.22
675	8/2/2006 9:01	-0.38	3.436	080203	242.79	183.98	0.45	0.25
737	8/2/2006 10:03	-0.4	3.525	080204	147.95	123.97	0.49	0.29
795	8/2/2006 11:01	-0.39	3.481	080205	34.91	23.39	0.51	0.30
856	8/2/2006 12:02	-0.38	3.436	080206	319.23	264.64	0.54	0.33
917	8/2/2006 13:03	-0.42	3.612	080207	77.10	54.39	0.59	0.37
978	8/2/2006 14:04	-0.24	2.730	080208	638.49	488.88	0.65	0.41
1035	8/2/2006 15:01	-0.33	3.202	080209	304.90	239.97	0.73	0.47
1095	8/2/2006 16:01	-0.31	3.103	080210	301.30	236.86	0.78	0.52
1156	8/2/2006 17:02	-0.3	3.053	080211	259.22	212.43	0.84	0.56
1213	8/2/2006 17:59	-0.32	3.153	080212	198.06	156.35	0.88	0.59
1281	8/2/2006 19:07	-0.32	3.153	080213	240.22	178.05	0.92	0.63
1357	8/2/2006 20:23	-0.3	3.053	080214	198.30	162.49	0.97	0.67
1420	8/2/2006 21:26	-0.33	3.202	080215	28.56	22.93	1.00	0.69
1450	8/3/2006 8:50	-0.31	3.103	080301	185.43	183.82	1.01	0.70
1501	8/3/2006 9:41	-0.3	3.053	080302	375.85	288.97	1.05	0.73
1564	8/3/2006 10:44	-0.32	3.153	080303	144.49	135.69	1.10	0.77
1634	8/3/2006 11:54	-0.31	3.103	080304	185.41	170.65	1.14	0.81
1667	8/9/2006 10:17	-0.29	3.001	080901	60.77	44.05	1.15	0.82
1725	8/9/2006 11:15	-0.3	3.053	080902	208.69	152.94	1.17	0.84
1792	8/9/2006 12:22	-0.3	3.053	080903	226.96	168.01	1.22	0.87

Elapsed Time (min)	Date	Extraction P differential (in wc)	Extraction Flow cubic metres/min	Sample #	Pentane ug/L	Hexane ug/L	Pentane Removed (kg)	Hexane Removed (kg)
1848	8/9/2006 13:18	-0.3	3.053	080904	226.49	164.52	1.26	0.90
1907	8/9/2006 14:17	-0.29	3.001	080905	164.88	125.32	1.29	0.92
1967	8/9/2006 15:17	-0.28	2.949	080906	200.80	148.11	1.32	0.95
2030	8/9/2006 16:20	-0.29	3.001	080906	181.05	128.55	1.36	0.97
2089	8/9/2006 17:19	-0.28	2.949	090808	188.41	131.47	1.39	1.00
2150	8/9/2006 18:20	-0.28	2.949	080909	272.52	216.30	1.43	1.03
2232	8/9/2006 19:42	-0.28	2.949	090910	180.30	147.62	1.49	1.07
2246	8/10/2006 8:06	-0.29	3.001	091001	281.43	190.57	1.50	1.08
2330	8/10/2006 9:30	-0.29	3.001	081002	209.77	158.98	1.56	1.12
2431	8/11/2006 17:31	-0.31	3.103	081102	162.13	118.68	1.62	1.17
2494	8/11/2006 18:34	-0.34	3.250	081103	191.30	136.35	1.65	1.19
2520	8/12/2006 10:46	-0.35	3.297	081201	161.30	113.48	1.67	1.20
2641	8/12/2006 12:47	-0.35	3.297	081202	202.30	139.27	1.74	1.25
2808	8/12/2006 15:34	-0.35	3.297	081203	176.13	120.38	1.84	1.32
2930	8/12/2006 17:36	-0.36	3.344	081204	158.73	105.05	1.91	1.37
3037	8/12/2006 19:23	-0.31	3.103	081205	222.85	153.99	1.98	1.41
3159	8/12/2006 21:25	-0.3	3.053	081206	231.60	154.16	2.06	1.47
3222	8/12/2006 22:28	-0.31	3.103	081207	245.54	167.59	2.11	1.50
3231	8/14/2006 11:28	-0.27	2.896	081401	630.72	299.10	2.12	1.51
3404	8/14/2006 14:21	-0.29	3.001	081402	73.07	48.38	2.30	1.60
3434	8/14/2006 14:51	-0.3	3.053	081403	175.86	129.13	2.31	1.60
3508	8/14/2006 16:05	-0.27	2.896	081404	217.89	144.76	2.35	1.64
3565	8/14/2006 17:02	-0.27	2.896	081405	214.78	145.20	2.39	1.66
3664	8/15/2006 10:10	-0.27	2.896	081501	108.45	72.22	2.43	1.69
3732	8/15/2006 11:18	-0.25	2.787	081502	56.91	38.75	2.45	1.70
3769	8/15/2006 11:55	-0.21	2.554	081503	32.82	20.60	2.45	1.70
3793	8/15/2006 17:25	-0.23	2.673	081504	94.13	71.62	2.46	1.71
3845	8/15/2006 18:17	-0.25	2.787	081505	119.79	84.84	2.47	1.72
3908	8/15/2006 19:20	-0.25	2.787	081506	131.14	91.20	2.50	1.73
3964	8/15/2006 20:16	-0.24	2.730	081507	157.13	106.82	2.52	1.75

Elapsed Time (min)	Date	Extraction P differential (in wc)	Extraction Flow cubic metres/min	Sample #	Pentane ug/L	Hexane ug/L	Pentane Removed (kg)	Hexane Removed (kg)
4049	8/15/2006 21:41	-0.23	2.673	081508	193.11	129.70	2.56	1.78
4500	8/16/2006 5:12	-0.24	2.730	081601	272.51	191.46	2.84	1.97
4566	8/16/2006 6:18	-0.22	2.614	081602	276.13	201.19	2.89	2.01
4618	8/16/2006 7:10	-0.23	2.673	081603	272.03	203.68	2.93	2.03
4670	8/16/2006 8:02	-0.25	2.787	081604	177.18	132.05	2.96	2.06
4734	8/16/2006 9:06	-0.26	2.842	081605	279.05	216.71	3.00	2.09
4885	8/18/2006 11:07	-0.26	2.842	081801	126.24	80.43	3.09	2.15
4942	8/18/2006 12:04	-0.24	2.730	081802	38.81	21.93	3.10	2.16
4961	8/22/2006 13:55	-0.26	2.842	082201	123.17	71.20	3.11	2.16
5020	8/22/2006 14:54	-0.26	2.842	082202	89.39	60.65	3.12	2.18
5082	8/22/2006 15:56	-0.27	2.896	082203	115.69	82.28	3.14	2.19
5141	8/22/2006 16:55	-0.27	2.896	082204	136.28	113.16	3.16	2.20
5201	8/22/2006 17:55	-0.27	2.896	082205	156.39	108.91	3.19	2.22
5267	8/22/2006 19:01	-0.27	2.896	082206	159.85	110.68	3.22	2.24
5343	8/22/2006 20:17	-0.24	2.730	082207	155.74	108.06	3.25	2.27
5401	8/22/2006 21:15	-0.27	2.896	082208	164.76	113.57	3.28	2.29
5463	8/22/2006 22:17	-0.27	2.896	082209	159.19	111.54	3.31	2.31
5496	8/23/2006 8:44	-0.34	3.250	082301	175.39	117.39	3.33	2.32
5557	8/23/2006 9:45	-0.26	2.842	082302	175.71	123.08	3.36	2.34
5621	8/23/2006 10:49	-0.25	2.787	082303	189.74	133.24	3.39	2.36
5702	8/23/2006 12:10	-0.25	2.787	082304	201.83	145.41	3.44	2.39
5753	8/23/2006 13:01	-0.25	2.787	082305	201.13	144.31	3.46	2.42
5821	8/23/2006 14:09	-0.27	2.896	082306	198.38	141.86	3.50	2.44
5867	8/23/2006 14:55	-0.27	2.896	082307	192.11	139.80	3.53	2.46
5929	8/23/2006 15:57	-0.27	2.896	082308	197.65	144.38	3.56	2.49
5988	8/23/2006 16:56	-0.27	2.896	082309	210.19	153.31	3.60	2.51
6058	8/23/2006 18:06	-0.27	2.896	082310	199.52	146.58	3.64	2.54
6125	8/23/2006 19:13	-0.29	3.001	082311	198.21	145.58	3.68	2.57
6177	8/23/2006 20:05	-0.29	3.001	082312	198.06	148.69	3.71	2.60
6232	8/23/2006 21:00	-0.28	2.949	082313	193.72	146.48	3.74	2.62

Elapsed Time (min)	Date	Extraction P differential (in wc)	Extraction Flow cubic metres/min	Sample #	Pentane ug/L	Hexane ug/L	Pentane Removed (kg)	Hexane Removed (kg)
6292	8/23/2006 22:00	-0.29	3.001	082314	187.09	139.95	3.78	2.64
6318	8/24/2006 14:03	-0.29	3.001	082401	205.20	124.38	3.79	2.66
6374	8/24/2006 14:59	-0.31	3.103	082402	172.09	124.74	3.82	2.68
6470	8/24/2006 16:35	-0.29	3.001	081403	187.85	141.16	3.88	2.72
6542	8/24/2006 17:47	-0.29	3.001	082404	191.31	144.42	3.92	2.75
6813	8/24/2006 22:18	-0.29	3.001	082405	196.59	151.99	4.08	2.87
6868	8/24/2006 23:13	-0.29	3.001	082406	184.46	141.16	4.11	2.89
7128	8/25/2006 3:39	-0.25	2.787	082501	197.01	153.19	4.25	3.00
7282	8/25/2006 6:13	-0.26	2.842	082502	204.07	160.37	4.34	3.07
7349	8/25/2006 7:20	-0.26	2.842	082503	197.25	158.56	4.37	3.10
7428	8/25/2006 8:39	-0.27	2.896	082504	182.15	145.40	4.42	3.13
7508	8/25/2006 9:59	-0.26	2.842	082505	183.19	146.99	4.46	3.17
7624	8/25/2006 11:55	-0.28	2.949	082506	208.80	157.56	4.53	3.22
7693	8/25/2006 13:04	-0.28	2.949	082507	215.74	173.26	4.57	3.25
7748	8/25/2006 13:59	-0.27	2.896	082508	219.79	180.22	4.60	3.28
7931	8/25/2006 17:02	-0.29	3.001	082510	234.57	196.26	4.73	3.38
8015	8/25/2006 18:26	-0.3	3.053	082511	228.00	190.35	4.79	3.43
8088	8/25/2006 19:39	-0.29	3.001	082512	236.69	202.29	4.84	3.48
8134	08/27/2006 17:03	-0.27	2.896	082701	244.63	152.30	4.87	3.50
8195	08/27/2006 18:04	-0.27	2.896	082702	215.00	170.44	4.91	3.53
8273	08/27/2006 19:22	-0.26	2.842	082703	208.69	172.35	4.96	3.57
8368	08/27/2006 20:57	-0.25	2.787	082704	198.07	170.80	5.01	3.61
8450	08/27/2006 22:19	-0.24	2.730	082705	208.59	179.28	5.06	3.65
8985	08/28/2006 07:14	-0.25	2.787	082801	269.74	255.62	5.41	3.97
9035	08/28/2006 08:12	-0.25	2.787	082802	268.51	257.41	5.45	4.01
9113	08/28/2006 09:30	-0.25	2.787	082803	253.93	241.70	5.51	4.06
9158	08/28/2006 10:15	-0.24	2.730	082804	180.94	162.87	5.53	4.09
9270	9/27/2006 14:40	0.23	2.673	09271	50.76	5.24	5.57	4.11
9290	9/27/2006 15:00	0.24	2.730	09272	353.56	265.46	5.58	4.12
9450	9/28/2006 12:52	0.37	3.390	09282	290.44	303.51	5.73	4.26

Elapsed Time (min)	Date	Extraction P differential (in wc)	Extraction Flow cubic metres/min	Sample #	Pentane ug/L	Hexane ug/L	Pentane Removed (kg)	Hexane Removed (kg)
9536	9/28/2006 14:18	0.4	3.525	09283	257.73	314.95	5.82	4.35
9608	9/28/2006 15:30	0.35	3.29738832	09284	185.5692	213.2725	5.87	4.42
10698	9/29/2006 9:40	0.25	2.786801768	09291	85.37422	106.9342	6.33	4.96
10748	9/29/2006 10:30	0.25	2.786801768	09292	513.7453	508.7818	6.38	5.01
10808	9/29/2006 11:30	0.3	3.052788384	09293	164.9047	211.2333	6.43	5.07
10898	9/29/2006 13:00	0.32	3.152906285	09294	326.1723	332.9906	6.50	5.15
10958	9/29/2006 14:00	0.34	3.24994141	09295	152.7481	198.7415	6.55	5.20
11018	9/29/2006 15:00	0.32	3.152906285	09296	215.1586	250.7655	6.58	5.24
12128	9/30/2006 9:30	0.3	3.052788384	09301	250.1631	252.3897	7.38	6.11
12158	9/30/2006 10:00	0.3	3.052788384	09302	197.0655	192.6943	7.40	6.13
12193	10/3/2006 11:21	0.26	2.841991319	10031	287.4901	146.0281	7.43	6.14
12262	10/3/2006 12:30	0.27	2.896129352	10032	74.08636	65.14094	7.47	6.16
12327	10/3/2006 13:35	0.29	3.001477361	10033	80.02277	75.05611	7.48	6.18
12372	10/3/2006 14:20	0.27	2.896129352	10034	33.41763	11.41091	7.49	6.18
12412	10/3/2006 15:00	0.28	2.949273773	10035	109.1836	87.33175	7.50	6.19
12452	10/3/2006 15:40	0.3	3.052788384	10036	105.3379	104.0596	7.51	6.20
13552	10/4/2006 10:00	0.29	3.001477361	10041	171.0612	206.9389	7.97	6.72
13602	10/4/2006 10:50	0.29	3.001477361	10042	228.0275	241.7968	8.00	6.75
13662	10/4/2006 11:50	0.3	3.052788384	10043	218.3034	235.4107	8.04	6.79
13722	10/4/2006 12:50	0.3	3.052788384	10044	19.86524	3.815323	8.06	6.82
13782	10/4/2006 13:50	0.29	3.001477361	10045	105.807	129.2828	8.07	6.83
13842	10/4/2006 14:50	0.31	3.103251114	10046	231.1434	212.0338	8.10	6.86
13902	10/4/2006 15:50	0.29	3.001477361	10047	122.3884	118.5321	8.14	6.89
14962	10/5/2006 9:30	0.38	3.435799969	10052	67.17696	67.96884	8.45	7.20
15001	10/5/2006 11:30	0.34	3.24994141	10053	125.0005	131.4271	8.46	7.22
15041	10/5/2006 12:10	0.35	3.29738832	10054	141.9294	148.9203	8.48	7.23
15101	10/5/2006 13:10	0.36	3.344162122	10055	183.7275	196.1181	8.51	7.27
15161	10/5/2006 14:10	0.32	3.152906285	10056	161.9626	171.7655	8.55	7.30
15221	10/5/2006 15:10	0.32	3.152906285	10057	144.524	164.6899	8.58	7.34
15241	10/5/2006 15:30	0.36	3.344162122	10058	133.2941	153.6296	8.59	7.35

Elapsed Time (min)	Date	Extraction P differential (in wc)	Extraction Flow cubic metres/min	Sample #	Pentane ug/L	Hexane ug/L	Pentane Removed (kg)	Hexane Removed (kg)
16141	10/6/2006 8:30	0.39	3.480714293	10061	44.04524	39.98201	8.86	7.64
16161	10/6/2006 8:50	0.38	3.435799969	10062	47.10322	43.12542	8.86	7.64
16191	10/6/2006 9:20	0.39	3.480714293	10063	40.22278	37.72086	8.86	7.65

Appendix I

Phase II Soil Sampling Results

Core	Depth	Sample	Colour	Pentane (mg/kg)	Hexane (mg/kg)	Pentane (mL/kg)	Hexane (mL/kg)
1	91	1	clear	0.00	8.78	0.00	0.01
1	104	11	clear	0.00	5.70	0.00	0.01
1	118	3	Very Pink	67.85	497.35	0.11	0.75
1	132	5	Slight Pink	398.53	429.88	0.64	0.65
1	145	6	Clear	17.48	31.75	0.03	0.05
1	159	7	Clear	8.08	26.35	0.01	0.04
1	172	9	Clear	3.10	16.21	0.00	0.02
1	186	10	Clear	0.00	10.60	0.00	0.02
1	211	2	clear	15.24	51.82	0.02	0.08
1	224	12	Clear	0.00	27.76	0.00	0.04
1	238	13	Pink	20.63	116.44	0.03	0.18
1	252	15	Clear	86.06	243.58	0.14	0.37
1	265	16	Clear	8.15	34.17	0.01	0.05
1	279	17	Clear	0.00	17.86	0.00	0.03
1	292	18	Clear	0.00	0.00	0.00	0.00
1	306	19	Clear	0.00	5.16	0.00	0.01
1	331	21	clear	0.00	0.00	0.00	0.00
1	344	22	clear	0.00	0.00	0.00	0.00
1	358	23	clear	0.00	0.00	0.00	0.00
1	372	25	clear	0.00	0.00	0.00	0.00
1	385	26	clear	0.00	0.00	0.00	0.00
1	399	27	clear	0.00	0.00	0.00	0.00
1	412	28	clear	0.00	0.00	0.00	0.00
1	426	29	clear	0.00	0.00	0.00	0.00
2	105	31	Clear	2.83	32.62	0.00	0.05
2	120	32	Very Pink	29.26	112.03	0.05	0.17
2	135	34	Very Pink	58.61	362.94	0.09	0.55
2	150	35	Clear	0.00	25.08	0.00	0.04
2	165	36	Clear	0.00	10.33	0.00	0.02
2	180	37	Clear	0.00	5.89	0.00	0.01
2	195	38	Clear	2.50	20.19	0.00	0.03
2	225	40	Clear	10.57	27.88	0.02	0.04
2	240	42	Pink	52.86	176.91	0.09	0.27
2	255	43	Clear	14.10	54.07	0.02	0.08
2	270	44	Pink	6.87	29.43	0.01	0.04
2	285	45	Pink	7.00	56.74	0.01	0.09
2	300	46	Clear	0.00	50.77	0.00	0.08
2	315	47	Clear	0.00	41.94	0.00	0.06
2	338	49	Clear	0.00	0.00	0.00	0.00
2	353	50	Clear	0.00	0.00	0.00	0.00
2	368	51	Clear	0.00	0.00	0.00	0.00
2	383	52	Clear	0.00	0.00	0.00	0.00
2	398	54	Clear	0.00	0.00	0.00	0.00
2	413	55	Clear	0.00	0.00	0.00	0.00
2	428	56	Clear	0.00	0.00	0.00	0.00
2	440	57	Clear	0.00	0.00	0.00	0.00
3	102	58	Slight Pink	11.11	39.74	0.02	0.06

Core	Depth	Sample	Colour	Pentane (mg/kg)	Hexane (mg/kg)	Pentane (mL/kg)	Hexane (mL/kg)
3	118	59	Pink	15.03	120.73	0.02	0.18
3	135	60	Slight Pink	92.59	417.60	0.15	0.63
3	152	61	Clear	5.95	9.78	0.01	0.01
3	169	62	Pink	11.53	68.56	0.02	0.10
3	186	63	Slight Pink	7.43	119.35	0.01	0.18
3	203	64	Clear	0.00	8.82	0.00	0.01
3	219	66	Clear	0.00	0.00	0.00	0.00
3	234	67	Clear	0.00	0.00	0.00	0.00
3	255	68	Clear	0.00	0.00	0.00	0.00
3	272	70	Clear	0.00	0.00	0.00	0.00
3	289	71	Slight Pink	7.58	44.78	0.01	0.07
3	306	73	Pink	139.09	647.60	0.22	0.98
3	322	74	Slight Pink	0.00	6.09	0.00	0.01
3	339	75	Clear	0.00	0.00	0.00	0.00
3	356	76	Clear	0.00	0.00	0.00	0.00
3	373	78	Clear	0.00	0.00	0.00	0.00
3	383	79	Clear	0.00	0.00	0.00	0.00
4	113	80	Slight Pink	213.08	732.18	0.34	1.11
4	127	81	Pink	322.66	863.55	0.52	1.31
4	141	82	Pink	340.42	839.18	0.55	1.27
4	155	84	Slight Pink	48.56	113.51	0.08	0.17
4	170	85	Clear	21.43	51.39	0.03	0.08
4	184	86	Clear	41.84	106.05	0.07	0.16
4	198	88	Pink	376.48	831.00	0.61	1.26
4	215	89	Clear	90.20	173.01	0.15	0.26
4	229	90	Very Pink	962.59	2989.64	1.55	4.53
4	243	91	Pink	525.44	1459.41	0.85	2.21
4	257	93	Pink	27.62	1174.13	0.04	1.78
4	271	94	Clear	7.24	15.90	0.01	0.02
4	285	95	Clear	0.00	0.32	0.00	0.00
4	299	97	Clear	0.00	0.00	0.00	0.00
4	316	98	Clear	0.00	0.00	0.00	0.00
4	331	99	Clear	0.00	0.00	0.00	0.00
4	345	100	Clear	0.00	0.00	0.00	0.00
4	359	101	Clear	0.00	0.00	0.00	0.00
4	373	104	Clear	0.00	0.00	0.00	0.00
4	387	105	Clear	0.00	0.00	0.00	0.00
4	401	106	Clear	0.00	0.00	0.00	0.00

Appendix J

Analysis of Pentane and Hexane Vapours

ANALYSIS OF PENTANE AND HEXANE VAPORS

Organic Geochemistry Laboratory
Department of Earth Science
University of Waterloo

Analyst/Method Development: Marianne VanderGriendt ext. 35180

PARAMETERS: Pentane, Hexane

SCOPE AND APPLICATION:

This method describes the analysis of vapor phase samples of pentane and hexane in ambient air.

SAMPLE COLLECTION:

Pentane and hexane are highly volatile compounds which often make representative sampling difficult. In this case, vapor samples were collected from a dual phase extraction system used at a field site. Pressurized vapor outflow from the extraction system was placed under water. Duplicate vapor samples were collected in inverted glass vials (40ml) by displacing water from within the vials and trapping the exiting vapor phase. Vials were filled full and capped with Teflon® lined septa and screw caps. Initial tests were preformed to ensure reproducibility of the duplicate vapor samples and to determine acceptable sample holding times (7-14 days).

SAMPLE PREPARATION AND GAS CHROMATOGRAPHIC ANALYSIS:

The vapor samples were analyzed with a Shimadzu 9A capillary gas chromatograph and a flame ionization detector. A 500µl vapor sample was removed through the septa of the sample vial with a 1 ml Hamilton GasTight® glass/Teflon® syringe. The vapor sample was immediately flushed into a 100µl gas sampling valve (Valco Instruments) and loaded on column into a split injection port. The column used for gas chromatographic analysis was a 0.32mm I.D. x 60 m length, supelcowax 10 (Supelco) with a 0.5µm stationary phase of carbowax 20. The helium carrier gas column flow rate was 5 ml/min with a make-up gas flow rate of 50 ml/min. Detector/injector temperatures were 200^{o} C and column oven temperature was 35^{o} C. Chromatographic analysis run time was 3 minutes. Data integration was completed with a Shimadzu CR3A integrator.

CALIBRATION AND QUALITY ASSURANCE DATA:

Calibrations were made in external standard mode and standards were run in triplicate at five different concentrations of pentane/hexane vapor, covering the expected sample range. To prepare standards, neat quantities of pentane/hexane were injected through Teflon® septa screw caps into 1 L glass bottles. Standard bottles were allowed to equilibrate for 1-2 hours. After equilibration a 500µl vapor sample was removed through

the septa and loaded on column in the same way as samples. A multiple point linear regression was performed to determine the linearity and slope of the calibration curve. Quality control information on calibration curves (percent relative standard deviation and percent error) and blank information were included with reported data. Laboratory duplication on 10% of field samples was performed, and results were acceptable when they agreed within 10% of their average. Method detection limits for pentane and hexane were 7.86 and 8.64 µg/L respectively.

REFERENCES:

EPA Method 5000 – Sample Preparation for Volatile Organic Compounds

EPA Method 5021 – Volatile Organic Compounds in Soils and Other Solid Matrices Using Equilibrium Headspace Analysis

EPA Method 8000B – Determinative Chromatographic Separations

EPA METHOD 8015B – Non Halogenated Organics using GC/FID

EPA Method 8260B – Volatile Organic Compounds by Gas Chromatography/Mass Spectrometry (GC/MS)

Longbottom, James E., Lichtenberg, James J., Ed. (1982). "Methods for Organic Chemical Analysis of Municipal and Industrial Wastewater", EPA-600/4-82-057, USEPA/EMSL: Cincinnati, OH, Appendix A – Definition and Procedure for the Determination of the Method Detection Limit.

Appendix K

Analysis of Pentane and Hexane (Aqueous Samples)

VOLATILE ORGANIC COMPOUND ANALYSIS

CRITICAL PARAMETERS: Pentane, Hexane

AUTOMATED HEADSPACE PROCEDURE

SAMPLE PREPARATION:

Samples are collected in 40mL EPA glass vials, capped with tegrabond Teflon septa and screw cap (20mm) and stored in a 4 ºC refrigerator until analyzed. Prior to analysis they are decapped, 14.5 mL of sample quickly removed (with a 20mL glass syringe) and transferred to a 22mL glass vial (leaving a 8mL headspace) with a crimp top seal. Sample vials to be analysed are then stored upside down at room temperature over night (this helps maintain a constant response) and then placed in the autosampler carousel.

Calibration standards are prepared by filling the same 22-ml autosampler vials with organic-free water and then removing 8 ml from the total volume. Vials are quickly spiked with appropriate standards (dissolved in methanol) and sealed. Standards are also stored overnight upside down at room temperature.

GAS CHROMATOGRAPHIC (GC) ANALYSIS:

The prepared samples and calibration standards are run on a Hewlett Packard 5890 gas chromatograph equipped with a split injection port, capillary column, PID (photoionization detector) and a Varian Genesis headspace autosampler. Peak areas are measured by a 3392A HP integrator.
Linear regressions are completed using an excel spreadsheet. An external standard method of calibration is used.

Detection limits for these compounds were found to be between 2 - 4 μg/L using the EPA procedure for Method Detection Limit (MDL).
GC CONDITIONS:

Column:	DB-VRX 30 m x 0.32 mm I.D., 1.8 μm film thickness
Carrier:	Helium at 2.5 ml/min
Oven:	Temperature Program: Initial temperature 40EC, hold 5.0 min, then ramp at 12EC/min to 80EC, hold for 1.5 min
Injector:	Split 12:1, 150EC
Detector:	PID (11.7 eV), 65EC; helium makeup gas at 30 ml/min

HEADSPACE ANALYZER CONDITIONS:

Vial volume:	22.3 ml
Water volume:	14.3 ml
Platen temperature:	65EC
Sample equilibrium time:	30.0 min
Mixing time:	4.0 min
Pressurization time:	1.0 min
Loop fill time:	0.3 min
Loop equilibrium time:	0.2 min
Loop size:	1.0 ml
Injection time:	0.3 min
Valve temperature:	165EC
Line temperature:	165EC

Appendix L

Analysis of Soltrol 130 (Aqueous Samples)

ANALYSIS OF SOLTROL 130 (AQUEOUS SAMPLES)

Organic Geochemistry Laboratory
Department of Earth Sciences
University of Waterloo

Analyst/Method Development: Marianne VanderGriendt ext. 35180

PARAMETERS: Soltrol® 130 Isoparaffin – C10-C13 Isoalkanes

SCOPE AND APPLICATION:

Groundwater samples were taken from a field site cell contaminated with Soltrol® 130. Soltrol® 130 consists of isoalkanes in the C10 to C13 range (diesel fuel range). The chromatographic analysis for Soltrol® 130 is markedly different from that of single component analysis. The chromatogram consist of compounds that will produce well resolved peaks, as well as components that are not chromatographically resolved. This unresolved complex mixture results in a "hump" in the chromatogram that is characteristic of gasoline and diesel fuels. The response used for calibration must represent the entire area of the chromatogram within the retention time range for Soltrol® 130, including the unresolved complex mixture that lies below the individual peaks. This method describes the micro-solvent extraction and gas chromatographic analysis of Soltrol® 130 in groundwater.

SAMPLE COLLECTION:

Water samples were collected in Teflon® screw cap 40ml glass vials. Vials were filled full and stored at 4^{o} C until analyzed. Analysis occurred within 7 days of sample collection.

SAMPLE PREPARATION AND GAS CHROMATOGRAPHIC ANALYSIS:

To solvent extract a sample, the vial was uncapped and 5ml of groundwater was removed. Two ml of dichloromethane, containing internal standard m-fluorotoluene, was quickly added. The vial was then recapped and agitated on its side on a platform shaker for 20 min. at 350 rpm. After shaking, the vial was inverted and the phases were allowed to separate for 30 minutes. With the vial inverted, 1.0 ml of the methylene chloride phase was removed and placed in a 2ml autosampler vial and crimp sealed with a Teflon® cap. Samples were analyzed with a HP 5890 capillary gas chromatograph, a HP7673A autosampler, and a flame ionization detector. Three microliters of methylene chloride was injected in splitless mode onto a 0.25mm x 30 M DB5 column (Supelco), with a stationary phase film thickness of 0.25µm. The helium carrier gas flow rate was 2 ml/min with a make-up gas flow rate of 30ml/min. Injection temperature was 275 ^{o}C, detector temperature was 325 ^{o}C and initial column oven temperature was 35^{o}C, held for 0.5 min., then ramped at 12 ^{o}C/min., to a final temperature of 300 ^{o}C, and held for 2 minutes.

Chromatographic run time was approximately 21 minutes. Data integration was completed with a HP 3396A integrator.

CALIBRATION AND QUALITY ASSURANCE DATA:

Calibrations were made in internal standard mode and standards were run in triplicate at five (or more) different concentrations of Soltrol® 130, covering the expected sample range. Several levels of methanolic stock Soltrol® 130 standards were prepared gravimetrically, by injecting Soltrol® 130 through a septum into a 60ml aliquot of methanol. Calibration standards were prepared by spiking water with small quantities of methanolic stock standard. Standards were extracted and analyzed by gas chromatography, in the same way as samples. For the calibration, all areas of peaks eluting between retention times of 6.0 and 10.4 were summed. These areas were generated by projecting a horizontal baseline between the retention times. A multiple point linear regression was performed to determine the linearity and slope of the calibration curve. Quality control information on calibration curves (percent relative standard deviation and percent error) and blank information were included with reported data. Extraction duplicates were performed on samples and results were acceptable when they agreed within 10%. The method detection limit for Soltrol® 130 was 36.98 µg/L.

REFERENCES:

EPA Method 5000 – Sample Preparation for Volatile Organic Compounds

EPA Method 8000B – Determinative Chromatographic Separations

EPA METHOD 8015B – Non Halogenated Organics using GC/FID

Henderson, J.E., G.R. Peyton and W.H. Glaze (1976). A convenient liquid-liquid extraction method for the determination of halomethanes in water at the parts-per-billion level. IN: Identification and analysis of organic pollutants in water. Keith, L.H. ed. Ann Arbor Science Publishers Inc., Ann Arbor, MI.

Longbottom, James E., Lichtenberg, James J., Ed. (1982). "Methods for Organic Chemical Analysis of Municipal and Industrial Wastewater", EPA-600/4-82-057, USEPA/EMSL: Cincinnati, OH, Appendix A – Definition and Procedure for the Determination of the Method Detection Limit.

Appendix M

Analysis of Pentane and Hexane from Soil Samples

ANALYSIS OF PENTANE AND HEXANE FROM SOIL SAMPLES

Organic Geochemistry Laboratory
Department of Earth Science
University of Waterloo

Analyst/Method Development: Marianne VanderGriendt ext. 35180

PARAMETERS: Pentane, Hexane

SCOPE AND APPLICATION:

Soil cores, taken from a field cell contaminated with pentane and hexane, were analyzed to determine pentane/hexane concentration distribution. It was necessary to desorb these hydrocarbons from the soil. This method describes the techniques for desorption and gas chromatographic analysis of pentane and hexane from contaminated soils.

SAMPLE COLLECTION:

In the field, 1 to 2 g of soil samples were collected in pre-weighed Teflon® crimp sealed 18ml hypovials® containing 8ml of carbon disulfide (and internal standard m-fluorotoluene (MFT) - 100µl/500ml). Special coring and sample allocation techniques were utilized to prevent the loss of pentane and hexane during sampling. Soil extraction vials were ranked for pink/red colour due to the presence of dye #4, spilled along with the hydrocarbons in the field.

SAMPLE PREPARATION AND GAS CHROMATOGRAPHIC ANALYSIS:

After arrival in the laboratory, samples were re-weighed and shaken vigorously for 12 hours. One ml of carbon disulfide was then transferred to a 2ml autosampler vial and crimp sealed with a Teflon cap. Samples were analyzed with a HP 5890 capillary gas chromatograph, a HP7673A autosampler, and a flame ionization detector. One microliter of carbon disulfide was injected in split mode (purge on 0.05 min, purge off 4.0 min) onto a 0.25mm x 30M length, DB5 capillary column with a stationary phase film thickness of 0.25µm. Helium column flow rate was 2ml/min. and make-up gas flow rate was 30ml/min. Injection temperature was 250^{o}C, detector temperature was 300^{o}C and initial column oven temperature was 35 ^{o}C held for 4 min, then ramped at 12 ^{o}C/min to a final temperature of either 70 ^{o}C or 250 ^{o}C (if chromatogram was dirty). Data integration was completed with a HP 3396A integrator.

CALIBRATION AND QUALITY ASSURANCE DATA:

Calibrations were made in internal standard mode and standards were run in triplicate at five (or more) different concentrations of pentane/hexane, covering the expected sample

range. Several levels of stock carbon disulfide standards, were prepared gravimetrically, by injecting pentane and hexane through a septum into a 60ml aliquot of carbon disulfide. Calibration standards were prepared by spiking small quantities of carbon disulfide stock standards into autosampler vials containing 1 ml of carbon disulfide (with MFT). Standards were analyzed by gas chromatography in the same way as samples. A multiple point linear regression was performed to determine the linearity and slope of the calibration curve. To determine method extraction efficiency, clean Borden sand was used to prepare matrix spikes in the same way samples were prepared. Average percent recovery of pentane and hexane over 5 concentration ranges with soil present was 97.48% and 100.86, respectively. Quality control information on calibration curves (percent relative standard deviation and percent error) and blank information were included with reported data. Extraction duplicates were performed on samples and results were acceptable when they agreed within 10%. Method detection limits for pentane and hexane were 3.97 and 3.32 mg/Kg of soil, respectively.

REFERENCES:

Modification of "Analysis of Pentane and Hexane Vapors Collected on Activated Charcoal/ Carbon" Developed by Marianne VanderGriendt.

Ball, W.P., G. Xia, D.P. Durfee, R. D. Wilson, M. J. Brown, and D. M. Mackay. 1997. Hot methanol extraction for the analysis of volatile organic chemicals in subsurface core samples from Dover Air Force Base, Delaware. Groundwater monitoring and remediation 17,no. 1:104-121.

Huang, L.Q., and J. J. Pignatello. 1990. Improved extraction of atrazine and metolachlor in field samples. Journal of the Association of Analytical Chemists 73, no. 3: 443-446.

Longbottom, James E., Lichtenberg, James J., Ed. (1982). "Methods for Organic Chemical Analysis of Municipal and Industrial Wastewater", EPA-600/4-82-057, USEPA/EMSL: Cincinnati, OH, Appendix A – Definition and Procedure for the Determination of the Method Detection Limit.

Sawhaney, B.L., J. J. Pignatello, and S. M. Steinberg. 1988. Determination of 1,2-dibromoethane (EDB) in field soils: Implications for volatile organic compounds. Journal of Environmental Quality 17, no. 1:149-152.

Appendix N

Analysis of Pentane and Hexane Vapours Collected on Activated Carbon

ANALYSIS OF PENTANE AND HEXANE VAPORS COLLECTED ON ACTIVATED CHARCOAL/CARBON

Organic Geochemistry Laboratory
Department of Earth Science
University of Waterloo

Analyst/Method Development: Marianne VanderGriendt ext. 35180

PARAMETERS: Pentane, Hexane

SCOPE AND APPLICATION:

Water and vapor samples containing pentane and hexane were passed through activated carbon filters in the field as a remedial procedure. It was necessary to desorb these hydrocarbons to estimate vapor phase mass removal in the field. This method describes the techniques for desorption and gas chromatographic analysis of pentane and hexane vapors that have been adsorbed from air/water onto activated charcoal/carbon.

SAMPLE COLLECTION:

Activated charcoal/carbon samples were collected in Teflon® screw caped 40 ml glass vials. Vials were filled full to eliminate headspace and stored at 4^{o}C until analyzed.

SAMPLE PREPARATION AND GAS CHROMATOGRAPHIC ANALYSIS:

Samples were extracted with carbon disulfide which contained the internal standard, m-fluorotoluene (MFT) (100µl MFT/500ml). An activated charcoal/carbon sample (0.4g) was quickly weighed into 4mls of carbon disulfide (with MFT), in an 18ml hypovial, and sealed with a Teflon crimp cap. Samples were shaken vigorously and left to equilibrate for 12 hours. After equilibration, 1ml of carbon disulfide was transferred to a 2ml autosampler vial and crimp sealed with a Teflon cap. Samples were analyzed with a HP 5890 capillary gas chromatograph, a HP7673A autosampler, and a flame ionization detector. One microliter of carbon disulfide was injected in split mode (purge on 0.05 min, purge off 4.0 min) onto a 0.25mm x 30M length, DB5 capillary column with a stationary phase film thickness of 0.25µm. Helium column flow rate was 2ml/min with a make-up gas flow rate of 30ml/min. Injection temperature was 250^{o}C, detector temperature was 300^{o}C and initial column oven temperature was 35 ^{o}C held for 4 min, then ramped at 12 ^{o}C/min to a final temperature of either 70 ^{o}C or 250 ^{o}C (if chromatogram was dirty). Chromatographic run time was 10 minutes. Data integration was completed with a HP 3396A integrator.

CALIBRATION AND QUALITY ASSURANCE DATA:

Calibrations were made in internal standard mode and standards were run in triplicate at five (or more) different concentrations of pentane/hexane, covering the expected sample range. Several levels of stock carbon disulfide standards, were prepared gravimetrically, by injecting pentane and hexane through a septum into a 60ml aliquot of carbon disulfide. Calibration standards were prepared in the same way as samples. A clean activated charcoal/carbon sample (0.4g) was quickly weighed into 4mls of carbon disulfide in an 18ml hypovial®, spiked with carbon disulfide stock standard solution, and sealed with a Teflon® crimp cap. Samples were shaken vigorously and left to equilibrate for 12 hours. Standards were analyzed by gas chromatography in the same way as samples. A multiple point linear regression was performed to determine the linearity and slope of the calibration curve. To confirm method validity, extraction efficiency of hexane and pentane was determined with and without activated charcoal/carbon present. Extraction efficiency, with activated charcoal/carbon present, was in the acceptable range of 92.3% for pentane and 90.94% for hexane. However, since the calibration standards were prepared with activated charcoal/carbon present, no data correction for extraction efficiency is necessary. Quality control information on calibration curves (percent relative standard deviation and percent error) and blank information were included with reported data. Extraction duplicates were performed on samples and results were acceptable when they agreed within 10%. Method detection limits for pentane and hexane were 16.23 and 18.89 mg/Kg of activated charcoal/carbon, respectively.

REFERENCES:

ASTM Standard Designation: D 3687-01. Standard Practice for Analysis of Organic Compound Vapors Collected by the Activated Charcoal Tube Adsorption Method. In: *Annual Book of ASTM Standards*, Vol 11.03

ASTM Standard Designation: D3686-95 (Reapproved 2001). Standard Practice for Sampling Atmospheres to Collect Organic Compound Vapors (Activated Charcoal Tube Adsorption Method). In: *Annual Book of ASTM Standards*, Vol 11.03

Eiler, Peter M., ed. NIOSH Method 1500, Hydrocarbons, BP 36-126oC. In: *NOISH Manual of Analytical Methods*, Third Edition, U.S. Gov't. Printing Office, Washington, D.C., 1987. p.1500-1

EPA SOP#2103, Charcoal Tube Sampling in Ambient Air, Date 10/24/94, Rev. #0.0

Longbottom, James E., Lichtenberg, James J., Ed. (1982). "Methods for Organic Chemical Analysis of Municipal and Industrial Wastewater", EPA-600/4-82-057, USEPA/EMSL: Cincinnati, OH, Appendix A – Definition and Procedure for the Determination of the Method Detection Limit.